The effect of sub-catchment industrialisation on the health of Ahuriri Estuary

A thesis presented in partial fulfillment of the requirements for the degree of

Master Environmental Management

at Massey University, Manawatū, New Zealand.

Hannah Ludlow

2021

ABSTRACT

Ahuriri Estuary is steeped in geological and cultural history. In 1931 a magnitude 7.8 earthquake uplifted the bed of the former Ahuriri Lagoon by approximately 2 metres. The drainage, diversion of the Tutaekuri River, channelisation of waterways, and urban development of the surrounding catchment which ensued formed the modern 275-hectare estuary in the centre of Napier City.

To investigate the effects of sub-catchment industrialisation on the health of Ahuriri Estuary, research outlined in this thesis involved undertaking a multi-temporal land use change assessment using historic aerial photographs of the Onekawa and Pandora sub-catchments. In 2018, 41.9ha of grasslands remained within the sub-catchments compared to 254.8ha in 1936, with 223.3ha of impervious industrial development spanning the sub-catchments. The waterways which flow through the Onekawa and Pandora Industrial zones have shown elevated dissolved and sediment-bound heavy metal concentrations.

Six sediment cores were retrieved from tributary discharge zones within Ahuriri Estuary. Visual observations of grain sizes and fossil macrofauna densities accompanied Itrax™ core scanning for chemical constituents. Results for marine and terrigenous sediment ratios identified the 1931 earthquake. To investigate the relationship between sub-catchment industrialisation and the health of the modern Ahuriri Estuary, heavy metal peaks were assigned approximate depositional timeframes using calculated sediment accumulation rates.

The early 1970s registered across five of the six cores as a time of excessive heavy metal contamination delivered to Ahuriri via the urban tributaries. Extreme zinc and lead pollution from the Pandora Industrial zone lasting several years from 1973-1976 exceed levels found in the literature of Itrax™ XRF-scanned estuarine cores. Zinc levels are high across the cores compared to the available literature. Above identified peak zones, heavy metal trends across five of the six cores gradually reduce towards the core surface. Despite observed heavy metal reductions, recent toxicity assessments using surficial sediment suggest that Ahuriri Estuary is in a state of poor ecological health, meaning its functionality as an important spawning ground and nursery for aquatic species is undermined.

Once land-based contaminant mobilisation is reduced via improvements to land and freshwater management, rehabilitation options for contaminated sediment within the Ahuriri Estuary can be investigated for feasibility.

ACKNOWLEDGEMENTS

First and foremost; thank you to my two supervisors, Prof. Diane Pearson, and Dr Alastair Clement. Your strong but humble guidance kept me on track.

Secondly; to Napier City Council, and Cameron and Jon for accommodating this opportunity, allowing time during a busy schedule to work towards this goal.

Thirdly; to everyone involved in the collection of sediment cores; Alix, Andrew, Caitlin, Chloe, Cameron, Alastair and Mum. It's not the easiest process!

Thanks to Bob Dagg, Chris Moy and Amelia Morris at Otago University for your patience with some challenging sediment core samples!

Thanks to Hawke's Bay Regional Council's Dr Anna Madarasz-Smith, who shares a common passion for Te Whanganui-a-Orotū and in how the community can work together to prevent its further degradation. Without the Hawke's Bay Regional Council Coastal Grant, sediment core sampling would not have been viable.

To the surf crew; our surf & coffee outings toward the end of the thesis helped keep me sane!

Finally, to my family, and to Ryan, thank you for everything you are. Thank you for being the strength when the pressure got to me, especially when I overestimated the available time!

TABLE OF CONTENTS

LIST OF FIGURES

LIST OF TABLES

1 INTRODUCTION

Estuarine health in populated catchments is affected by sub-catchment urbanisation and an accumulation of land-derived heavy metals (Buggy & Tobin, 2008; Clark et al., 2020; Jartun et al., 2008; Ministry for the Environment, 2020; Swales et al., 2005). Recognised as important spawning grounds and sheltered nurseries for aquatic species and wading birds, estuaries play a critical role in the aquatic food webs (Vasconcelos et al., 2011), carbon sequestration (Chmura et al., 2003), oceanic food security, the economy (Ministry for the Environment, 2020), and marine recreation (Borja et al., 2011). Monitoring of future sea level change shows that estuaries may keep in pace with vertical and landward transgression in sea level rise scenarios, maintaining a natural buffer protecting coastal settlements against storm swells (Pethick, 2001; Plater & Kirby, 2011). It is paramount that estuarine health is assessed and understood in order to prevent further degradation to economically and environmentally beneficial coastal systems (O'Brien et al., 2016), prior to planning adaptation to relative sea level change in populated catchments.

New Zealand estuaries are critical habitats for juvenile endemic fishes (McDowall, 1976), despite many being under threat from sedimentation and the effects of catchment urbanisation (Borja et al., 2011; Charry et al., 2018; Heinrich et al., 2016). Hawke's Bay's Te Whanganui-a-Orotū (Ahuriri Estuary) is a tidal lagoon on the east coast of New Zealand's North Island (Hume et al., 2016). Situated in central Napier City within a mixed rural-urban catchment, the estuary has a rich history of morphodynamic change. Ahuriri Estuary is a nationally significant wildlife reserve acting as an important nursery for several native aquatic species (Hawke's Bay Regional Council, 2004). Despite this, the estuary is in a poor state of health from urban freshwater tributaries delivering excessive sediment and heavy metals.

Previous research from Ataria et al. (2007), Charry et al. (2018), Heinrich et al. (2016), Kelly (2018), and Smith (2014) on the Ahuriri Estuary has focused on surface sediment quality and its relation to benthic health. Each of these research projects linked the relatively high heavy metal concentrations compared to other New Zealand estuaries to biological disruption in brackish species: particularly from sediment collected adjacent the Thames-Tyne discharge. Aside from the research of Chagué-Goff et al. (2000), the quality of sediment deposited since the 1931 earthquake has had little exploration, and no research to date has investigated the heavy metal concentrations within sediment deposited in every urban tributary discharge zone since 1931.

The aim of this thesis was to build a holistic picture to understand the current estuarine health of Ahuriri Estuary using a combination of available water quality data, multi-temporal sub-catchment change analysis, and sediment core physicochemical analysis. The study focused on addressing identified knowledge gaps within the literature about Ahuriri Estuary that consider the relationship between estuarine health and land system change at the sub-catchment scale. From identifying and addressing these gaps in the literature, this thesis has built upon existing knowledge on the sediment quality of Ahuriri Estuary within discharge zones of the urban tributaries. This provides a valuable contribution towards holistically understanding the effect of the development of Napier City on the health of the estuary.

There are four objectives that act as the foundation of different chapters and sub-sections to address the overarching aim of the study:

1. *Review recent environment quality research undertaken in the Ahuriri Estuary, including geomorphology, hydrodynamics, sedimentary history, sediment quality, water quality, and ecology.*
2. *Undertake land system change analysis using aerial imagery to investigate gradual effects of industrial development on Ahuriri Estuary.*
3. *Utilise previous hydrodynamic modelling of the central estuary to guide sampling locations for extraction of sediment cores representing discharge depositional zones of different tributaries. Undertake physicochemical analysis on retrieved sediment core samples to investigate connections between industrial development and temporal sediment quality.*
4. *Prepare recommendations on the future management of Ahuriri Estuary to reduce known actions which catalyse contaminant accumulation and prevent further degradation of the estuary.*

This thesis follows a scientific structure. Chapter 1 presents the introduction, Chapter 2 provides background information for the study area, and Chapter 3 presents a literature review summarising previous research on the Ahuriri Estuary. The methodologies for the thesis are presented in Chapter 4. Chapters 5 and 6 present the results of the sub-catchment change assessment and the sediment physicochemical analysis, respectively. Chapter 7 discusses the implications of the results identified in the previous chapters. Chapter 8 then concludes the thesis by summarizing the findings and presenting recommendations for future research.

2 SITE DESCRIPTION

Ahuriri Estuary is a tide-dominated estuary situated in Napier City, Hawke's Bay on the East Coast of New Zealand's North Island (Figure 2.1). The modern Ahuriri Estuary catchment is approximately 144 km^2 (Ataria et al., 2007) and includes rural, urban, residential, and industrial land uses. Within the catchment, three local government bodies influence land management. These are the Napier City Council (NCC), Hastings District Council (HDC) and Hawke's Bay Regional Council (HBRC) (Figure 2.2). Ngāti Kahungunu are tangata whenua for Napier and hold mana whenua through a series of Post Settlement Government Entities (PSGEs) (Brooker's Ltd., 1995; Parsons, 1992). Despite being recognised as a nationally significant wildlife reserve through its importance as a nursery for several native aquatic species (Hawke's Bay Regional Council, 2004), Ahuriri Estuary is in poor health, with shellfish being deemed unsafe for consumption (Smith et al., 2018). The estuarine recreational zone also experiences semi-frequent closures due to elevated microbiological counts (Ludlow, 2020).

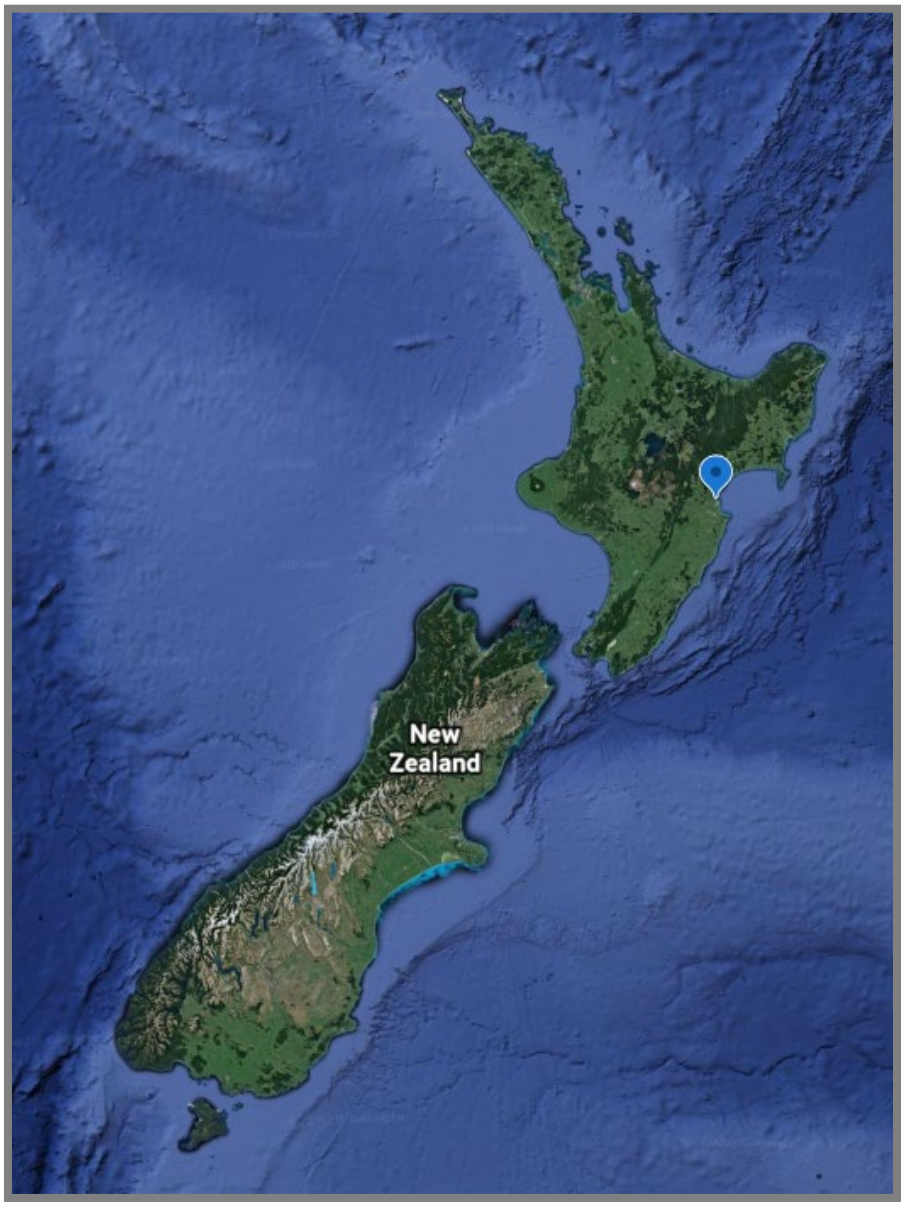

Figure 2.1: Ahuriri Estuary, Napier, East Coast of New Zealand's North Island (Google, n.d.-a).

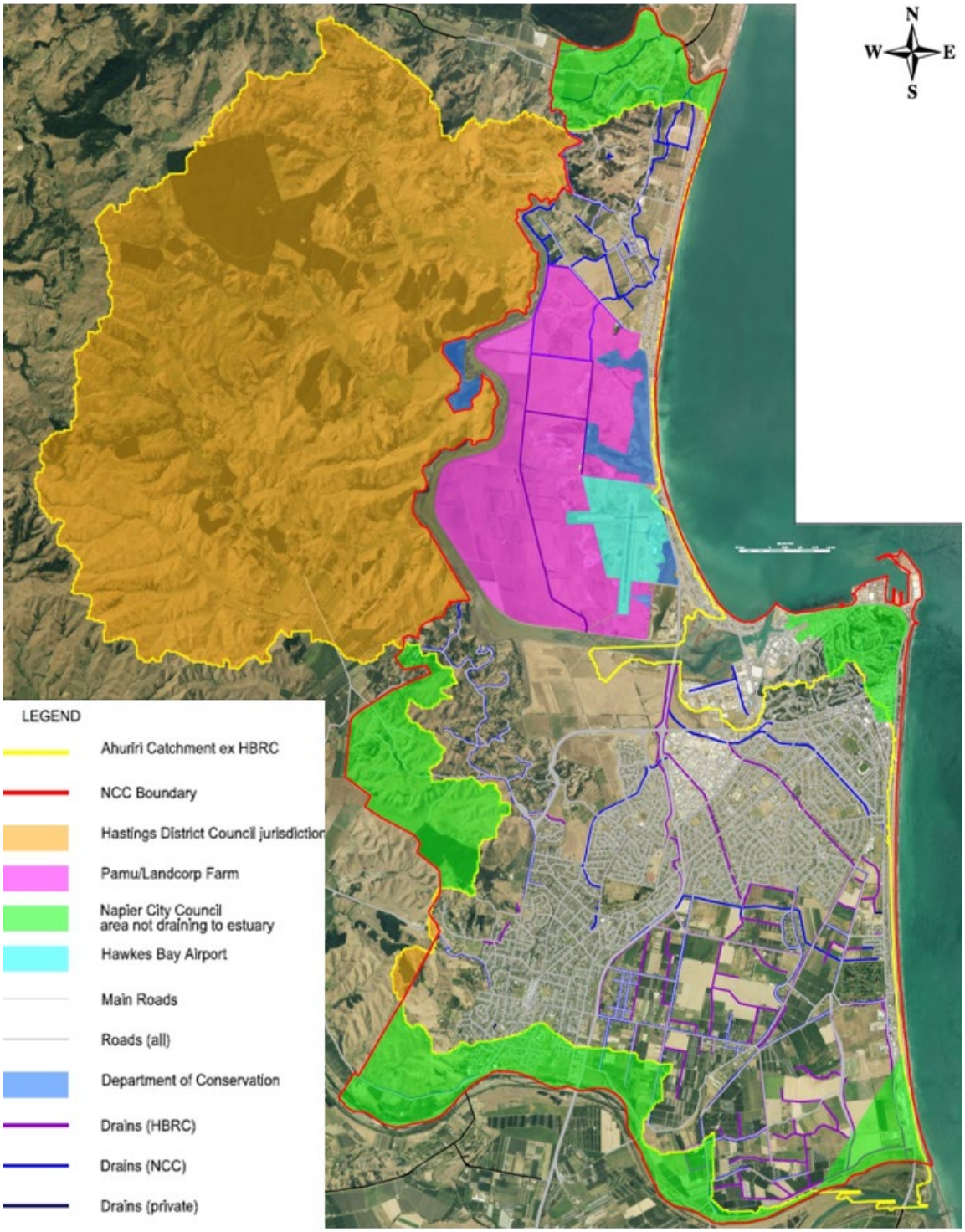

Figure 2.2: The mixed governance of the Te Whanganui-a-Orotū land and surface water catchment (Burton, 2018).

2.1 Morphological zones of Ahuriri Estuary

The modern Ahuriri Estuary can be split into five distinct zones (Figure 2.3). From east to west:

- the inner harbour;
- the central estuary;

- the main channel
- the upper estuary; and
- the fringing wetlands.

The estuary is hydraulically driven by a dominant semi-diurnal tidal exchange of approximately 495 million litres, leading to approximately 275 ha of water coverage at high tide (Ataria et al., 2007; Eyre, 2009; Hume et al., 2016). The tectonically-forced diversion of the Esk River, and the engineered diversion of the Tutaekuri River (Figure 2.4) has resulted in Ahuriri Estuary's high saltwater to freshwater ratio of 10:1 (Ataria et al., 2007). Modern freshwater inflow is restricted to a series of pumped urban channels containing shallow groundwater and run off from Napier City, and indirect surface water run-off from Poraiti Hills at the estuary's western border (under 'Hastings District Council jurisdiction in Figure 2.2).

Figure 2.3: Aerial view with labelled zones of Ahuriri Estuary. Base image from Google (n.d.-a) Inset retrieved from (Google, n.d.-a).

Table 2.1 identifies key morphological, ecological, and anthropogenic features of these five zones.

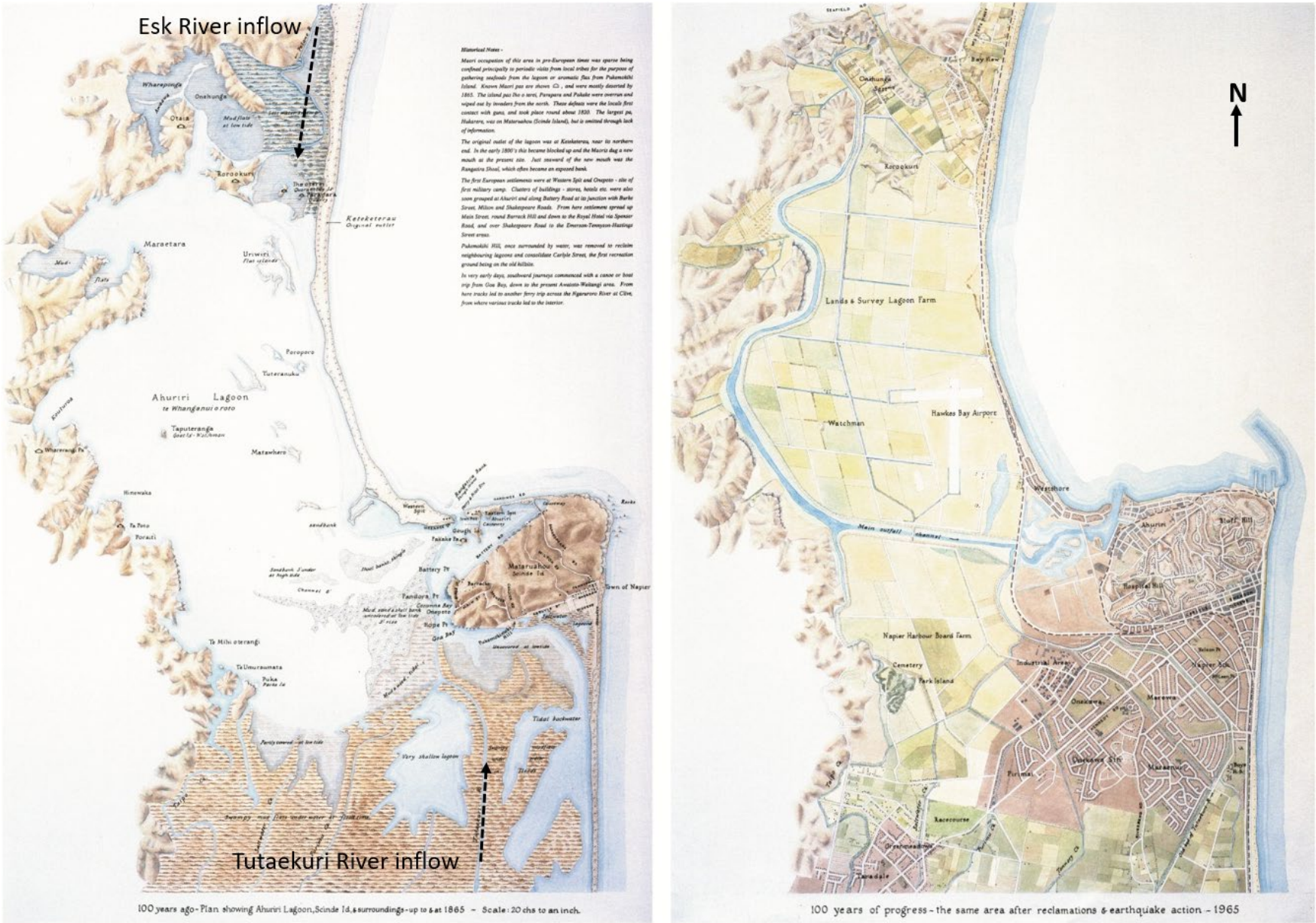

Figure 2.4: '100 years of progress' sketch of Napier: 1865 prior to the 1931 earthquake and uplift (left) showing Esk River and Tutaekuri River inflows, and 1965 post uplift (right). Adapted from Museum Theatre Gallery Hawke's Bay (n.d.).

Table 2.1: The five zones of Ahuriri Estuary (Figure 2.3), including distinctive anthropogenic, ecological and morphological features.

	Photo	Morphological features	Ecological features	Anthropogenic features
Inner harbour		○ Entirely subtidal; & ○ Mostly saline.	○ Semi-frequent bioluminescent algal blooms (Laing, 2021).	○ Live-aboard boats; ○ Berthed boats; ○ Rock wall revetment; ○ Wharfs; ○ 'Iron Pot' resource consent discharge (Hawke's Bay Regional Council, 2007).
Central estuary		○ Ebb-dominated subtidal channels; & ○ Flood dominated intertidal mudflats (Eyre, 2009).	○ Wading birds; ○ Black-billed gull nesting zone (Department of Conservation, n.d.); ○ Area of highest *Austrovenus stutchburyi* density; ○ DOC native plantation; ○ Beaded glasswort (*Sarcocornia quinqueflora*) intertidal zone dominance; ○ Invasive cone snails (Ludlow, 2020).	○ Westshore bridge; ○ Pandora Pond recreational zone; ○ Embankment bridge; ○ State Highway 2 bridge; ○ Three urban drainage channel discharge outlets: the Thames-Tyne, Purimu, and Old Tutaekuri Riverbed (the combined Plantation, County and Georges); ○ Recreational boardwalk.

	Photo	Morphological features	Ecological features	Anthropogenic features
Main channel		○ Low energy environment.	○ Beaded glasswort (*Sarcocornia quinqueflora*) intertidal zone dominance; ○ Invasive cone snails.	○ Remnants of historic bridge; ○ Stopbanks; ○ Napier Airport stormwater pump station; ○ Pāmu Farm stormwater pump station; ○ Lagoon Farm stormwater pump station.
Upper estuary		○ Low energy environment; & ○ Mostly freshwater.	○ Invasive tubeworm.	○ Rural overland flow paths (Poraiti Hills); ○ Taipo urban drainage channel.
Fringing constructed wetlands		○ Settling/depositional/low energy environment.	○ Rare birds (Bittern, bar tailed Godwit) (Department of Conservation, n.d.).	○ Area recently re-developed; ○ Boardwalks; & ○ Recreational pathways.

2.2 Inflows into Ahuriri Estuary

The central estuary accommodates the three major drainage channel discharges from Napier City, each of which are authorised by conditional resource consents under the Resource Management Act 1991 (RMA) (Parliamentary Counsel Office, 1991). Two waterways either side of the State Highway 2 Bridge (Figure 2.5) discharge via tidal gates, which work to reduce the tide travelling upstream particularly in a time of high rainfall and waterway flow coinciding with a flood tide. The discharge of drainage and storm waters via these waterways (The Purimu and the Old Tutaekuri Riverbed, the latter which combines the flows of the Georges Drive, Plantation, and County urban streams - Figure 2.6) to the Ahuriri Estuary is legislated under a jointly held resource consent between NCC and HBRC. These waterways convey drainage and storm water from semi-rural Meeanee, through residential land, then through heavy industrial land prior to discharge (Figure 2.6).

A further resource consent exists for the discharge of stormwater via the Thames & Tyne Waterways servicing the heavy wet Pandora Industrial area on the south border of the central estuary (Figure 2.6). These tidal waterways combine prior to discharging via ebbing tides into the estuary adjacent to Humber St, Pandora, and are tidally driven, meaning they discharge on an ebbing tide. Resource consent DP110266W is solely under NCC's jurisdiction.

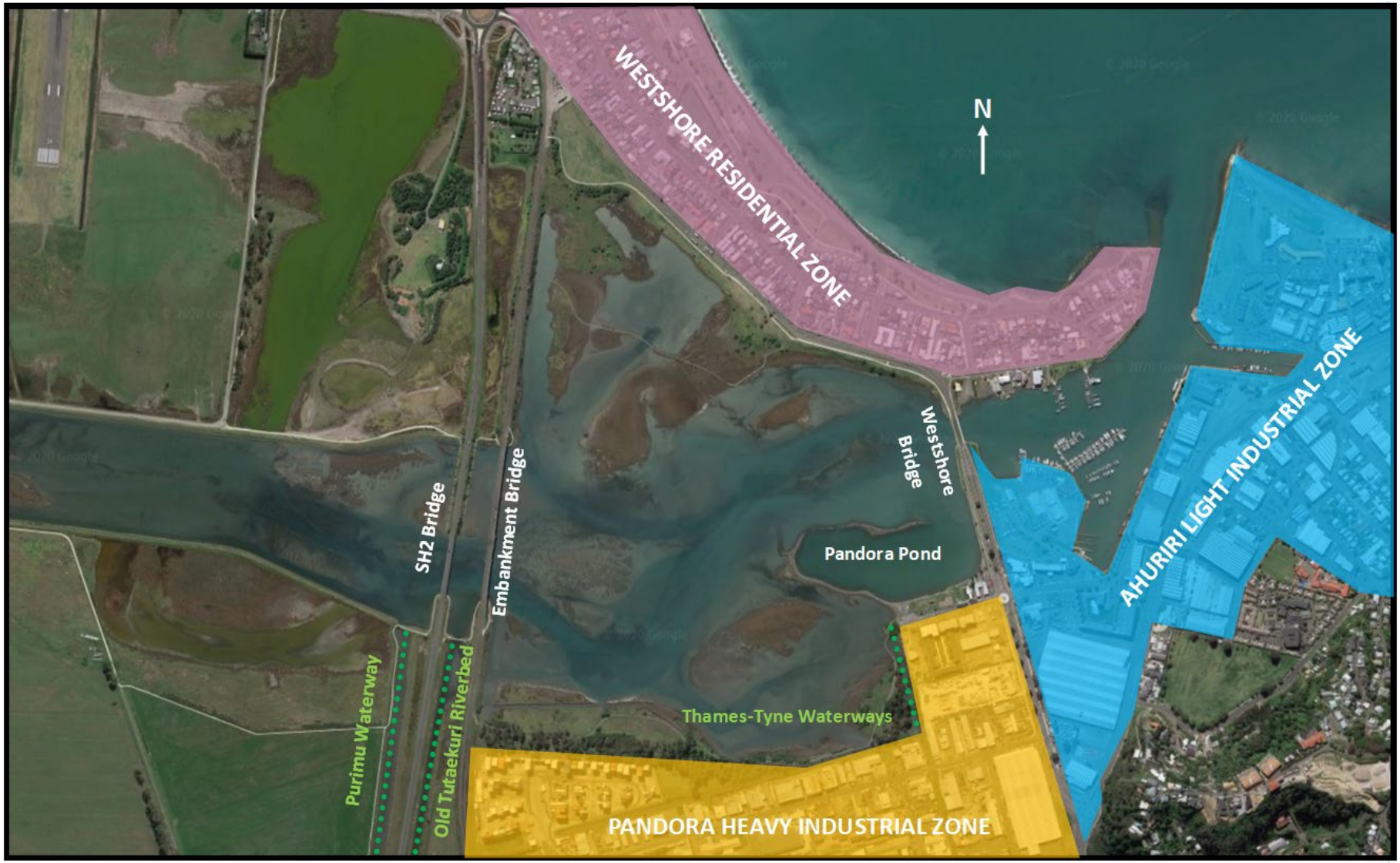

Figure 2.5: Aerial view of the central estuary, highlighting key zones of residential and industrial activity, the three primary urban waterway discharges, the Pandora Pond recreational area, and the three bridges constraining this zone (Google, n.d.-a).

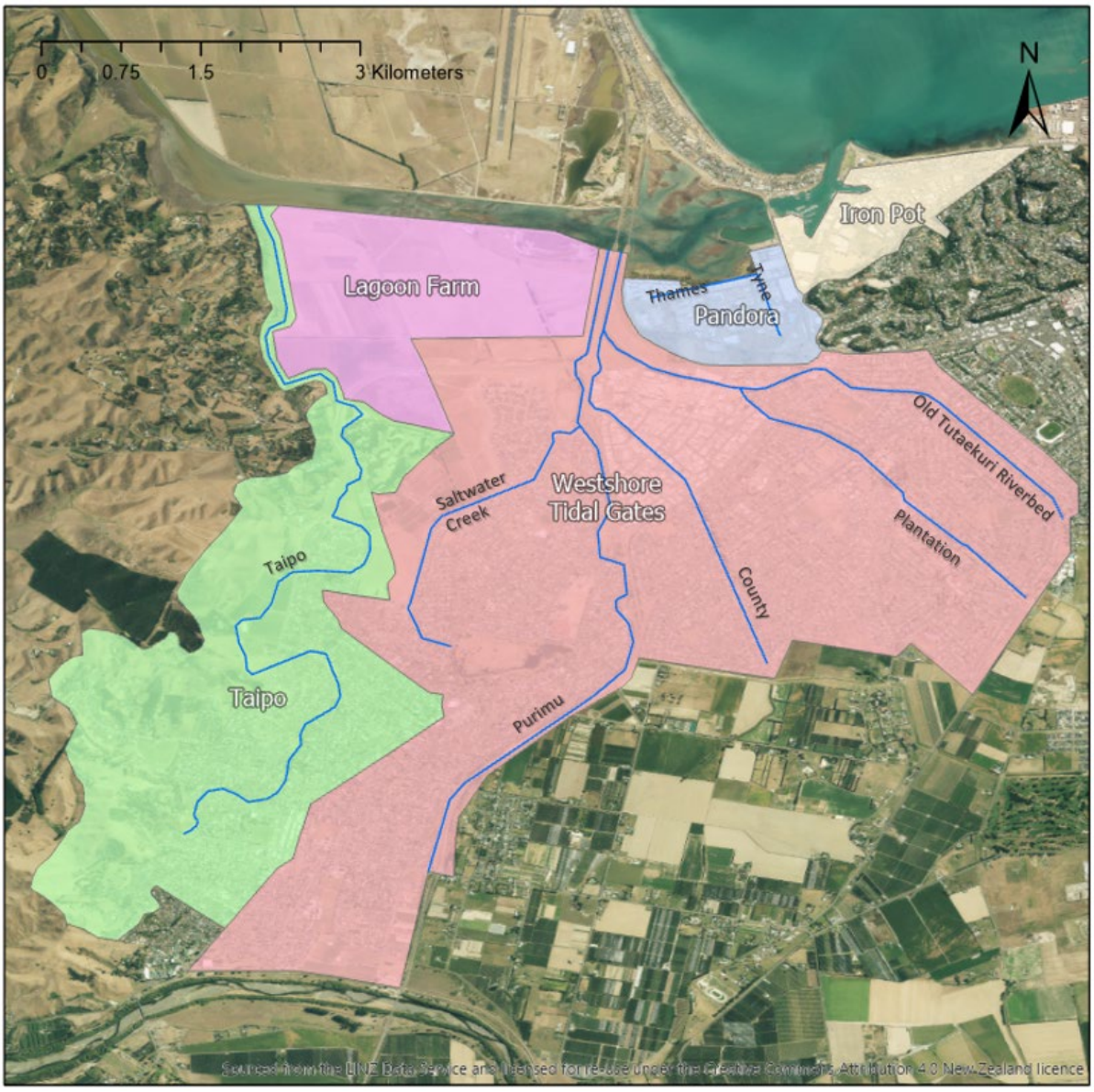

Figure 2.6: Major southern fringing catchments within the greater Ahuriri Estuary catchment. Background image from ESRI Inc. (2019).

2.3 Geology

The tectonic setting of New Zealand has been characterized by the subduction of the major Pacific Plate beneath the Australian Plate (Komar, 2007). Dissecting the South Island of New Zealand along the alpine fault, then curving eastward off the coast of the North Island, the subduction zone exhibits as the shallow marine Hikurangi Trench approximately 160km off the coast of Napier (Hull, 1986; Komar, 2007) (Figure 2.7). Complex surface folding and faulting (McLintock, 1966) is common across Hawke's Bay, stretching between the forearc basin to the west, and accretionary wedge to the east (Cashman & Kelsey, 1990). The frequency of earthquakes in the region over the previous thousand years have made the region one of the most tectonically active in New Zealand (Hull, 1986; Komar, 2007). Fringing the western Pacific Ocean, the region is additionally at risk from distant-source tsunamis.

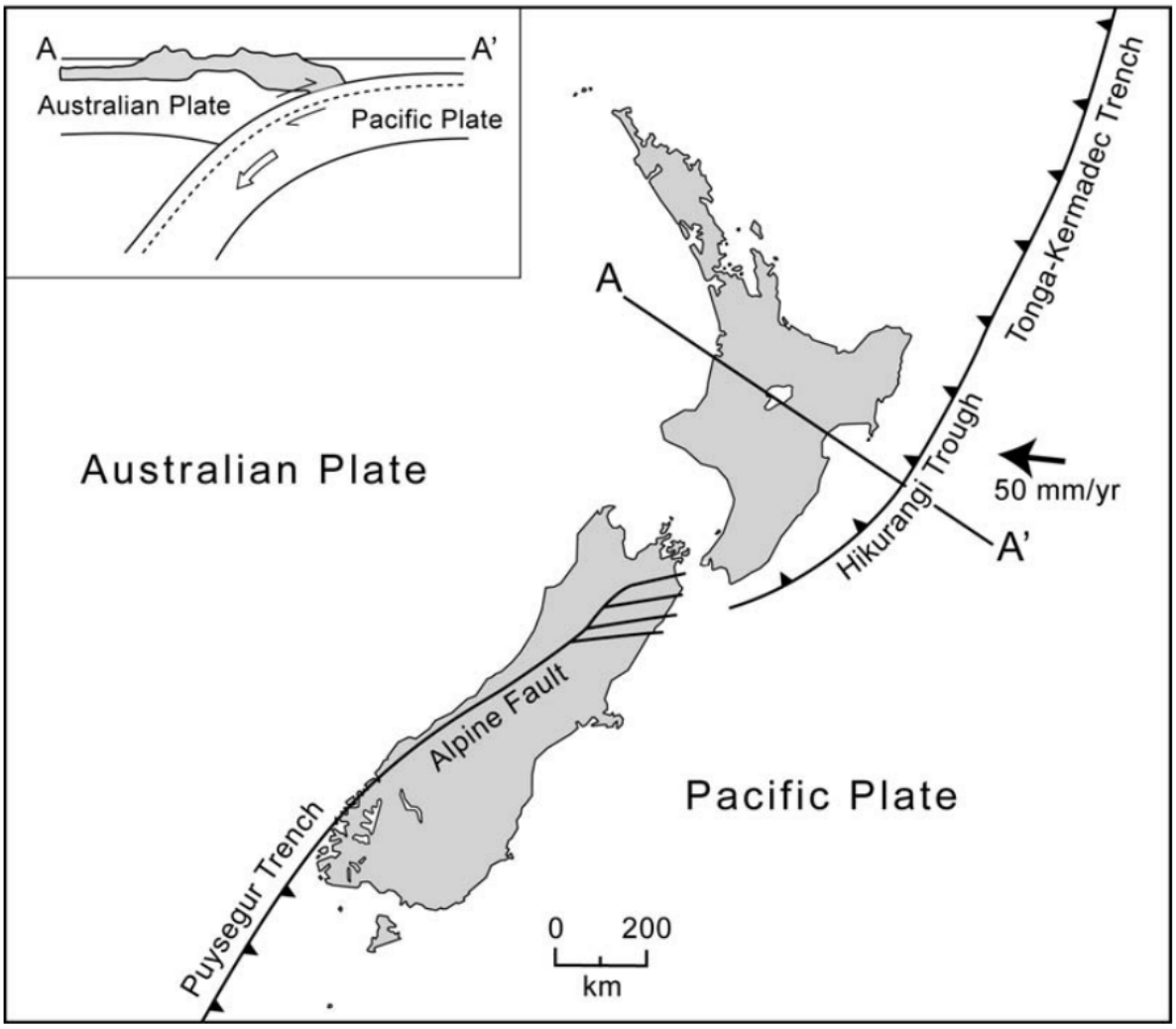

Figure 2.7: Surface geological features of the Pacific-Australian Subduction Zone, showing Hikurangi Trough to the West of Hawke's Bay (Komar, 2007).

In 1931, a surface wave magnitude 7.8 earthquake originating approximately 30km north of Napier resulted in widespread damage to the established Napier Township. The Ahuriri Lagoon was forcibly uplifted approximately 2 metres (Figure 2.8) by a north-south tectonic tilt ranging between -1m at Te Awanga to an estimated 3 metres at Tangoio north of Napier City (Hull, 1990; Komar, 2007).

This uplift has characterised the surface soils of the modern Napier City. Much of the central city consists of marine soil, with some areas comprised of various infill from post-earthquake land reclamation (see Figure 2.9). Mataruahou (Napier Hill) in the central city is comprised of Pliocene fossiliferous marine rock, and Tertiary sandstones are common across the remainder of the city (McLintock, 1966). A series of gravel barrier beach systems from Cape Kidnappers, to the south of Napier, to Mahia Peninsula north of the city display greywacke clasts typically transported from axial Triassic-Jurassic Kaweka and Ruahine Ranges (McLintock, 1966) via fluvial systems (Komar, 2007).

Figure 2.8: Stranded horse mussels of Te Whanganui-a-Orotū after the 1931 Hawke's Bay earthquake (Parsons, 1992).

Figure 2.9: Land reclamation works adjacent to Ahuriri Estuary, circa 1936 (Parsons, 1992).

2.4 Climate

The median annual temperature in coastal Hawke's Bay averaged 13.5°C for the years 1981-2010 (Chappel, 2013). Measured as July to June, each hydrological year from 2013/14 to 2017/18 in the Hawke's Bay region recorded mean minimum and mean maximum temperature anomalies, ranging between +0.1°C and 1.0°C (Smith et al., 2018). Figure 2.10 and Figure 2.11 show the median average daily maximum temperature distribution in the Hawke's Bay region for the summer and winter months between the years 1981-2010.

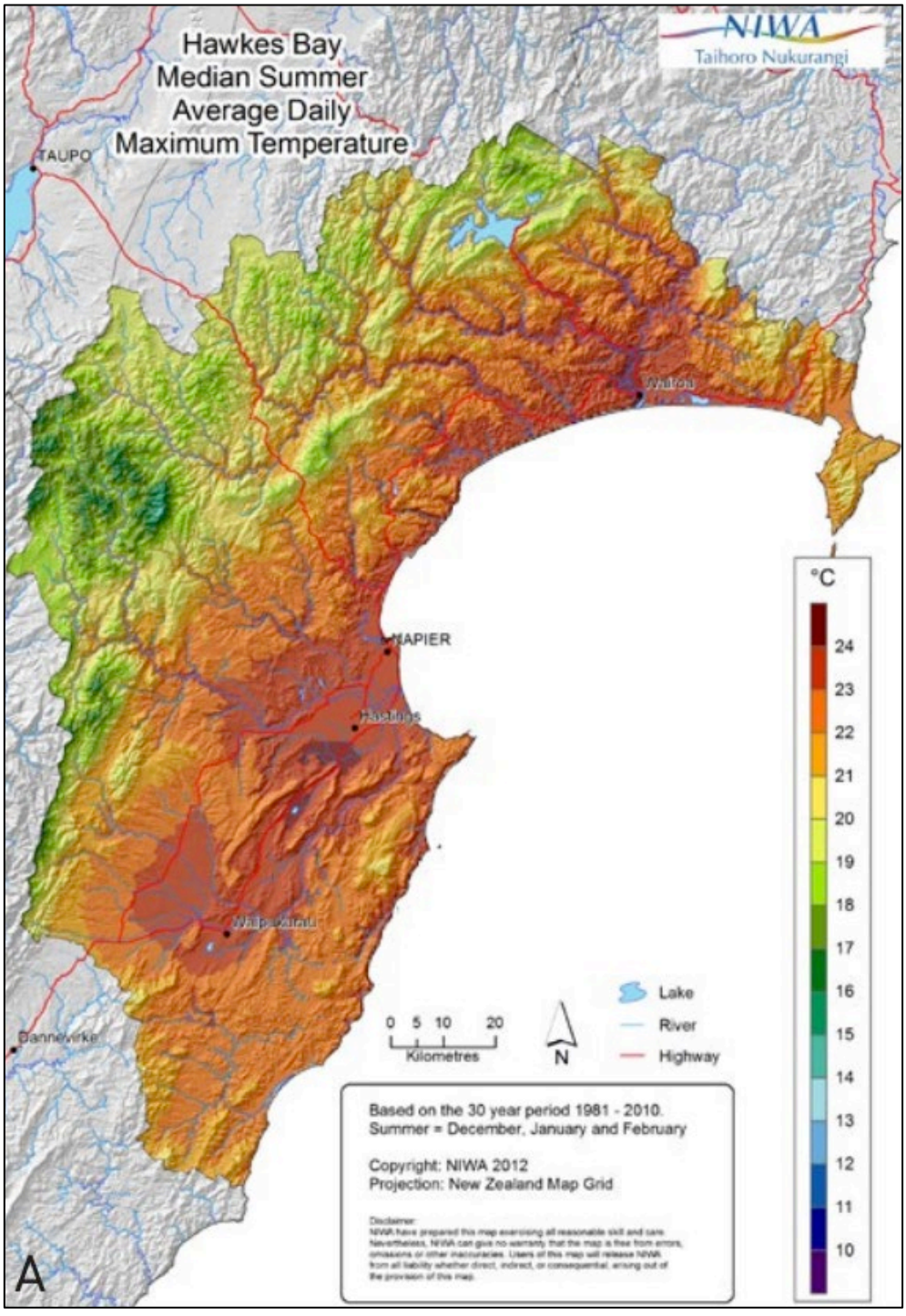

Figure 2.10: Median summer daily maximum temperature - Hawke's Bay region (Chappel, 2013)

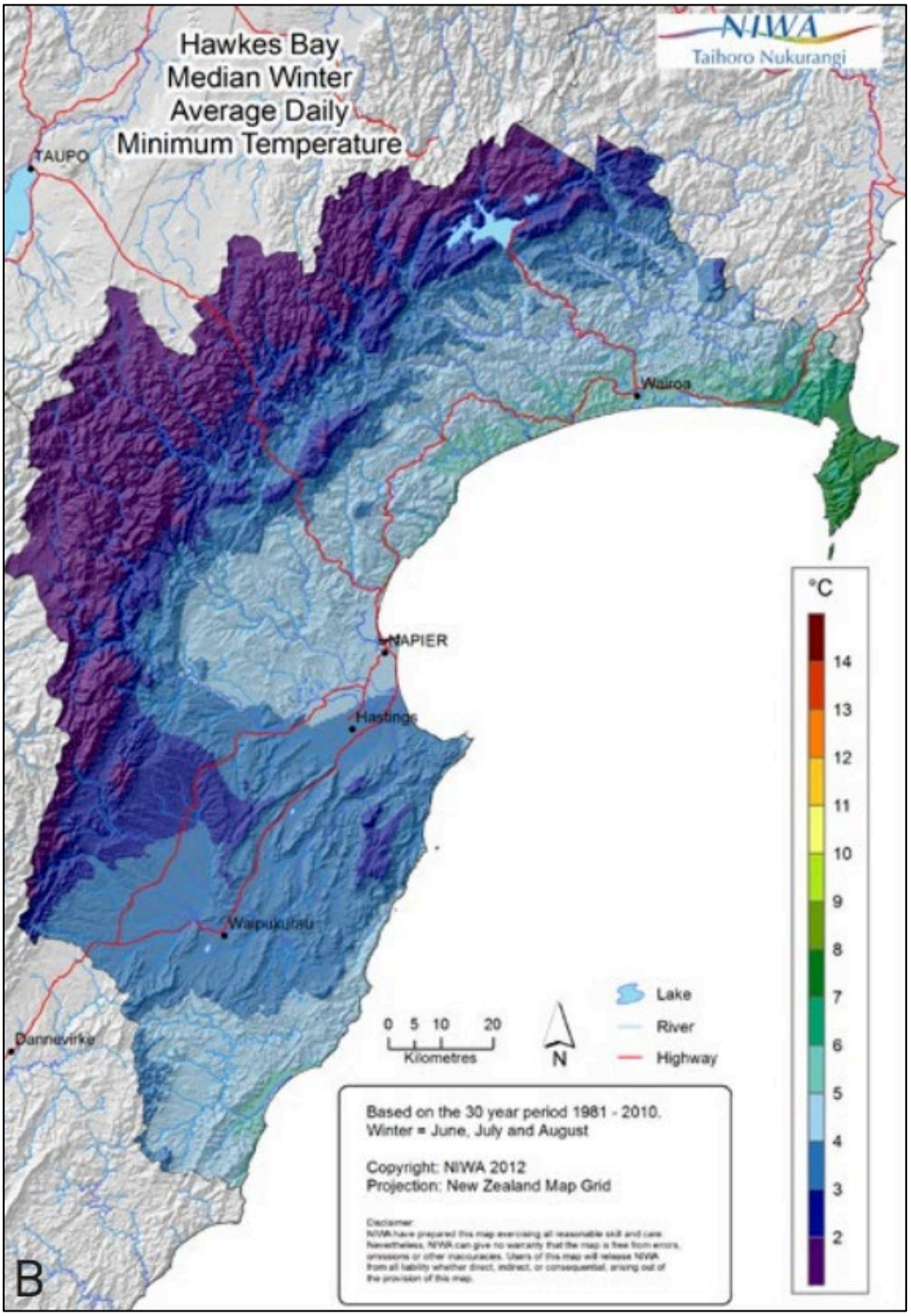

Figure 2.11: Median winter daily maximum temperature - Hawke's Bay region (Chappel, 2013).

A report by NIWA (2013) explains that Napier City is sheltered from prevailing westerly winds in the Hawke's Bay region by the western Kaweka range, resulting in higher frequencies of light winds compared to other coastal areas of New Zealand (Chappel, 2013). Chappel (2013) highlights the high spatiotemporal irregularity of rainfall in Hawke's Bay, with Napier City receiving typically less than 800mm per annum, 60% of which is driven by south to southeast winds. Figure 2.12 shows the annual total median rainfall for the Hawke's Bay region based on data from 1981-2010. By contrast to this 30-year period, 650mm of total cumulative rainfall recorded by a NIWA weather station in Nelson Park,

Napier in the year 2019 is shown in Figure 2.13 (National Institute of Water and Atmospheric Research, n.d.-b).

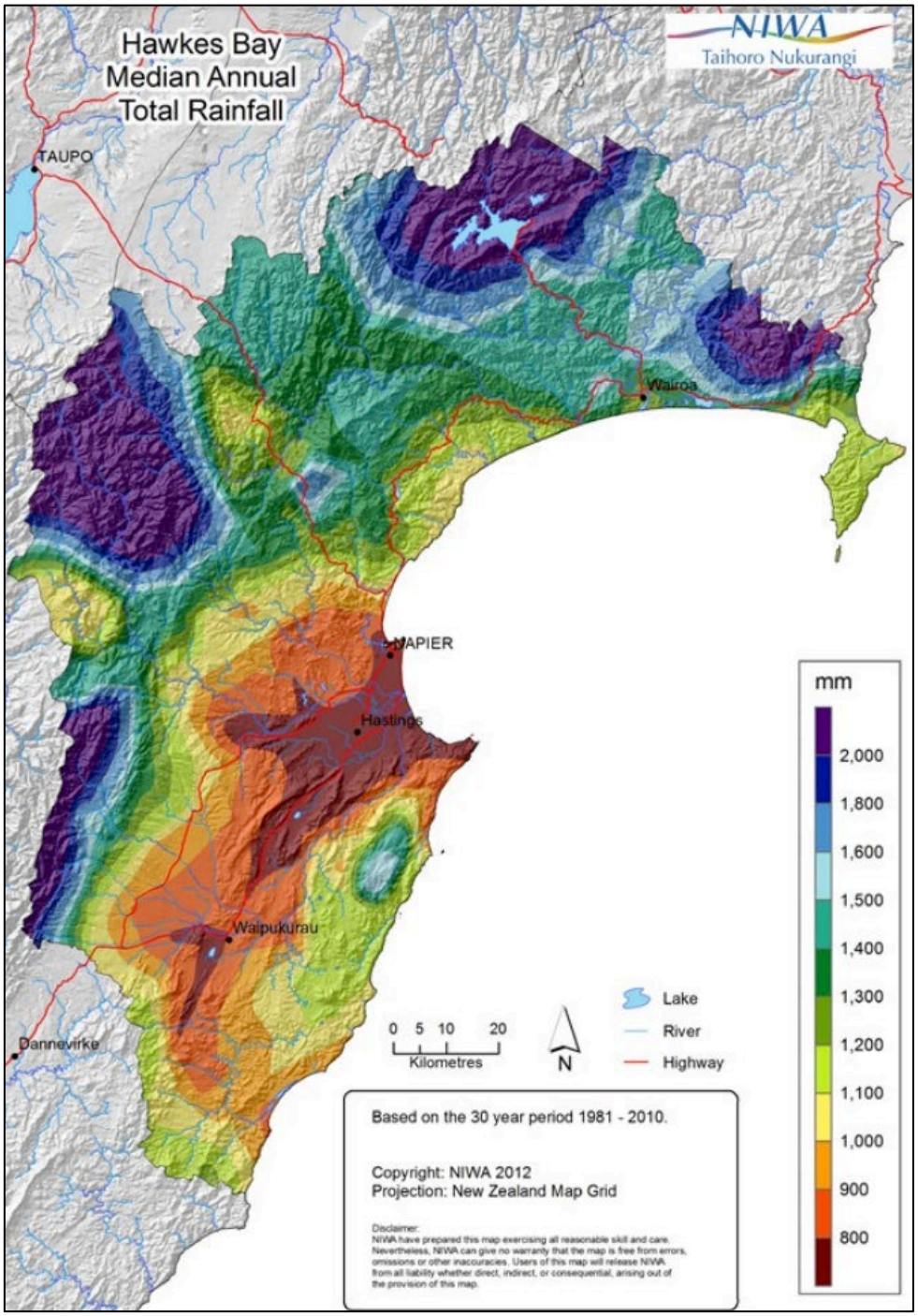

Figure 2.12: 1981-2010 Hawke's Bay median annual total rainfall (Chappel, 2013).

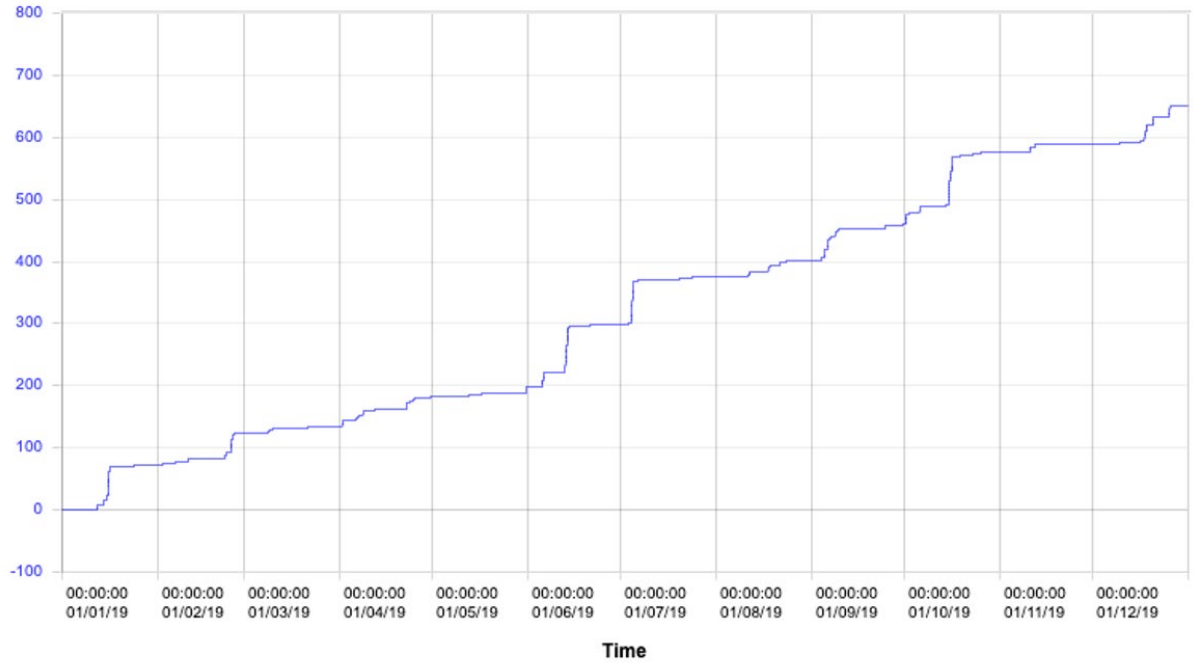

Figure 2.13: 2019 cumulative rainfall data from Nelson Park, Napier City (National Institute of Water and Atmospheric Research, n.d.-b).

2.5 Settlement

2.5.1 Pre-1931 earthquake

Māori are estimated to have arrived in Hawke's Bay between 800 and 650 years ago (Komar, 2007; Ogden et al., 2006) with Ngati Whatumamoa and Ngati Awa believed to be two of the first formed local iwi prior to the conquering of Heretaunga by Ngati Kahungunu in about 1550 (Brooker's Ltd., 1995). The arrival of people saw small-scale vegetation clearance for establishment of settlements, having identified the reliable abundance of kaimoana within Ahuriri Lagoon as a lifeline prompting settlement around its shores (Ogden et al., 2006; Swales et al., 2005).

European settlers arrived in Napier in the mid-1800's (Parsons, 1992). A report by Parsons (1992) presents a compilation of personal accounts from Māori of Ahuriri and European settlers from 1850 through to the 1931 earthquake. A defining moment in the history of Napier is the miscommunication around the sale of Ahuriri Lagoon, and the contravention of te Tiriti o Waitangi by the 1851 Ahuriri Deed of Purchase, through the transferal of legal right to the tidal waters of Ahuriri Lagoon to the crown for trading opportunities (Parsons, 1992).

European land ownership and the Crown governance over Te Whanganui-a-Orotū expanded, by way of both agreed negotiations, and miscommunications (Brooker's Ltd., 1995). Significant forest and vegetation clearance ensued (Ogden et al., 2006; Swales et al., 2005). Port development saw Pukemokimoki Hill, the growth location of the fern *Doodia fragrans*, and translated from Te Reo in an early deed of settlement as the 'only portion of Mataruahou reserved for ourselves' destroyed and used for infill (Brooker's Ltd., 1995). Dredging for accessibility to the port began a slow ecological shift in Te Whanganui-a-Orotū from dominance of freshwater fish such as tuna and inanga to saltwater

species such as kahawai and taniwe as a result of dredging of Ahuriri Heads (Brooker's Ltd., 1995; Parsons, 1992).

In 1921, development continued in the Ahuriri Lagoon with the construction of the Embankment Bridge (Figure 2.5) funded by the County, Government and Napier Harbour Board (Parsons, 1992). This effectively cordoned off the tidal flow to upper margins of the estuary (Parsons, 1992). Oral accounts reflected the gradual decline of the sheer abundance of kai moana in the lagoon linking it to the reduction in tidal flow, as well as effluent discharges from the western margin of the lagoon, and the sewerage discharge to the sea from Mataruahou (Parsons, 1992). Diminishing reliance on the lagoon as a food source happened gradually, with the events aforementioned contributing to this slow decline in abundance and quality, as well as the uplift from the 1931 earthquake, prompting the eventual public warning against kaimoana consumption (Brooker's Ltd., 1995).

2.5.2 Post-1931 earthquake

Prior to the uplift from the 1931 earthquake, the Esk River had two mouths: one via the Petane stream into Ahuriri Estuary (Figure 2.3) and the other into the ocean (Brooker's Ltd., 1995). Uplift reduced the Petane Stream's discharge to a trickle (Parsons, 1992). The Tutaekuri River continued its discharge into the southern Ahuriri Estuary until 5 years after the earthquake, when physical works saw the full diversion of the river to the Pacific Ocean via Awatoto completed on 4 June, 1936 (Parsons, 1992).

Land reclamation and stopbank development on the estuary edge provided sheltered grasslands for grazing animals, serviced by over 600km of drainage channels (Parsons, 1992) (Figure 2.9). Some of this reclamation work provided ground for the Onekawa and Pandora Industrial area developments (initiated in 1948 and 1962, respectively (Parsons, 1992). Drainage channels servicing these industrial zones were linked to the central estuary to prevent flooding in previously submerged land (Parsons, 1992). Further residential development on pre-1931 land and reclaimed land continues through to today, as well as engineering stabilization works on the fringes of the estuary (Komar, 2007).

Today, a boardwalk surrounding the central estuary provides recreational accessibility. The Pandora Pond area is commonly used for water-based recreation, recently becoming less popular for contact recreation (submersing) in summer due to unpredictable bacterial fluctuations (Figure 2.14) which occasionally exceed the upper threshold of 550 cfu/100mL of *Escherichia coli* (Ministry for the Environment & Ministry of Health, 2003).

Figure 2.14: Public warning notice for water safety for Pandora Pond recreational zone, Napier City, 2018.

2.6 Summary

Prior to the uplift from the 1931 Napier Earthquake, Ahuriri Lagoon covered a vast area and its abundance of kaimoana supported Māori and eventually European settlements around its shoreline. In February of 1931, a magnitude 7.8 earthquake uplifted Napier City, and much of the former Ahuriri Lagoon was drained and reclaimed to what is now Ahuriri Estuary. The diversion of the Tutaekuri and Esk rivers in the 1930's has reduced the estuary's modern freshwater to urban tributaries and surface run-off. The estuary is now poor in health and experiences closures to recreational use due to semi-frequent excessive microbiological counts (Ludlow, 2020).

3 LITERATURE REVIEW

3.1 Introduction

Estuarine health does not have a universal definition or assessment approach (O'Brien et al., 2016). Therefore, understanding the impact of industrial development on an estuary first requires a review of available assessment techniques. This chapter firstly provides a brief overview of some monitoring-based approaches in assessing estuarine health. A literature review of research undertaken in the Ahuriri Estuary then follows. A synthesis of aspects of estuarine health evaluation and the identification of gaps in the available literature then builds the model which will be adopted to assess the current health of Napier's Ahuriri Estuary.

3.2 Assessing estuarine health

Being the downstream transitional zone between terrigenous freshwater and the marine environment, estuaries are exposed to the condition of their tributary fluvial environments (Gadd et al., 2020; Ministry for the Environment, 2020) and act as depositional contaminant sinks for mobilized land-based contaminants (Chen et al., 2018; Feng et al., 1998; Gadd et al., 2020; Smith, 2014). Though natural stressors such as sea level change and tectonic forcing can impact the geomorphology and ecological quality of estuaries (Chagué-Goff et al., 2000; Hayward et al., 2006; Zeldis et al., 2011), studies have shown that industrial development (with the associated vegetation and grassland conversion for impervious surfacing) has catalysed estuarine sedimentation and sediment heavy metal accumulation (Gadd et al., 2020; Jartun et al., 2008; Shi et al., 2007; Swales et al., 2005). The interconnectedness of the hydrological cycle ensures that water, as a universal solvent, mobilises exposed land-based contaminants via rainfall runoff (Chen et al., 2018; Jartun et al., 2008; Johnson et al., 2017; Shi et al., 2007) and the shallow groundwater network (Wu & Sun, 2016). Freshwater tributaries and their estuarine depositional environments can subsequently be loaded with excessive volumes of dissolved and particulate-bound zinc, copper, and lead, from urban and industrial runoff (Gadd et al., 2020; Hwang et al., 2016; McKenzie et al., 2009; Napier City Council, 2021a; Pitt et al., 1995).

Assessing estuarine function by integrating one or more biophysicochemical aspects with catchment assessments provides the opportunity for a holistic system status assessment. Birch et al. (2016) linked Sydney Estuary's water quality and the concentration of metal contaminants in sediment to topographically delineated sub-catchments. Using sediment chemistry to determine ecological risk to aquatic communities as well as the degree of anthropogenic contamination, the authors found a statistically significant correlation between sediment metal concentrations and higher risk industrial sub-catchments. Though not estuarine, Arunyawat and Shrestha (2016) employed a similar approach for northern Thailand, where multi-temporal aerial catchment assessments, combined with hydrology and biodiversity surveys, have allowed the classification of the state of a terrestrial system affected by land development to inform future decision making.

Swales et al. (2005) undertook an assessment of estuarine ecological health from the populated Whāingaroa Harbour in Raglan. Swales et al. (2005) used ^{210}PB and ^{137}Cs dating of recent estuarine

sediment, as well as pollen grain (palynomorph) identification to model sediment accumulation rates (SAR) to build a holistic awareness of the state of the estuary having been affected by anthropogenic sedimentation. The authors distinguished the effects of gradual deforestation and land conversion to productive grasslands within estuarine sediment and drew conclusions as to the relative changes in SAR through time markers. Swales et al. (2005) concluded that gradual land use change had increased sedimentation rates threefold in one arm of the harbour.

In a similar catchment-based assessment, Al-Naswari et al. (2018) used a suite of monitoring techniques to assess the eco-geomorphic state of Towamba Estuary in Australia as a result of anthropogenic stressors. The extensive study included in-field calibrated multi-temporal digital elevation modelling (DEM) to assess morphological changes through shoreline and barrier migration, and bathymetric change. The authors modelled catchment elevation, coverage, waterbody, and land-use features to provide linkage to potential anthropogenic effects on estuarine health. Spatial water quality samples provided a point-in-time reference of salinity, turbidity, pH and dissolved oxygen, and 35 surface sediment samples were analysed for grain size and loss on ignition (LOI) to compare terrigenous to marine-origin sediment ratios. Using a multi-faceted assessment such as in Al-Naswari et al. (2018) reduces potential assumption error in drawing conclusions as to the effect of catchment changes on the estuary's health.

Combining approaches such as Al-Naswari et al. (2018), Arunyawat and Shrestha (2016), Birch et al. (2016), and Swales et al. (2005) allows a unique assessment of estuarine health by summarising catchment change information and biophysicochemical factors of the estuary itself. Catchment development, water quality, benthic ecology, sediment quality, and identification of sediment depositional time markers can lead to a holistic understanding of the functional state of an estuarine system and subsequently prompt management changes to prevention further ecological decline.

3.3 Research from Ahuriri Estuary

The quality of Ahuriri Estuary is poor (Hawke's Bay Regional Council, 2004), with semi-frequent closures to recreational use and public advised against the collection and consumption of kai moana from health officials (Smith et al., 2018). In this section, relevant research on the quality of the Ahuriri Estuary to meet the criteria of Objective One is summarised:

Objective One: Review recent environment quality research undertaken in the Ahuriri Estuary, including geomorphology, hydrodynamics, sedimentary history, sediment quality, water quality, and ecology.

3.3.1 Ahuriri Estuary: Morphology and hydrodynamics

There is research on the historical morphology of Ahuriri Estuary. Using in-channel measurements and topographic LiDAR with a specified mean sea level of 10.3m, Goodier (2003) from HBRC derived an aerial bathymetric map (Figure 3.1).

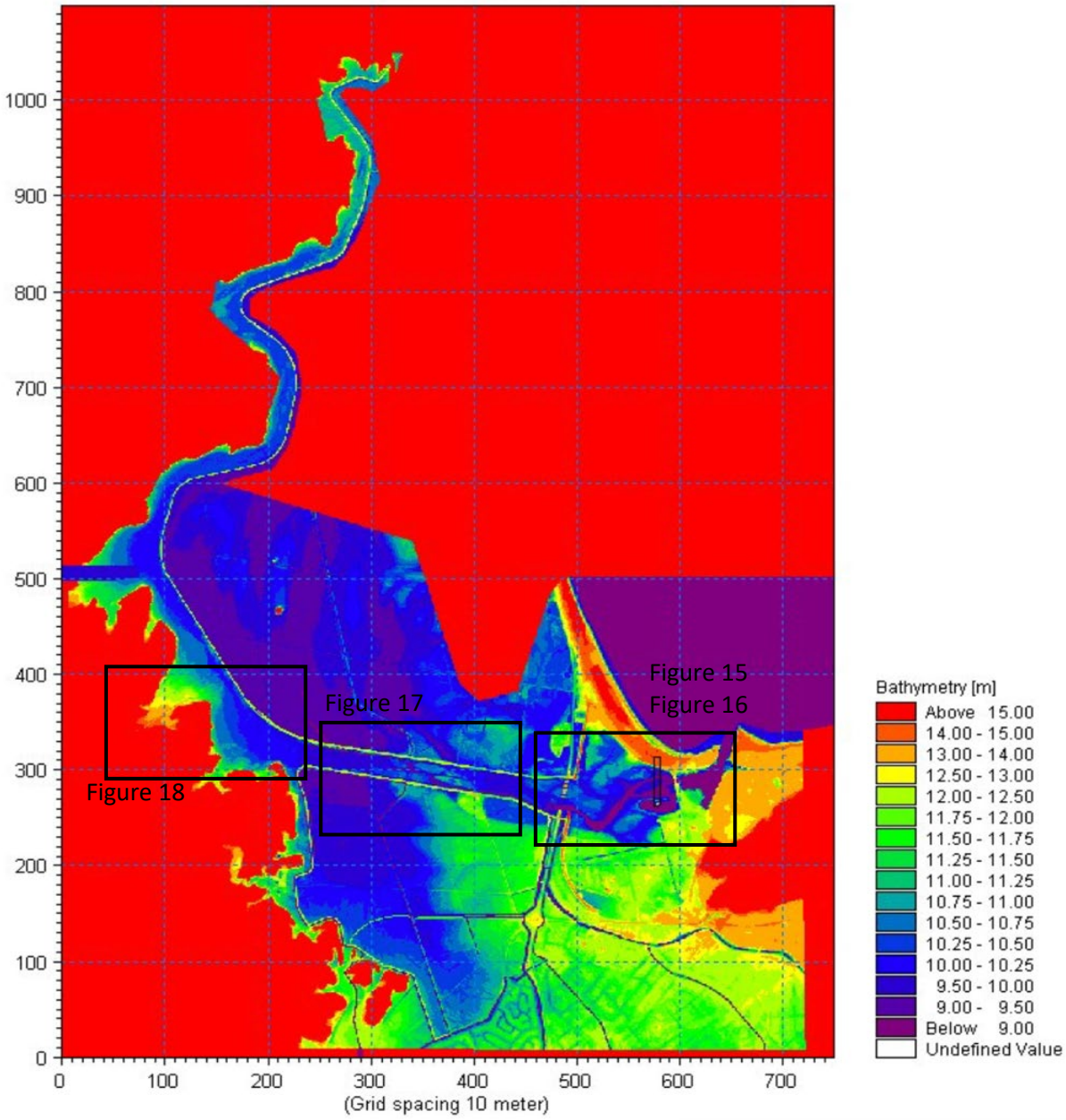

Figure 3.1: LiDAR-derived bathymetric map of Ahuriri Estuary and surrounds, Goodier (2003) as found in Eyre (2009). Black boxes indicate location of following figures: Figure 3.2 - Figure 3.5.

The hydrodynamics of the estuary have similarly had historic investigation. Using the bathymetric map in Figure 3.1, Eyre (2009) developed a two-dimensional tidal MIKE 21 Flow model of Ahuriri Estuary. The author reported that strong tidal flows are largely restricted to the main channel in the central estuary (Figure 3.2 and Figure 3.3) with the model detecting low-velocity feeding currents in the central intertidal mudflats on an incoming tide (Figure 3.2). Eyre (2009) identified the main channel as having relatively strong tidal velocities (Figure 3.4), and the upper estuary as unaffected by tidal regimes (Figure 3.5). In the inner harbour the model detects a circulatory current, where high velocities underneath the Pandora Rd bridge on an ebb and flood tide cause shear, reflection, refraction and prevent sediment settling (Eyre, 2009). From this hydrodynamic modelling, Eyre (2009) summarised Ahuriri Estuary as a well-mixed ebb-tidal dominant system with limited stratification due to a low freshwater input and with a net seaward sediment transport.

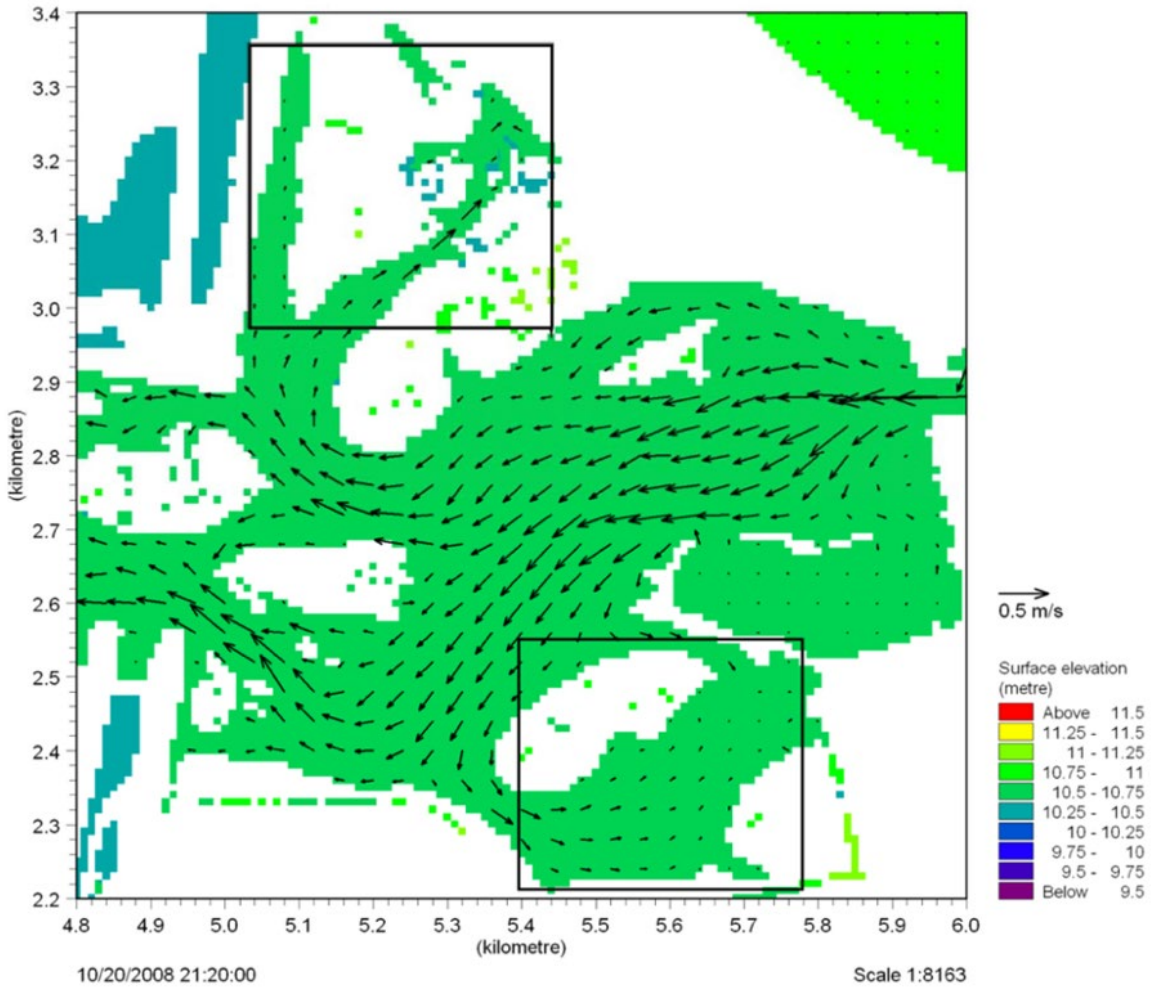

Figure 3.2: Velocity map of modelled hydrodynamics on an incoming spring tide, Central Estuary, Ahuriri Estuary. Black boxes show zones of measurable incoming tidal velocities over intertidal mudflats. From Eyre (2009).

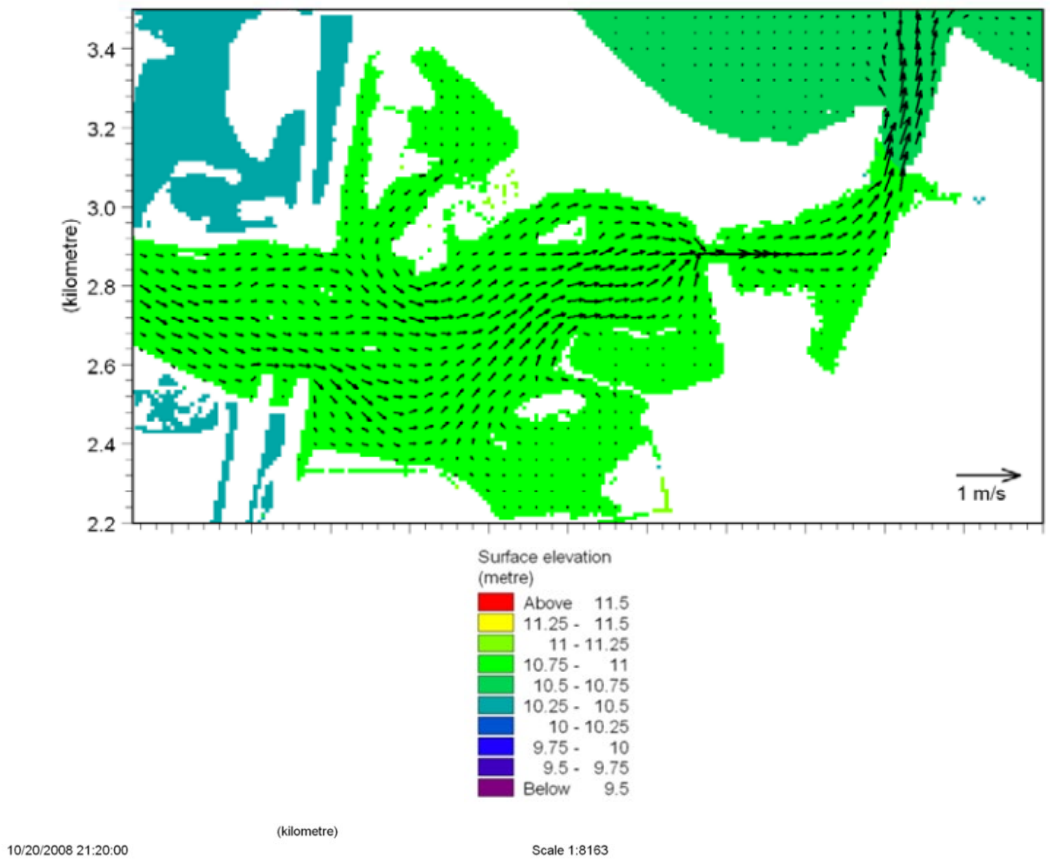

Figure 3.3: Velocity map of modelled hydrodynamics on an outgoing spring tide, Central Estuary, Ahuriri Estuary. From Eyre (2009).

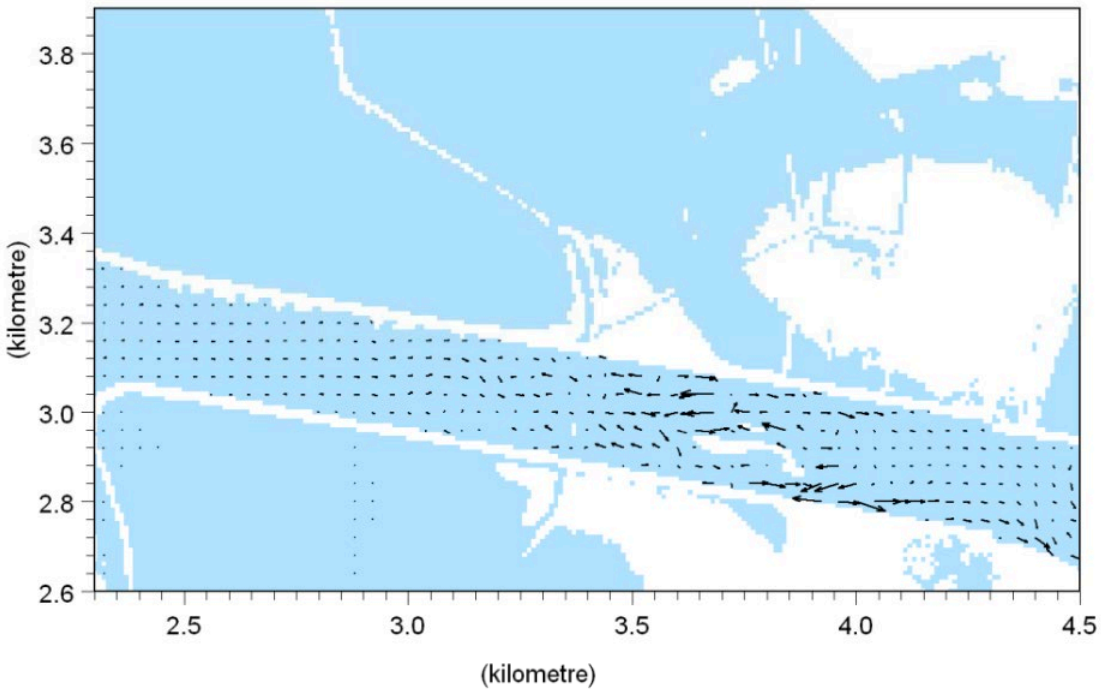

Figure 3.4: Velocity map of modelled hydrodynamics averaged over two tidal cycles, Main channel. From Eyre (2009).

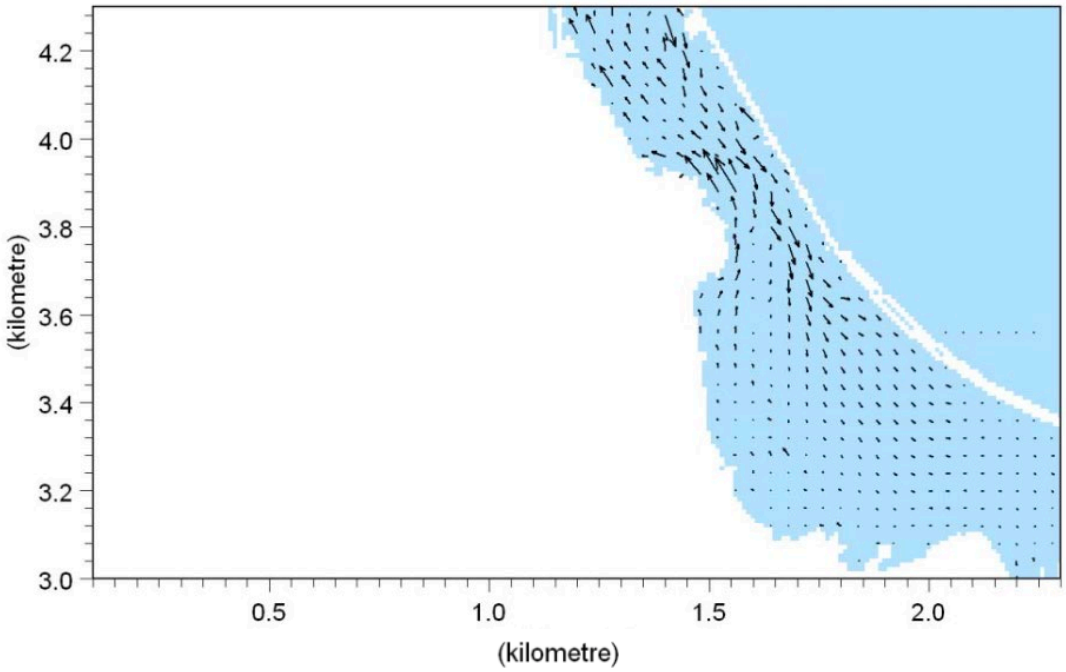

Figure 3.5: Velocity map of modelled hydrodynamics averaged over two tidal cycles, Upper Ahuriri Estuary. From Eyre (2009).

The model developed by Eyre (2009) was relatively coarse and based on a LiDAR-derived bathymetric model of the estuary. Consideration of freshwater open channels discharging into the central estuary and upper estuary would have contributed to a higher resolution model. However, limitations on time, resource and budget can restrain such studies. Overall, the model provides a sound initial overview for the otherwise unknown hydrodynamic behaviour of the Ahuriri Estuary, in the notable absence of flow meters on any of the major freshwater tributaries.

3.3.2 Ahuriri Estuary: Sediment transport

Eyre (2009) investigated the sediment transport of Ahuriri Estuary using MIKE 21 Mud modelling software. The author simulated sediment release into the Ahuriri Estuary via the Taipo Stream in storm conditions, measuring cumulative and instantaneous sediment flow past three estuarine sites downstream of the Taipo discharge. Figure 3.6 shows the flux measurement sites used by Eyre (2009).

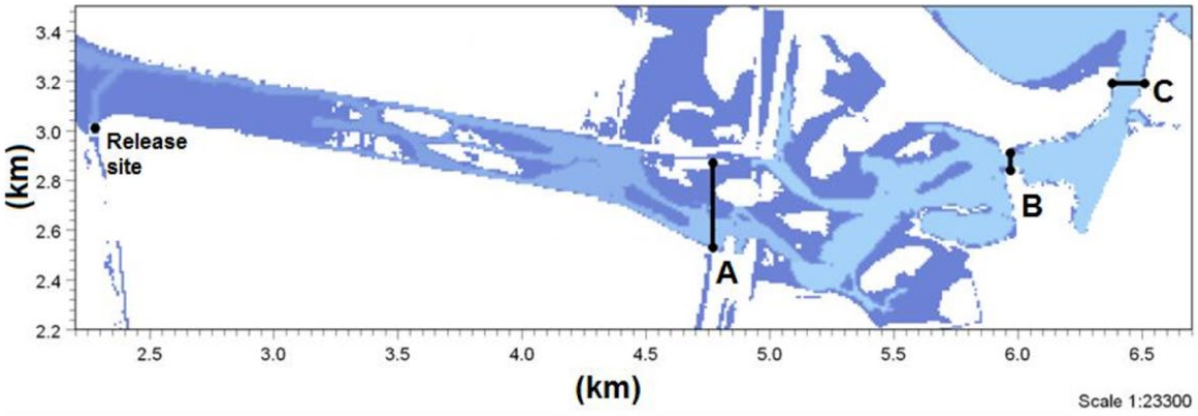

Figure 3.6: Sediment flux simulation by Eyre (2009) showing release site and 'site' delineations A, B, and C for quantitative assessment.

A total of 96 scenarios covering a grain size range of 10-105µm, spring and neap tidal conditions, ranging times of sediment release relative to tidal stage and rainfall event intensities between 20-100mm were modelled by Eyre (2009). The author found that the timing of release of sediment generally controlled the path of sediment transport, with sediment released on an incoming tide largely flushed back into the Taipo waterway and subject to resuspension on the outgoing tide. Sediment released on the mid-ebb tide showed greatest net downstream transport, coinciding with an approximate 3 hour lag on observable tidal turnaround at the discharge zone (Eyre, 2009).

Eyre (2009) then modelled sediment settling of a range of grain sizes under varying conditions at four sites and reported that sediment transport was largely dependent on grain size, with a lower grain size showing a higher net transport from the modelled Taipo release zone. The author sub-sectioned Ahuriri Estuary into 8 zones (Figure 3.7) to generalise sediment deposition from the model simulations, finding that Zone 2 being the channel from the Taipo downstream showed the highest quantitative SAR for the 10µm, 60µm and 105µm grain sizes. Zone 1 upstream of the Taipo discharge followed, with a higher 10µm accumulation than downstream zones due to a lower flow velocity, while Zones 6, 7, and 8 showed lower sedimentation rates than Zones 1 and 2; however, rates within Zones 6, 7, and 8 generally increased downstream. Modelling for the 60µm and 105µm sediment fractions for all storm event scenarios only showed considerable accumulation in Zone 2.

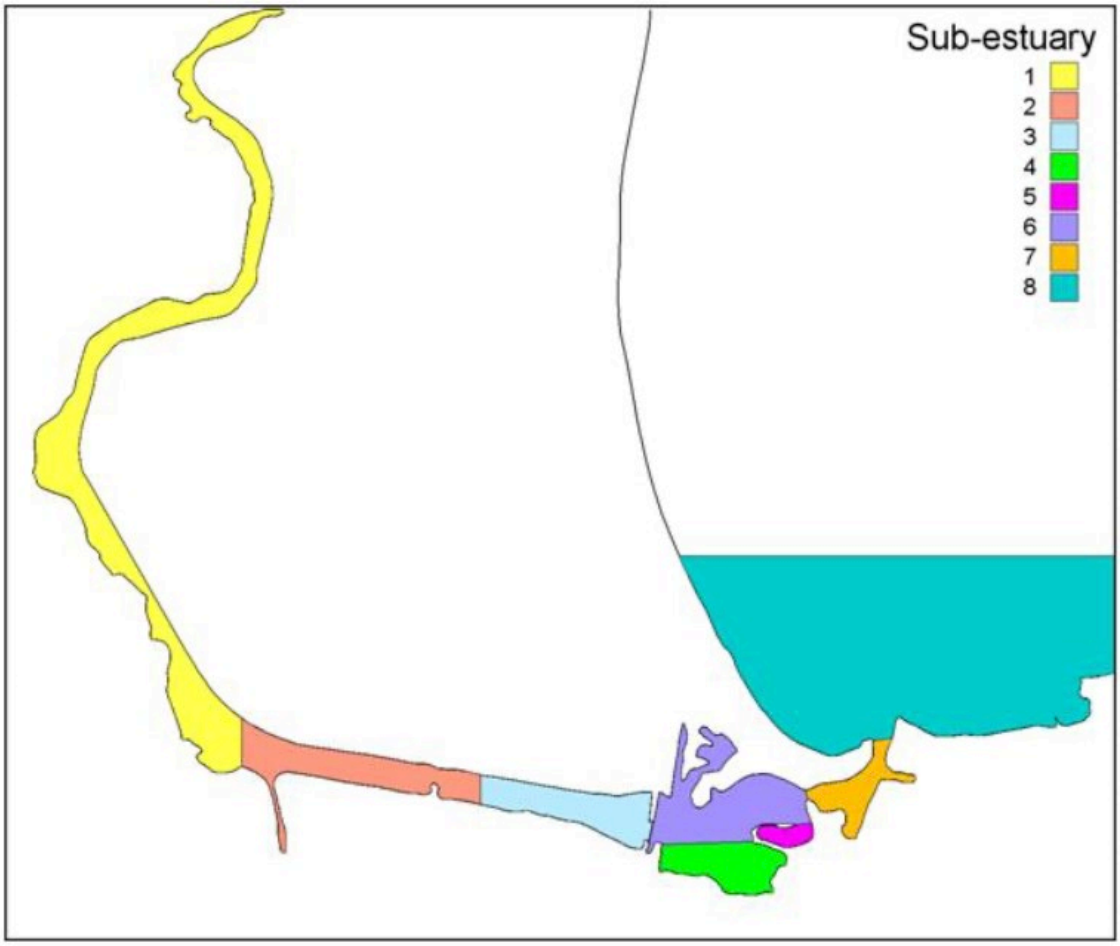

Figure 3.7: Sub-sections of Ahuriri Estuary for sediment transport modelling, by Eyre (2009).

From model simulations on sediment resuspension, Eyre (2009) concluded that tidal velocities were insufficient to erode bed-load or sediment ≥105µm diameter with the exception of where flow is channelised by intertidal islands with high SAR. Secondary reworking was found to be restricted to the main channel in the central estuary. Importantly, Eyre (2009) highlighted that tidal velocities under normal flow and subsequent shear stress remains too low to erode intertidal mudflats, lending to the observation of laminar accretion of fine sediment. This finding is supported by the literature discussing intertidal SAR (Plater & Kirby, 2011), and the mid-estuarine maxim (Buggy & Tobin, 2008). Eyre (2009) provides a conceptualisation of sedimentation patterns in the central estuary to summarise the implied accretion/erosion patterns (Figure 3.8).

Figure 3.8: Conceptual model of sedimentation behaviour, central Ahuriri Estuary Eyre (2009).

There is one aspect to the models developed by Eyre (2009) which undermines their quantitative representation of the morphodynamics of the estuary. The models are based on the freshwater input of the Taipo tributary alone, which is quoted as "the only freshwater discharge into the estuary of significance" (Eyre, 2009). This is fundamentally flawed as the consented Purimu, Old Tutaekuri Riverbed and Thames-Tyne open channels convey pumped and gravity-flow surface and drainage water from Napier City continuously (Figure 2.6). Considering these discharges, as well as the Taipo, it is expected that accretion would still occur in the zone between the Taipo and the Central Estuary (Zone 2 and 3 in Figure 3.7) as discovered by the models. However, it is likely that accretion is underestimated in the intertidal zones adjacent to the three unconsidered significant freshwater discharges. The models by Eyre (2009) remain representative when considering tidal velocity shear over intertidal versus subtidal zones though the quantitative assessments made for SAR by zones are challengeable. As the sole insight to the morphodynamic behaviour of Ahuriri Estuary, these models still provide invaluable guidance as hydrodynamic behaviour, sediment quality, and the health of estuaries are inextricably linked.

3.3.3 *Ahuriri Estuary: Sedimentary history*

Chagué-Goff et al. (2000) conducted a study investigating the effect of external forces on Ahuriri Estuary, namely urban anthropogenic effects and natural catastrophic events, and discovered that anthropogenic effects from the previous century are preserved in estuarine sediment. The authors recovered sediment cores from three morphologically diverse areas of Ahuriri Estuary: the northern intertidal zone of the central estuary, the southern intertidal zone of the central estuary adjacent to the Pandora Industrial area and the subtidal right bank of the main channel immediately downstream of the Taipo discharge. Chagué-Goff et al. (2000) subsampled the cores for ^{210}Pb radioisotope, trace element, and grain size analyses. Chagué-Goff et al. (2000) deduced from ^{210}Pb analysis that the top 140mm of core S0 (Figure 3.9) was deposited between 1964 and the year of sample collection (1998), corresponding to an averaged SAR in Ahuriri Estuary's south-central intertidal zone of 4.1mm yr^{-1}.

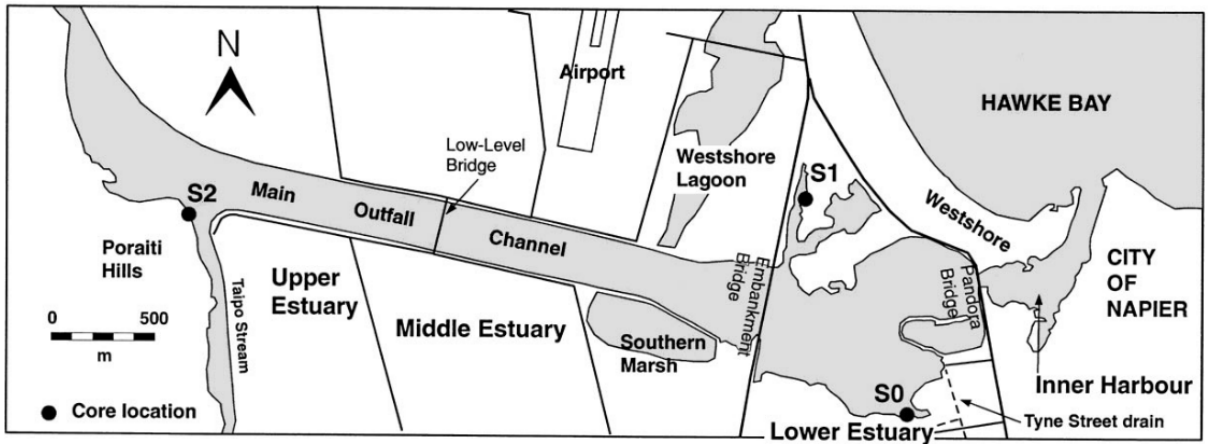

Figure 3.9: Map of core locations from Chagué-Goff et al. (2000).

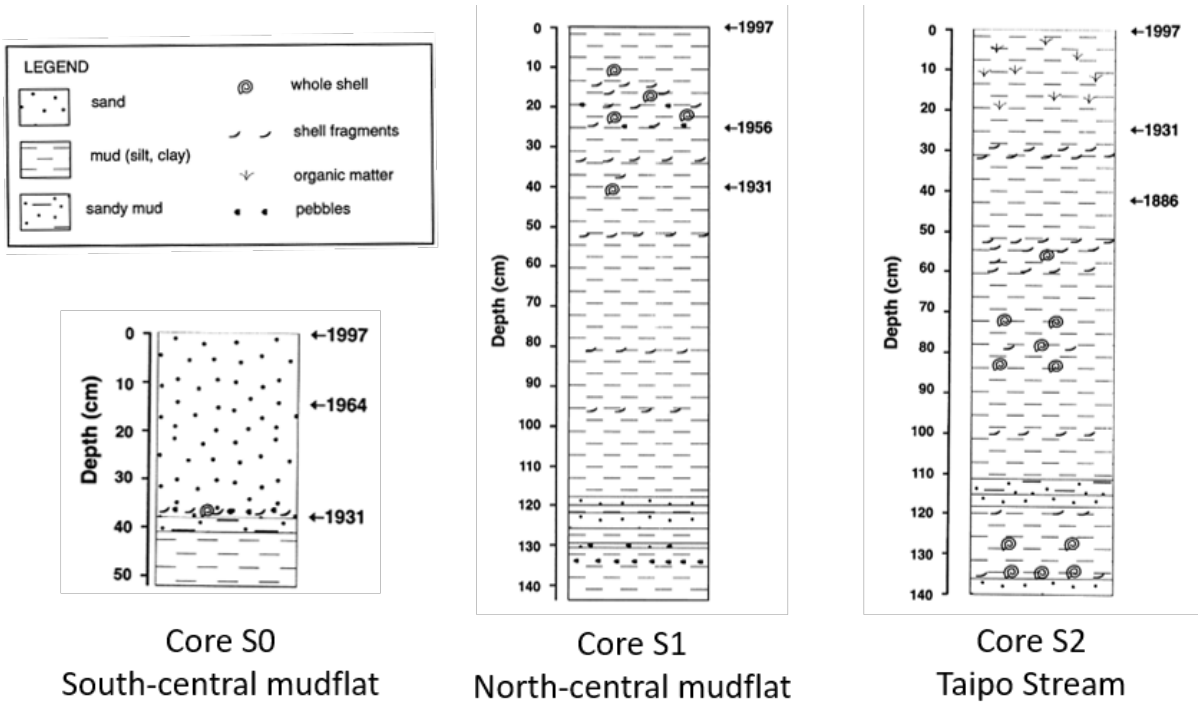

Figure 3.10: Stratigraphy and radioisotope age derivation of cores S0, S1 and S2, Ahuriri Estuary. Compiled from Chagué-Goff et al. (2000).

In the north-central estuary, Chagué-Goff et al. (2000) calculated core S1 expressed an average sedimentation rate of 6.1mm yr^{-1}, while the upper estuarine core S2 was calculated as 3.1mm yr^{-1} average accumulation, with this lower rate attributed to lack of tidal sediment input at this location. This finding is consistent with the sediment transport models designed by Eyre (2009). As a critical time marker for Ahuriri Estuary and Napier City's subsequent development, Chagué-Goff et al. (2000) recognised the 1931 earthquake in each of the three cores using radioisotope data and grain size changes.

Hayward et al. (2006) also undertook core sampling around Ahuriri Estuary to investigate palaeotidal elevation history by assessing eleven land-based sediment core samples representing the pre-1931 Ahuriri Lagoon. Hayward et al. (2006) analysed sediment core samples via radiocarbon dating of spatially varying diatom and foraminiferal assemblages (particularly *Austrovenus stutchburyi* and *Amphibola crenata*), tephra glass shard comparisons to known historic deposits, dating wood deposits within the sediment core samples, land elevation record comparisons, and visual sediment assessments.

Hayward et al. (2006) collected one sample from the northern modern Pāmu farm, one from the central Pāmu Farm, three from the corner of the Taipo and the modern Lagoon Farm to present a composite core, and five from Te umu Roimata south of Lagoon Farm. The core samples reflected a combined 8.5m subsidence from a series of downthrow events, followed by 1.5m uplift in 1931. In the northern sample, Taupō and Waimihia tephra deposits were identified in the three metres below the 1931 earthquake. At the time of the study, the samples beside the Taipo showed a surface land compaction 0.2m below extreme low water spring. Relative sea level changes are observable in the irregularity of bioturbated zones at 2.48m, 1.8m, and 0.85m depth. Above 0.3m depth, Hayward et al. (2006) observed foraminifera reflective of low marsh environments and suggest this is a visual result of the uplift from the 1931 earthquake. All cores reflected three major sea level rise scenarios between 1.8-2m depth approximately 3000 cal. BP, and some cores reflected a degree of microfossil displacement potentially caused by earthquake or tsunami events.

In a more recent study, Hayward et al. (2015) discussed Holocene sedimentary sequences that are poorly constrained. This recent study presents foraminiferal, tephrostratigraphic and radiocarbon analyses from 45 sites in the historic Ahuriri Lagoon. Three general zones were selected as building upon the 2006 study: Te Umu Roimata, Ohingaroa and the central Lagoon Farm or 'Poraiti Lane'. The 'A' samples from Poraiti Lane show a distinctive time series of tidal flats, salt marsh and peat swamp depositional environments (Figure 3.11), fluctuating as a result of both sea level and tectonically-driven land elevation changes (Hayward et al., 2015).

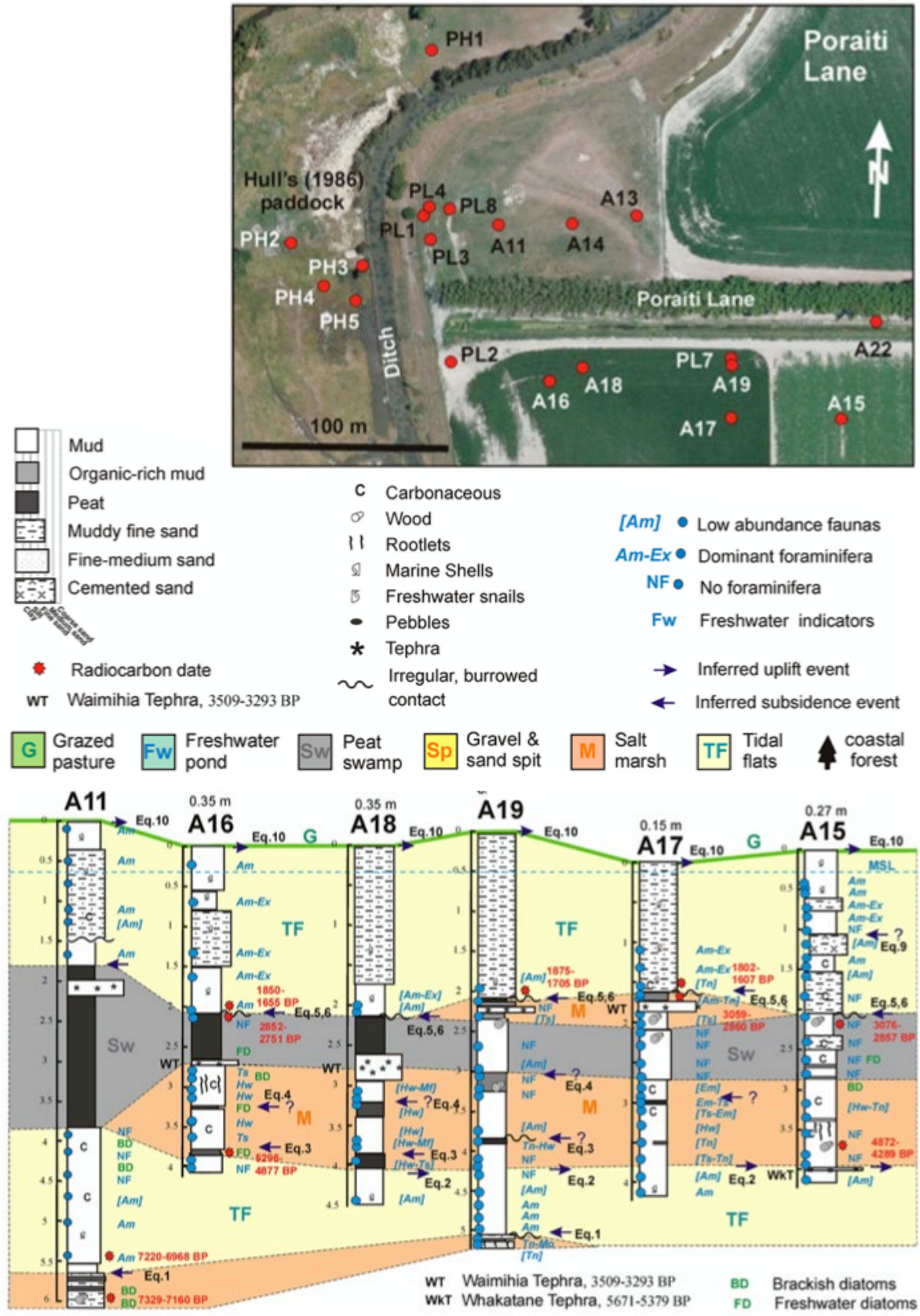

Figure 3.11: Location and schematic of lithologies in analysed core samples in 'Poraiti Lane' Lagoon Farm, Napier. All years in cal. BP. Compiled from Hayward et al. (2015).

From both studies (Hayward et al., 2006; Hayward et al., 2015), the balance of net 7m subsidence over eight earthquakes (including seven subsidence events and one major uplift) from the previous 7200 years is a finding consistent with Hull (1986) who created a composite sedimentary log from the base of the Poraiti Hills using radiocarbon dating of peat, wood, human bones and shells. Hull (1986) described the changes in sea level by comparing depositional environments to stratigraphic observations suggesting the fluctuations of sea level at the site of the sample were due to tectonic changes. In Hull (1990), the author then investigated the 1931 earthquake surface faulting and deformation. Both papers concluded that the sedimentary record of the uplift was well preserved in Ahuriri Estuary.

3.3.4 Ahuriri Estuary: Sediment quality

Alongside isotope analysis using ^{210}Pb and ^{222}Ra calculations, the study by Chagué-Goff et al. (2000) tested the three cores for grain size, iron, aluminium, lithium, arsenic, chromium, copper, nickel, lead, rubidium, vanadium, zinc, chlorine, bromine and Sulphur using a combination of spectrometry and X-ray fluorescence (XRF). As expected from progressive urban development, Chagué-Goff et al. (2000) identifies generally increasing trends in trace metal concentrations in the three sediment core samples from time markers such as the 1931 earthquake. Figure 3.12, Figure 3.13 and Figure 3.14 taken from Chagué-Goff et al. (2000) show trace metal concentrations with depth for each core sample. Notably, levels of urban indicator contaminants copper, chrome and lead (Gadd et al., 2020; Hwang et al., 2016; Pitt et al., 1995) generally increase towards present, particularly in S1. This is suggestive of recent rises in discharge rates of these three metals and increases in fine sediment accumulation (Chester & Jickells, 2012; Smith et al., 2018; Thrush et al., 2004).

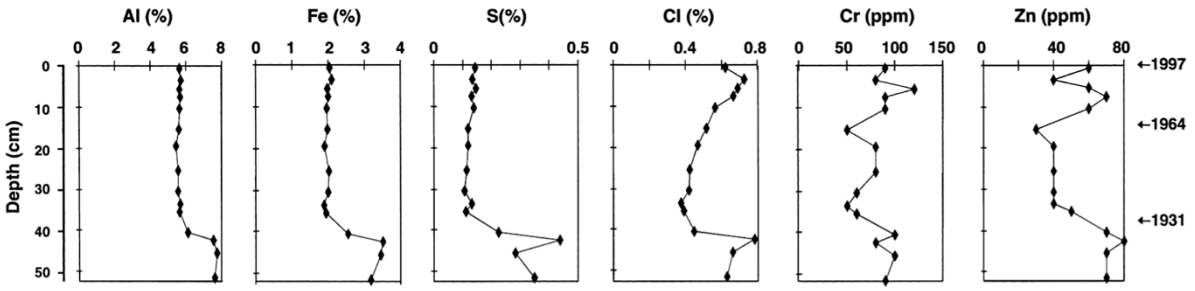

Figure 3.12: Trace metal distribution in core 'S0': adjacent the Thames-Tyne discharge in the South-central Ahuriri Estuary (Chagué-Goff et al., 2000).

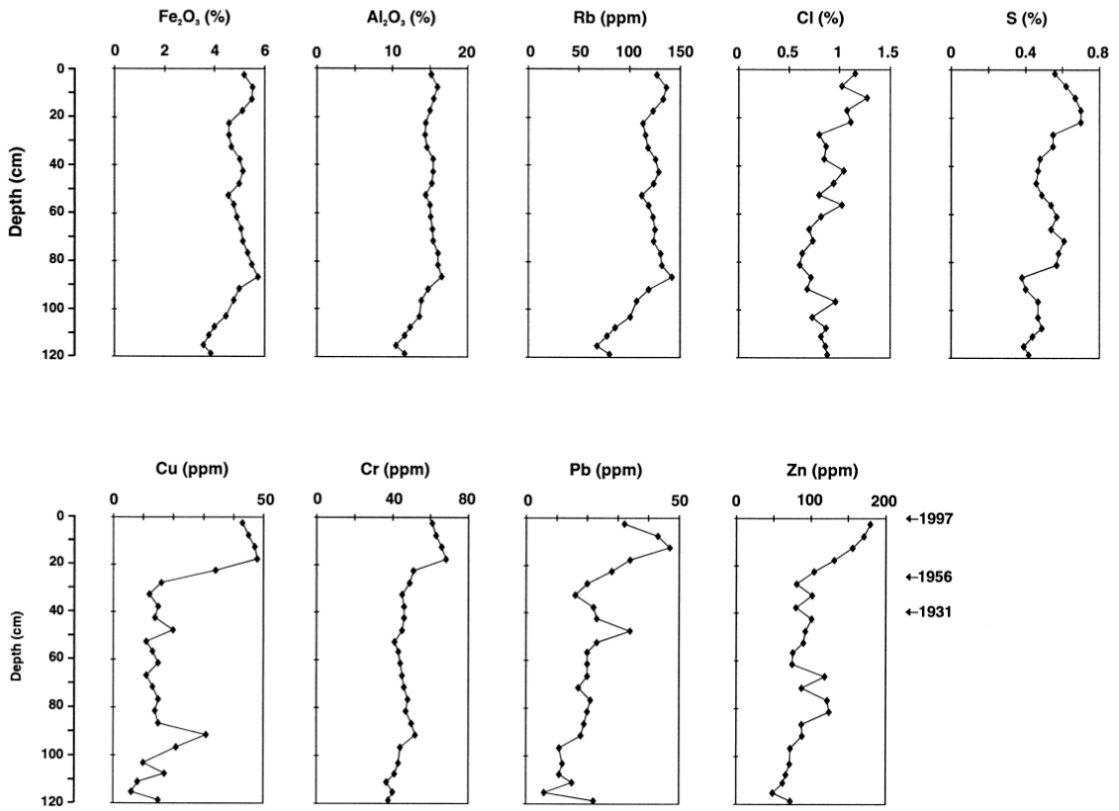

Figure 3.13: Trace metal distribution in core 'S1' in the north-central Ahuriri Estuary (Chagué-Goff et al., 2000).

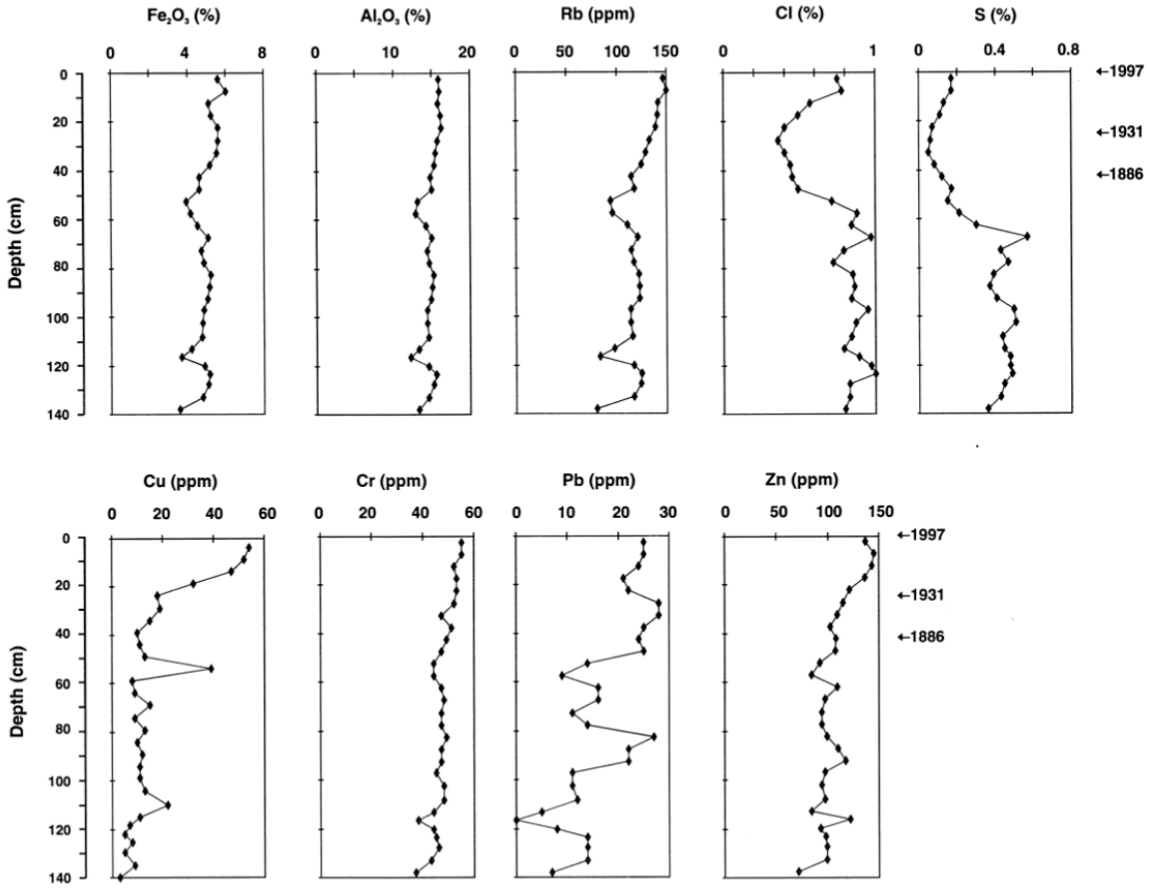

Figure 3.14: Trace metal distribution in core 'S2': adjacent the Taipo discharge, Ahuriri Estuary (Chagué-Goff et al., 2000).

The sediment trace metal concentrations studied by Chagué-Goff et al. (2000), who attributed contamination to the effects of urbanisation, are consistent with Strong (2005) who compared trace metal concentrations in surface sediments from 12 estuaries in Hawke's Bay. Strong (2005) reiterated the high zinc and lead concentrations in Ahuriri Estuary and provided a comparison to other estuaries in the Hawke's Bay (Figure 3.15). The copper, lead, arsenic, cadmium, chromium, nickel, zinc, iron and manganese measurements at urbanised Ahuriri Estuary are higher than at Waitangi Estuary, a restored rural-urban estuary, and Mahia's Mangawhio Lagoon, a low-population rural-residential estuary (Strong, 2005).

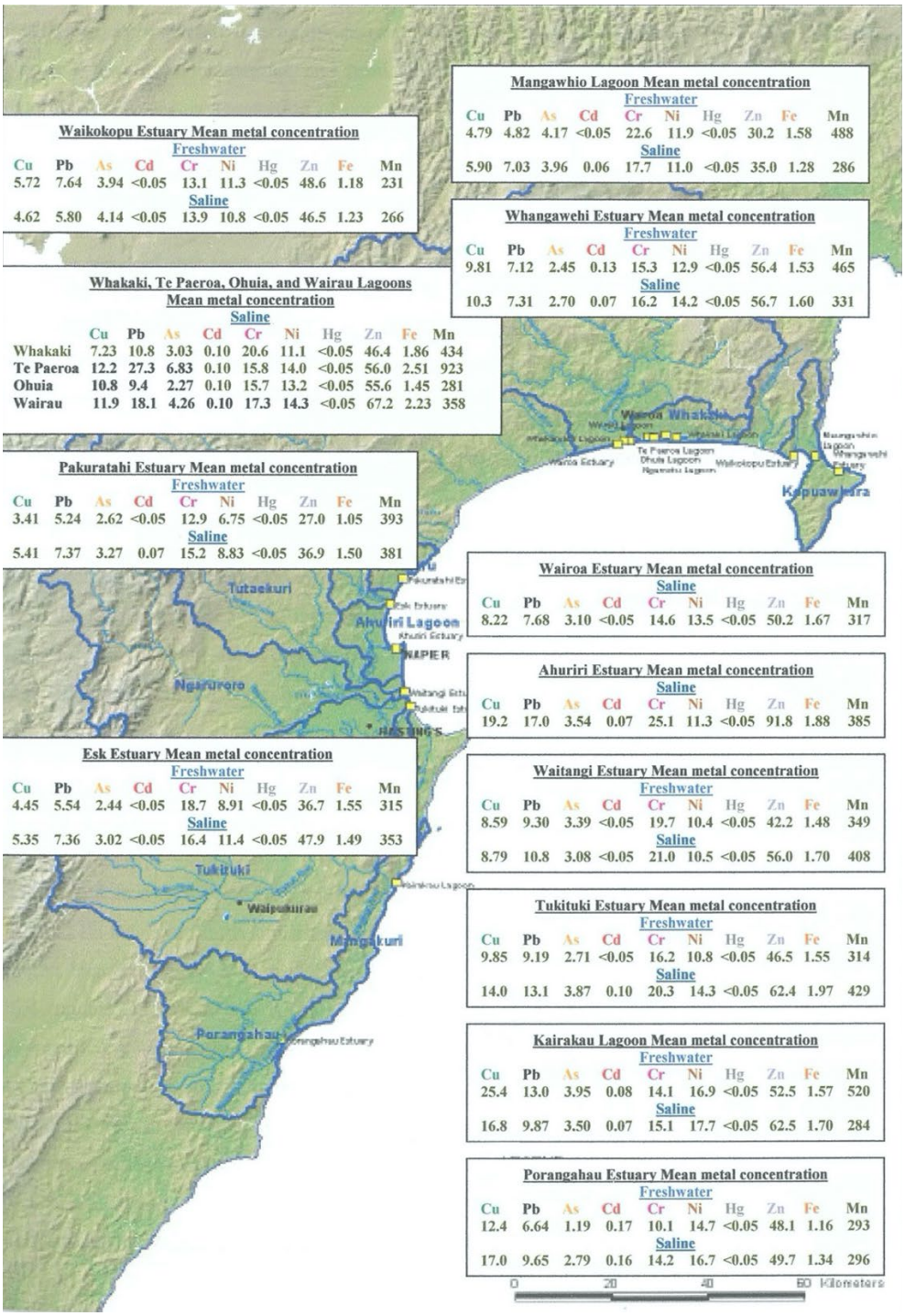

Figure 3.15: Mean trace metal concentration in surface sediment samples, Hawke's Bay estuaries (Strong, 2005).

Some conclusions drawn in the Chagué-Goff et al. (2000) study regarding anthropogenic effects as found in the sediment of Ahuriri Estuary can be challenged. The authors attribute the primary source of anthropogenic pollution in Ahuriri Estuary proper to the Thames-Tyne discharge from conveyance of surface water through the Pandora Industrial area. The Thames-Tyne discharge is only one urban tributary discharge in Ahuriri Estuary's multi-faceted hydrodynamic system. In the context of the Chagué-Goff et al. (2000) study, it is intuitive that the southern core shows the highest sediment-metal concentration levels of the three cores, as the other two core sites are not directly influenced by urban surface water discharges. The decision to take a core sample from the Taipo as a control site is questionable as the Taipo Stream conveys residential surface water which can contain an array of dissolved contaminants as well as contaminated particulate terrigenous sediment. To repeat a core sampling program in Ahuriri Estuary to determine anthropogenic effects on the estuary as captured in sediment, it would be wise to incorporate samples from areas of Ahuriri as determined by point source depositional zones.

Ataria et al. (2007) present *He Moemoea*, a report on behalf of Ngā Pae o Māramatanga as an assessment on the health of Ahuriri Estuary and a vision plan for prevention of further decline. The health assessment included the retrieval of seven shallow sediment cores (10cm depth) from sites immediately in point-source discharge zones of surface waterways (Figure 3.16) and analysis for recoverable cadmium, chromium, copper, mercury, lead, nickel and zinc.

Figure 3.16: 10cm depth sediment core collection sites, He Moemoea study and vision plan (Ataria et al., 2007).

The findings of Ataria et al. (2007) echo those of Chagué-Goff et al. (2000) and Strong (2005) in the excessive metal concentrations, particularly zinc and lead, found adjacent to the Thames-Tyne

discharge (site 1, Figure 3.16) with polycyclic aromatic hydrocarbon (PAH) levels an order of magnitude higher than from the other six core sites, reiterating conclusions of Chagué-Goff et al. (2000).

Unlike Chagué-Goff et al. (2000), Ataria et al. (2007) considered many more point sources as potential sites of anthropogenic contamination than just the Thames-Tyne and included them in the comparative assessment. It is suggested in the conclusions of the *He Moemoea* study that the sediment in the vicinity of the Thames-Tyne discharge has a generally higher concentration of contaminants than elsewhere in Ahuriri Estuary. The authors attribute the higher concentrations adjacent the Thames-Tyne to the channelisation of the waterway system. Considering hydrodynamic assessments by Eyre (2009), it may be suggested that channelisation is less of a contributor than the tidal regime due to the system's location. In addition, the openness and low gradient of the system (Ludlow, 2020) allows contaminant conveyance from relatively faster channelised flow into the low energy adjacent southern-central mudflats.

In another surficial sediment quality assessment akin to Strong (2005), Kelly (2018) analysed the results of 73 20-mm sediment samples from the central Ahuriri Estuary. Heavy metal analyses echo the findings of Ataria et al. (2007), Chagué-Goff et al. (2000) and Strong (2005) featuring the high levels of sediment-bound zinc in particular around the Thames-Tyne discharge zone (Figure 3.17 and Figure 3.18). The thorough surficial sediment profiling study by Kelly (2018) shows high concentrations of zinc around the Purimu discharge and the Old Tutaekuri Riverbed discharge: a result which Ataria et al. (2007) also identified. A study by Smith (2014) identified that the Old Tutaekuri Riverbed discharge zone had the highest sampled concentration of mean normalised trace zinc (Figure 3.19) when comparing 2014 surficial sediment results to other New Zealand reference estuaries.

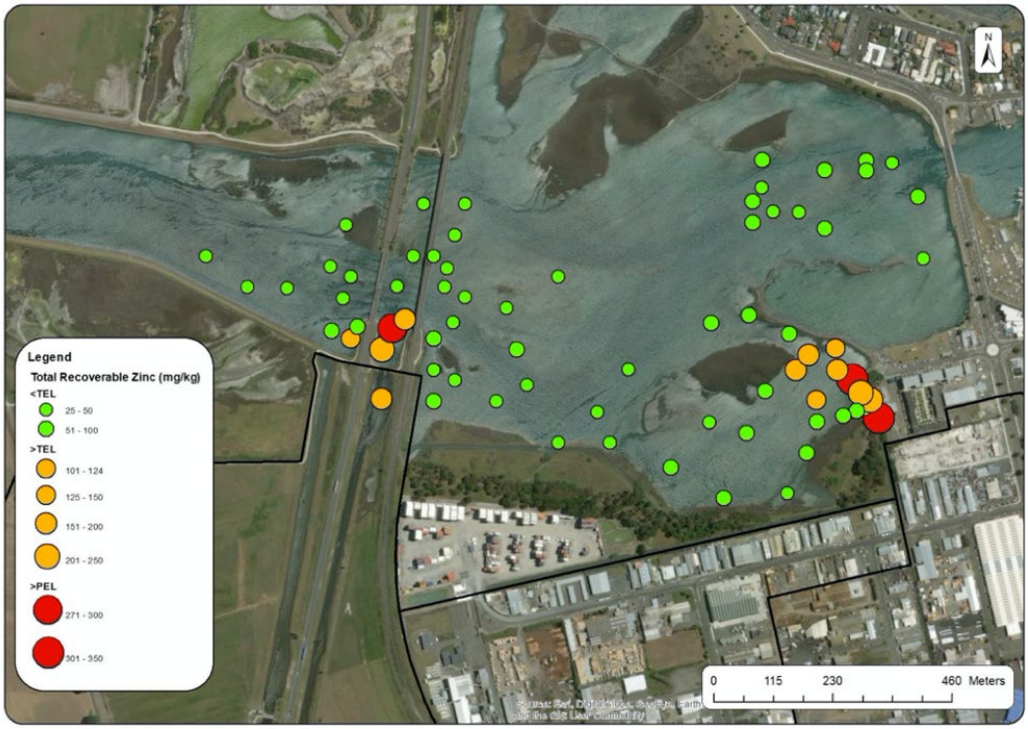

Figure 3.17: Total recoverable zinc from the <2mm fraction of surficial sediment samples (Kelly, 2018).

Other high concentrations of sediment trace metals in both the Smith (2014) and Kelly (2018) studies included chromium, copper, arsenic and lead, with higher concentrations largely restricted to the immediate intertidal discharge zones of the Thames-Tyne and Old Tutaekuri Riverbed. This likely reflects the influences on the estuary of both the Pandora Industrial and the Onekawa Industrial catchments, respectively.

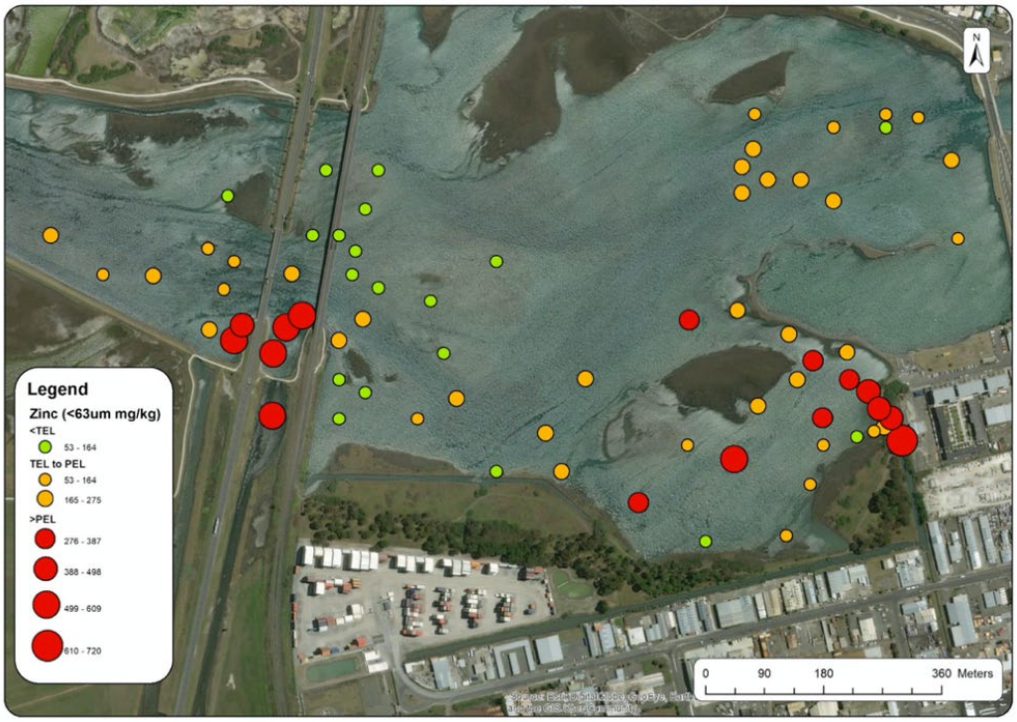

Figure 3.18: Total recoverable zinc from the <63µm fraction of surficial sediment samples (Kelly, 2018).

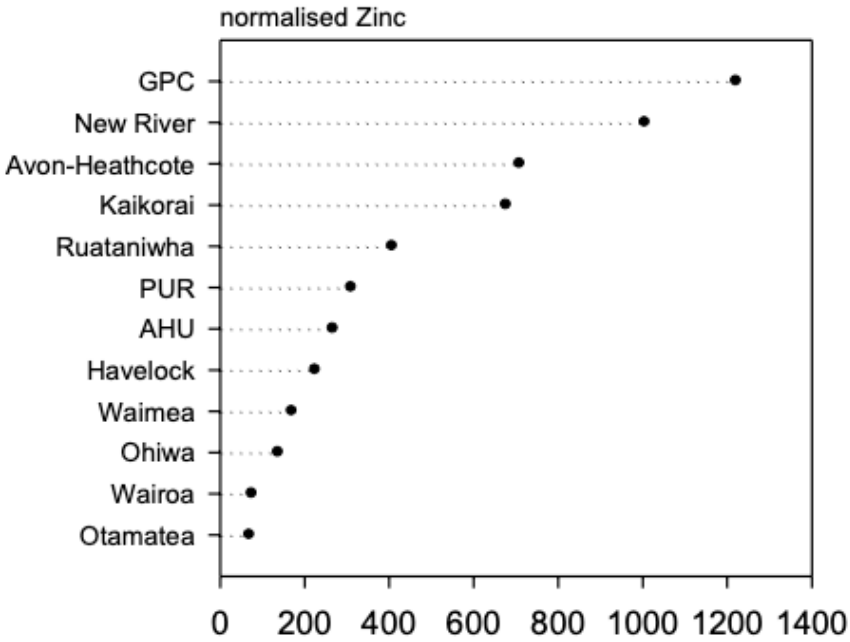

Figure 3.19: Mean normalised trace zinc in estuarine sediment with New Zealand reference estuaries as comparisons. 'GPC' is the Old Tutaekuri Riverbed (Figure 3.36), 'PUR' is the discharge zone of the Purimu (Figure 3.36), and 'AHU' is a reference site for the Smith (2014) study (Figure 3.35).

3.3.5 Ahuriri Estuary: Tributary water quality

Water quality monitoring can be a cost-effective indicator for assessing point-in-time estuarine health. However, physical parameters such as dissolved oxygen, conductivity, temperature and pH are largely reliant on external factors such as biological activity, salinity, estuarine tidal stages, weather, season time of day and additional chemical constituents. Ideally, water quality monitoring programs are developed which address spatial (i.e., across several sites within a waterbody), and temporal differences, which include across full tidal cycles, different times of the day (due to biological activity and oxygen depletion overnight), across seasons, and different weather events and years.

Water quality is a vital constituent to understanding estuarine health, yet it can display extreme spatiotemporal variability, meaning physical parameter readings can be misrepresentative if extrapolated to a water body as point-in-time sampling; spot sampling can miss high-concentration yet brief contaminant pulses (Birch et al., 2000). Therefore, relevant and informative water quality data for the major tributaries of Ahuriri Estuary will be summarised in this section and will not be further investigated in the thesis. This analysis of surface water quality will act as a linkage between Objectives Two and Three: land use change assessment and the physicochemical quality of Ahuriri Estuary.

A Napier city-wide surface water quality study was initiated by NCC in 2019. 22 sites across Napier city (Figure 3.20) have since been visited monthly to retrieve a grab-sample for analysis of chemical, physical and microbiological parameters (Napier City Council, 2021a). As this city-wide surface water quality monitoring program is ongoing, this is unpublished data which is part of a developing dataset.

Figure 3.21 through to Figure 3.32 are bubble plot maps of mean annual concentrations of various chemical parameters to allow an understanding of the current state of surface water quality of the freshwater tributaries of Ahuriri Estuary. Concentrations are colour-coded to represent the 12-month means as ‘below’ or ‘above’ guideline values from the Australia New Zealand Environment and Conservation Council (ANZECC) 2000 and the Australia New Zealand (ANZG) 2018 guidelines for the protection of aquatic species (Napier City Council, 2021b). Points are additionally sized to represent degrees of difference to these guidelines. As the monitoring was initiated in a time of localised drought, some of the sites within the dataset were frequently dry and samples were therefore unable to be collected. This means there is a slight skew within the dataset regarding sites which allowed sampling only in wet weather, such as Plantation at Harakeke (Site 17 in Figure 3.20). The number of grab samples which comprise the means presented in the bubble plots are listed in Table 3.1, as well as parent waterway and Ahuriri Estuary sub-catchment detail for each site.

Figure 3.20: Map of numbered sites; Napier city-wide waterway monitoring project. Site names referenced in Table 3.1. Data obtained from Napier City Council (2021b).

Table 3.1: Site name, label on Figure 3.20, waterway, catchment, and number of grab samples contributing to mean values in bubble plots Figure 3.21 - Figure 3.32. Data obtained from Napier City Council (2021a)

Name	Label (Figure 3.20)	Waterway	Catchment	Number of grab samples	Dry-weather samples (0-5mm rainfall in previous 72hr)	Wet-weather samples (>5mm rainfall in previous 72hr)
Onehunga at base of Pump Station	1	Onehunga	Bayview-Onehunga	11	7	4
Purimu 10m downstream Meeanee Road	2	Purimu	Westshore Tidal Gates (WTG)	11	8	3
Purimu 10m upstream Burness Road	3	Purimu	WTG	11	8	3
Purimu 50m downstream Saltwater Creek	4	Purimu	WTG	10	7	3
Purimu 50m downstream Pump Station	5	Purimu	WTG	11	8	3
Taipo at Ngarimu Road	6	Taipo	Taipo	8	5	3
Taipo 50m upstream Church Road	7	Taipo	Taipo	10	7	3
Taipo at Prebensen Road/Lagoon Farm	8	Taipo	Taipo	10	7	3
Anderson Park west pond outlet	9	Saltwater Creek	WTG	6	3	3
Saltwater Creek Westminster/Wharerangi	10	Saltwater Creek	WTG	10	7	3
Saltwater Creek 50m downstream Orotu Drive	11	Saltwater Creek	WTG	9	6	3
Waverley at Tannery/Ulyatt Road	12	Waverley	WTG	9	6	3
County at Harold Holt	13	County	WTG	11	8	3
County 50m upstream Taradale Road	14	County	WTG	9	6	3
County 50m downstream Taradale Road	15	County	WTG	6	3	3
County 50m downstream Pump Station	16	County	WTG	8	5	3
Plantation at Harakeke	17	Plantation	WTG	9	6	3
Plantation 50m upstream Latham Street	18	Plantation	WTG	10	7	3
Combined Plantation-OTRB at Ford Rd Bridge	19	Plantation-OTRB	WTG	10	7	3
OTRB at Nuffield Avenue	20	OTRB	WTG	10	7	3
OTRB 50m upstream Kennedy Road	21	OTRB	WTG	10	7	3
Forgotten Creek	22	OTRB	WTG	5	4	1

The water chemistry in the tributaries of Ahuriri Estuary is variable, with several noticeable trends. Dissolved reactive phosphorus and total phosphorus (Figure 3.24 and Figure 3.25) are universally excessive across all of the 22 sites with many sites significantly above the guideline value for total phosphorus. Mean Chemical Oxygen Demand (COD) (Figure 3.26) also exceeds guideline values across all sites with the Onehunga Pump Station site adjacent to and discharging to the upper Ahuriri Estuary significantly above reference. Onehunga Pump Station shows an excessive 12-month mean for dissolved copper (Figure 3.21) and is the only site to exceed the value for dissolved lead (Figure 3.23).

The plot of 12-month means for Nitrate-N shows that 15 of the 22 sites are below the reference value for the protection of aquatic species. The 12-month means for the remaining seven sites exceed this nitrate reference value with Forgotten Creek (site 22) and County at Harold Holt (site 13) showing very high readings. Nitrite-N 12-month means are universally excessive with County at Harold Holt again proving a nutrient-enriched section of the waterway. Chlorophyll *a* density can be considered a reliant factor on nitrogen bioavailability (Borja et al., 2011) and the 12-month means for Chlorophyll *a* show an averaged excess over six of the 22 sites with County at Harold Holt again showing highly excessive concentrations. Where Nitrate-N and Chlorophyll *a* is concerned, there does not appear to be a suburb based, waterway specific, or sub-catchment pattern to the exceedances.

The 12-month mean plot for Total Suspended Solids (TSS) indicates that the Napier urban waterways experience higher sediment loading than advised by the guideline values for aquatic species protection. Mobilisation of terrigenous sediment into waterways is catalysed by rainfall (Chester & Jickells, 2012). Table 3.1 shows that the 12-month means for the majority of the 22 sites encapsulates only three samples collected during a rainfall event (with greater than 5mm cumulative rainfall in the previous 72 hours) (Napier City Council, 2021b). With many of the samples being collected in dry weather, the implication is that most sites often exceed reference values for TSS. This can be further explained by similar trends seen in dissolved versus total zinc and copper, with particulate-bound Zn and Cu represented by the total minus the dissolved fraction. The 12-month means for total zinc (Figure 3.28) and total copper (Figure 3.22) are higher than the dissolved means. Higher 12-month mean total copper concentrations trend toward the upper reaches of the waterways except for County Pump Station (site 16). Total zinc is much more universal with particularly high concentrations observable in and around the Onekawa Industrial area.

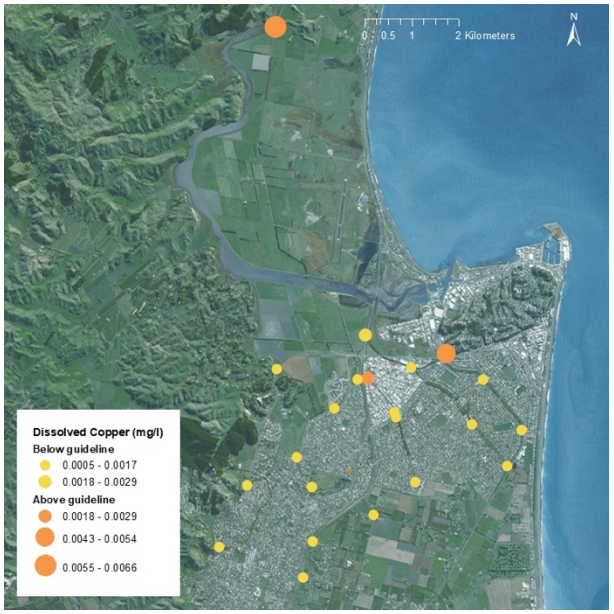

Figure 3.21: 12-month mean dissolved copper concentration.

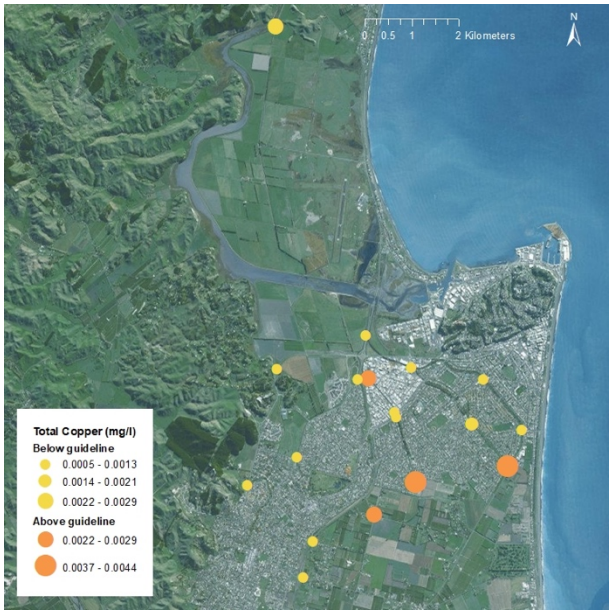

Figure 3.22: 12-month mean total copper concentration.

Figure 3.23: 12-month mean dissolved lead concentration.

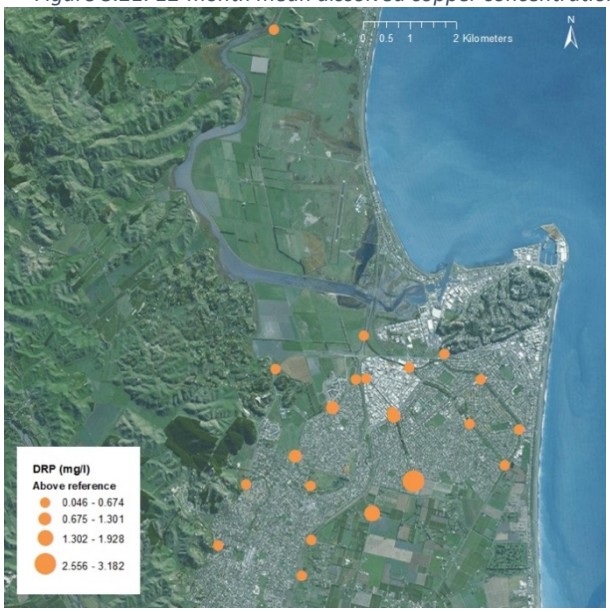

Figure 3.24: 12-month mean dissolved reactive phosphorus concentration.

Figure 3.25: 12-month mean total phosphorus concentration.

Figure 3.26: 12-month mean Chemical Oxygen Demand (COD) concentration.

Figure 3.27: 12-month mean dissolved zinc concentration.

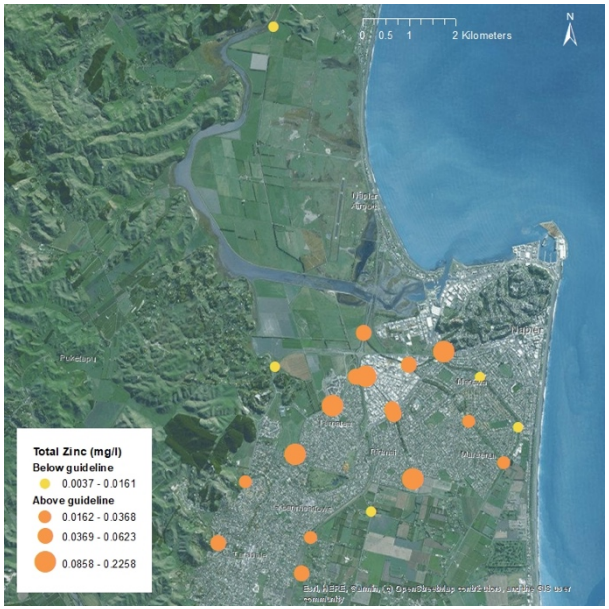

Figure 3.28: 12-month mean total zinc concentration.

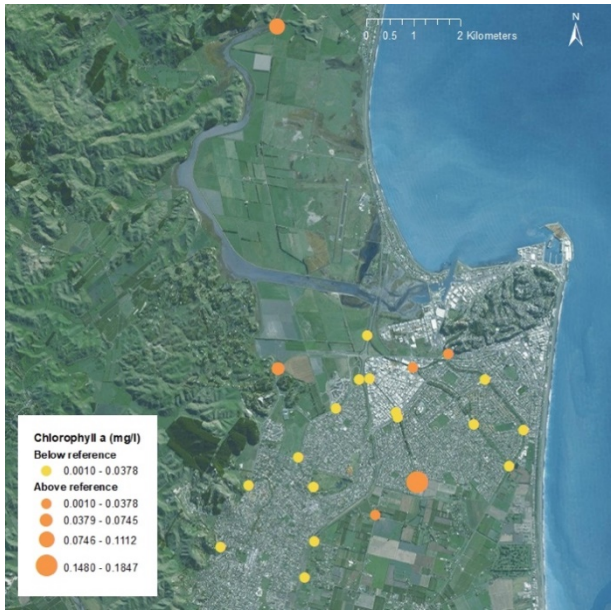

Figure 3.29: 12-month mean Chlorophyll a concentration.

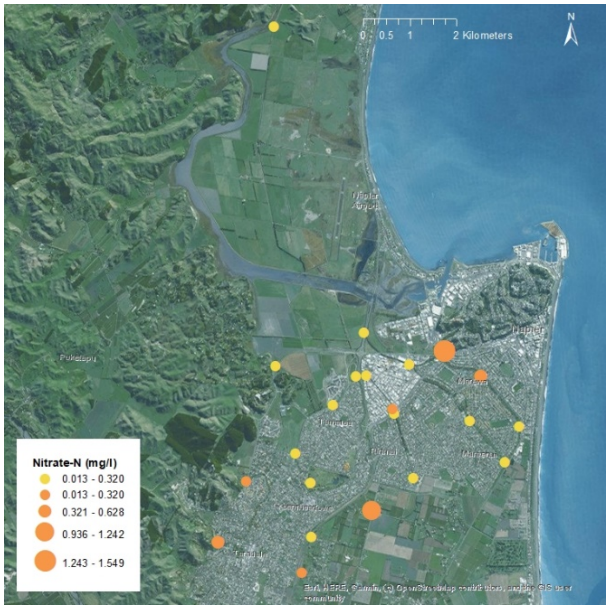

Figure 3.30: 12-month mean Nitrate-N concentration.

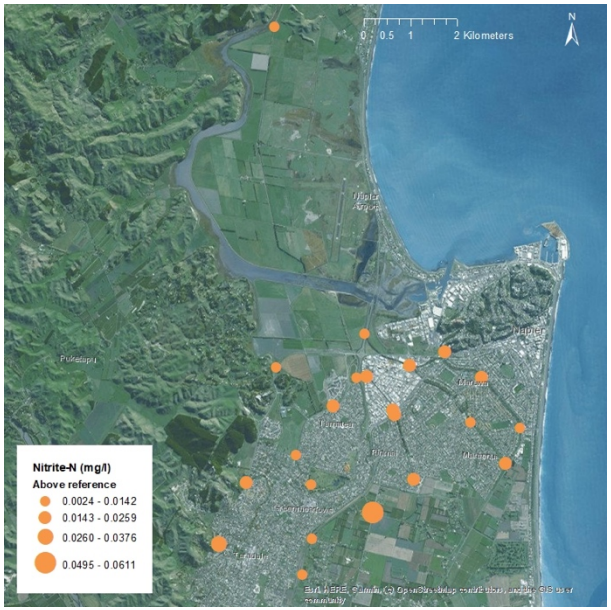

Figure 3.31: 12-month mean Nitrite-N concentration.

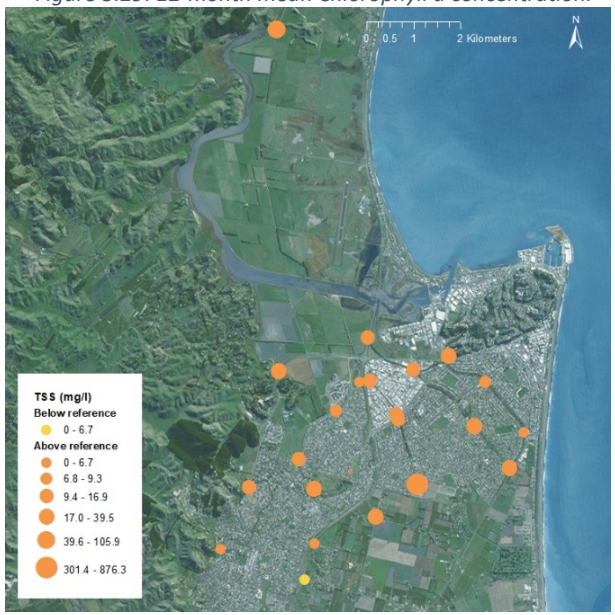

Figure 3.32: 12-month mean Total Suspended Solids (TSS) concentration.

3.3.6 Ahuriri Estuary: Ecology

Under resource consent DP110266W held by NCC for stormwater discharged via the Thames-Tyne network, ten benthic ecological samples from approximately 50m downstream of the footbridge at low tide ('Mid Thames-Tyne' in Figure 3.33) and 200m west of the footbridge are required annually in October ('Outer Thames-Tyne' in Figure 3.33) with 2019 marking the third year of collection (Ludlow, 2020). Ludlow (2020) reported that as an endemic indicator species of estuarine health, 59 *Austrovenus stutchburyi* individuals were found across the ten 2019 benthic samples. Of the 31 cockles collected from 50m downstream of the Thames-Tyne discharge, 29% of these were measured as <10mm diameter: their size potentially suggestive of juvenile individuals. By comparison, 41 cockles were collected in the previous year's monitoring with the 50m downstream site having a 13% <10mm ratio. The number of taxa for both areas were similar for 2018 and 2019 (Ludlow, 2020). Both 2018 and 2019 data reported more *Austrovenus stutchburyi* individuals than were found in the same 2017 monitoring. The author reports that the impact of the zinc and microbiologically enriched discharge from the Thames-Tyne waterways may have inhibited *Austrovenus stutchburyi* growth rates, meaning individuals which are considered juveniles in an unpolluted estuarine setting may instead be mature individuals with a stunted growth (Ludlow, 2020).

Figure 3.33: Map showing benthic ecological monitoring zones 'Mid Thames-Tyne', and 'Outer Thames-Tyne'. From Kelly (2018) as cited in Ludlow (2020).

Upstream of the Thames-Tyne discharge, a 2014 study on the benthic effects of urban stormwater from the Westshore Tidal Gates resource consent (Hawke's Bay Regional Council, 2011) on three sites in Ahuriri Estuary by Smith (2014) involved the collection of benthic ecological cores up to 150mm depth. Endemic *Austrovenus stutchburyi* cockles dominated all sites, being AHU downstream of

Embankment Bridge (Figure 3.35), PUR adjacent the Purimu discharge and GPC adjacent the Old Tutaekuri Riverbed discharge (Figure 3.36). Comparison to a similar 2006 study, and a replica 2010 study, highlights a general decline in taxonomic numbers across sites PUR and GPC between 2006 and 2014, while AHU generally increased. Individual counts between 2010 and 2014 experienced decline across each of the three sites.

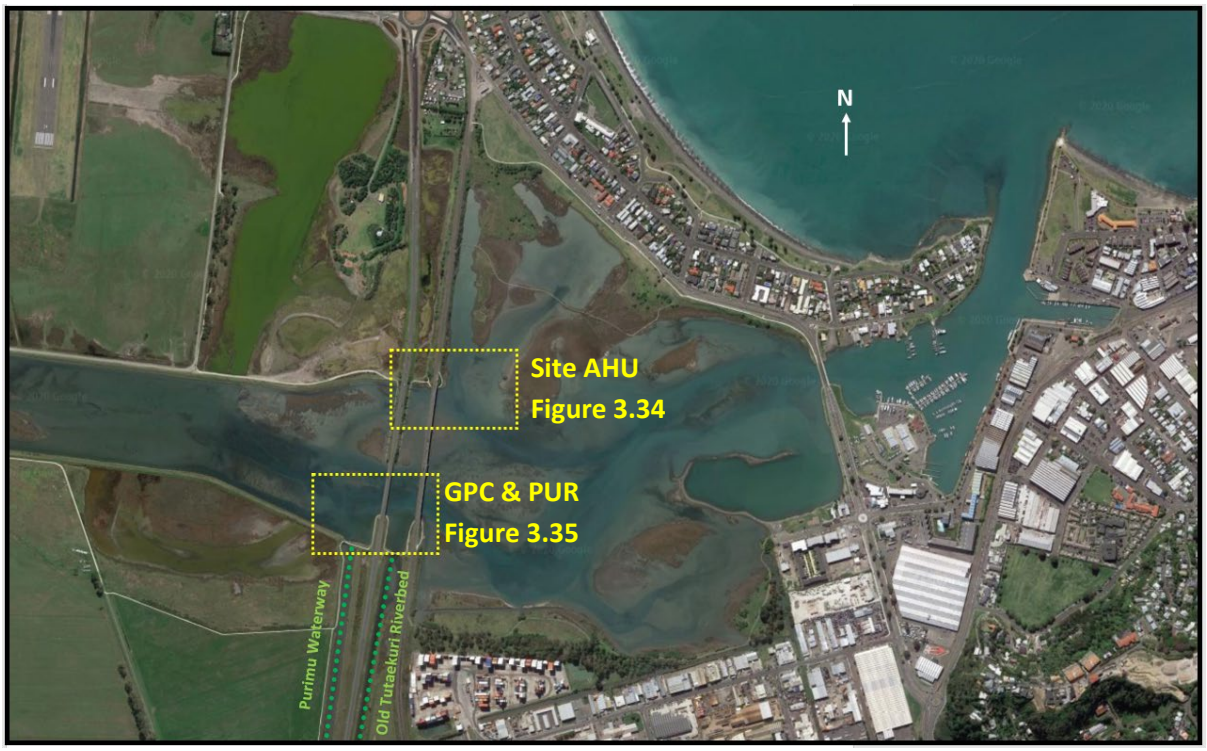

Figure 3.34: Location map of Smith (2014) study sites. Background image from Google (n.d.-a).

Figure 3.35: Sample site location; east of Embankment Bridge, Ahuriri Estuary. Blue sites denote 2010 survey, red sites represent 2014 survey (Smith, 2014).

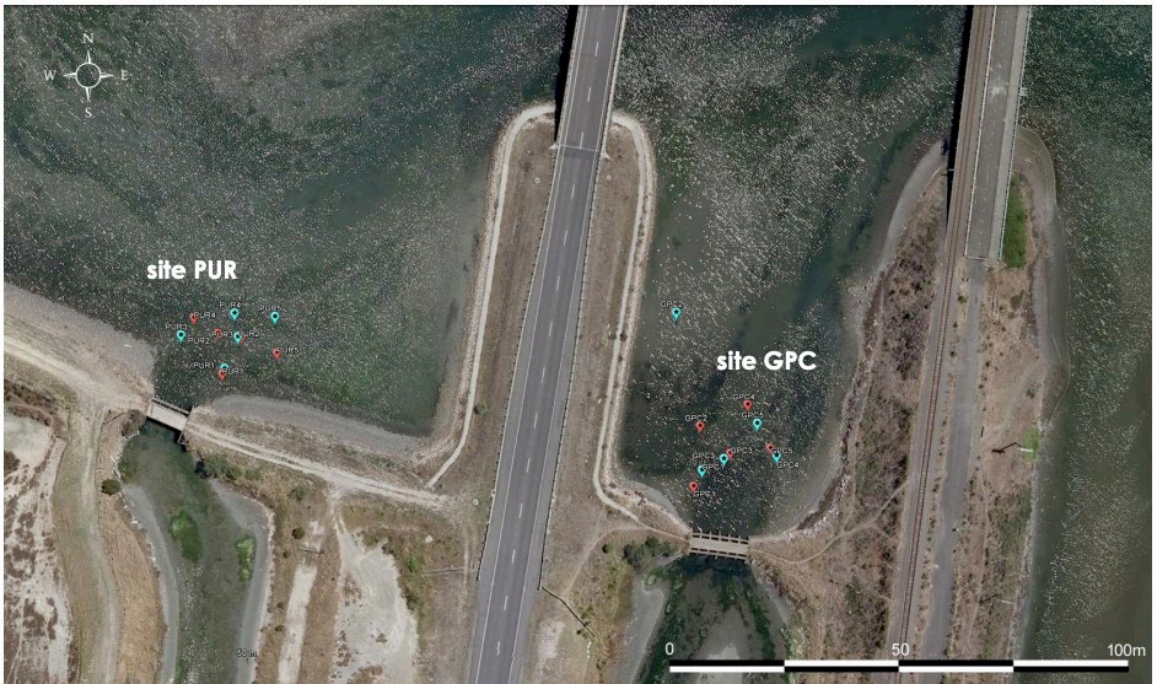

Figure 3.36: 2010 (blue) and 2014 (red) in-estuary sample sites adjacent the Purimu and Old Tutaekuri Riverbed discharges (Smith, 2014).

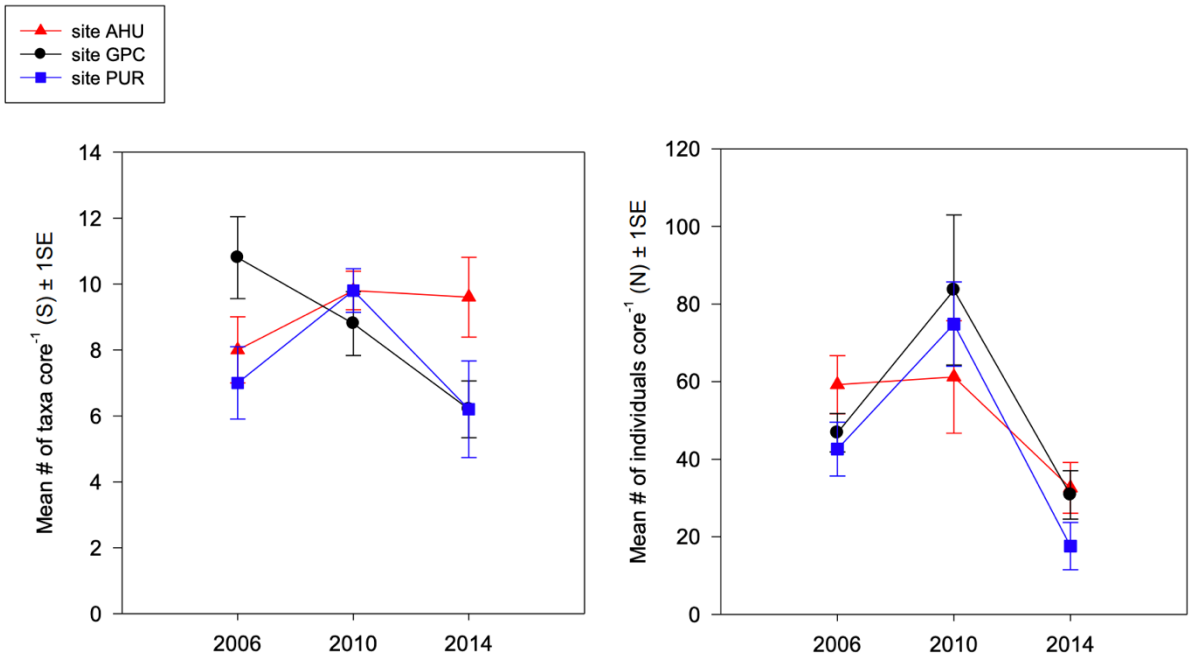

Figure 3.37: Temporal comparison of mean taxa numbers per core, and mean number of individuals per core, for surveys 2006, 2010 and 2014 (Smith, 2014).

The urban stormwater-driven ecological results from both Ludlow (2020) and Smith (2014) need to be carefully interpreted due to potential biological spatiotemporal heterogeneity; each within a limited three-round dataset.

As well as taxonomic and individual counts, previous biological studies undertaken in Ahuriri Estuary have referenced sediment toxicity to bioassays. Charry et al. (2018) selected 4 sites for 50mm surficial

sediment collection for use in elutriate toxicity testing, copepod cell counts and chemical analysis testing. Endemic bioassay *Quinquelaophonte* sp. and Australian *Gladioferens pectinatus* were isolated and grown in a controlled salinity and temperature environment. For the 14-day study, Charry et al. (2018) conducted three replicate tests using Erlenmeyer flasks with continuous water circulation; each flask containing 10g of collected sediment and 15 male and 15 female copepods. A fourth flask was organised for physicochemical analysis. For the 6 day elutriate testing, gravid *G. pectinatus* females, nauplii, and new hatchlings were exposed to the sediment samples having been centrifuged with saline water (Charry et al., 2018).

Charry et al. (2018) reported low benthic copepod survival in the sediment toxicity (Figure 3.39) and elutriate toxicity (Figure 3.40) testing when compared to a control. Testing from Waitangi estuary shows a marked overall difference comparably to the four sites in Ahuriri Estuary with Ahuriri's site B, C and D (Figure 3.38) scoring zero or close to zero percent survival rate for sediment toxicity. For elutriate testing, Charry et al. (2018) discovered little difference between sites in Ahuriri and Waitangi estuaries, yet there was a marked difference between all sites and the control. The conclusions drawn from this testing is that sediment from Ahuriri Estuary contains bioavailable chemicals which can be genotoxic and are likely to inhibit benthic and pelagic organism reproduction, particularly highlighted in samples retrieved from the Thames-Tyne and Old Tutaekuri Riverbed tributaries: a result echoing sediment quality analyses by Ataria et al. (2007), Chagué-Goff et al. (2000), Kelly (2018), Smith (2014) and Strong (2005).

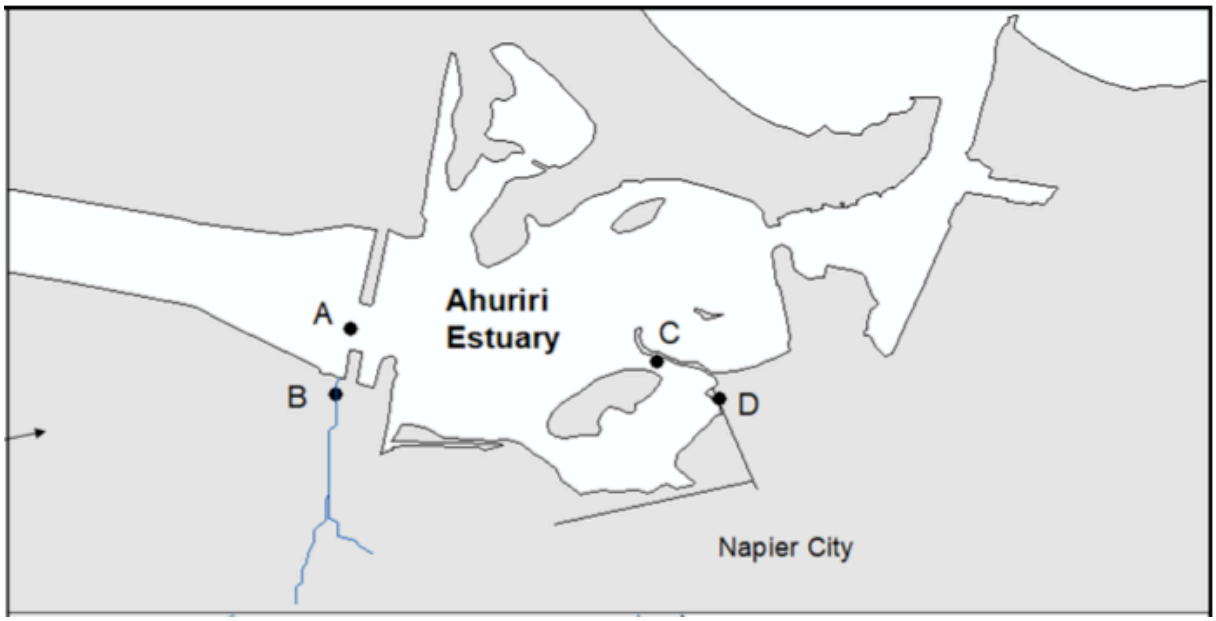

Figure 3.38: Sample sites; sediment toxicity and elutriate testing (Charry et al., 2018). Not pictured: the Waitangi Estuary sample site, on the southern border of Napier City with Hastings District.

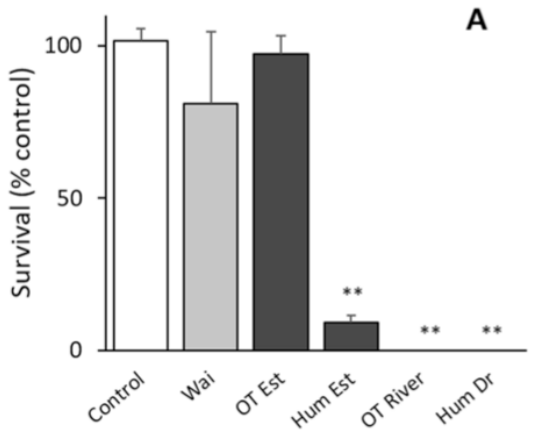

Figure 3.39: Graph A as 14-day sediment toxicity test from sites in Ahuriri and Waitangi Estuary. Columns represent site results as a percentage of survival against the control. 'Wai' - Waitangi Estuary, 'OT Est' - site A in Figure 3.38, 'Hum Est' - Site C, 'OT River' - site B, & 'Hum Dr' - site D (Charry et al., 2018).

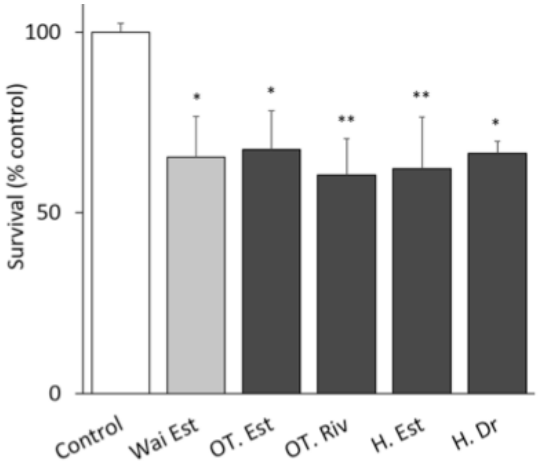

Figure 3.40: Elutriate testing from sites in Ahuriri and Waitangi Estuary as percentage survival rate against the control (Charry et al., 2018).

In a similar study to Charry et al. (2018), Heinrich et al. (2016) collected 25cm core samples at three sites representative of the Ahuriri Estuary (Figure 3.41) and in the New River Estuary in Invercargill to compare the effect of industrial activity on sediment between both estuaries using cytotoxicity, genotoxicity and ethoxyresorufin-O-deethylase (EROD) induction testing. All sediment samples retrieved from both estuaries resulted in EROD and cytotoxicity assay responses, while Humber B and the Old Tutaekuri samples show high levels of toxicity and toxic potential respectively with Humber A marginally lower than Humber B. While difficult to compare against the study by Charry et al. (2018) due to different testing methodologies, the high toxicity readings in Humber B and A from the Heinrich et al. (2016) study are consistent with the sediment toxicity survival percentage test (Figure 3.39), where 'Hum Est' or site C, and 'Hum Dr' or site D also highlight the effect of Ahuriri Estuary's tributary-affected sediment on aquatic species' biological functionality. EROD testing in the study by Ataria et al. (2007) is analogous to this Heinrich et al. (2016) study with reports of PAH concentrations in Ahuriri Estuary generating EROD responses in yellowbelly flounder.

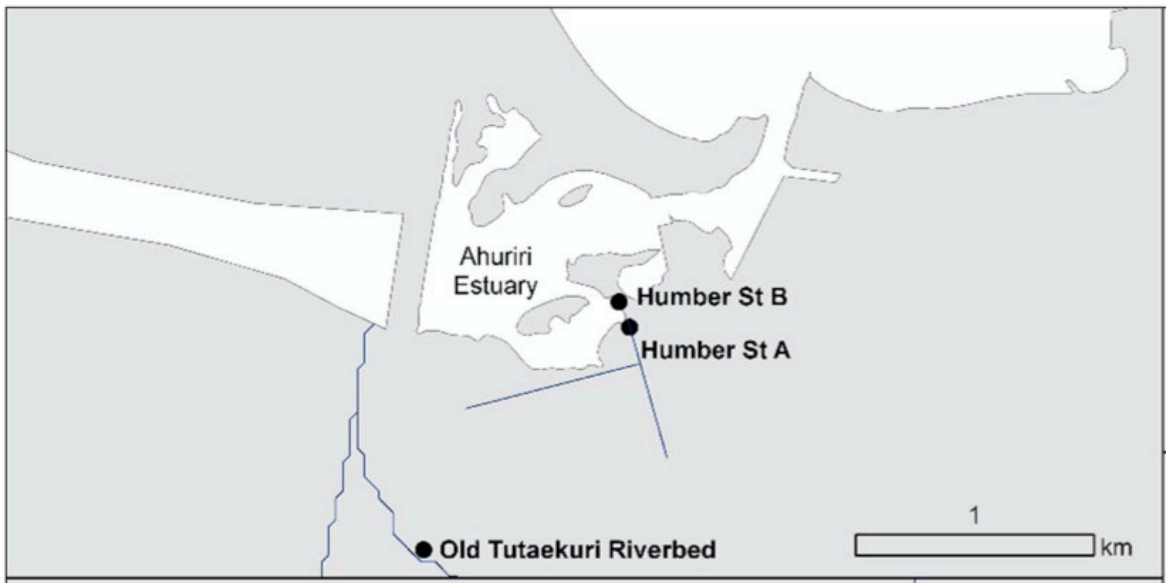

Figure 3.41: Ahuriri Estuary tributary sample sites, Heinrich et al. (2016).

Each of these studies, including those which have investigated sediment quality in part 1.4, indicate potential effects from urban tributaries on estuarine sediment quality and the subsequent benthic and pelagic functionality and community structures of Ahuriri Estuary.

3.4 Gap identification and summary: Recent Ahuriri Estuary research

Considering the coverage of the research undertaken to understand Ahuriri Estuary, a key gap has been identified. Depositional zones of tributary waterways have not been investigated with a focus on sub-catchment industrial development since 1931. Though there have been three recent sediment core sampling programs in and around Ahuriri Estuary, Chagué-Goff et al. (2000) was the only program to have collected sediment at a depth beyond 10cm within the wetted estuary proper. The three samples taken by Chagué-Goff et al. (2000), however, do not lend to identifying the effects of the major Onekawa industrial zone, nor do they focus on the effects of all major tributaries to the estuary.

To address this gap, and guided by the studies of Al-Naswari et al. (2018), Birch et al. (2016), and Swales et al. (2005) in particular, this thesis presents a three-part adapted synthesis for assessing the current health of Ahuriri Estuary and preventing further degradation:

1. A multi-temporal sub-catchment land cover change, using aerial imagery to gauge the development of Napier City's Onekawa and Pandora Industrial zones.
2. An estuarine sediment physicochemical assessment on core samples from urban tributary discharge depositional zones, identifying time markers using visual tools and chemical cues.
3. Recommendations for prevention of further degradation of Ahuriri Estuary.

Overall, the state of knowledge of Ahuriri Estuary would benefit from a cohesive catchment-based analytical approach to identifying causes and effects of the development of Napier City. Chagué-Goff et al. (2000) suggest that a record of sedimentological and chemical expressions is well preserved in sediment in the Ahuriri Estuary from the previous 100 years. This bodes well for an expansion on previous sediment core sampling work focusing on tributary depositional zones and the effect of urban contaminants. Figure 3.42 presents a flow chart on the processes within this thesis to understand the current health of Ahuriri Estuary as a result of progressive sub-catchment industrialisation.

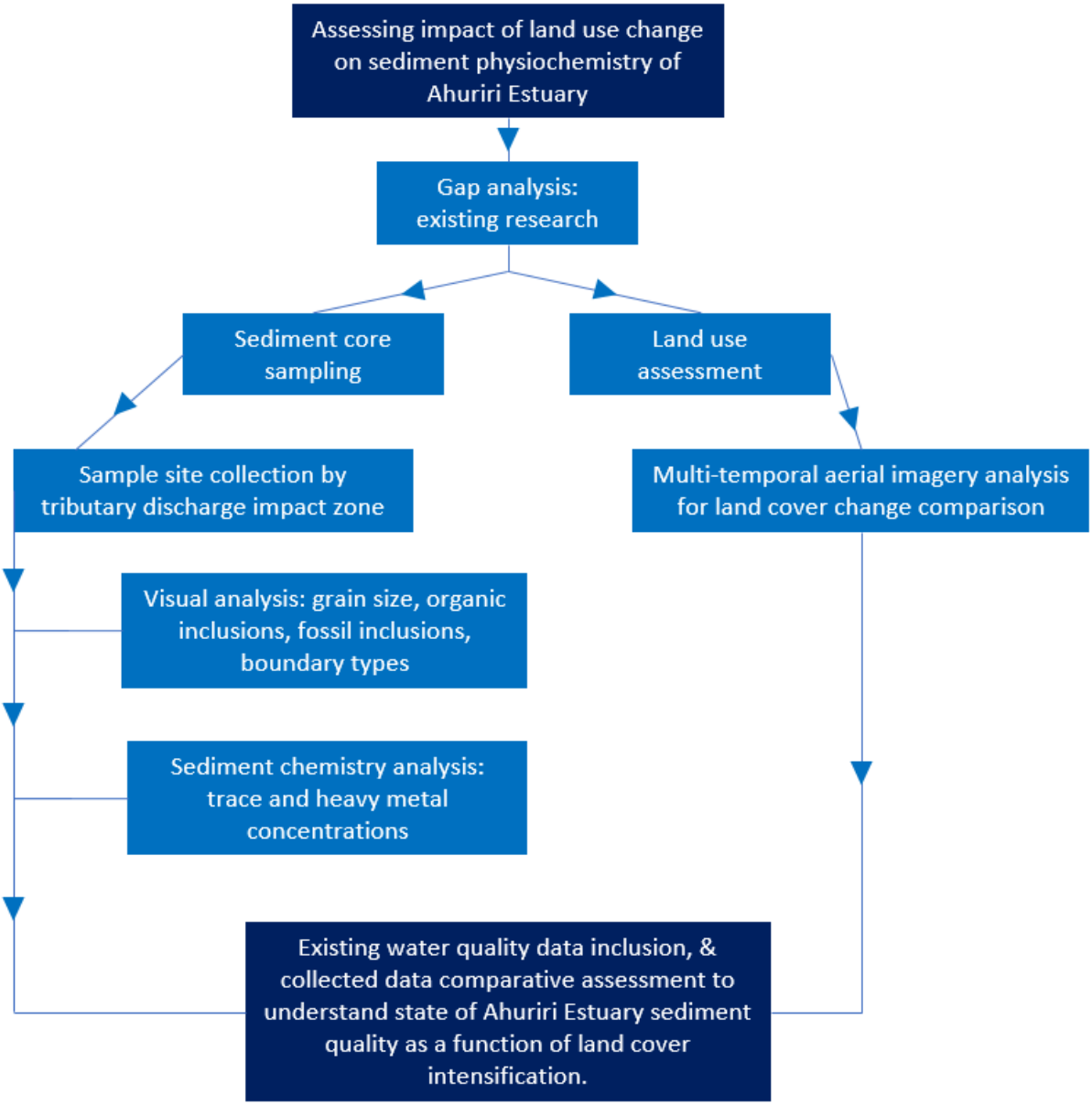

Figure 3.42: Thesis flow chart.

Objectives two, three and four will be addressed individually in the following chapters. Consolidating the findings of each objective's results will allow an informed derivation of the current sedimentary health of Ahuriri Estuary.

4 METHODOLOGY

4.1 Introduction

This chapter outlines the methodology employed to determine the effects of progressive industrialisation on the sediment quality of the Ahuriri Estuary. Two techniques were used to investigate the effect of sub-catchment industrialisation on estuarine sediment. These techniques were:

1. Multi-temporal sub-catchment land use change assessment; and
2. Estuarine sediment core sample physicochemical analysis.

This chapter will present a description of the methodologies chosen for each of the two techniques following brief reviews of available tools to undertake these analyses. These two techniques address overarching objectives two and three, being:

Objective Two: Undertake land system change analysis using aerial imagery to investigate gradual effects of industrial development on Ahuriri Estuary.

Objective Three: Utilise previous hydrodynamic modelling of the central estuary to guide sampling locations for extraction of sediment cores representing discharge depositional zones of different tributaries. Undertake physicochemical analysis on retrieved sediment core samples to investigate connections between industrial development and temporal sediment quality.

4.2 Sub-catchment change

4.2.1 Review of sub-catchment change assessment tools

Common techniques for catchment mapping to determine land use effects on surface waters include:

- Digital Elevation Modelling (DEM) for sediment mobility and catchment connectivity model development, such as per Jones (2002) and Zingaro et al. (2019);
- Multi-temporal land use change assessments based on topographic or aerial imagery such as undertaken by Arunyawat and Shrestha (2016) to determine the effects on ecosystem services such as sediment retention, habitat quality and water yield; and
- GIS-integrated software 'CLUES' (Catchment Land Use for Environmental Sustainability model) assessments of water quality parameters total nitrogen, *Escherichia* coli, sediment, and total phosphorus as a function of catchment-scale land use change (National Institute of Water and Atmospheric Research, n.d.-a).

With the majority of Napier City at low-lying elevation, a DEM becomes inappropriate for analysis with an urban-industrial focus. To understand the effect of land use change on sediment quality of the Ahuriri Estuary at a sufficient depth to reflect sub-catchment industrialisation, a multi-temporal land use assessment is required.

4.2.2 Sub-catchments of the Ahuriri Estuary

The wider Ahuriri Estuary catchment contains a multitude of land uses within several sub-catchments (Figure 2.2 and Figure 2.6). For this assessment, two sub-catchments were utilised to investigate and

demonstrate the effect of land system changes. These sub-catchments are Westshore Tidal Gates and Pandora. For mapping urban intensification over different times since the 1931 Napier Earthquake, only the industrial zones of these catchments were delineated, these being Onekawa Industrial and Pandora Industrial. These two zones represent the primary industrial activity within the Ahuriri Estuary catchment and, as such, are likely to have contributed higher concentrations of heavy metal contaminants to Ahuriri Estuary (Crane, 2019; Gadd et al., 2020; Jartun et al., 2008). It can be anticipated that the time of development of these two key industrial zones may be recognisable in the chemistry of the receiving estuarine sediment at specific depths.

There is one other industrial zone which feeds to the Ahuriri Estuary, this being in the Iron Pot catchment (Figure 2.6), to the east of the Inner Harbour. Due to its location, the Ahuriri Industrial zone does not directly impact the sediment quality of the central and upper estuary, as surface water from this zone discharges into the lower Inner Harbour.

4.2.3 Georeferencing historic imagery

Historic imagery of the Ahuriri Estuary catchment was sourced from the open source RetroLens database (RetroLens, n.d.), and the NCC internal mapping system IntraMaps (Napier City Council, n.d.-a). The boundaries of the Pandora and Onekawa Industrial zones were mapped using the NZ Imagery basemap in ArcGIS Pro (Table 4.1), guided by an NCC digital elevation model of the study area (Figure 4.3). The boundaries of the industrial zones were mapped from contemporary imagery to transpose the same boundaries to the historic images, keeping the reference area the same size.

Table 4.1: Details of imagery utilised for multi-temporal catchment change assessment - Onekawa and Pandora industrial zones. Imagery retrieved from ESRI Inc. (2019), Napier City Council (n.d.-b), Napier City Council (n.d.-c), RetroLens (2016), RetroLens (2019a), RetroLens (2019b), RetroLens (2020).

Year	Image source	Name	Type	Image size	Altitude (m)
1936	NCC IntraMaps	AerialPhotos1936	Raster dataset	N/A	N/A
1964	RetroLens	Crown_1654_3845_38 Crown_1654_3846_38	Jpg Jpg	7268 x 6903 7272 x 6907	11500
1969	RetroLens	Crown_3183_4199_25	Jpg	7228 x 6864	16500
1980	RetroLens	Crown_5752_I_18	Jpg	9015 x 8542	25000
2004	NCC IntraMaps	AerialPhotos2004	Raster dataset	N/A	N/A
2018	ArcGIS Pro default 'NZ Imagery' basemap.	NZ Imagery	Default basemap	N/A	N/A

The New Zealand Transverse Mercator (NZTM) 2000 was used as the geographic coordinate system for each map. The selected image downloaded from RetroLens was georeferenced against the default 2018 'NZ Imagery' basemap, via matching a point on the historic aerial imagery to an unchanged 'control' point on the basemap, such as an apex or corner of a roof, with an awareness that some degree of misfit was likely as the images were off nadir. A transformation was then applied to stretch the image to fit while maintaining a proportional perimeter as well as low forward and inverse residuals (Table 4.2).

Table 4.2: Applied transformation, forward residuals, inverse residuals, and number of control points for georeferencing historic aerial imagery source: RetroLens (2016), RetroLens (2019a), RetroLens (2019b), RetroLens (2020).

Name	Year	Transformation	Forward (m)	Inverse (m)	Forward-Inverse (m)	Control points
Crown_1654_3845_38	1964	Adjust	0.000016	0.000015	0.000019	13
Crown_1654_3846_38	1964	Spline	0.000008	0.000004	0.000013	13
Crown_3183_4199_25	1969	Spline	0.0	0.0	0.000007	15
Crown_5752_I_18	1980	Spline	0.0	0.0	0.000007	14

Imagery downloaded from the NCC IntraMaps system had been previously georeferenced in NZTM coordinates by default, so did not require further transformation.

4.2.4 Defining land use changes

Figure 4.1 outlines the process taken for undertaking the multi-temporal sub-catchment industrialisation assessment. The first step in deciphering land use changes across the six chosen years was to define a boundary polygon covering the Pandora and Onekawa industrial zones together. This would become the reference polygon copied to each of the six maps to allow comparison of changes within a set 293.5ha area. Onekawa and Pandora industrial zones were defined by recognising the large size of industrial buildings and the high reflectivity of impervious land, as well as visual cues for overland flow paths such as railway lines (which are typically elevated compared to surroundings) and main highways. Comparatively, residential zones typically have smaller building footprints, coloured roofs, and a higher area of grassy or vegetated ground. Knowledge of the piped stormwater network (Figure 4.2) and the low topography of the industrial areas (Figure 4.3) was also utilized.

Once the boundary of the polygon was delineated, 'merge' and 'split' editing tools were used to define the Pandora and Onekawa Industrial zones, at a 1:3536 scale for consistency. Major waterways and drainage channels were split inclusive of an approximately 5m bank width. In the polygon attribute table, key fields were added to categorise land-use, relevant catchment and suburb, allowing colour differentiation of each sub-classification. Attribute tables for each of the six years were then copied into Microsoft Excel to utilise graphing and statistical comparison functions for area change assessments.

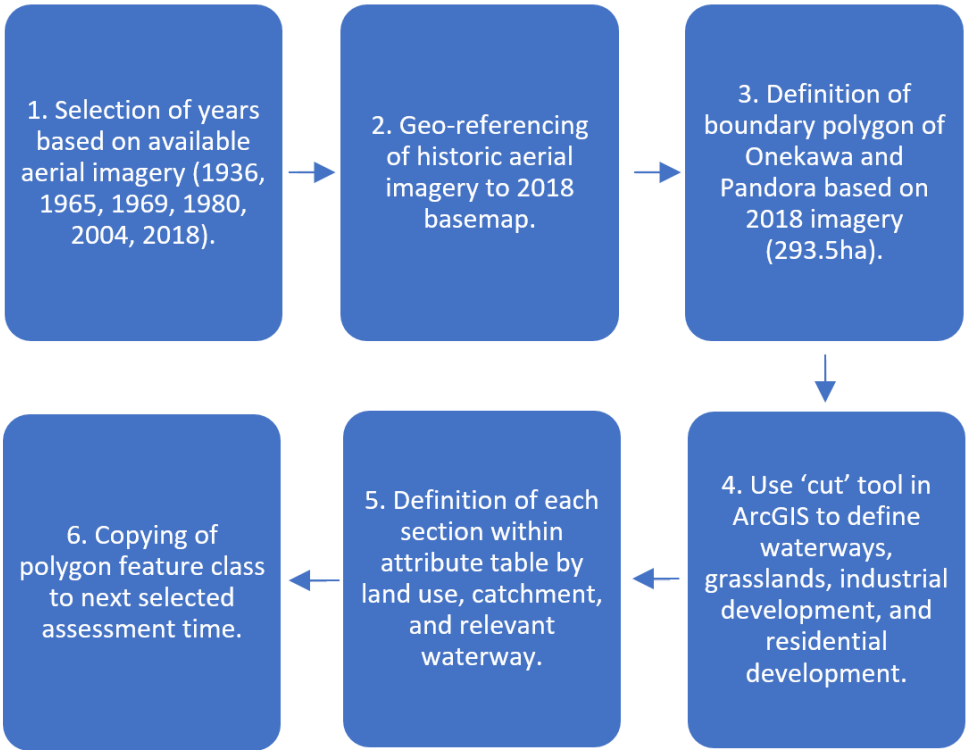

Figure 4.1: Flow chart process for georeferencing historic aerial imagery and defining land use for multi-temporal sub-catchment industrialisation assessment.

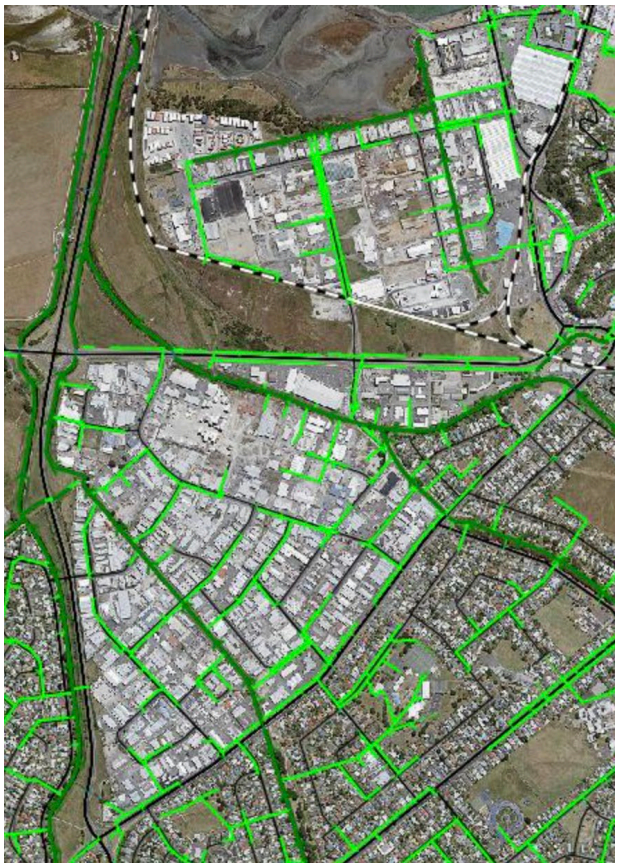

Figure 4.2: Aerial map of piped stormwater mains; Pandora and Onekawa Industrial zones, Napier City (Napier City Council, n.d.-f).

Figure 4.3: LiDAR 1m contour topographic map, Pandora and Onekawa industrial zones, Napier City. Image captured at 5424m elevation (Napier City Council, n.d.-e)

4.3 Sediment physicochemistry

4.3.1 Review of sediment core sampling techniques

While use of a manually operated surface dredge is common in surficial sediment sampling, sediment core sampling provides a visual and tactile representation of unbroken sub-surface geomorphology. Compared to other core extraction methodologies, single-drive vibracoring is advantageous for environments with a high water content such as alluvium or marine sediment (Finkl & Khalil, 2005) as vibrations reduce compaction by overcoming the high friction of water-saturated sediment. A vibracoring rig was used for sediment core sample collection for this thesis due to the saturated and unconsolidated nature of the estuarine sediment, and for its ease of use for sample collection. Collection of unbroken cores also provided appropriate samples for the scanning of heavy metals.

4.3.2 Review of sediment chemistry analysis methodologies

Laboratory analysis for sediment chemistry typically involves sub-sampling (Kelly, 2018) and x-ray fluorescence (XRF) (Tjallingii et al., 2007; University of Otago, n.d.). Analysing sub-samples using acid digestion, sieving (Buggy & Tobin, 2008) and Inductively Coupled Plasma-Mass Spectrometry (ICPMS) (Crane, 2019) can result in a loss of resolution through homogenisation as analysis for heavy metal concentrations requires at least 100g of dry sediment (A. Heron, personal communication, September 29, 2020). An advantage of concentration-based methodology of testing is in the provision of qualitative results standardised units such as mg/kg dry weight allowing for straightforward comparison to common estuarine health assessment guideline standards such as the ANZECC sediment ISQG-high and ISQG-low levels for species protection (Kelly, 2018).

In the case of the Ahuriri Estuary sediment core samples, surficial scanning using an Itrax™ XRF Corescanner was selected due to the ability to scan whole, unbroken core lengths and count concentrations of heavy metals with a far higher resolution than sub-sampling (Jarvis et al., 2015; MacLachlan et al., 2015). This provided high-resolution readings at the millimetre scale: an advantage for relating peaks in concentrations to depositional timeframes considering Chagué-Goff et al. (2000) estimates of Ahuriri Estuary's SAR were in the order of 3-6mm per annum. Ideally, a combination of both ICP-MS and Itrax would be used to convert spectral peaks into quantitative measurements, though this was beyond the scope of the study.

A limited number of XRF core scanning studies have utilised Itrax™ methodologies to assess heavy metal pollution in estuarine sediment in New Zealand. The studies that have undertaken Itrax™ heavy metal assessments have typically included assessments of organic elements such as calcium (Ca) and silicon (Si) to investigate sediment type, as well as the incoherent/coherent scatter ratio as a proxy for organic matter and interstitial water content (Davies et al., 2015; Rodríguez-Germade et al., 2014; Rodríguez-Germade et al., 2015). Within these studies, elemental data is often normalised against the incoherent value to reduce the interference that a high water content may have on Itrax™ elemental counts per second (CPS) (Rothwell & Croudace, 2015). Investigation to date suggests that elements such as Ca and Si are much more sensitive to water content than heavy metals (MacLachlan et al., 2015).

The ratios potassium/incoherent scatter (K/Inc) and bromine/incoherent (Br/Inc) can be used in conjunction in estuarine cores to determine relative changes in terrigenous and marine content

(Rodríguez-Germade et al., 2014; Rothwell & Croudace, 2015). A study by Rothwell and Croudace (2015) suggests that bromine can be used as an indicator of high marine organic matter as it occurs in crustal rocks and marine organisms synthesize bromine compounds. Therefore, a high Br normalized to the incoherent value (Br/Inc) implies high marine organic influence. Comparatively, Rothwell and Croudace (2015) explain that terrestrial sediment is poor in bromine, though high potassium counts can indicate the presence of land-derived siliciclastics. The authors discuss that normalising counts can reduce interference in scanning of varying interstitial water content and sediment organic levels.

4.3.3 Site selection

Site selection for Ahuriri Estuary core sampling was based on the sediment quality gaps identified in Ataria et al. (2007) and Chagué-Goff et al. (2000) as well as the sediment transport, hydrodynamic and erosion modelling by Eyre (2009). Site selection has also been informed by the requirement to identify the effect of industrial sub-catchments on sediment metal concentrations in tributary depositional zones of Ahuriri Estuary; a gap identified in the review of recent literature on the Ahuriri Estuary.

Three of six samples in the central estuary (being SCAE, TT, and OTRB in Figure 4.4) were collected from intertidal mudflats due to their higher potential for accreting metal-contaminated fine sediment from urban tributaries, as well as ease of accessibility. Sample PUR was collected from a subtidal zone as there is no intertidal mudflat at the point where the Purimu Stream discharges into the estuary. While there exists an intertidal zone opposite the Purimu tidal gate, the discharge is mostly swept under the State Highway 2 Bridge meaning the opposite intertidal area is too far from the discharge impact zone. The remaining two subtidal cores were collected from the Taipo discharge zone (TAI) and in the upper estuary (UAE). Site UAE was selected due to its distance from tributary discharges and its subsequent ability to act as a control site. Figure 4.5 shows the six selected core sample collection sites.

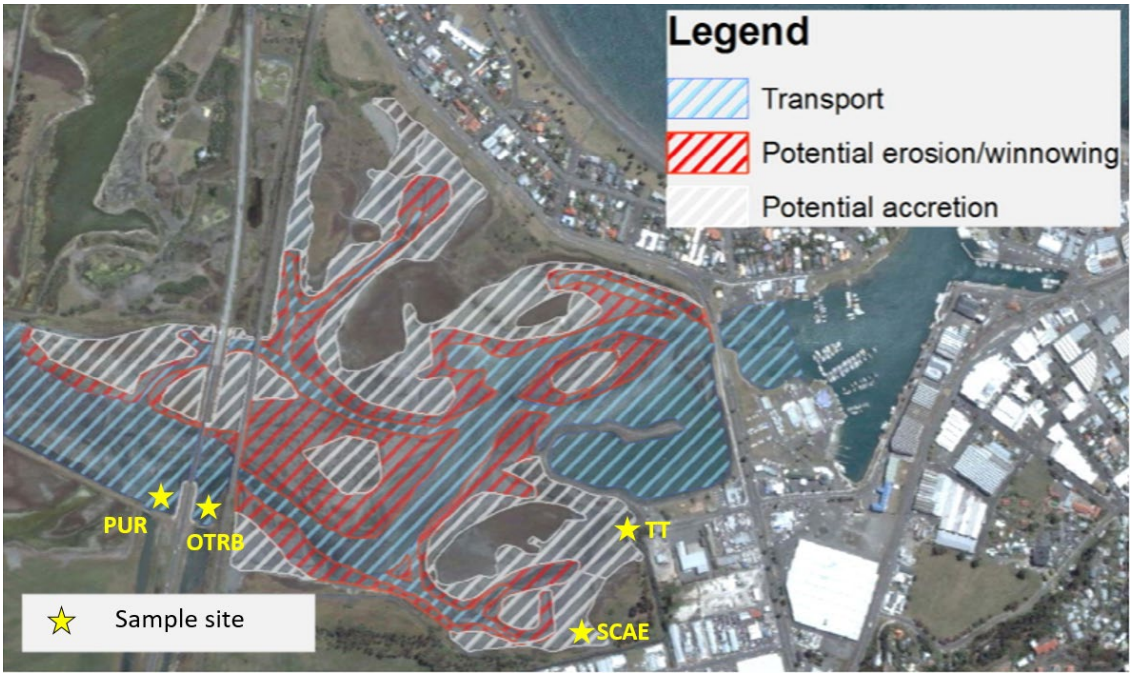

Figure 4.4: Superimposed Central Ahuriri Estuary sediment core sampling sites, over modelled pattern of sedimentation, Ahuriri Estuary by Eyre (2009)

Figure 4.5: Superimposed sediment core sampling sites, Ahuriri Estuary. Image taken from 5404m elevation (Google, n.d.-a).

4.3.4 Sample collection

Sampling was undertaken over four different days, as three of the core samples informed an additional NCC project. Sampling was undertaken as close to low tide as possible for ease of accessibility to the intertidal zones. Sample depths varied with compaction rates and with site-specific drilling capabilities. Collection dates, times, tidal stages, site locations, sample lengths and compaction measurements are as per Table 4.3.

Samples were collected in 80mm diameter 1.25m length aluminium barrels. A petrol generator powered an electric pneumatic concrete vibrator (PCV) which was inserted into a welded t-shaped steel attachment bolted to each barrel. With the generator and PCV switched on, the vibrating aluminium barrel was guided into the estuarine sediment until approximately the top 20cm of the barrel remained above the sediment surface. Compaction was measured by the difference between the internal and external distance from the top of the barrel to the sediment. A drain twist plug was inserted into the top of the barrel to create a vacuum seal, and the barrel was hoisted by a chain block supported by a steel tripod. Once the barrel was retrieved, the base was tightly plugged with paper towels and taped. The welded attachment and the drain plug were removed and the top end was tightly plugged with paper towels in the same manner. The core barrel and each end were labelled ready for processing.

For the low energy environment TAI and UAE samples, the sediment was too fine for safe wading. In the interest of safety, the 80mm aluminium barrel was pushed into the sediment by hand for these two sites only metres from the banks. This avoided the requirement to wade and the use of machinery for retrieval. Compaction readings for TAI and UAE were not excessive considering the range of readings from the other cores (Table 4.3).

Table 4.3: Site, date, tide, and compaction details for collected sediment core samples, Ahuriri Estuary.

Code	Site	Zone	NZGD 2000	NZGD 2000	Sample date	Sample time	Tidal stage	Sample depth (cm)	Int. to sediment (cm)	Ext. to sediment (cm)	Compaction (cm)
TT	Thames-Tyne discharge zone	Central Estuary	176 53 14.09494 E	39 29 12.87716 S	9/11/2020	6:30am	Low	70.0	51.0	47.0	4.0
SCAE	South-Central Ahuriri Estuary	Central Estuary	176 53 11.45226 E	39 29 19.51524 S	9/11/2020	9:30am	Low tide +3hr	100.0	16.1	20.2	-4.1 (expansion)
OTRB	Old Tutaekuri Riverbed discharge zone	Central Estuary	176 52 36.41533 E	39 29 11.77010 S	8/1/2021	8:00am	Low tide	75.0	32.0	21.0	11.0
PUR	Purimu discharge zone	Central Estuary	176 52 31.43829 E	39 29 11.06082 S	8/1/2021	6:30am	High tide +5hr	92.0	20.5	13.5	7.0
TAI	Taipo discharge zone	Main channel	176 50 47.74756 E	39 28 58.91307 S	11/1/2021	1:45pm	Low tide +3hr	84.0	39.5	21.5	18.0
UAE	Upper Ahuriri Estuary	Upper Estuary	176 50 06.06087 E	39 28 14.57394 S	17/11/2020	3:30pm	Low tide +1hr	58.0	65.0	60.0	5.0

4.3.5 Processing & visual analysis

Core barrels were split lengthways by cutting two lines at 180° to each other along the length of each barrel (Figure 4.6). The paper towels which acted as a holdfast in the field were aligned in one of the half barrels, which was then shrink wrapped, labelled and inserted into layflat plastic for shipping to Otago University. The other half barrel was assessed against a tape measure from the top of the core downwards for grain size, fossil and gravel inclusions, layer boundary types, and colour using a Munsell® Soil Color Chart. Once analysed, sediment from the visual analysis half barrel was segmented into 10cm blocks, placed in plastic zip bags and frozen as back-ups in the instance of core scanning errors.

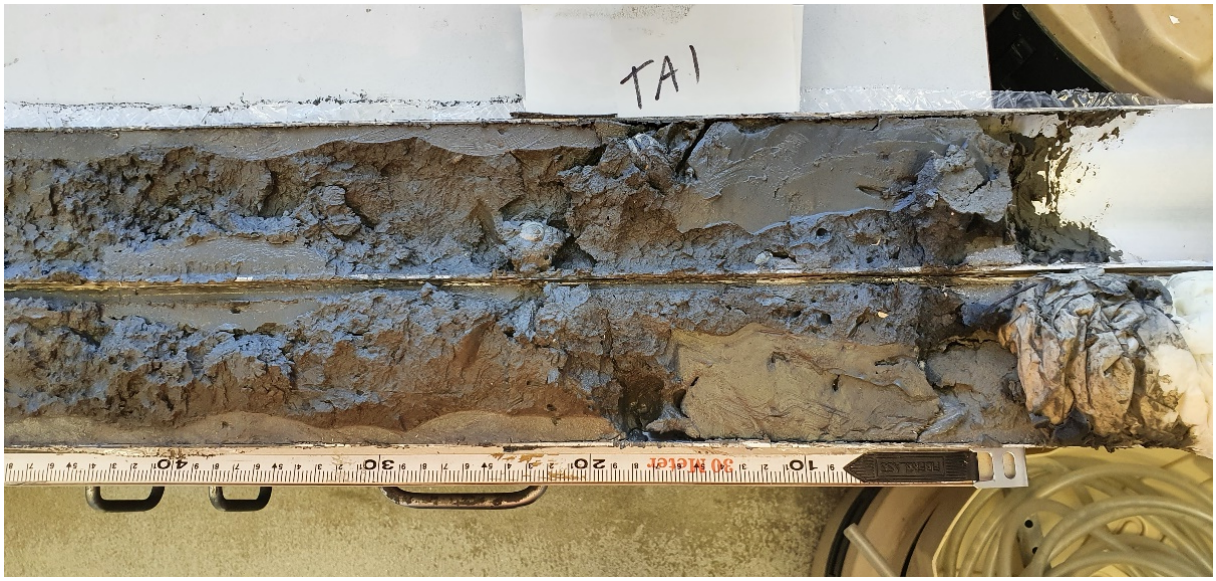

Figure 4.6: Split barrel of upper 50cm of TAI core sample prepared for visual analysis. One half of each barrel is plugged at the ends and shrink wrapped in preparation for shipping to the University of Otago.

4.3.6 Storage & shipping

Core samples prepared for shipping to Otago University were kept refrigerated at 4°C until shipping to prevent algal growth which may have otherwise interfered with sediment core scanning. Controlled temperature shipping from Palmerston North to Dunedin at 5°C minimised the risk of algal growth.

4.3.7 Itrax™ laboratory analysis

Sample analysis was undertaken by University of Otago staff using a Cox Analytical Systems Itrax™ XRF Corescanner (University of Otago, n.d.). A molybdenum (Mo) tube was used for scanning each of the six cores. It is noted that the Mo tube is less accurate for the scanning of lighter elements compared to a chromium (Cr) tube. Preparing samples for analysis involved grinding of bivalves and exposed gravels to ensure a flat surface for scanning. Scan lengths, resolutions, and exposure times for each of the six samples are as per Table 4.4.

Table 4.4: Total scan length, resolution, and exposure time and sample reparation details for the six Ahuriri Estuary sediment core samples.

Sample name	Scan length	Resolution	Exposure time
UAE	580mm	2mm	50s
TAI	840mm	3mm	50s
PUR	920mm	2mm	50s
OTRB	750mm	2mm	50s
SCAE	1000mm	2mm	50s
TT	700mm	2mm	50s

4.3.8 Data analysis

4.3.8.1 Sediment physiology

To calculate the true length of the sample without in-field compaction, the length of collected sediment plus the compaction (internal – external measurement from the top of the barrel) was divided by the length of material in the core. Equation 1 exemplifies the compaction ratio calculation from the PUR sediment core.

Equation 1: Compaction ratio calculation for PUR sediment core sample.

$$Compaction\ ratio\ (PUR) = \frac{Compacted\ length + compaction}{Compacted\ length} = \frac{920 + 70}{920} = 1.076$$

True layer depths from compaction ratio calculations as well as results of visual analysis were compiled using a combination of the digital stratigraphic log tool sedlog-3.1, and InkScape 1.0beta2.

4.3.8.2 Itrax™ sediment chemistry

Analysis of sediment chemistry was undertaken using Microsoft Excel version 16.5. Data was provided and graphed in counts per second (CPS), as opposed to a running mean, to identify the scale of individual peaks which may indicate individual pollution events. Overall CPS and validity provided an insight into each segment's results reliability, where a '0' for validity was indicative of the scanner lifting off the surface of the sediment. As such, validity '0' indicates an unreliable reading.

Raw heavy metal counts for copper, chromium, zinc and lead were plotted against scan depths that were corrected for compaction. These four elements in particular were selected due to their frequent quantification in various research undertaken previously in Ahuriri Estuary, and their subsequent discovered prominence in the depositional zones of industrially influenced waterways. Lead data was unavailable for the Upper Ahuriri Estuary (UAE) and Purimu (PUR) cores. Arsenic, mercury and cadmium were investigated for each of the six cores though no significant trends were found to justify their inclusion into the analysis. The ratios K/Inc and Br/Inc were also plotted to give insight into terrigenous content and marine organic matter, respectively. The Inc/Co values were investigated as MacLachlan et al. (2015) suggest that a water content of above 40% can affect peak areas of lighter elements such as silicon and calcium. However, the Inc/Co ratio was not included in the analysis as research to date on the relationship of water content to peak area and CPS reliability in the heavy metals Zn, Cr, Cu, and Pb is limited.

4.3.9 Caveats

It is important to note a particular effect that may emerge in the surface layer of the sediment core samples, being the occurrence of one of Napier City's largest flooding events on record of 247mm in 13hr, which occurred on 9/11/2020; immediately after the collection of TT and SCAE cores used to inform this thesis. While the feeding catchment to these sites - the Pandora Industrial zone - has few un-sealed sites or sites in development which may have contributed to sediment settling in the estuary due to this flood event, it is likely that the adjoining Mataruahou (Napier Hill) catchment would have contributed to sediment loading. It is not unreasonable to expect all other cores to show a recently deposited flood sediment layer and, therefore, surface readings between the two cores retrieved on 9/11/2020 and the remaining five core samples may show slight differences.

Three of six sediment cores were retrieved as part of a similar NCC project to assess sediment quality of the Thames-Tyne network. Resultantly, Munsell® Soil Color Chart assessments were only undertaken for three cores. In relation to colour determination, it is also recognized that Munsell® comparison can be subjective and down to the individual.

With Itrax™ data expressed in CPS, and the majority of previously collected sediment chemistry data in the literature expressed as weight ratios, cross-comparison between the two is extremely limited. However, as aforementioned, Itrax™ was selected in this thesis due to its ability to profile whole, unbroken cores at a higher resolution for detecting pollution 'events' than sub-sampling for mass spectrometry would allow.

4.4 Summary

Assessing the effect of progressive sub-catchment industrialisation on the sediment quality of Ahuriri Estuary has been undertaken in stages:

1. Sub-catchment assessments including historic aerial imagery to support changes in grain size ratios and concentrations of metals at different depths.
2. Sediment core collection in depositional zones of tributaries. Site selection was guided by the hydrodynamic and sediment transport models by Eyre (2009), the historic core sites of Chagué-Goff et al. (2000) and by the surficial sediment quality results of Kelly (2018) which show zones of metal concentrations adjacent to the estuary tributaries. Sediment cores then prompted:
    a. visual assessment including grain size, colour, inclusions, and structure; and
    b. Itrax™ XRF core scanning to determine heavy metal counts.
    c. assessment of heavy metal peak chronology using SAR previously derived by Chagué-Goff et al. (2000)

The results of the multi-temporal sub-catchment change assessment are presented in Chapter 5. The results from sediment core sampling results can be found in Chapter 6. The results from both techniques will be interpreted in the discussion in Chapter 7 to determine the effect of sub-catchment industrialisation on the health of Ahuriri Estuary.

5 RESULTS: SUB-CATCHMENT CHANGE

5.1 Introduction

This chapter presents the results obtained from undertaking a multi-temporal sub-catchment land use analysis focusing on two major industrial zones in the immediate vicinity of Ahuriri Estuary. This multi-temporal sub-catchment assessment for the Pandora and Onekawa Industrial zones will assist in the determination of the effects of industrial intensification on the sediment quality of the Ahuriri Estuary.

The Pandora Industrial area is zoned to support heavy, wet industrial activity such as tanneries, galvanisers, slaughterhouses, hydro-excavators, fuel stations, timber treatment facilities and wineries, as well as mechanics, fertiliser works, and container yards (Napier City Council, 2011). The Onekawa Industrial area is zoned to support general industrial processes (Napier City Council, 2011). Under the Hawke's Bay Waterway Design Guidelines, many of these processes pose a relatively high risk to surface water quality with a high likelihood of sediment and metal mobilisation (Hawke's Bay Regional Council, 2009a).

As outlined in Chapter 4, the six years selected for investigating the development of the Onekawa and the Pandora Industrial zones were 1936, 1964, 1969, 1980, 2004, and 2018. This chapter presents the results of each year covered in the assessment of the Onekawa and Pandora Industrial zones and ends with a summary of observations. Observations made of features outside the fixed area of focus which may have additionally impacted the sediment quality history of the estuary are also noted.

This chapter aligns with Objective Two being:

Undertake land system change analysis using aerial imagery to investigate gradual effects of industrial development on Ahuriri Estuary.

5.1.1 Ahuriri Estuary catchment change

The modern Ahuriri catchment can be considered relatively young. This is due to the uplift of Napier City that resulted from the 1931 earthquake converting the Ahuriri Lagoon to a tidally dominant estuary. This project has a particular focus on heavy metal concentrations in estuarine sediment through Itrax™ XRF scanning of six estuarine core samples. Therefore, only the industrial zones of the Pandora and Onekawa sub-catchments were delineated (Figure 5.1) in the land use assessment to explore industrial progression since the 1931 Napier Earthquake. These two zones represent the primary industrial activity within the Ahuriri Estuary catchment and, as such, are likely to have contributed higher concentrations of heavy metal contaminants to Ahuriri Estuary (Crane, 2019; Gadd et al., 2020; Jartun et al., 2008) via the intersecting major urban tributary waterways. It can be anticipated that key developmental stages of these two industrial sub-catchments may be recognisable in the sediment geochemistry at specific depths of the cores recovered from the estuary.

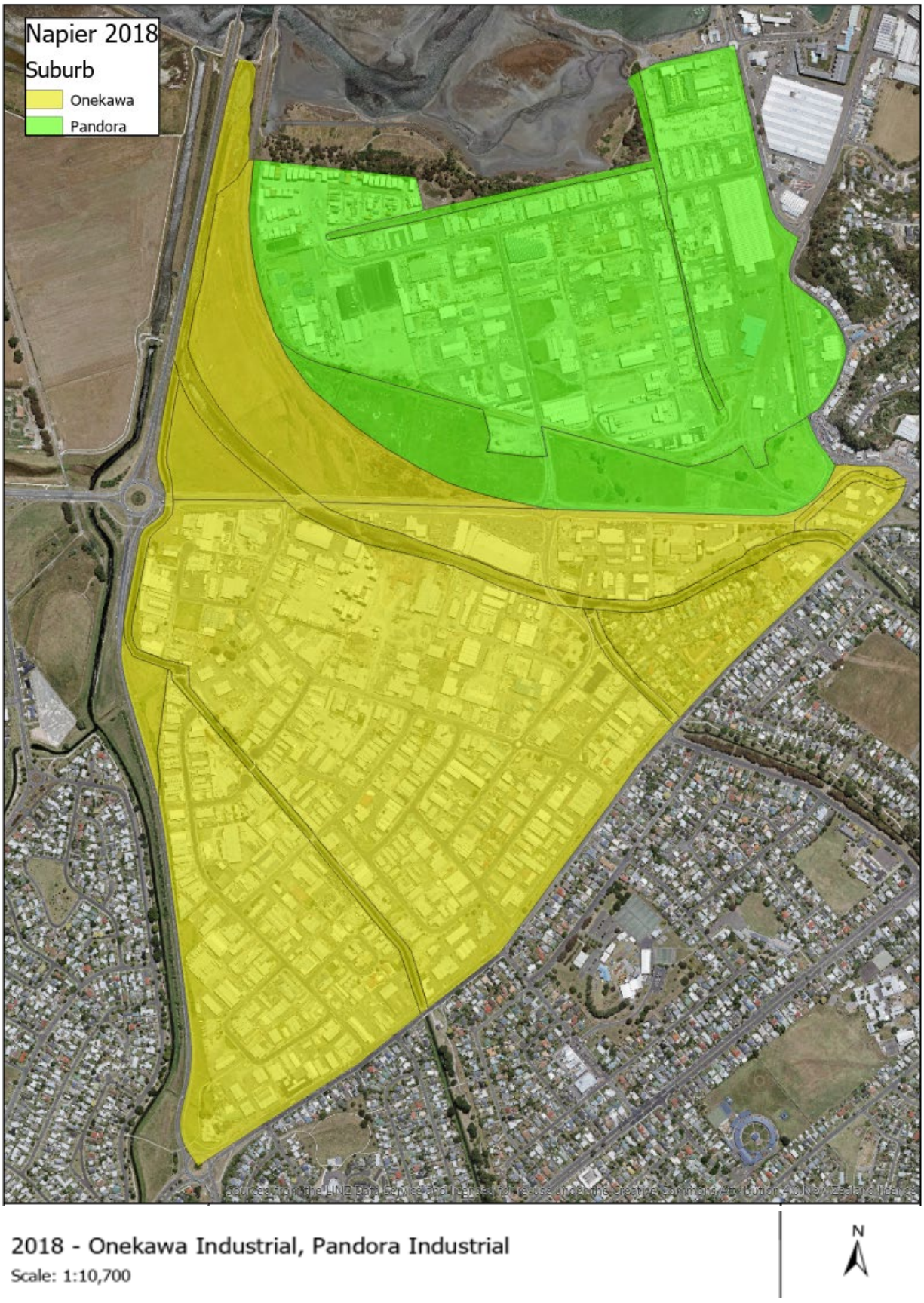

Figure 5.1: Reference polygon coverage of Onekawa (yellow) and Pandora (green) industrial zones, overlying 2018 aerial imagery.

5.2 Sub-catchment development – Onekawa and Pandora industrial zones

5.2.1 Onekawa & Pandora - 1936

The 1936 imagery is the earliest aerial imagery in the analysis and does not contain buildings or impervious surfaces within the 293.5ha reference area (Figure 5.2). The area is dominated by 254.8ha of grasslands intersected by 17.96ha waterways and drainage channels in the Onekawa suburb, and 20.7ha of estuary in Pandora. The first sign of infrastructure within the catchments is the Napier railway line, which acts as the topographic boundary for overland flow between what would eventually become the Onekawa and Pandora industrial zones.

There is evidence of waterway channelization in the 1936 imagery, with both the Plantation and the County Waterways running mostly linearly, prior to their confluence with the Old Tutaekuri Riverbed (OTRB). The meandering OTRB is a dominant feature within the polygon, with a larger width than the County and Plantation Waterways. The OTRB forms a wetland at its discharge to Ahuriri Estuary at the northwest of the polygon.

Within the polygon area, Ahuriri Estuary is visible at the north of the Pandora catchment, fringed by an apparent track or drainage channel. The 1936 imagery may also feature further wetland landforms connected to the Ahuriri Estuary, however, the high contrast of the aerial photograph has made some features difficult to perceive, so a conservative approach to land use mapping has been taken. Outside of the polygon area in the 1936 imagery, Embankment Bridge and Westshore Bridge marking the bounds of the central estuary have been constructed.

Table 5.1 shows areas of different land use categories in Onekawa, Pandora, and overall.

Table 5.1: 1936 land use types and areas per sub-catchment.

Napier 1936					
Total area (ha)		Onekawa (ha)		Pandora (ha)	
Total area	293.5	Total area	184.4	Total area	109.1
Estuarine	20.7	Estuarine	0.0	Estuarine	20.7
Grasslands	254.8	Grasslands	166.4	Grasslands	88.40
Industrial	0.0	Industrial	0.0	Industrial	0.0
Residential	0.0	Residential	0.0	Residential	0.0
Waterway	18.0	Waterway	18.0	Waterway	0.0

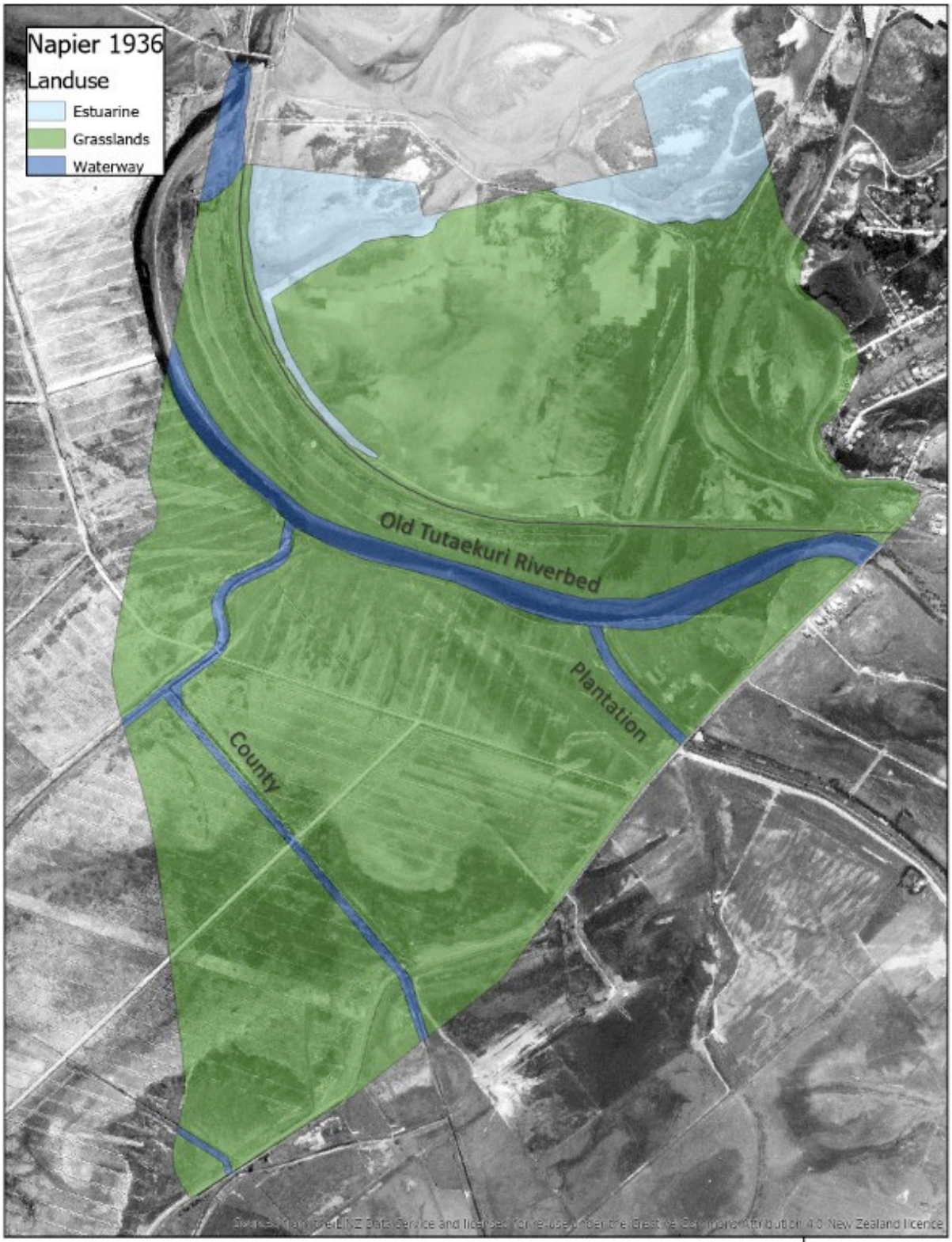

Figure 5.2: Land cover, Onekawa and Pandora, Napier, 1936. Base image source from (Napier City Council, n.d.-b).

5.2.2 Onekawa & Pandora - 1964

The two 1964 georeferenced aerial images from RetroLens highlight the rapid expansion of Onekawa's industrial and residential areas and the early developmental stages of the Pandora industrial zone. The primary zone of development sits between the County Waterway and the Plantation Waterway's confluence with the OTRB. An associated reduction in grassland area in Onekawa from 166.4ha in 1936 compared to 85.5ha in 1964, and a reduction in waterway widths to 14.1ha, has allowed for the development of 76.5ha of industrial land use (Table 5.2). The OTRB waterway has visibly reduced in width to accommodate this expansion (Figure 5.3), with development beginning to line the waterway banks, reducing pervious area within the sub-catchment and reducing available opportunity for ground soakage prior to rainfall run-off entry into the waterway. The County Waterway and Plantation Waterway pump stations have been developed, indicating the desire to create reliable flow in the low-elevation waterway channels.

In the Pandora industrial area, the southern margin of Ahuriri Estuary edge as seen in the 1936 aerial imagery has been pushed north to expand habitable grassland area. No estuary area is recovered within the bounds of the polygon from this time onward. The Tyne Waterway has been defined, and the beginnings of the Thames Waterway are visible, though the discharge point to the estuary is via the west of the Pandora sub-catchment compared to its modern confluence with the Tyne. In Pandora in 1964, 8.0ha of early industrial development was present, comprising 7.3% of the total catchment area.

Table 5.2: 1964 land use types and areas per sub-catchment.

Napier 1964					
Total area (ha)		Onekawa (ha)		Pandora (ha)	
Total area	293.5	Total area	184.4	Total area	109.1
Estuarine	0.0	Estuarine	0.0	Estuarine	0.00
Grasslands	179.7	Grasslands	85.5	Grasslands	94.2
Industrial	84.5	Industrial	76.5	Industrial	8.0
Residential	8.2	Residential	8.2	Residential	0.0
Waterway	21.1	Waterway	14.1	Waterway	7.0

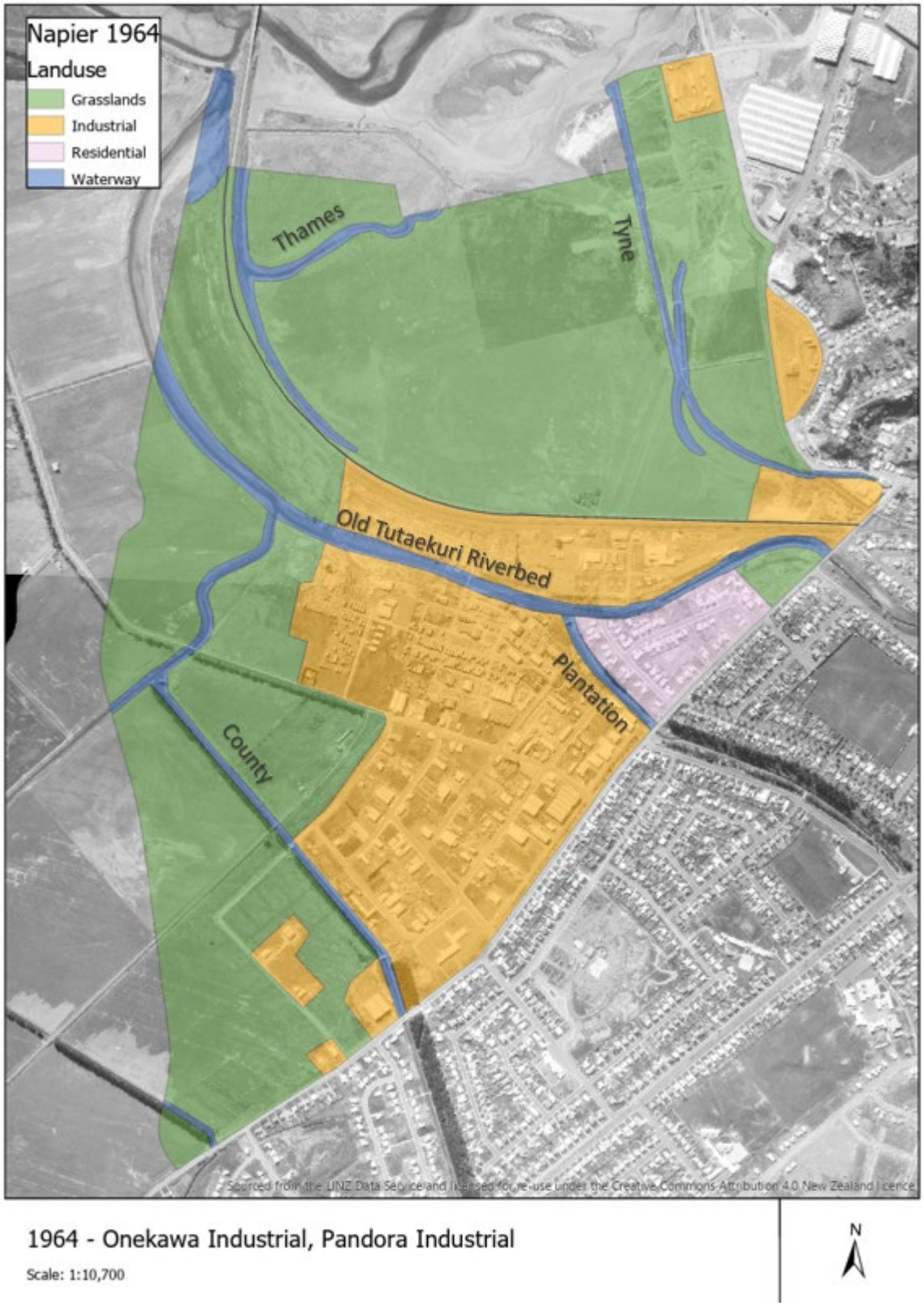

Figure 5.3: Land cover, Onekawa and Pandora, Napier, 1964. Base images source from RetroLens (2019a) and RetroLens (2019b).

5.2.3 Onekawa & Pandora - 1969

A marked increase in industrial development in both Onekawa and Pandora occurred in the five years between 1964 and 1969 (Figure 5.4). Since 1936, overall grassland area reduced by 49% (129.88ha), with 49.81ha grasslands converted between 1964 and 1969 alone to accommodate new industrial development (Table 5.3). All new development in the Onekawa area is focused along the true left bank of the County Waterway.

Thames Waterway has been channelised, and the stream is extended to meet the Tyne Waterway. Prior to the newly formed Thames-Tyne confluence, the Thames Waterway connects directly to Ahuriri Estuary in the absence of the modern estuary walkway. In the Pandora Industrial zone, development largely focused along the southern margin of the newly delineated Thames Waterway, with an additional extension to a developed area in the northeast of the polygon. In the georeferenced background imagery, there is an apparent wetted area increase at the southern edge of the Tyne Waterway. However, seeing as the 1964 imagery did not show this feature, the 1969 imagery may have been captured after heavy rainfall, for example.

Table 5.3: 1969 land use types and areas per sub-catchment.

Napier 1969					
Total area (ha)		Onekawa (ha)		Pandora (ha)	
Total area	293.5	Total area	184.4	Total area	109.1
Estuarine	0.0	Estuarine	0.0	Estuarine	0.0
Grasslands	129.9	Grasslands	62.5	Grasslands	67.4
Industrial	131.4	Industrial	97.8	Industrial	33.5
Residential	9.9	Residential	9.9	Residential	0.0
Waterway	22.4	Waterway	14.1	Waterway	8.2

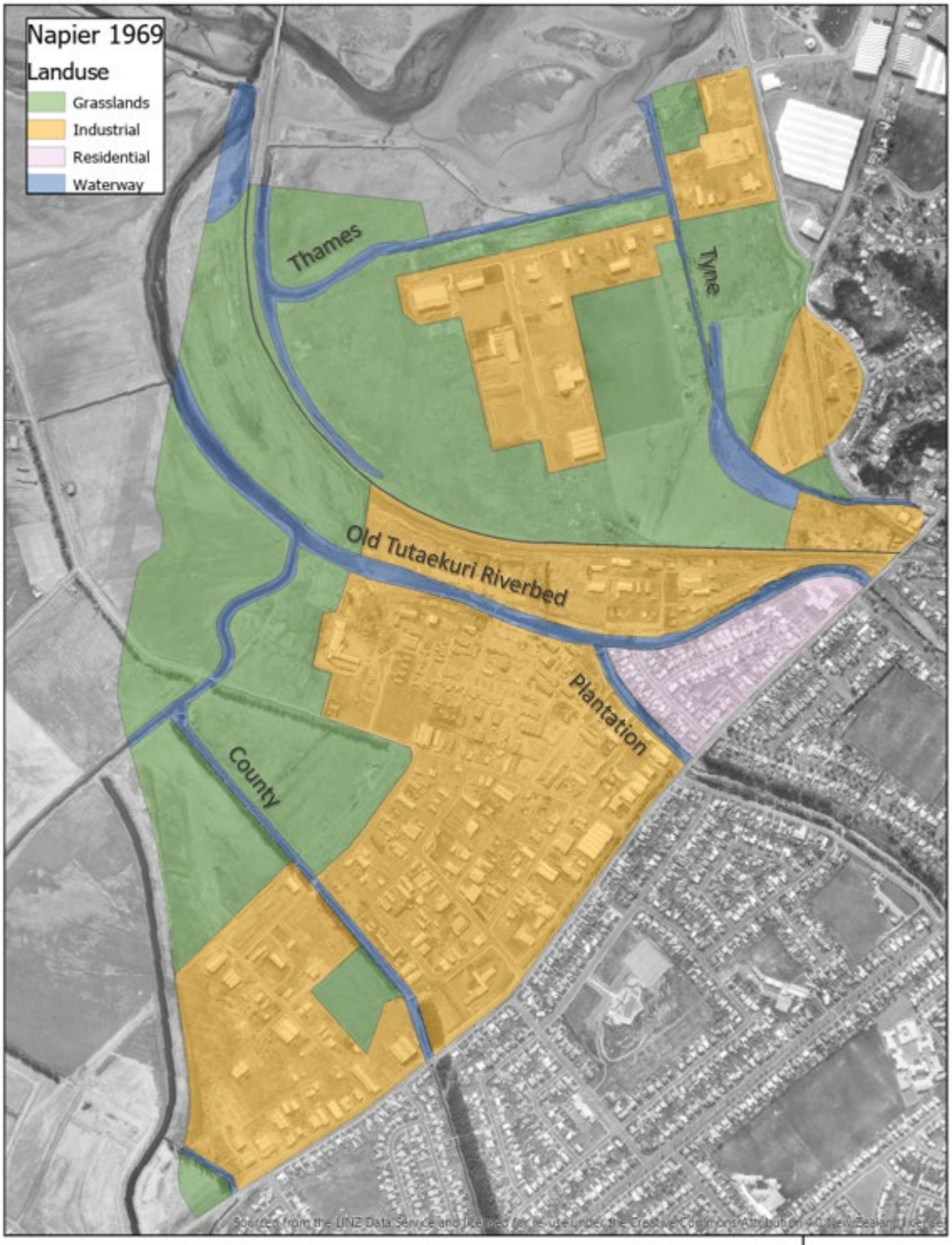

Figure 5.4: Land cover, Onekawa and Pandora, Napier, 1969. Base image source from RetroLens (2020).

5.2.4 Onekawa & Pandora - 1980

By 1980, further industrial development has occurred in Onekawa, with most of the original grassland between the three major waterways now built environment (Figure 5.5). In Onekawa, the reduction in grassland area between 1936 and 1980 is 71.11%.

Compared to 1936, grassland in the Pandora area has reduced by 45.83%. The Thames-Tyne network has been fully delineated with the Thames now separated from the western waterway channel to Ahuriri Estuary. The Thames Waterway still connects to Ahuriri Estuary directly via a new discharge upstream of its connection to the Tyne Waterway. Development in Pandora is largely centered on Mersey Street between the Tyne and the centre of the catchment and along the southern margin of the Thames Waterway. Extensions to existing building footprints are also visible in the centre of the sub-catchment.

Outside of the focus area, the Pandora Pond recreational area (Figure 2.5) has been dredged and the linear Purimu waterway has been formed.

Table 5.4 shows areas of different land use categories for 1980.

Table 5.4: 1980 land use types and areas per sub-catchment.

Napier 1980					
Total area (ha)		Onekawa (ha)		Pandora (ha)	
Total area	293.5	Total area	184.4	Total area	109.1
Estuarine	0.0	Estuarine	0.0	Estuarine	0.0
Grasslands	85.3	Grasslands	35.3	Grasslands	50.0
Industrial	178.7	Industrial	124.7	Industrial	54.0
Residential	9.9	Residential	9.9	Residential	0.0
Waterway	19.6	Waterway	14.5	Waterway	5.1

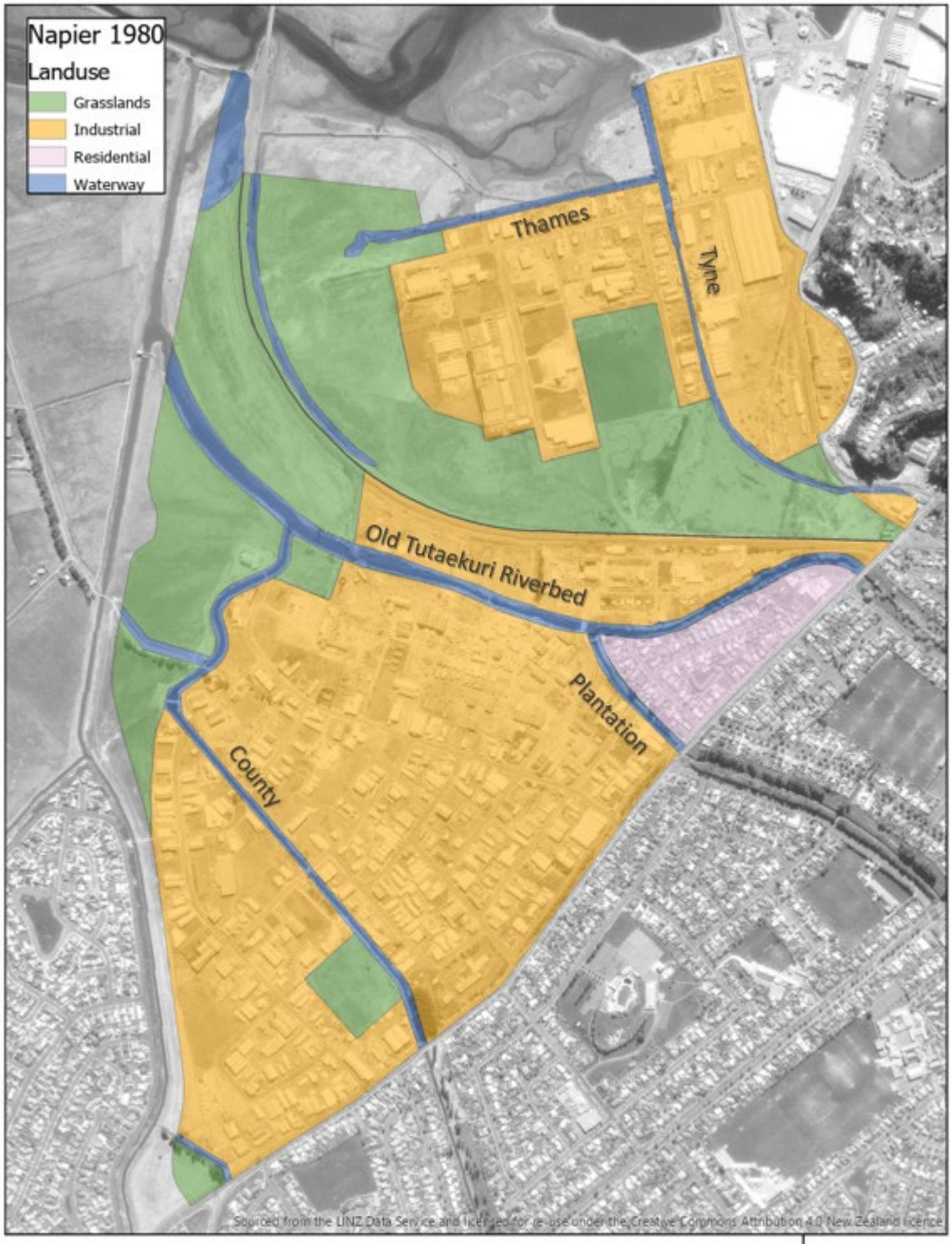

Figure 5.5: Land cover, Onekawa and Pandora, Napier, 1980. Base image source from RetroLens (2016).

5.2.5 Onekawa & Pandora - 2004

Between 1980 and 2004, several key changes have occurred. Most of the historic grasslands in the Onekawa Industrial zone have been filled by impervious surfaces including unsheltered concreted sites and warehouses with highly reflective zinc roofs (Figure 5.6). A section of the northern Onekawa Industrial zone appears to have been re-vegetated after 1980. Vegetated grassland area in Onekawa has been reduced to 14.1% of land coverage within the sub-catchment with 72.4% of the sub-catchment industrial by comparison (Table 5.5). The younger Pandora Industrial zone exhibits a similar development expansion with 65.7% industrial and 31.7% grasslands.

Much of this industrial expansion is reflected in the changes made to the urban waterways between 1980 and 2004. The Thames waterway has been fully channelised and now only discharges to the Ahuriri Estuary via its confluence with the Tyne. This is due to the Department of Conservation (DOC) walkway being commissioned and shutting off an historic discharge point. The northbound State Highway 2 has been developed splitting the Old Tutaekuri Riverbed into the modern Purimu Stream and a much narrower OTRB. The County Waterway has been further channelised with its natural meander straightened into a pathway which pushes its confluence with the OTRB further north. The upper Tyne Waterway has been split and shortened with the eastern split re-aligned into a new confluence with the OTRB, adding additional catchment area to the Onekawa Industrial zone.

Table 5.5: 2004 land use types and areas per sub-catchment.

Napier 2004					
Total area (ha)		Onekawa (ha)		Pandora (ha)	
Total area	293.5	Total area	188.8	Total area	104.7
Estuarine	0.0	Estuarine	0.0	Estuarine	0.0
Grasslands	59.8	Grasslands	26.6	Grasslands	33.2
Industrial	205.4	Industrial	136.7	Industrial	68.8
Residential	9.9	Residential	9.9	Residential	0.0
Waterway	18.4	Waterway	15.6	Waterway	2.8

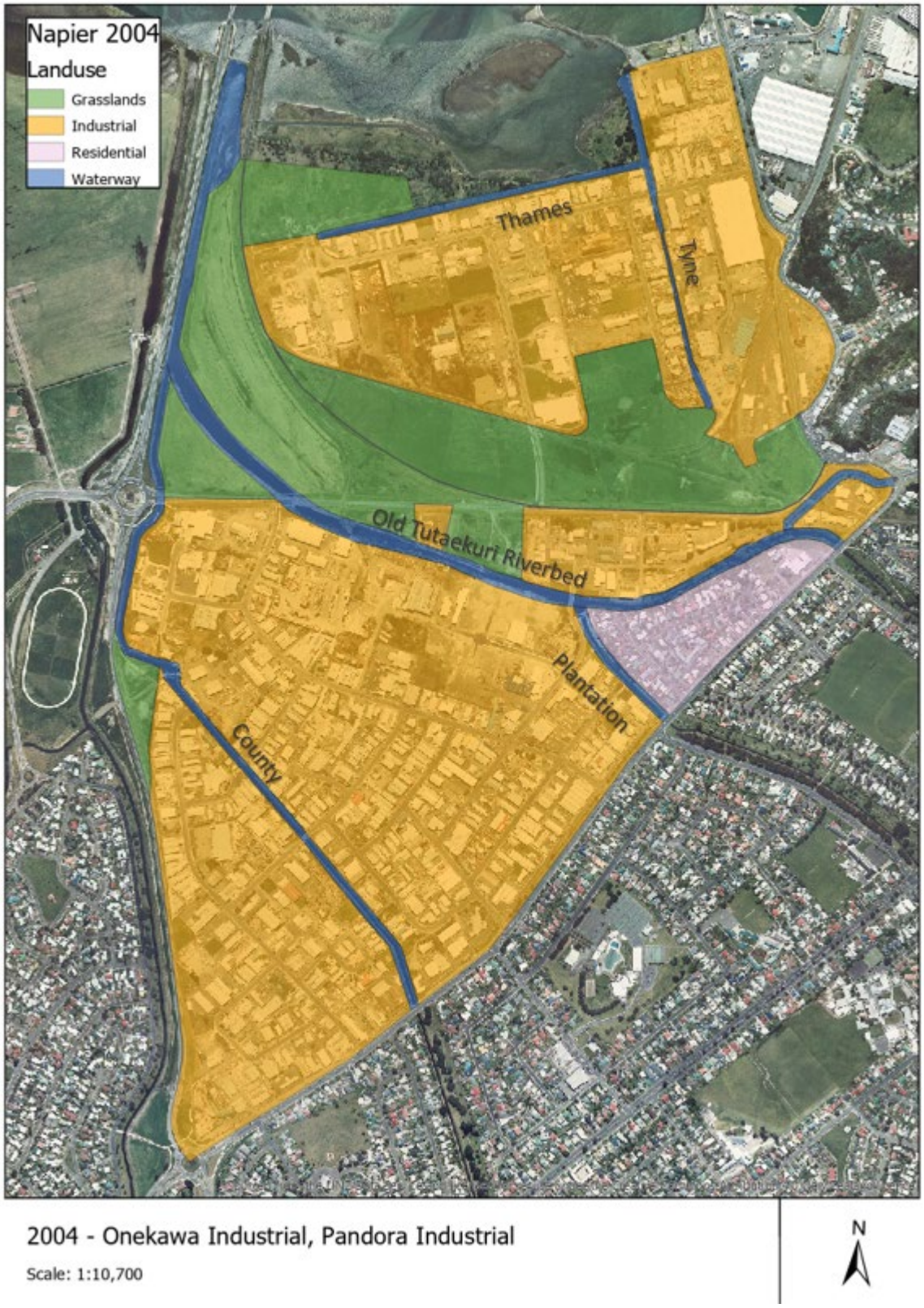

Figure 5.6: Land cover, Onekawa and Pandora, Napier, 2004. Base image source from (Napier City Council, n.d.-c).

5.2.6 Onekawa & Pandora - 2018

The most recent aerial image shows the largest area of industrial coverage in both the Onekawa Industrial and the Pandora Industrial sub-catchments (Figure 5.7). While the 293.5 ha polygon was comprised of 86.8% grasslands in 1936, this has reduced to only 14.3% in 2018, with industrial land use comprising most of the remaining area at 76.1%. Total waterway area is 6.3%. The southern side of main arterial road Prebensen Drive is fully developed, adding further industrial area to Onekawa. Pandora, now at 79% industrial coverage, has extended both northwards towards Ahuriri Estuary, and southwards towards its remaining grassland area.

Table 5.6 shows areas of different land use categories for 2018.

Table 5.6: 2018 land use types and areas per sub-catchment.

Napier 2018					
Total area (ha)		Onekawa (ha)		Pandora (ha)	
Total area	293.5	Total area	188.8	Total area	104.7
Estuarine	0.0	Estuarine	0.0	Estuarine	0.0
Grasslands	41.9	Grasslands	22.7	Grasslands	19.3
Industrial	223.3	Industrial	140.6	Industrial	82.7
Residential	9.9	Residential	9.9	Residential	0.0
Waterway	18.4	Waterway	15.6	Waterway	2.8

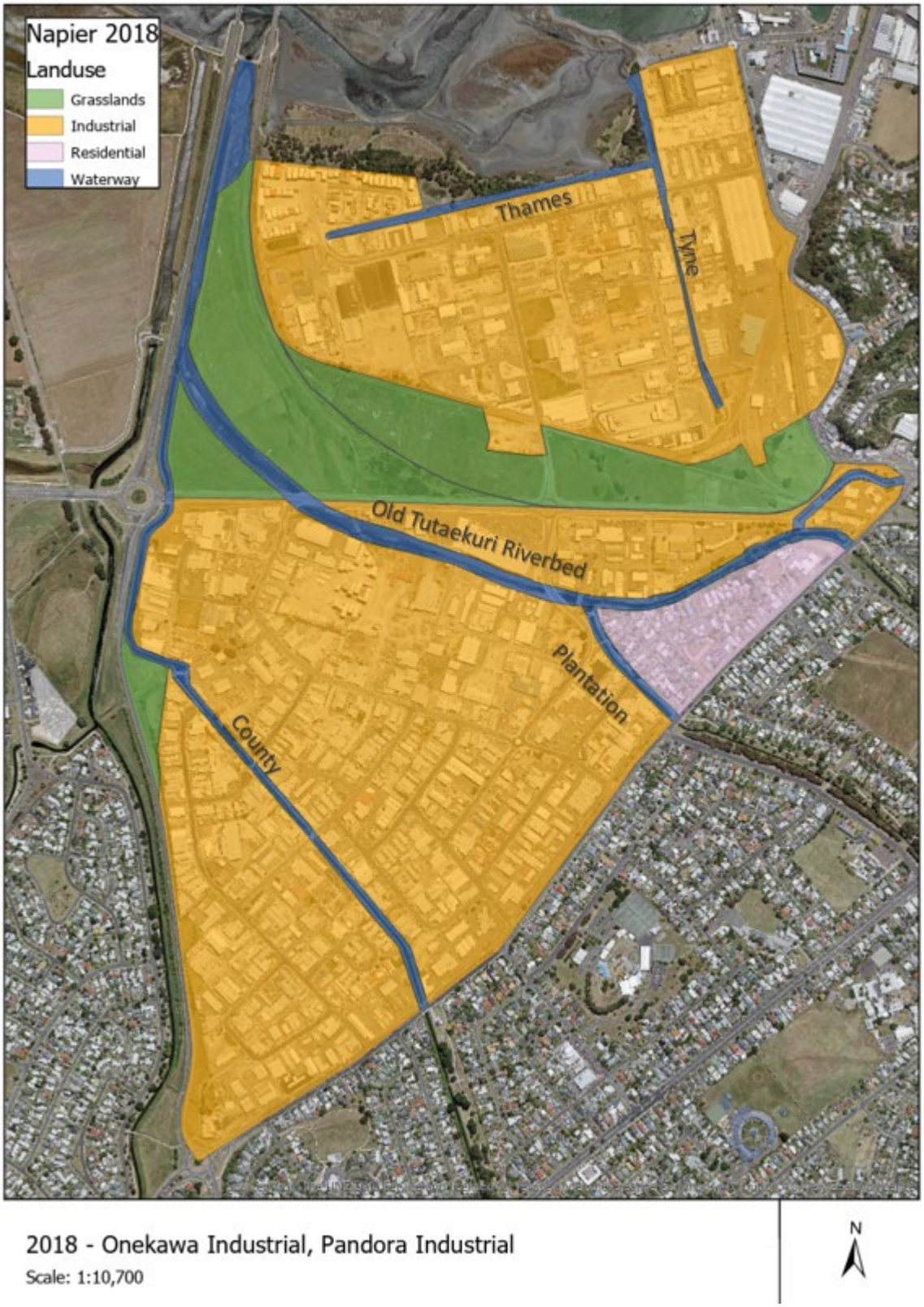

Figure 5.7: Land cover, Onekawa and Pandora, Napier, 2018. Base image source from ESRI Inc. (2019).

5.2.7 Land cover change between 1936 – 2018

From 1936 onward, both Onekawa and Pandora Industrial zones exhibit increasing areas of industrial development (Figure 5.8 through Figure 5.11), and proportionally-decreasing areas of vegetated land, as original grasslands are gradually converted to accommodate industry (Figure 5.10 and Figure 5.11). Table 5.7 shows area change over the six focus years for each land-use category compared to the 1936 baseline.

Table 5.7: Land use category change from 1936 within focus area.

Area change from 1936 (ha)						
	1936	1964	1969	1980	2004	2018
Total area	293.5	+0	+0	+0	+0	+0
Estuarine	20.7	-20.7	-20.7	-20.7	-20.7	-20.7
Grasslands	254.8	-57.1	-124.9	-169.4	-195.0	-212.9
Industrial	0.0	+84.5	+131.3	+178.7	+205.4	+223.3
Residential	0.0	+8.2	+9.9	+9.9	+9.9	+9.9
Waterway	18.0	+3.1	+4.4	+1.6	+0.4	+0.4

Figure 5.9 shows a noticeable improvement in grassland area in the Pandora Industrial zone from 1936 and 1964. This is the only increase in grassland land type within the reference area and is due to reclamation of the southern Ahuriri Estuary which occurred in the northern area of the Pandora Industrial zone. This change is observable between Figure 5.2 and Figure 5.3.

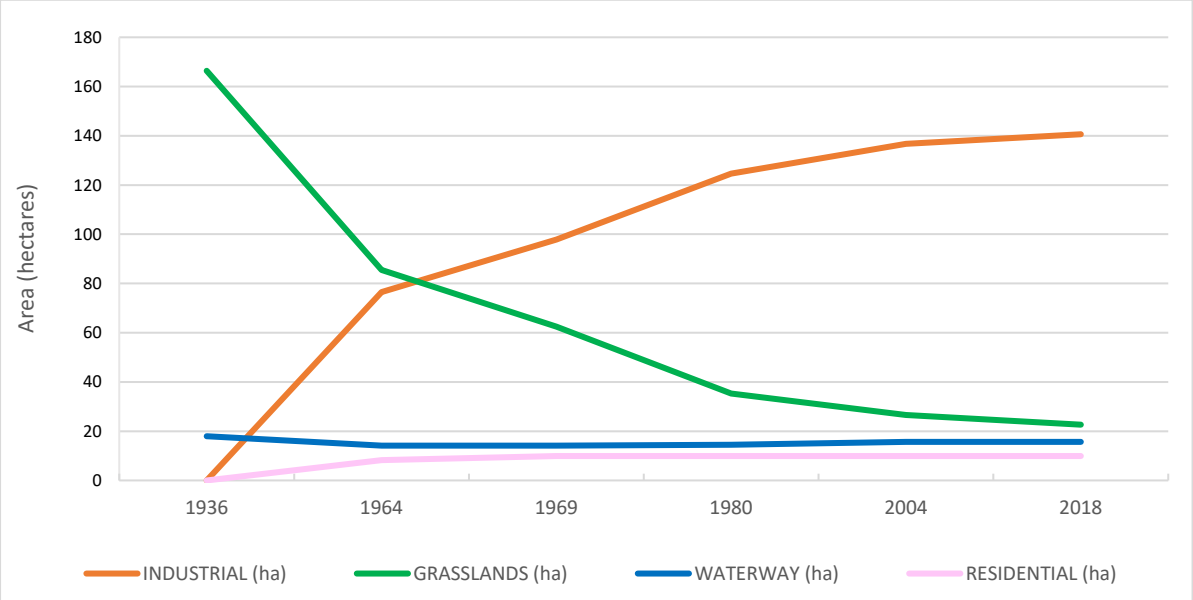

Figure 5.8: Onekawa land use area changes since 1936.

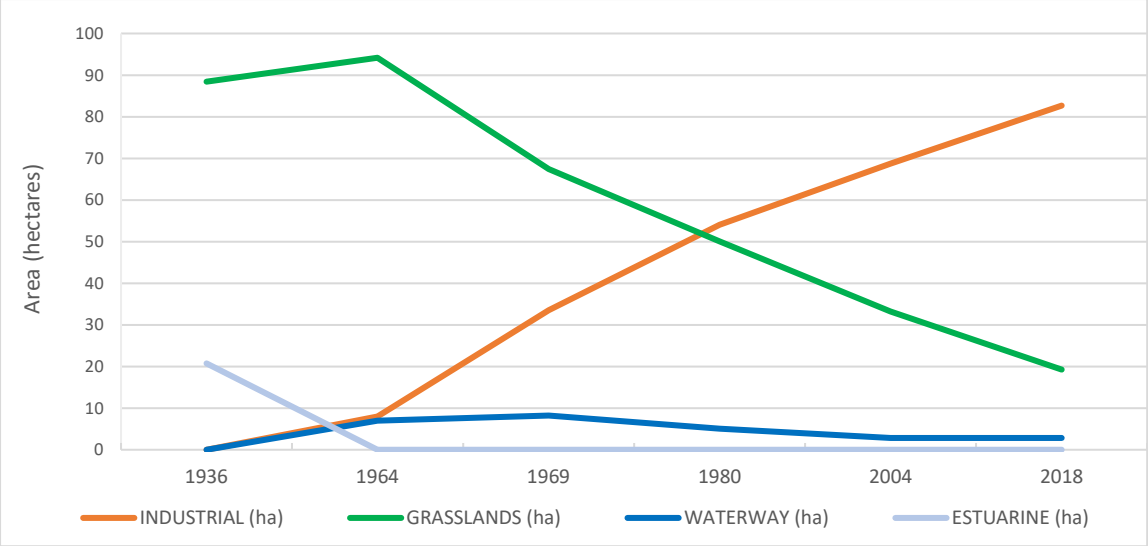

Figure 5.9: Pandora land use area changes since 1936.

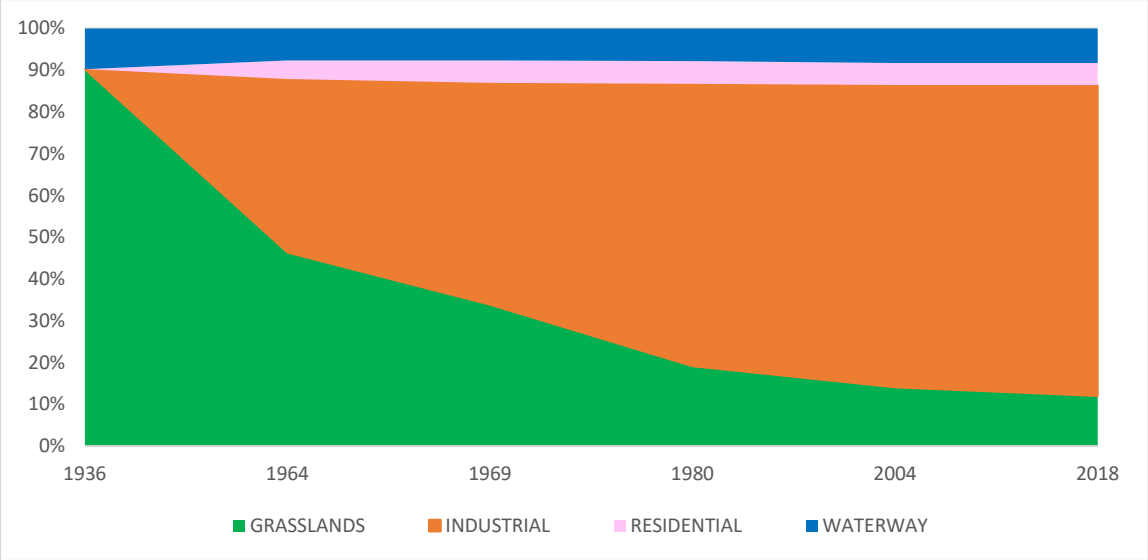

Figure 5.10: Onekawa proportional land use changes since 1936.

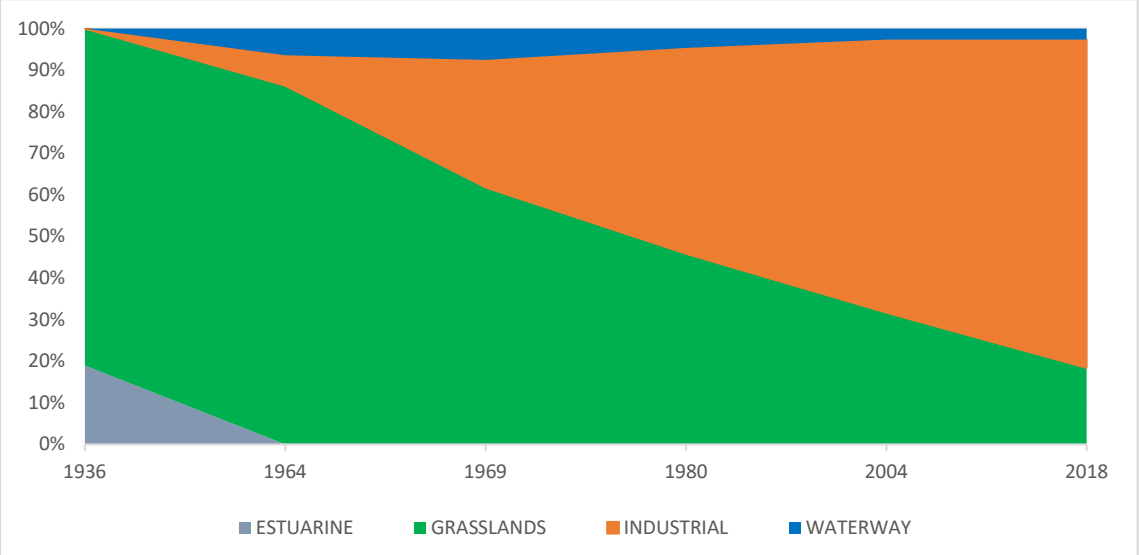

Figure 5.11: Pandora proportional land use changes since 1936.

The Onekawa Industrial zone experienced the initial largest proportional industrial development compared to the Pandora area (Figure 5.12) and this trend increased until 2018. In 2018, Pandora Industrial zone had overtaken Onekawa Industrial zone as containing the highest proportional area of industrial development relative to sub-catchment size.

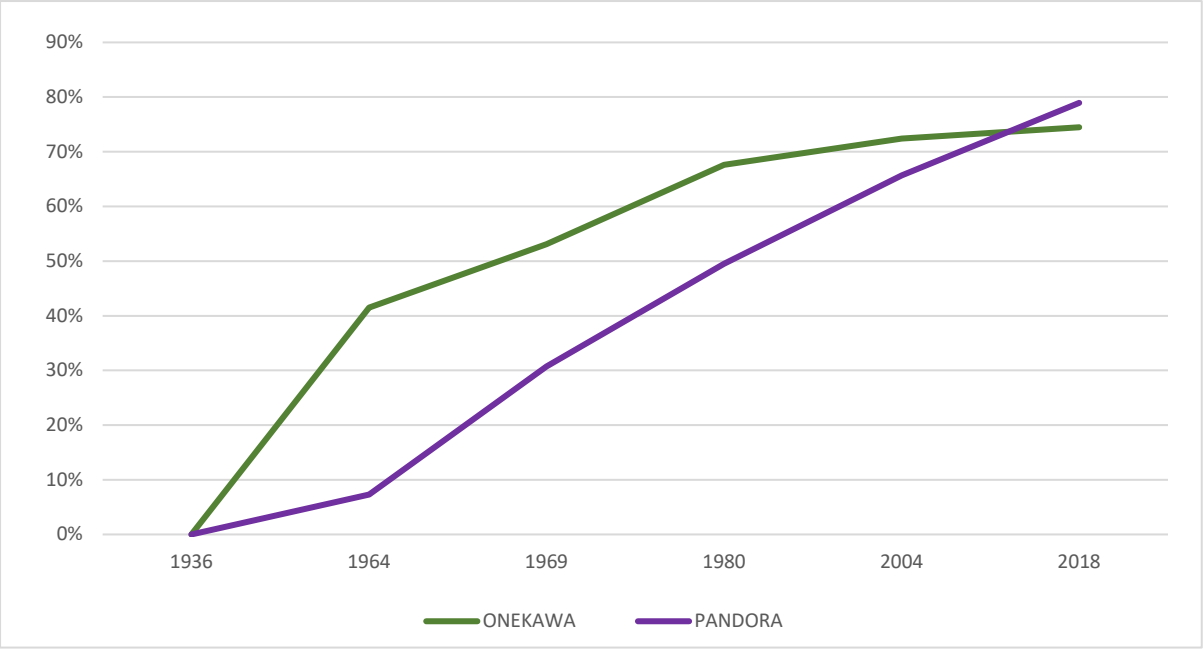

Figure 5.12: Industrial growth trends as proportion of total catchment area, Onekawa and Pandora industrial zones.

5.3 Post-earthquake observations outside of focus area

From the same 1936 imagery as used in the Onekawa and Pandora sub-catchment focus area mapping, several developments are worth noting when attempting to reference sediment physicochemical changes to a time in Napier City's development. Figure 5.13 is provided as a reference for the locations of Figure 5.14 through Figure 5.17. Figure 5.14 shows the 1936 aerial view of Pāmu Farm north of Ahuriri Estuary's main channel. The estuary-edge has been lined with what appears similar to the modern stopbanks. Pāmu Farm still appears marsh-like from the effects of the 1931 earthquake's uplift and has not yet been developed into a working farm. Figure 5.15 shows the residential settlement of Taradale well in development. In this image, the Taipo Stream is shown as largely in the same position as the modern waterway meandering through the western outskirts of the Taradale suburb.

The 1936 aerial imagery shows that the harbour mouth to the Ahuriri Estuary adjacent to the fringing Westshore settlement was largely unchanged through to 2018 (Figure 5.16). Embankment Bridge and the Westshore Bridge had additionally been developed as estuary crossings. The imagery shows development to the east of the Onekawa Industrial zone (Figure 5.17) in what is now the Napier Central Business District (CBD). Mataruahou additionally shows signs of the residential area which had been utilised since the late-1800s (Parsons, 1992).

Figure 5.13: Aerial map of Napier City showing 1936 overlay of focus sub-sections Pāmu Farm (expanded in Figure 5.14), Upper Taipo Catchment (Figure 5.15), Central Ahuriri Estuary (Figure 5.16), and Mataruahou and CBD (Figure 5.17). Base image retrieved from Google (n.d.-b), inset imagery from Napier City Council (n.d.-b).

Figure 5.14: 1936 aerial imagery of Pāmu Farm, north of Ahuriri Estuary (Napier City Council, n.d.-b).

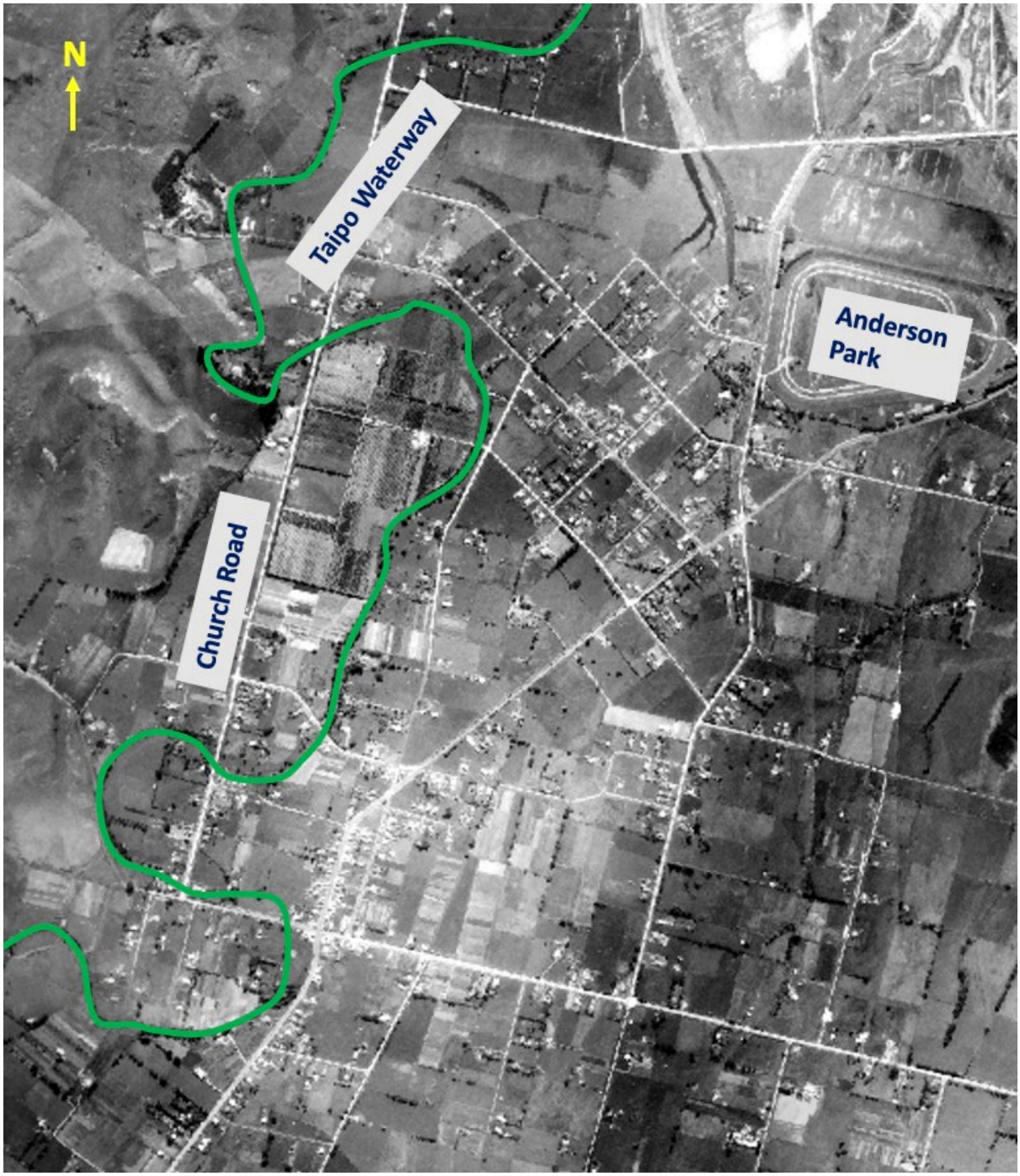

Figure 5.15: 1936 aerial imagery of Taradale Suburb, south-west Napier (Napier City Council, n.d.-b).

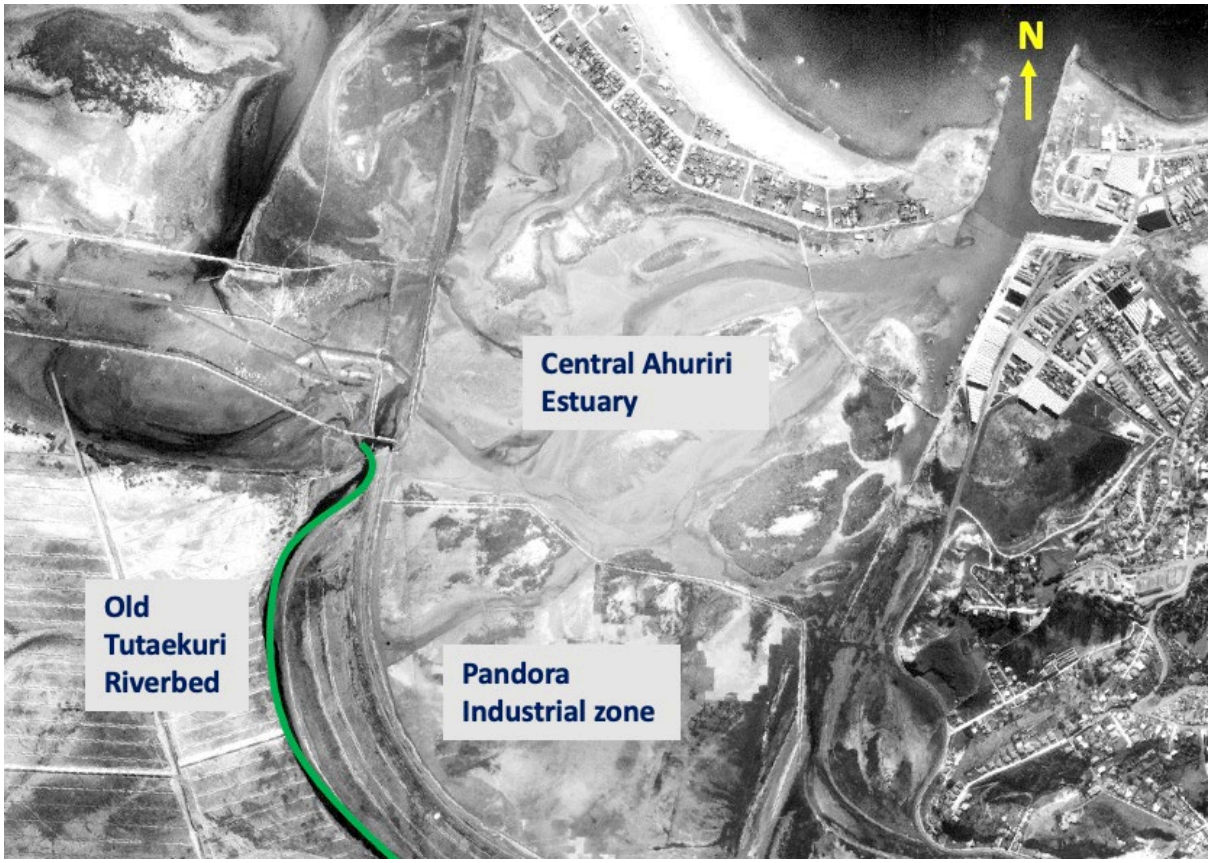

Figure 5.16: 1936 aerial imagery of central Ahuriri Estuary (Napier City Council, n.d.-b).

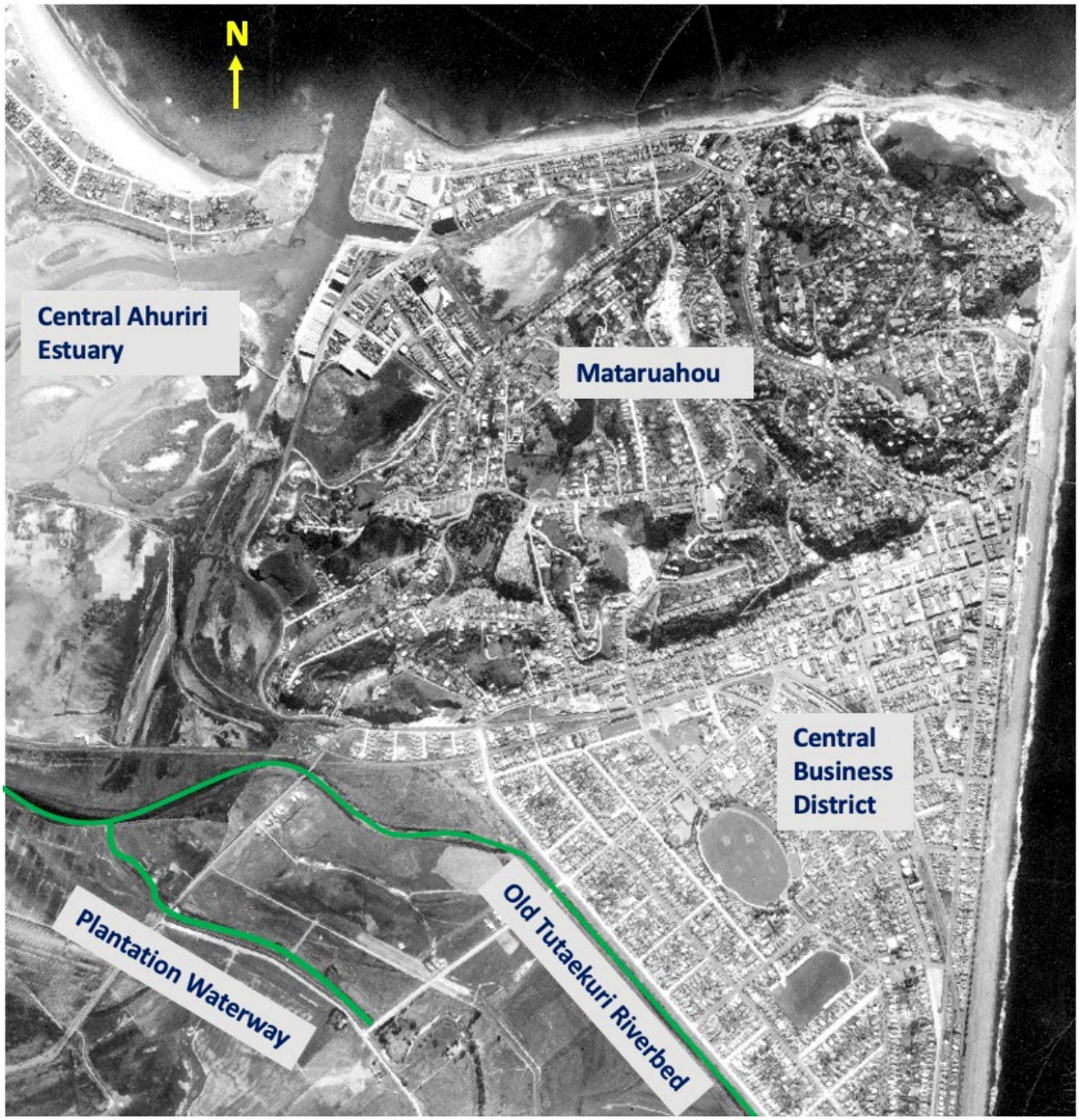

Figure 5.17: 1936 aerial imagery of Mataruahou and Napier CBD (Napier City Council, n.d.-b).

5.4 Summary

A summary of sub-catchment developments of note from within the 293.5ha Onekawa and Pandora Industrial zone reference area is presented in Table 5.8.

Table 5.8: Sub-catchment land use developments by year, Onekawa Industrial and Pandora Industrial zone.

	Onekawa	Pandora
1936	Railway delineating border between Onekawa and Pandora in existence. Evidence of stream channelisation in County and Plantation waterways.	Aside from the bordering railway line, no development within Pandora sub-catchment.
1964	Large-scale development of central Onekawa Industrial zone between County and Plantation/OTRB waterways. Residential development begun. OTRB width reduced to accommodate development.	Pandora Industrial zone still dominated by grasslands. Small segments of development on border of focus area. Reclamation of estuary creates further grassland area. Tyne Waterway delineated. Western reach of Thames Waterway developed.
1969	Large-scale development on either side of County Waterway. Residential section of Onekawa fully developed.	First signs of central Pandora Industrial Zone development including the partial channelisation of the modern Thames Waterway and its connection to the Tyne Waterway.
1980	Majority of central historic grasslands now developed with impervious area.	Thames Waterway separated from historic western discharge to estuary. North of Pandora, Pandora Pond has been dredged.
2004	Lower OTRB split into OTRB and PUR waterways via development of modern northbound State Highway 2 Bridge over Ahuriri Estuary. Old upper Tyne Waterway diverted into OTRB. Full channelisation of County Waterway.	Thames Waterway now only discharges via confluence of Thames and Tyne. Tyne Waterway shortened. Infilling of historic western Pandora stream.
2018	Southern side of Prebensen Drive developed into industrial land use.	Pandora extended north of Thames toward estuary.

Where applicable, sediment physicochemical changes will be referenced to these key sub-catchment industrial development stages in the discussion in Chapter 7, using Itrax™ XRF analytical results presented in Chapter 6.

6 RESULTS: SEDIMENT PHYSICOCHEMISTRY

6.1 Introduction

This chapter presents the results obtained from collection and physicochemical analysis of seven Ahuriri Estuary sediment core samples. This data will assist in the determination of the effects of sub-catchment industrial intensification on the current health of Ahuriri Estuary itself. This chapter aligns with Objective Three, being:

Utilise previous hydrodynamic modelling of the central estuary to guide sampling locations for extraction of sediment cores representing discharge depositional zones of different tributaries. Undertake physicochemical analysis on retrieved sediment core samples to investigate connections between industrial development and temporal sediment quality.

Itrax™ XRF scans were undertaken on samples compacted by the vibracoring process. All depths discussed herein have been corrected using compaction corrections for individual cores to represent in-situ estuarine sediment depths. Both the physical and chemical results are presented in the form of stratigraphic logs. XRF chemical analyses have been presented per analyte and ratio in table form for each core. Figure 6.1 shows the key for the stratigraphic logs presented in this chapter.

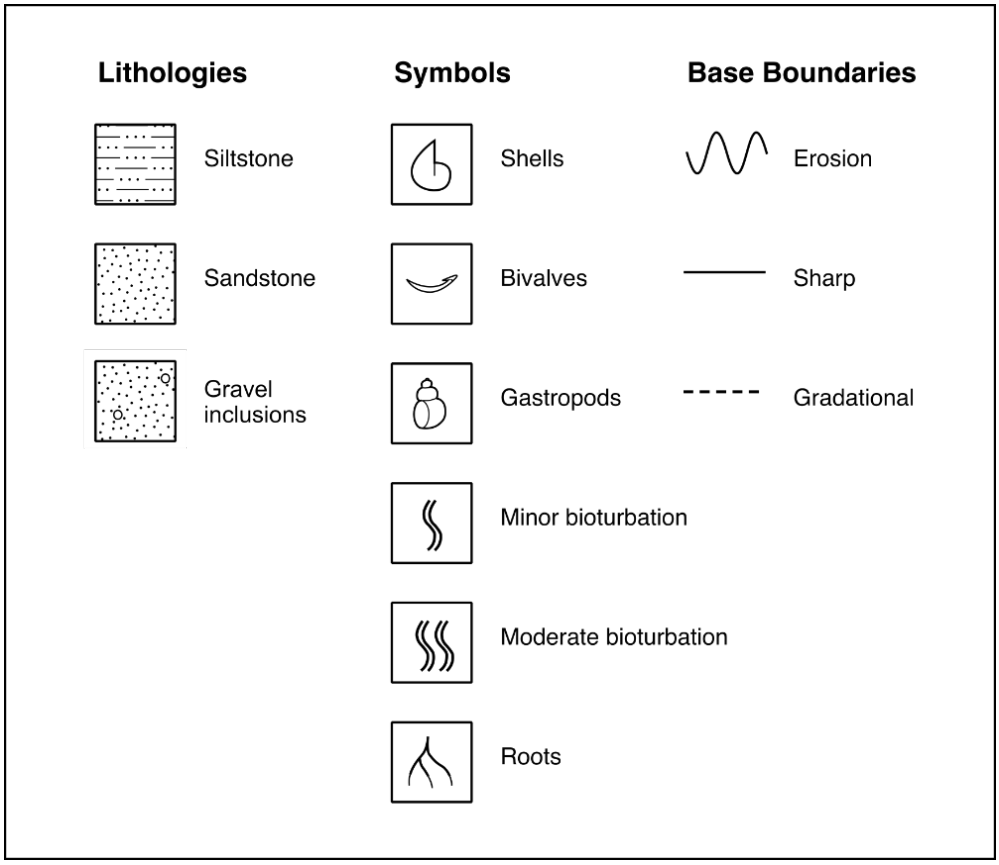

Figure 6.1: Stratigraphic log key.

6.2 Thames-Tyne discharge zone

6.2.1 Visual analysis

The 70cm core from the intertidal Thames-Tyne (TT) discharge zone was corrected to 74.2cm accounting for in-field compaction. Grain size ranged from silt to coarse sand with most of the core dominated by sandy silt (Figure 6.2). The core was rich in bivalve fossils and fragments with minor bioturbation. The upper core was rich in fine plant matter with one sandy silt layer (4.2cm-7.2cm) rich in gravel clasts. Rounded gravel clasts were observed in the lower 49.8cm-74.2cm coarse sand layer.

6.2.2 Sediment chemistry

The four analytes chromium (Cr), zinc (Zn), copper (Cu) and lead (Pb) were plotted against depth for the TT core (Figure 6.3). Cr resides around 3,500CPS for the length of the core without a discernable trend and spikes to 12,211CPS at 14.0cm depth. Zn shows an increase with decreasing depth with a trend about 3,000CPS in the lower 40cm of the core and about 16,000CPS in the upper 17.0cm. At 17.8cm depth, Zn spikes to 689,636CPS. Cu also peaks at 17.8cm depth to 9,020CPS from a trend of about 500CPS in the lower 40cm of the core and about 2,000CPS in the upper 17.0cm. Similarly, Pb spikes at 17.8cm to 566,681CPS from a lower core trend of about 1,000CPS and returns to a trend of about 2,200CPS in the top 17.0cm.

The two ratios potassium/incoherent (K/Inc) and bromine/incoherent (Br/Inc) were also plotted against depth for the TT core (Figure 6.3). The K/Inc ratio shows a general increase between 27.6-36.0cm depth with a small peak at 47.7cm depth and 59.2cm depth onwards showing dramatic ratio changes. Br/Inc exhibits a decreasing trend with increasing depth and spikes at 7.6cm, 17.8cm and 47.7cm depth.

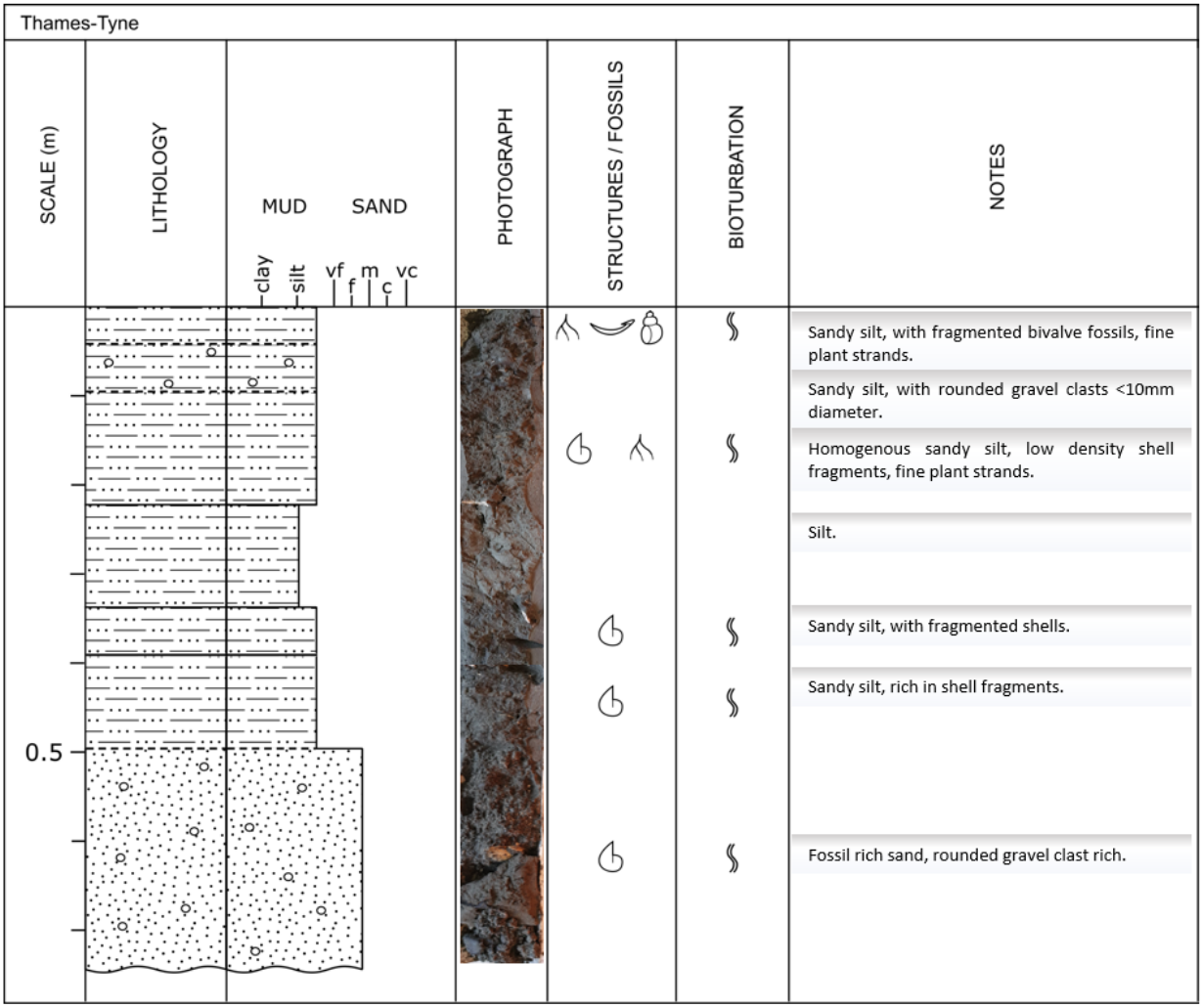

Figure 6.2: TT intertidal sediment core sample stratigraphic log.

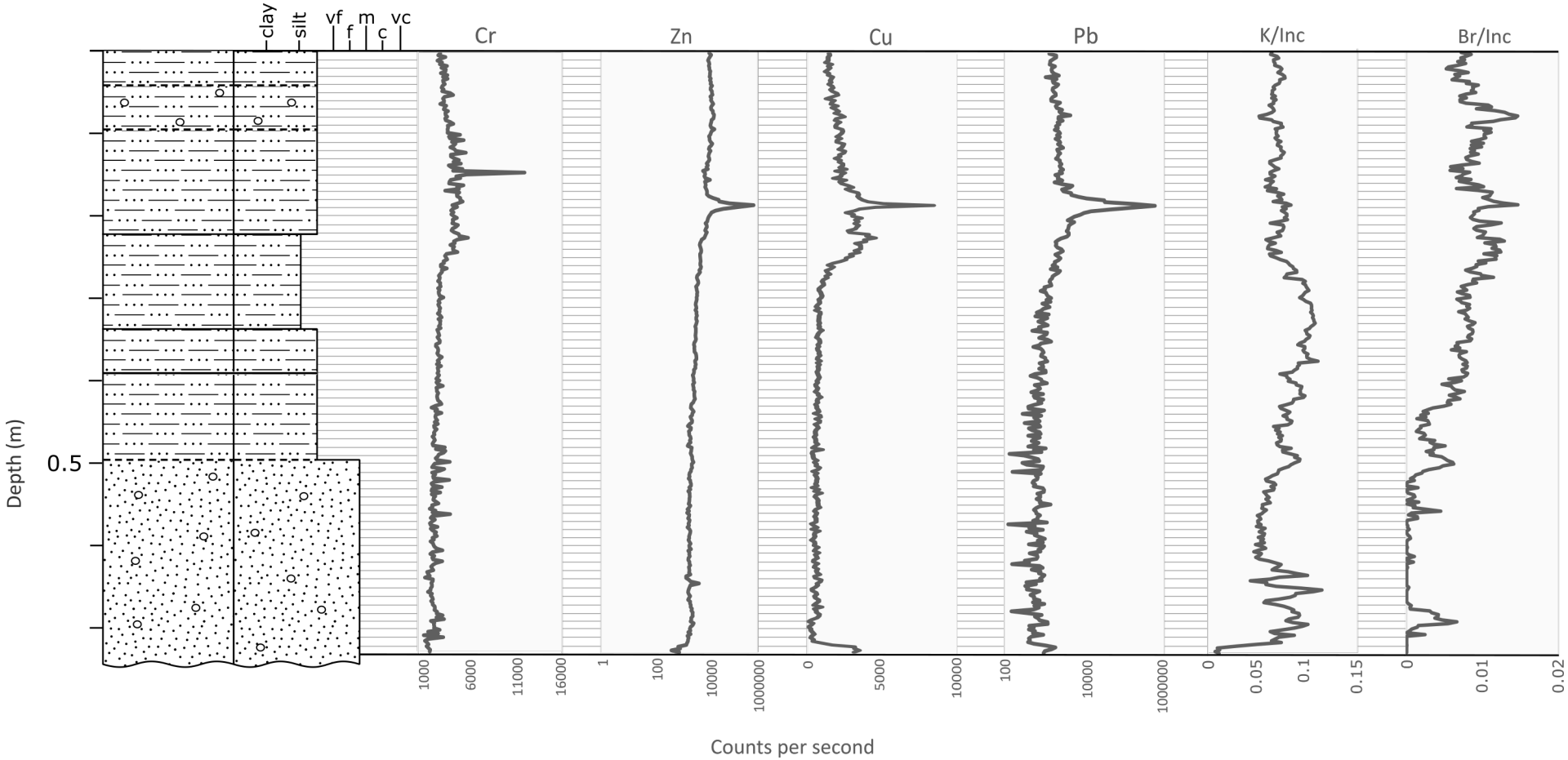

Figure 6.3: TT sediment core elemental and ratio results versus depth; Chromium (Cr), zinc (Zn), copper (Cu), lead (Pb), potassium/incoherent (K/Inc), and bromine (Br/Inc).

6.3 South Central Ahuriri Estuary

6.3.1 Visual analysis

The 100cm intertidal South Central Ahuriri Estuary (SCAE) sediment core was the only core of the six to undergo in-field expansion which resulted in the sample representing 95.9cm of estuarine depth. The top 38.4cm silt layer was the dominant layer with fine plant matter, indications of bioturbation and a low density of bivalve shells (Figure 6.4). Two silty sand layers with fine plant matter encompassed a sharp-boundaried coarse sand layer at 51.8-67.1cm. The bottom two layers exposed gravel clasts in medium-high densities along with fragmented shells.

6.3.2 Sediment chemistry

Cr in the SCAE core spikes to 7,188CPS at 36.1cm depth and 5,808CPS at 68.7cm depth from a trend of about 3,000CPS (Figure 6.5). The trend in Zn is split into two clear 'sections' by a peak area between 23.4-34.9cm depth which spikes to 10,391CPS at 32.8cm depth. Zn trends about 6,000CPS in the upper 23.4cm and about 3,000CPS from 34.9cm depth. Cu generally increases with decreasing depth with a peak of 1,548CPS at 14.6cm depth, and a surface reading of about 1,000CPS. Pb shows a fluctuating trend with the upper 30.4cm of the core increasing to a peak of 1,814CPS. Three key spikes in Pb of 1,980CPS, 2,097CPS and 2,222CPS occur at 53.1cm, 68.9cm and 87.1cm, respectively.

The K/Inc ratio fluctuates between 0.05-0.1 with a gradually decreasing trend to 63.9cm depth, a spike to 0.117 at 73.7cm, a drop to 0.036 at 91.7cm, then a spike to 0.109 at 93.6cm. Br/Inc gradually increases with depth from 0.004 at the surface to 0.013 at 34.5cm depth then decreases to a low at 64.4-69.6cm and at 73.7-75.6cm followed by a gradual increase toward the core base.

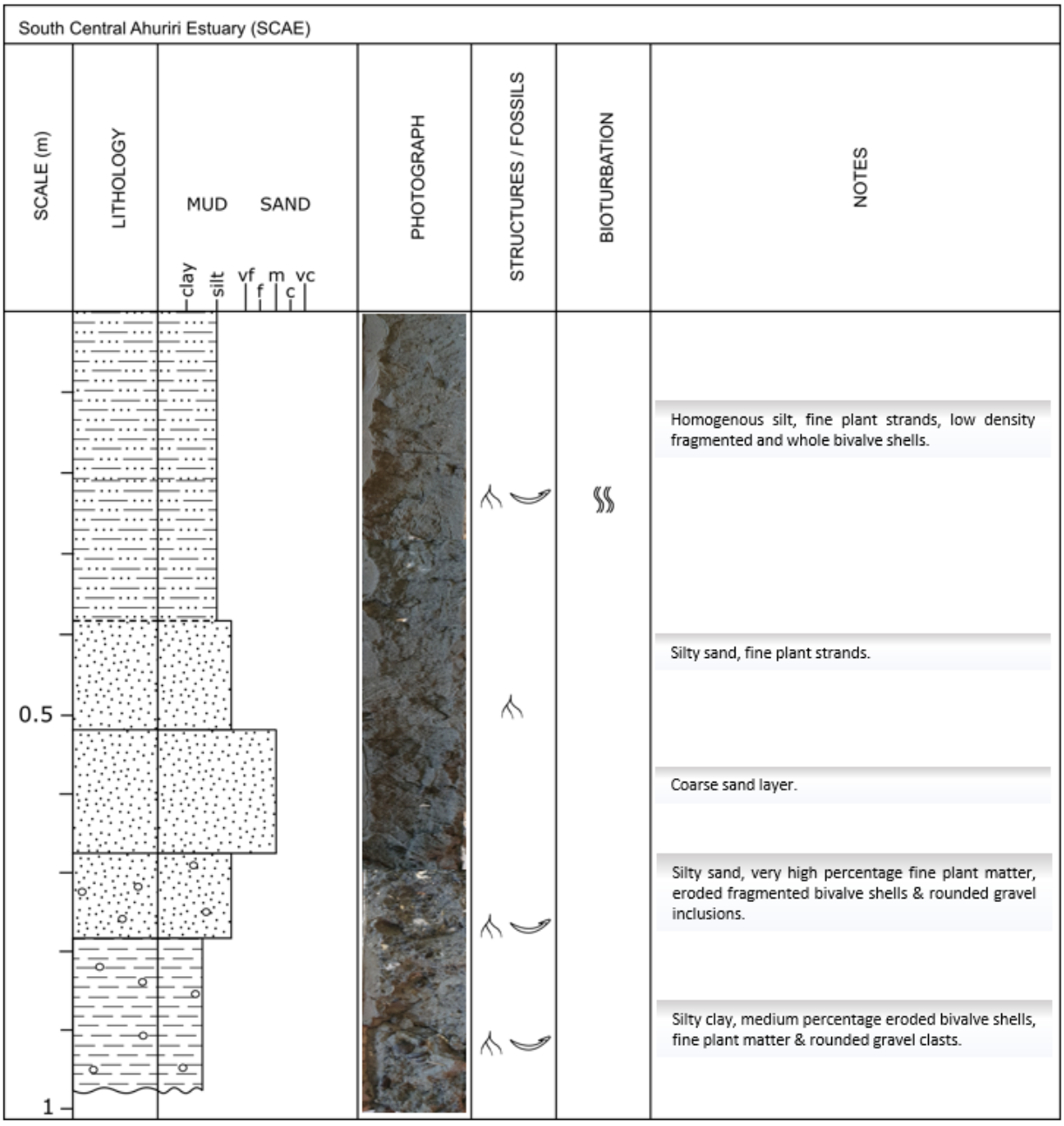

Figure 6.4: SCAE intertidal sediment core sample stratigraphic log.

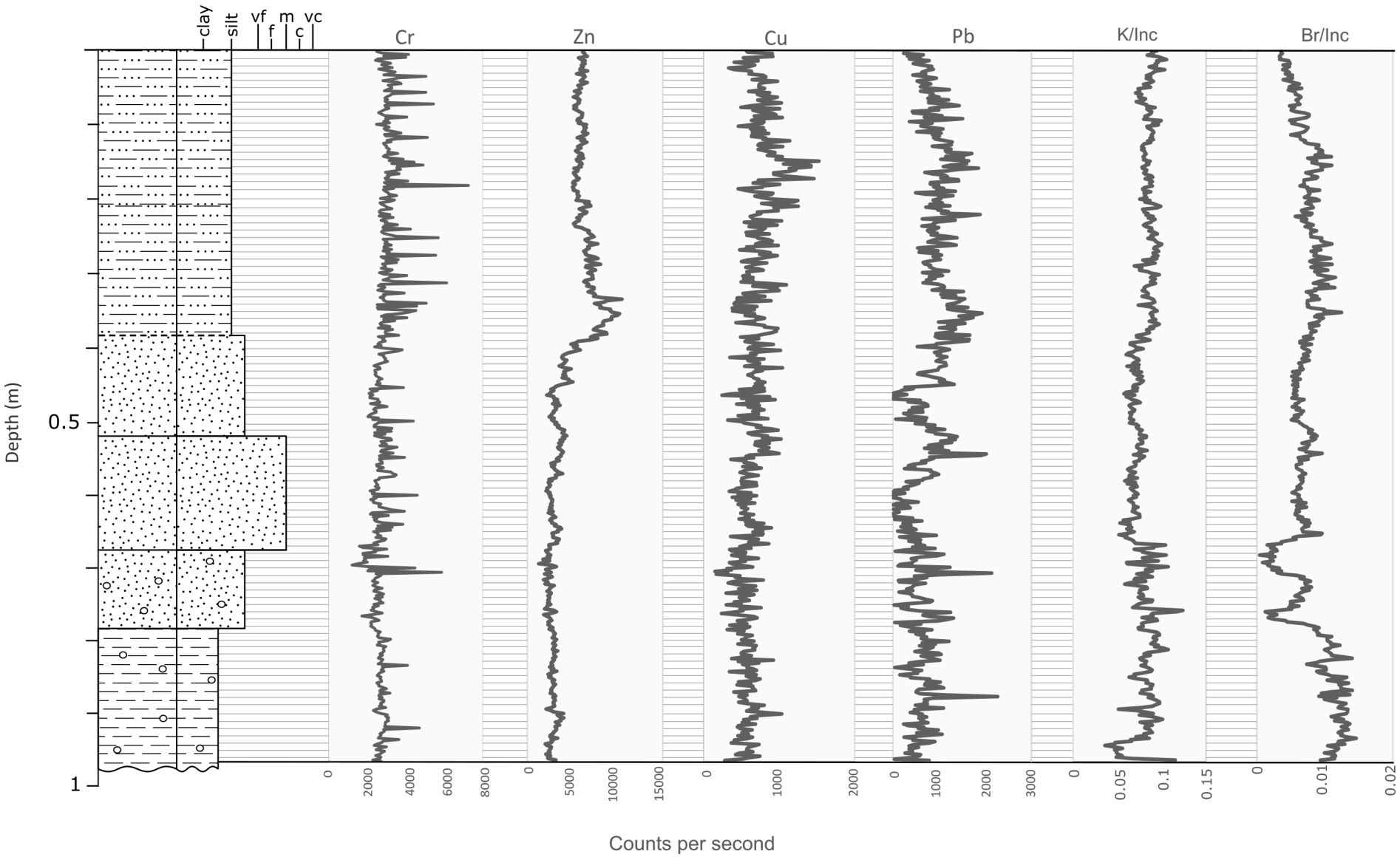

Figure 6.5: SCAE sediment core elemental and ratio results versus depth; Cr, Zn, Cu, Pb, K/Inc, and Br/Inc.

6.4 Old Tutaekuri Riverbed discharge zone

6.4.1 Visual analysis

The core retrieved from the intertidal Old Tutaekuri Riverbed (OTRB) discharge zone had an in-field length of approximately 85cm, though some material was lost through the base of the barrel while securing the ends of the core in field. With 75cm visual length and a compaction of 11cm, the core represents 86cm of estuarine sediment depth. The core alternates between sandy silt and medium sand with varying densities of preserved bivalve shell halves, shell fragments and minor bioturbation identified in the silt horizons (Figure 6.6). The upper 17.2cm comprises unconsolidated sandy silt, incorporating a low density of bivalve halves with a similar layer identified between 33-54cm. A densely packed large shell layer sits amongst fine-medium grained sand between 25cm-28.6cm. From 65cm down, the core consists of four alternating sand layers with very low densities of fine shell fragments and no gravels. The core was predominantly 5Y 2.5/2 and 5Y 3/2.

6.4.2 Sediment chemistry

The OTRB sediment core encountered scanning issues between 5.7-11.9cm and 66.5-71.6cm. Data validity between these sections is zero and therefore unreliable to include in the analysis.

Cr in the OTRB core averages about 3,000CPS without a clear trend and spikes to 6,299 at 33.7cm, 4,925 at 38.5cm and 6,685 at 50.2cm (Figure 6.7). Zn experiences a generally increasing trend with decreasing depth, with a zone of peak concentration of approximately 17,000-20,000CPS at 12.4-17.2cm. The trend then decreases toward 38.5cm, then enters a zone of relative stability around 3,500CPS from 35.8cm depth. Cu experiences a general increase with depth to a peak of 1,934CPS at 14.7cm, then decreases toward the base of the core. A spike in Cu counts of 1,543CPS stands out at 50.9cm depth. Pb is slightly higher between 0-26.6cm at about 1,200CPS, spikes to 4,165CPS at 26.6cm, and appears stable about 1,000CPS from 27.1cm down.

The OTRB K/Inc ratio experiences a gradual, almost linear increase with depth along core length, with a drop to 0.04 at 51.2cm depth. The Br/Inc ratio experiences a gradual decrease along core length, with a spike to 0.03 at 51.2cm depth.

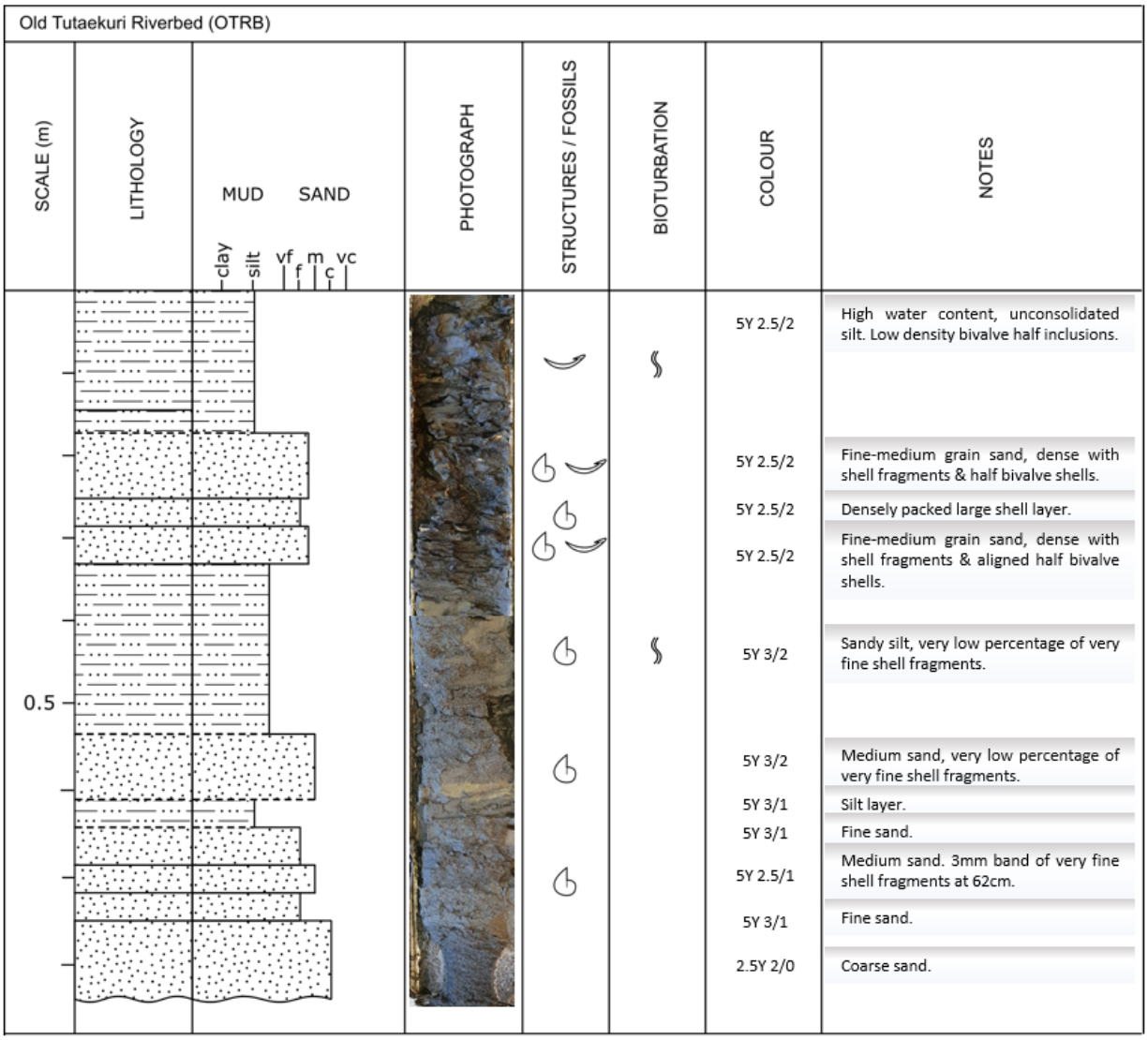

Figure 6.6: OTRB intertidal sediment core sample stratigraphic log.

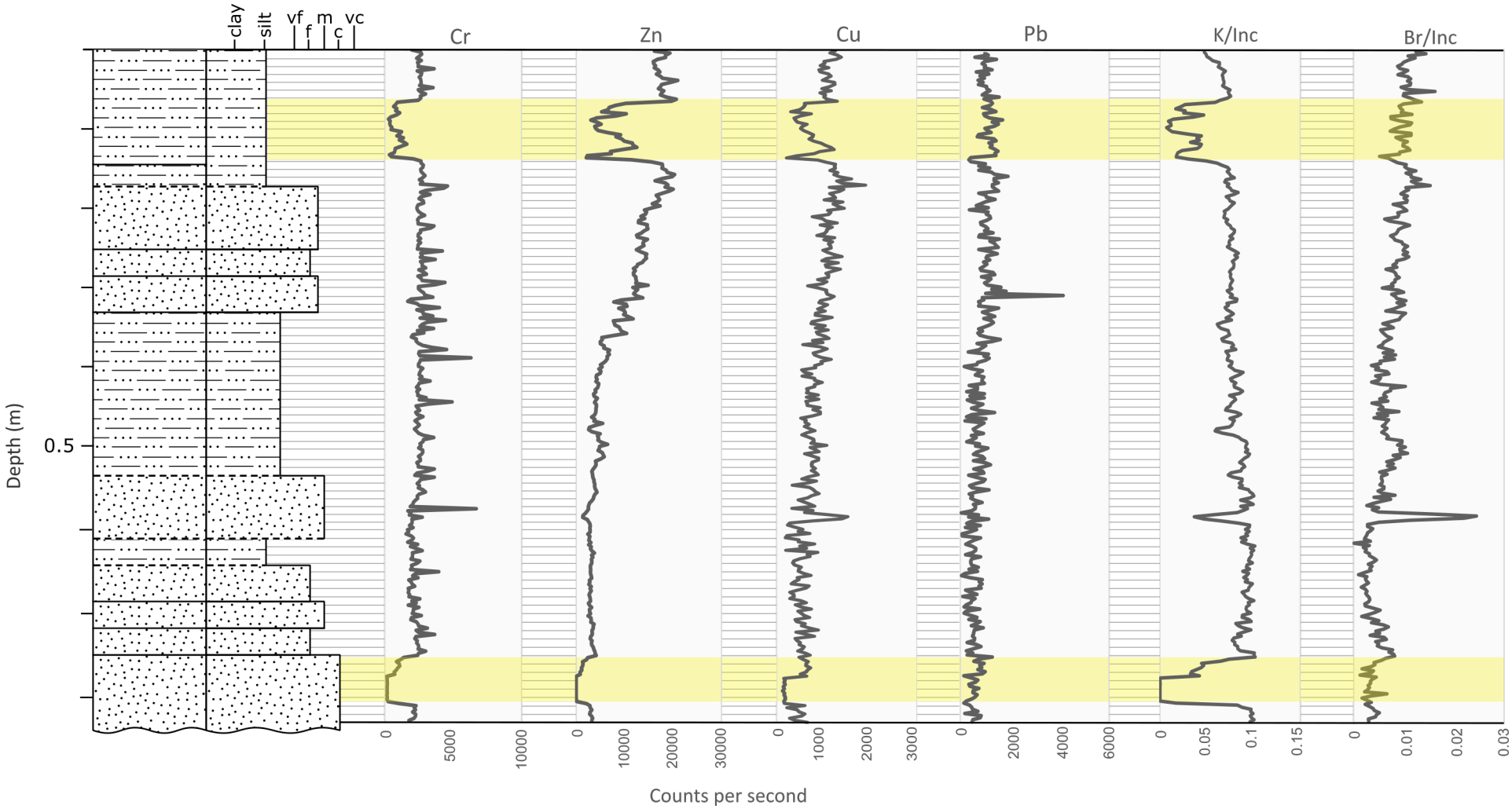

Figure 6.7: OTRB sediment core elemental and ratio results versus depth; Cr, Zn, Cu, Pb, K/Inc, and Br/Inc. Yellow shading represents validity = 0 data.

6.5 Purimu discharge zone

6.5.1 Visual analysis

The core retrieved from the subtidal Purimu (PUR) discharge zone was 92cm representing 99cm of estuarine sediment depth when accounting for in-field compaction. The core was dominated by sand, interspersed with rounded gravels and fine shell fragments (Figure 6.8). Thin layers of silt and sandy silt intersected the upper core and comprised the very base of the sample. Whole and fragmented bivalves and gastropods were recognized in the central and lower core with the lower core showing evidence of bioturbation. The colour of the core was dominated by 5Y 2.5/2 and 2.5Y 2/0.

6.5.2 Sediment chemistry

In the PUR core, Cr is relatively stable at 2,000-2500CPS with a spike at 35.7cm depth (Figure 6.9). Zn is divided into two clear sections by a zone of peak concentration at 20.0-31.0cm. Zn trends at approximately 6,000CPS in the upper 20cm and fluctuates between 2,500-3,500CPS in the lower section of the core with a spike to 4,937CPS at 44.1cm. Cu shows an increase in concentration with increasing depth, peaking at 46.1-54.9cm with the highest reading at 1,966CPS before the trend decreases after 54.9cm.

The K/Inc ratio in the PUR core is relatively stable between 0.04-0.1. The Br/Inc ratio has no clear trend though exhibits two distinctive zones between 0-34.0cm and 34.0cm to the base of the sample. In the upper 34.0cm the ratio generally increases with depth, spikes at 16.4cm and subsequently drops before rising to another peak at 26.7cm, and 44.3cm.

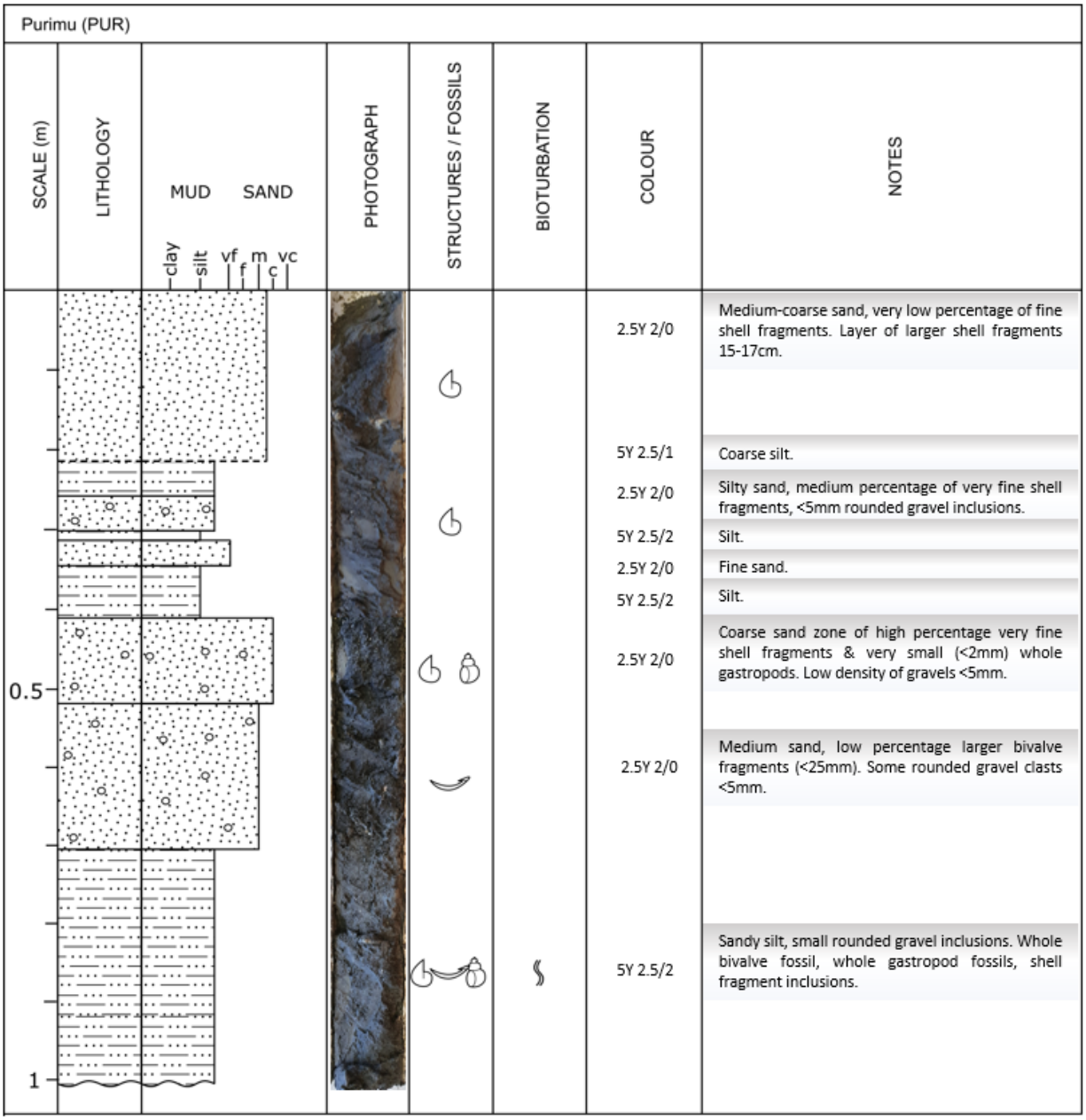

Figure 6.8: PUR sub-tidal sediment core sample stratigraphic log.

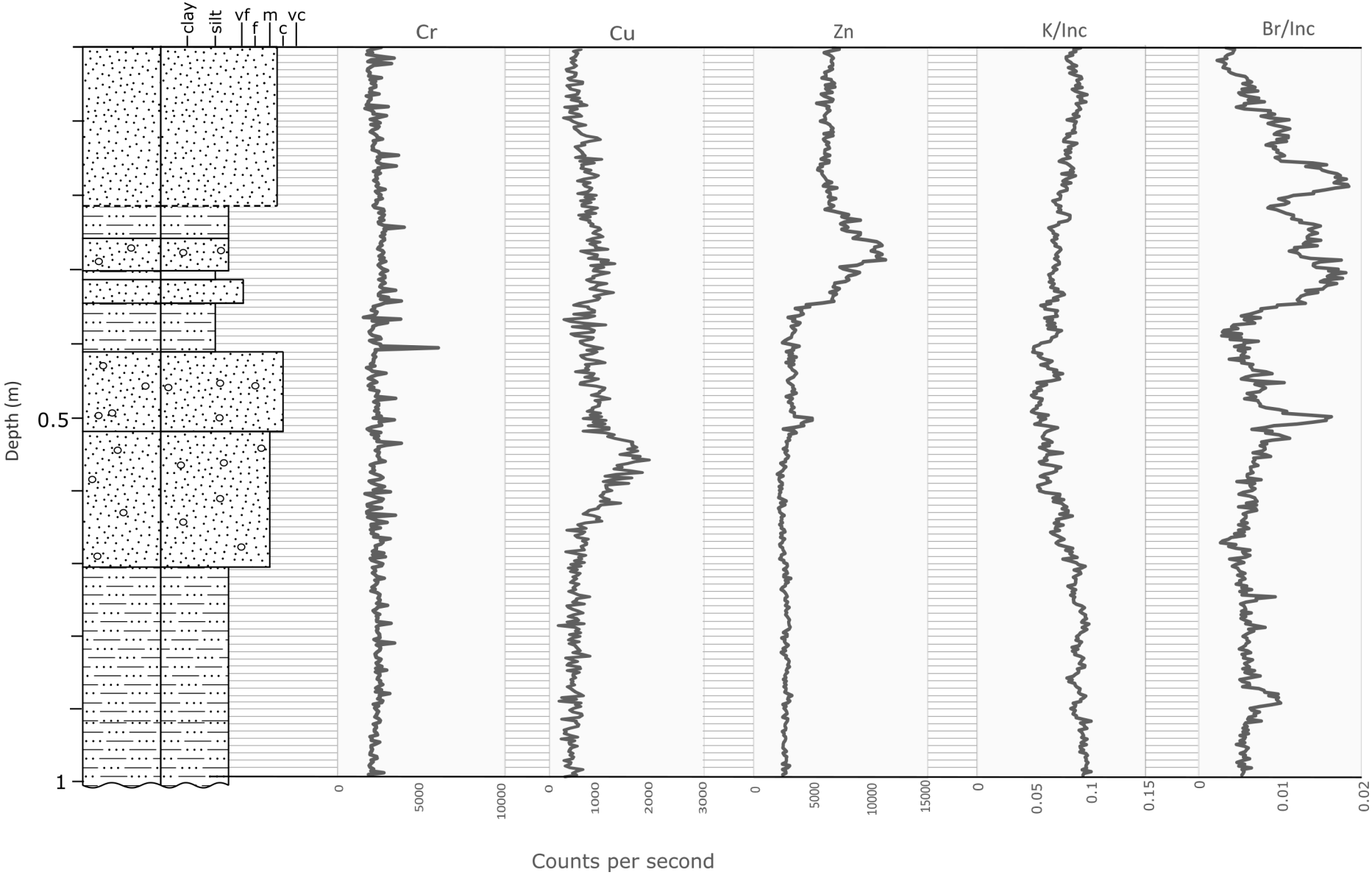

Figure 6.9: PUR sediment core elemental and ratio results versus depth; Cr, Zn, Cu, K/Inc, and Br/Inc.

6.6 Taipo discharge zone

6.6.1 Visual analysis

The 84cm core retrieved from the subtidal Taipo (TAI) discharge zone represented 101.6cm when corrected for in-field compaction. Four layers were identified in the sample, being the surface layer, a fine sand layer containing aligned shell fragments between 79.9cm-81cm and unconsolidated clayey-silt which comprised the body of the sample in layers two and four (Figure 6.10). Rounded gravel inclusions, shell fragments, large whole gastropod fossils and a whole bivalve were identified in the clayey silt. Munsell colour charts allowed identification of layers two, three and four as colour 5Y 2.5/2.

6.6.2 Sediment chemistry

The TAI sediment core encountered scanning issues between 53.5-55.0cm. Data validity in this section is zero and is therefore unreliable to include in the analysis.

In the TAI core, Cr is relatively stable at about 2,500CPS with a small peak to 3,124CPS at 60.8cm depth (Figure 6.11). Zn experiences a generally decreasing concentration from about 5,000CPS with increasing depth with a peak to 8,718CPS close to the surface of the core between 0.7cm-5.5cm. Cu shows a steady increase from 1,000CPS at the core surface to about 3,000CPS at the base of the core with a peak to 3,279CPS at 82.7cm depth. Pb does not show a clear trend fluctuating between 500-2,000CPS.

The K/Inc ratio for the TAI core resides about 0.09 at the core surface, declines to 0.056 at 37.5cm depth, then increases to 0.09 at 93.4cm depth. The Br/Inc ratio shows two distinctive zones, with the 0cm-57.5cm fluctuating about 0.016 and the lower core from 57.5cm fluctuating about 0.011.

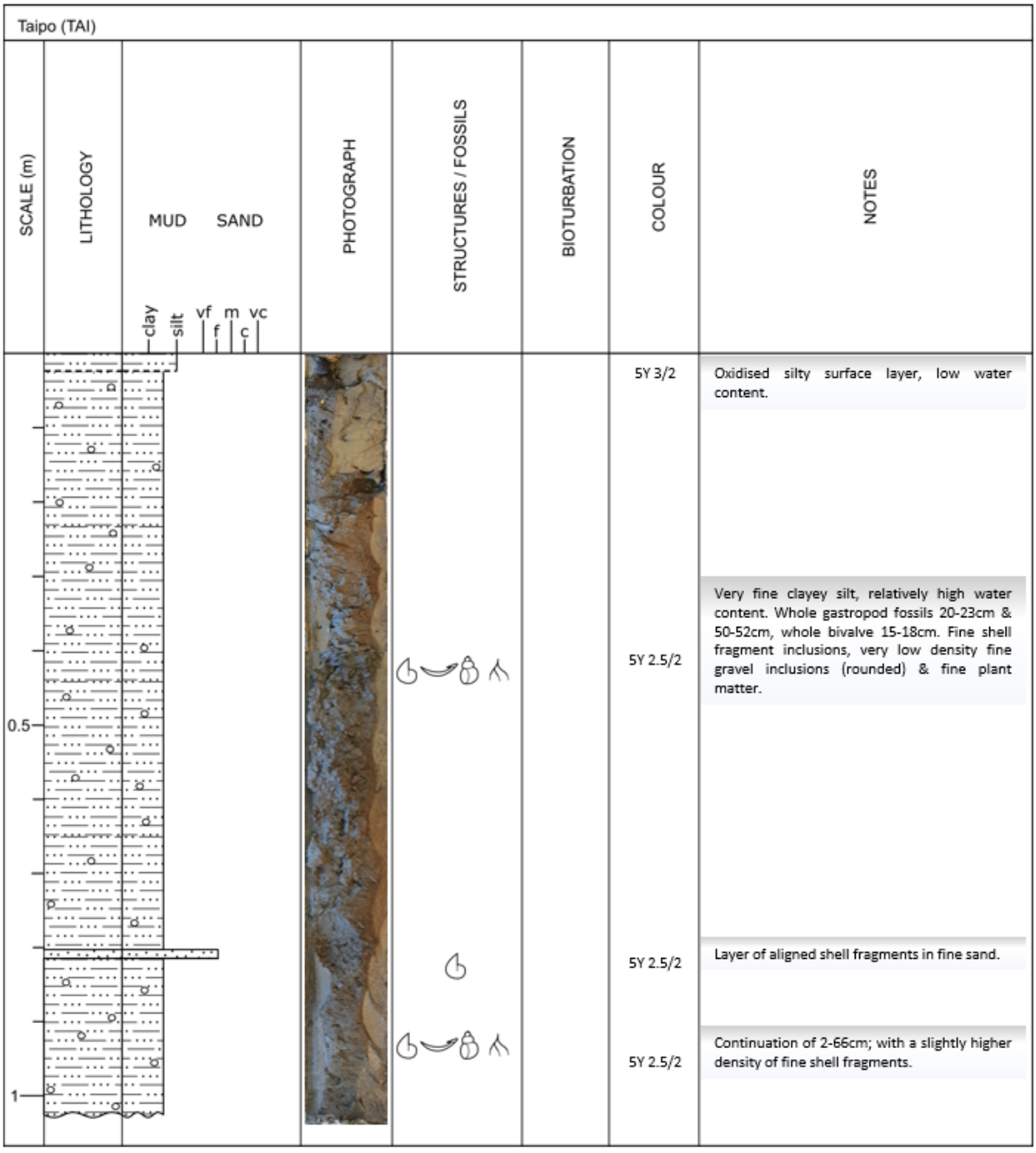

Figure 6.10: TAI sub-tidal sediment core sample stratigraphic log.

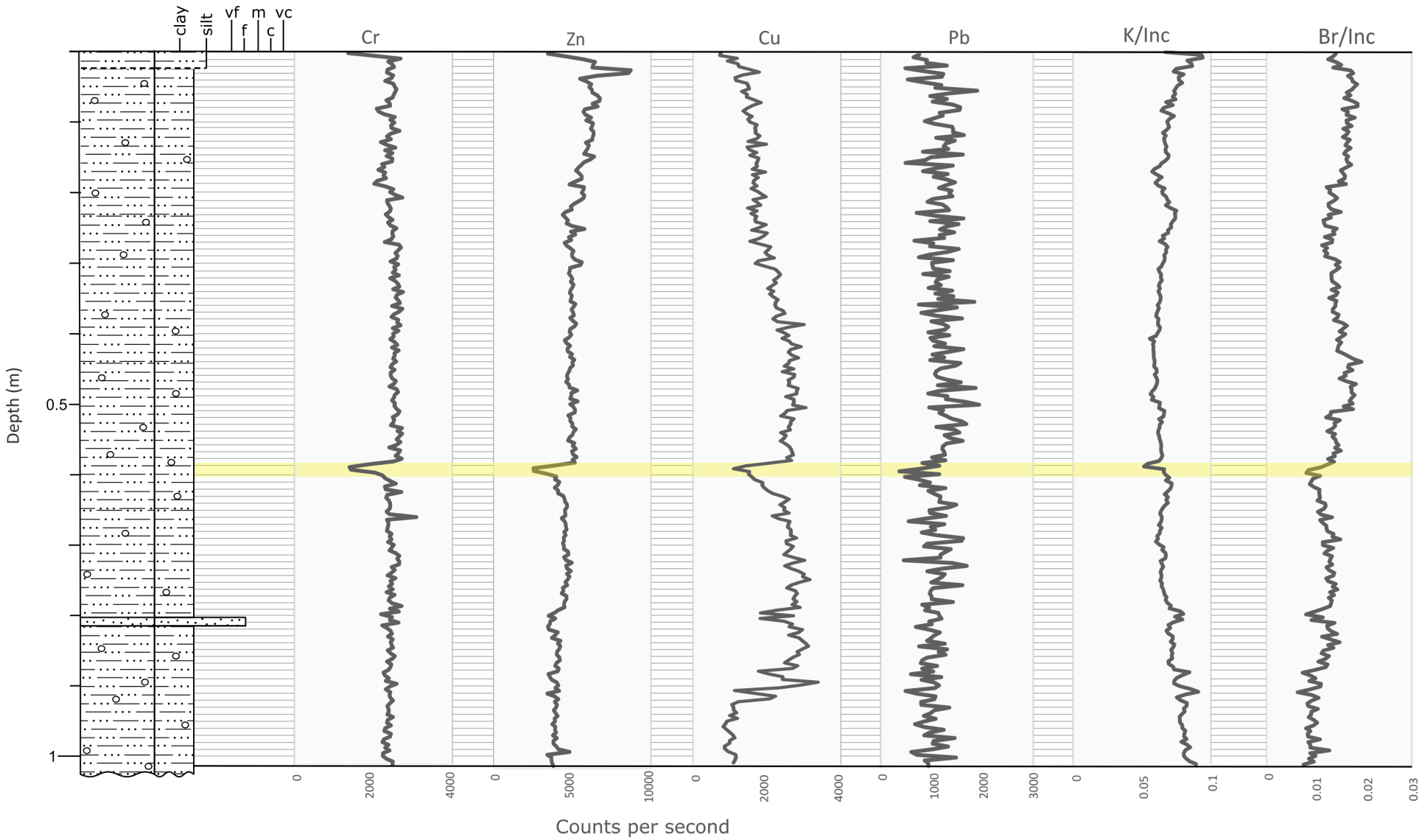

Figure 6.11: TAI sediment core elemental and ratio results versus depth; Cr, Zn, Cu, Pb, K/Inc, and Br/Inc. Yellow shading represents validity = 0 data.

6.7 Upper Ahuriri Estuary

6.7.1 Visual analysis

58cm of sediment was collected in the subtidal Upper Ahuriri Estuary (UAE) zone, representing a corrected estuarine depth of 63.2cm. The UAE core was silt-dominant, with varying densities of whole bivalve shells, shell fragments and minor bioturbation between 5.45cm-13.1cm (Figure 6.12).

6.7.2 Sediment chemistry

Cr in the UAE core is relatively stable about 3,000CPS with a peak to 4,156CPS at 5.2cm, and a drop to 2,406CPS at 26.1cm (Figure 6.13). Zn peaks at the surface of the core at 6,199CPS followed by a decline to 10.6cm depth where the trend stabilises downcore at about 3,500CPS. Cu peaks at the core surface at 691CPS followed by a decline to 21.9cm where concentration then fluctuates about 0CPS.

The K/Inc ratio for the UAE core exhibits a gradually increasing trend with depth in the upper 21.9cm, before no clear trend from 21.9cm downcore. A low ratio zone between 1.1-4.1cm is followed by a spike in K/Inc at 6.5cm to 0.1 then a drop to 0.08 at 21.5cm depth. Br/Inc shows a declining trend from the core surface with maximum reading of 0.02 to a stable trend of approximately 0.007 from 8.3cm depth. The Br/Inc ratio spikes to 0.025 at 21.5cm depth.

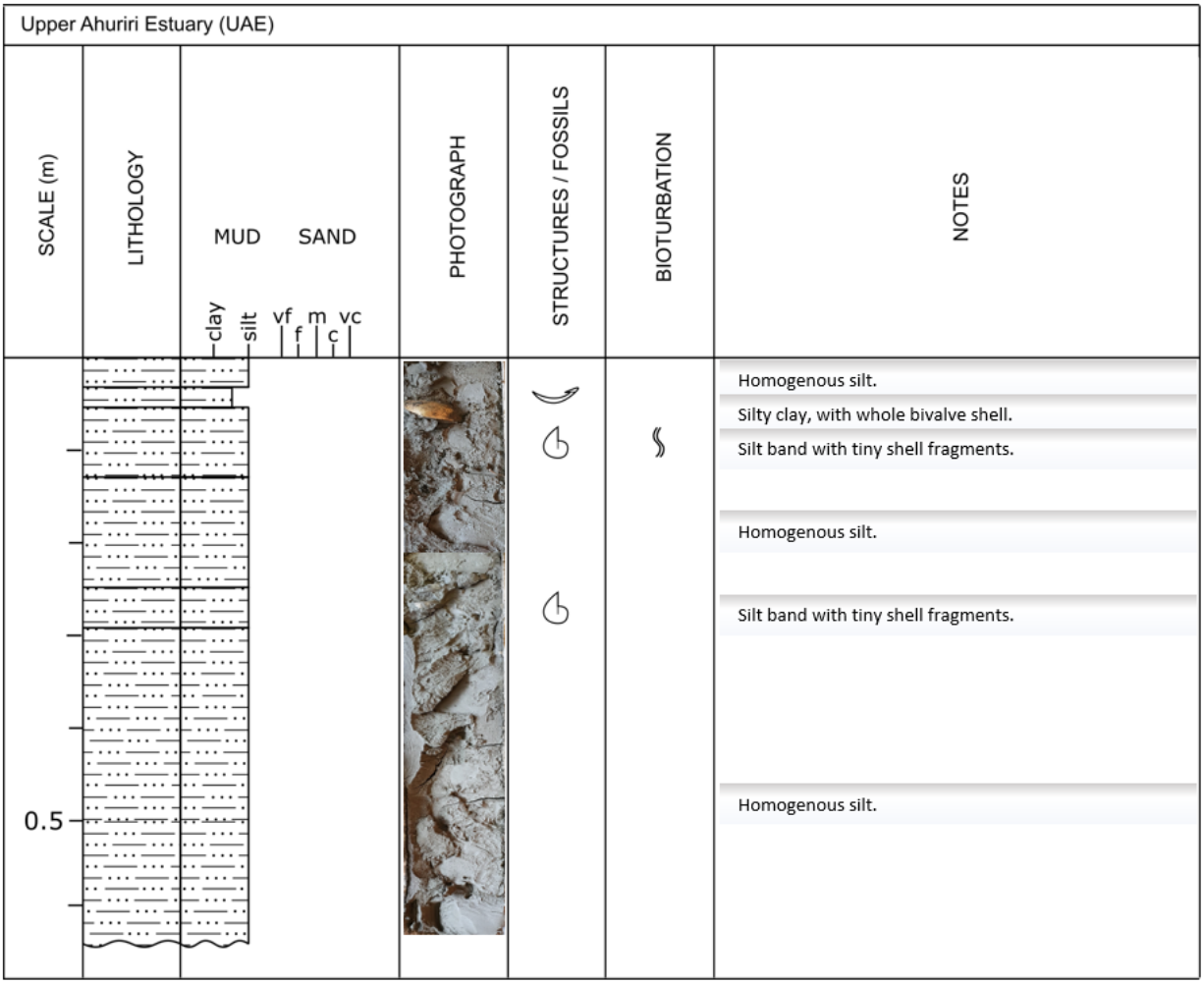

Figure 6.12: UAE sub-tidal sediment core sample stratigraphic log.

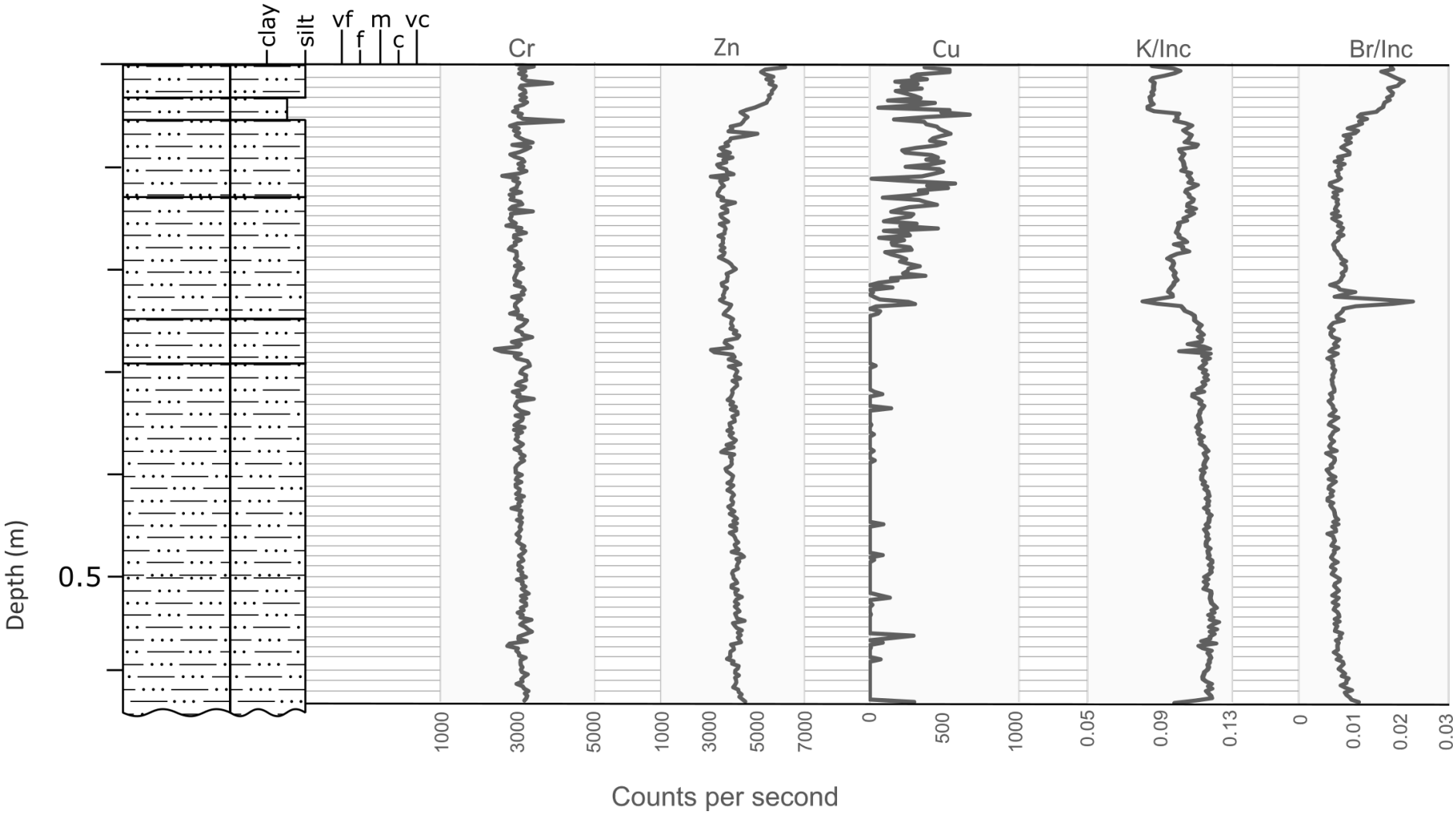

Figure 6.13: UAE sediment core elemental and ratio results versus depth; Cr, Zn, Cu, K/Inc, and Br/Inc.

6.8 Comparisons

Comparisons focused on the three samples retrieved in the discharge zones of waterways influenced by industrial zones in Napier City (being the Thames-Tyne (TT), Old Tutaekuri Riverbed (OTRB) and Purimu (PUR)) with the UAE sample overlain as a reference as a zone distant from urban tributaries. Three heavy metals Cr (Figure 6.14), Zn (Figure 6.16), and Cu (Figure 6.17) were graphed against corrected depth for these four cores while Pb (Figure 6.15) data was only available for TT and OTRB.

Comparative to the PUR, OTRB and UAE samples, the graphs highlight that the upper TT sample has excessive counts of Pb, Zn and Cu, each at 17.8cm depth and Cr at 14.0cm depth. In the case of Zn and Pb, the readings for the upper Thames-Tyne sample are enough to warrant a log plot. OTRB additionally shows high Pb levels which are exhibited throughout the upper portion of the core.

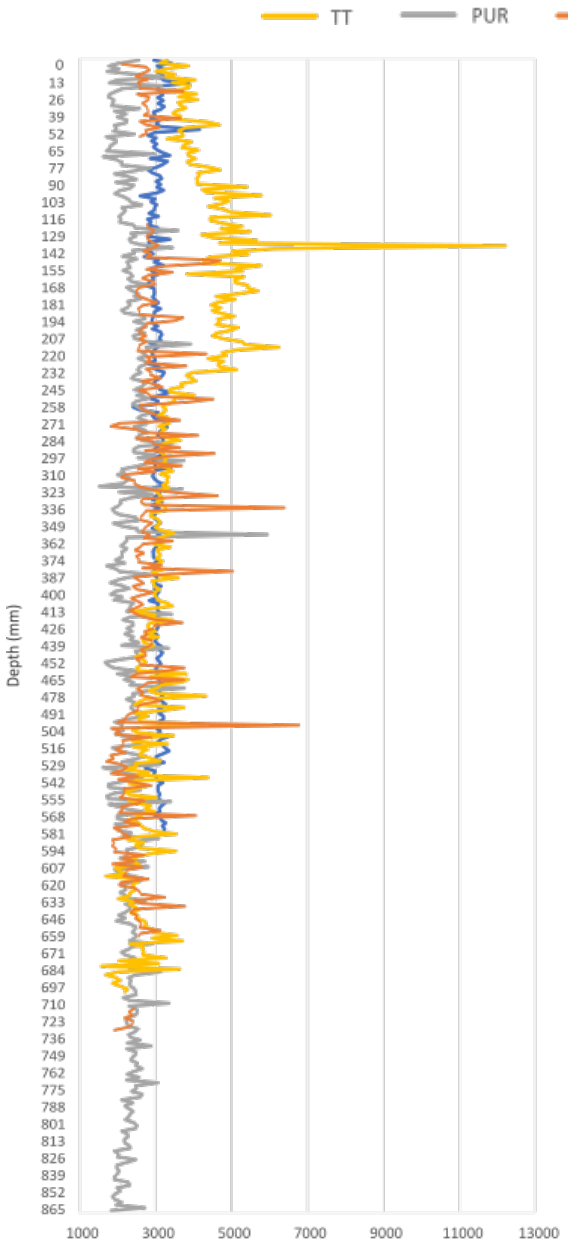

Figure 6.14: TT, OTRB, PUR and UAE chromium counts per second (CPS) comparisons by depth.

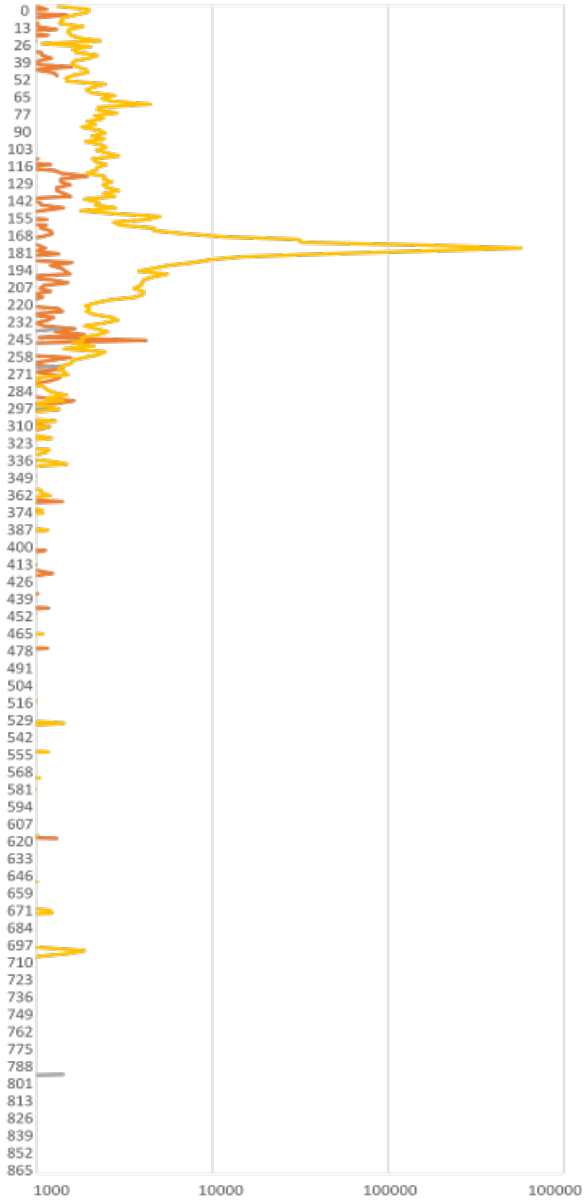

Figure 6.15: Log-scale TT and OTRB lead CPS comparisons by depth.

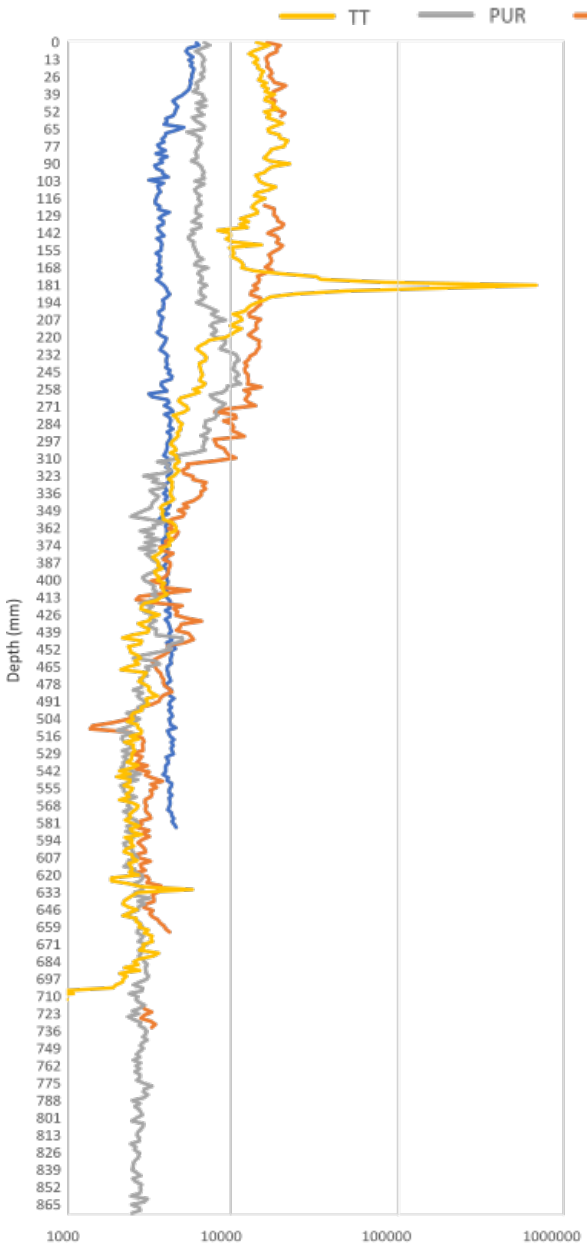

Figure 6.16: Log-scale TT, OTRB, PUR and UAE zinc CPS comparisons by depth.

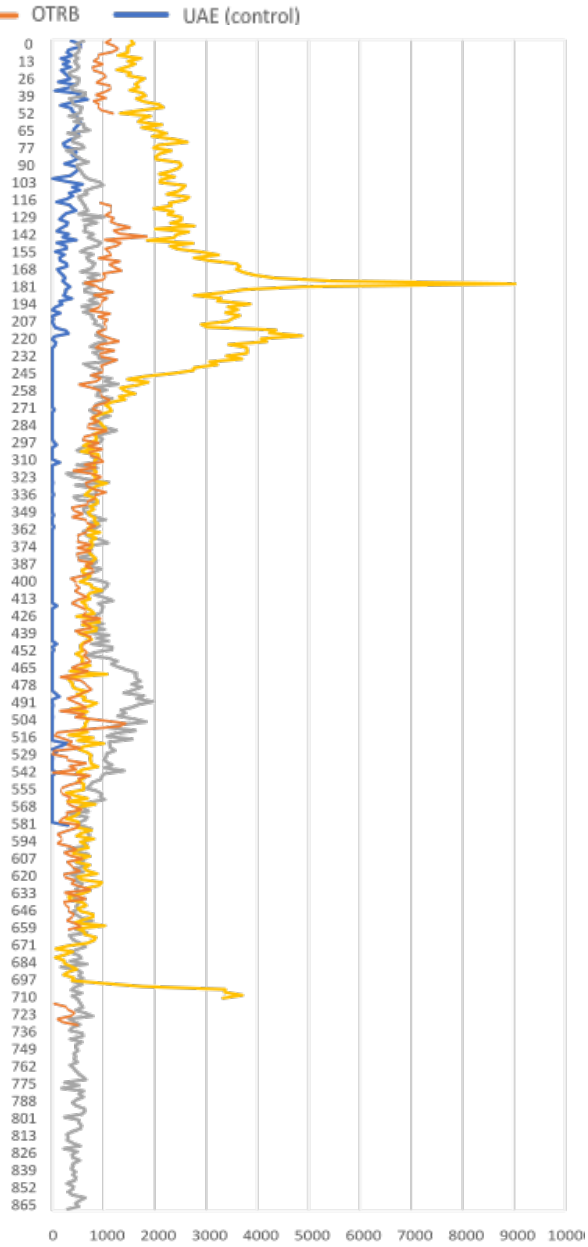

Figure 6.17: TT, OTRB, PUR and UAE copper CPS comparisons by depth.

6.9 Summary

This chapter presented physicochemical data from six Ahuriri Estuary sediment core samples. Where data were available, the four elements Cr, Cu, Pb, and Zn were plotted in CPS versus depth graphs as well as the ratios K/Inc, and Br/Inc. The OTRB and TAI core samples experienced minor issues with the Itrax™ XRF scanning which resulted in segments of zero validity.

Heavy metal trends typically showed higher counts in upper sections of the cores, with poignant spikes and dips from the trend visible across core lengths as well. Ratios similarly reflected changes in trends

across core lengths as well as prominent deviations. Inter-comparisons between the TT, PUR, OTRB and UAE core samples highlighted extreme differences in zinc in the TT and OTRB compared to the remaining two cores and in Pb between the TT and OTRB. The upper TT showed a zone of extremely excessive zinc, lead and copper counts at approximately 17.8cm depth with chromium showing an extreme spike at a shallower depth of 14.0cm. All cores showed a higher zinc concentration in the top 35cm of sediment.

In Chapter 7, these sediment physicochemical results are investigated and referenced to key developmental times in Napier City investigated in the multi-temporal sub-catchment assessment.

7 DISCUSSION

7.1 Introduction

This chapter discusses the findings of the study within the context of previous research. It focuses on the sub-catchment change assessment and the sediment physicochemistry analyses to investigate the interrelationship between the development of Napier City and the sedimentary health of Ahuriri Estuary. This chapter is split into six key sections:

1. identification of the 1931 Napier earthquake and sediment accumulation rates;
2. progressive sub-catchment industrialisation and the effects on Ahuriri Estuary;
3. placing the sediment physicochemistry results in the context of reviewed literature to identify the current health of Ahuriri Estuary;
4. discussing additional contributing factors to Ahuriri Estuary's current health; and
5. recommending tools for the prevention of further degradation of the estuary.

These six sections serve to address objectives two, three and four. In doing so, some of the identified gaps in the current knowledge of the health of Ahuriri Estuary are filled. Finally, this chapter briefly outlines the limitations of this thesis.

7.2 1931 Napier Earthquake & Sediment Accumulation Rates

7.2.1 Using sediment physicochemical data to locate the 1931 Napier Earthquake

7.2.1.1 Thames-Tyne and Southern Central Ahuriri Estuary

Based on the research of Chagué-Goff et al. (2000), identification of the uplift associated with the 1931 Napier earthquake is possible using grain size and sediment physicochemistry. In the TT core, a sharp grain size change at 49.6cm from medium sand to overlying sandy silt reflects a sudden change in depositional environment via a rapid reduction in hydrodynamic energy (Figure 6.2). A marked increase in the K/Inc ratio from 0.07 to 0.11 at 50.0cm suggests an increase in terrigenous input coinciding with the beginning of the sandy silt layer. From 50.0cm upward, Br/Inc also shows an increase to 0.015 with decreasing depth from a ratio near 0 at the very base of the core. The two ratios and the sharp grain size change from medium sand to overlying sandy silt indicate the 1931 earthquake is preserved at 50.0cm depth.

Moving up the TT core and mirroring the K/Inc trend, the Br/Inc ratio drops immediately after the identified 1931 earthquake at 50.0cm until increasing upcore from 42.0cm, reflective of a higher fluvial ratio and terrigenous input in the vicinity of the historic Tutaekuri flow path (Figure 7.1) until its engineered diversion in 1936. Both the B/Inc and the K/Inc trends begin to climb and become more variable with K/Inc dropping again from 29cm depth upward. Extensive drainage and reclamation within the Pandora sub-catchment explains this trend in K/Inc, with the channelisation and development of the modern linear Thames and Tyne waterways ongoing until 1980 (Figure 7.3) implying a time of higher terrigenous sediment loading at the TT core site.

Similar to the TT core, there is a sharp change in the SCAE core at 67.1cm depth (Figure 6.4) where a silty sand layer with gravel inclusions is overlain with coarse sand. Moving up the core, sediment

chemistry reflects a simultaneous drop in K/Inc to 0.05 and a spike in Br/Inc to 0.01 at 65.0cm depth, indicative of a decline in terrigenous input and a sudden increase in marine input. Due to the location of the SCAE core site, this can be attributed to a sudden reduction in fluvial input downstream of the historic Tutaekuri River discharge from the 1931 uplift followed by the diversion of the river itself.

7.2.1.2 Purimu and Old Tutaekuri Riverbed

The PUR core has a sharp change in grain size from silt to underlying coarse sand at 40.1cm depth (Figure 6.8), suggesting a change in depositional environment via a sudden reduction in hydrodynamic energy. The lowest K/Inc ratio is at 41-44cm depth. The Br/Inc ratio spikes at 44.3cm depth and becomes more irregular with decreasing depth. Guided primarily by the K/Inc ratio, and the change in grain size from silt to coarse sand at 40.1cm depth, the 1931 Napier earthquake can be attributed to an approximate depth of 41cm.

Similar to the TT, SCAE, and PUR cores, the OTRB core (Figure 6.6) exhibits a change in grain size between sandy silt and silty sand at 53.9cm depth, again suggestive of a rapid change in depositional environment. OTRB additionally shows a clear spike in Br/Inc to 0.03 and a drop in K/Inc to 0.04 at 50.9cm depth before both ratios return to a relative baseline level of 0.01 and 0.07 respectively throughout the lower part of the core. With the corresponding the change in lithology, this is suggestive of a sudden increase in marine input, and a simultaneous decrease in terrigenous input indicative of the 1931 earthquake.

In the PUR core, the Br/Inc ratio experiences a quiescence in the immediate depth above the suggested earthquake zone prior to fluctuating at increasing frequencies. This quiescence may also be attributed to the engineered diversion of the Tutaekuri River, for which the reduction in fluvial input exposed the core site to a higher marine hydrodynamic exposure. The PUR Br/Inc ratio shows fluctuations throughout the upper 34.2cm. This highlights its modern exposure to the tidal exchange through the constricted width of the main Ahuriri Estuary channel, as well as the geomorphological influences of the development of the State Highway 2 Bridge. The delineation of the Purimu channel from the OTRB waterway between 1969 and 1980 would have additionally altered the Br/Inc ratio through the new flow of freshwater over the PUR core site.

Below the identified 1931 earthquake in both the PUR and the OTRB cores are a series of sand and sandy silt layers. The coarser grain size of these pre-1931 sediments reflects the historic location of the PUR and OTRB sites as being in the centre of the historic Ahuriri Lagoon (Figure 7.1) likely exposed to high velocities from tidal exchange.

7.2.1.3 Taipo and Upper Ahuriri Estuary

Neither of the subtidal TAI and UAE cores showed distinctive sand to silt grain size changes (Figure 6.10 and Figure 6.12) indicative of changes in hydrodynamic energy as the four other cores. This is due to their location along the western margin of Ahuriri Estuary, and away from the tidal exchange (Figure 7.1). The TAI core experiences a heightened Br/Inc ratio of 0.02 indicative of increased marine input prior to a dip at 33.3cm depth, while K/Inc terrigenous input ratio experiences a minor low at 30.9cm depth. Due to the location of the core site close to the Poraiti Hills, this approximate zone between

30.9 and 33.3cm depth can be attributed to the effect of the 1931 earthquake uplift on the reduction in both marine and freshwater flow.

In the UAE core, there is a spike in the marine input Br/Inc ratio to 0.025 at 21.5cm. The ratio returns to baseline either side of this spike. The K/Inc ratio experiences a drop in ratio to 0.08 at 21.5cm. Due to the commonality in both ratios, the 1931 earthquake can be approximated to this depth, suggesting the upper 21.5cm of sediment has been deposited since.

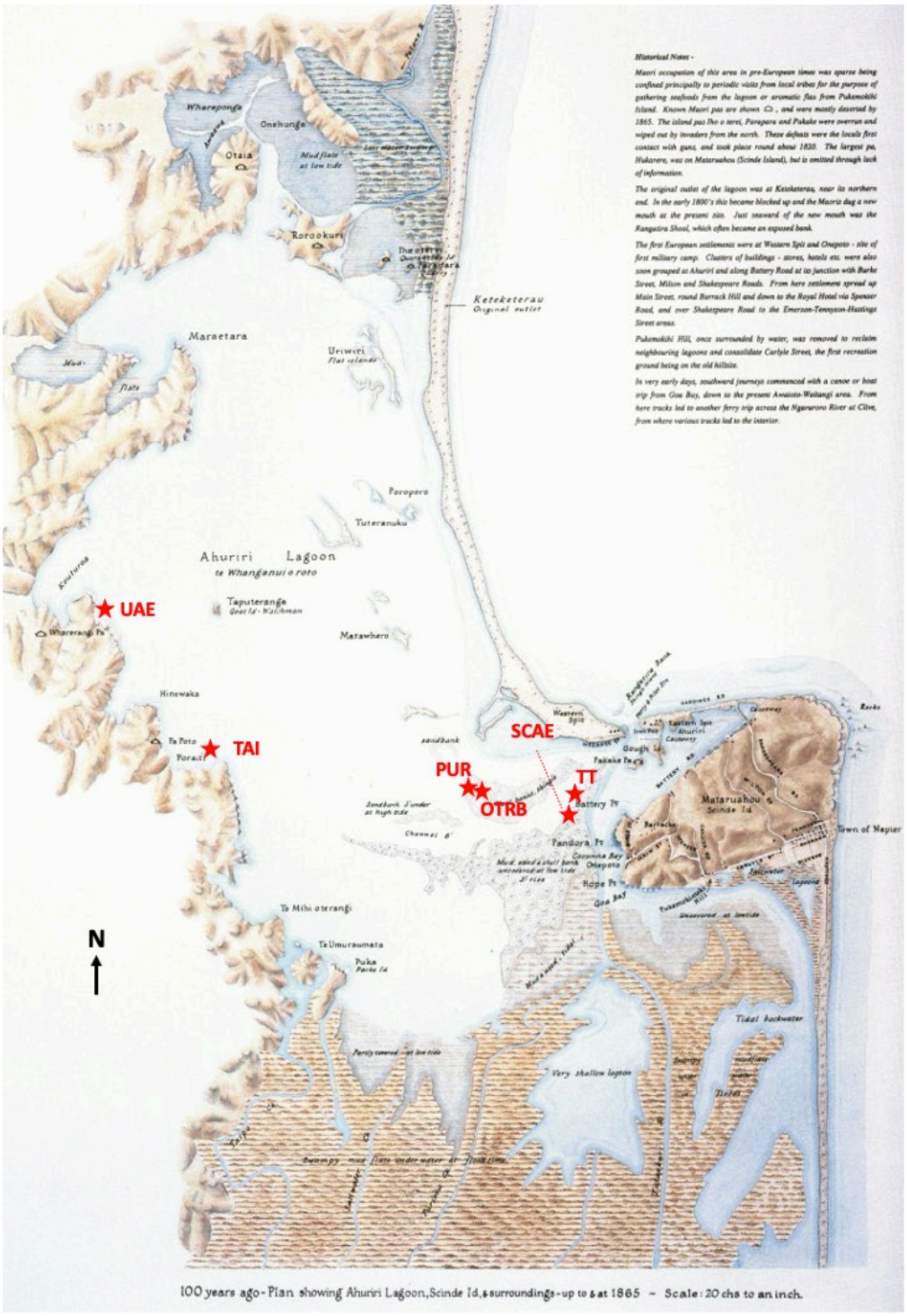

Figure 7.1: '100 years ago' sketched map of Napier City 1865 prior to the uplift of Ahuriri Lagoon. From Museum Theatre Gallery Hawke's Bay (n.d.). Six Ahuriri sediment core samples sites overlain in red.

7.2.2 Sediment accumulation rates

To date, sediment core sampling to assess impacts of sub-catchment industrialisation within Ahuriri Estuary has been limited. Of the studies that have taken place, Ataria et al. (2007) investigated sites representative of individual point-source discharges; however, cores were only collected to 100mm depth. Chagué-Goff et al. (2000) collected core samples to a depth which identified the 1931 Napier earthquake as well as undertook radioisotope analysis to determine SAR. However, Chagué-Goff et al. (2000) collected only three cores, missing essential discharge zone information from the Westshore Tidal Gates catchment which conveys surface water through the Onekawa Industrial area.

Sediment accumulation rates must be known to identify approximate depositional timeframes of key peaks in heavy metal counts across the six cores. Two of the six cores, being TT and TAI, have come from sites where Chagué-Goff et al. (2000) has previously assessed SAR using radioisotope analysis. Based on the SAR from the 'S0' and 'S2' cores collected in 1997 by Chagué-Goff et al. (2000), 103.2mm of sediment may have been deposited in the TT core vicinity and 91.2mm in the TAI core vicinity in the previous 24 years. In the remaining four cores, the identified depth of the 1931 Napier earthquake has been used as the basis for estimating average sediment accumulation rates over a 90-year period (Table 7.1).

Table 7.1: Application of Sediment Accumulation Rates (SAR) derived from Chagué-Goff et al. (2000) for TT and TAI cores, and 90-year averaged SAR for the four remaining cores.

Core	SAR from Chagué-Goff et al. (2000).	1931 depth from Chagué-Goff et al. (2000).	Indicative 1931 depth in 2020/21 cores using 1931 depth from Chagué-Goff et al. (2000).	1931 depth from grain size & Itrax™ ratio data	Averaged SAR
TT	4.3mm yr^{-1}	'S0' core: 41cm	51.3cm	49.6cm	3.7mm yr^{-1} since 1997
SCAE	-	-	-	67.1cm	7.5mm yr^{-1} since 1931
OTRB	-	-	-	53.9cm	5.9mm yr^{-1} since 1931
PUR	-	-	-	40.9cm	4.5mm yr^{-1} since 1931
TAI	3.8mm yr^{-1}	'S2' core: 25cm	34.1cm	30.9cm	2.6mm yr^{-1} since 1997
UAE	-	-	-	21.5cm	2.4mm yr^{-1} since 1931

The new estimated SAR for the TT and TAI cores are lower than those from Chagué-Goff et al. (2000), though not dissimilar. Vertical sedimentation in a dynamic estuarine environment is non-linear. Biological reworking, sediment autocompaction, land-based flood events and associated sediment deposition and/or erosion and the effects of high energy events such as storm-driven erosion and deposition have not been measured (Eyre, 2009; Hayward et al., 2006). In addition, excessive suspended sediment concentrations found at 21 of 22 sites within the tributary urban waterways likely affects true SAR. For an estuary which is ebb-tide dominated, with flood-tide dominance over the intertidal flats (Eyre, 2009), with an excessive fluvial terrigenous sediment input, and with cohesive fine sediment intertidal beds, it is plausible that average sedimentation rates are variable.

While the estimated accretion rate of SCAE is high compared to the remaining cores, it can be explained by its location within the upper margin of an intertidal zone which is unaffected by freshwater channel discharges and is exposed for most of the semidiurnal tidal cycle. This 7.5mm yr^{-1} rate is comparable to other urbanised estuaries in the populated Penobscot Estuary, Maine (Yeager et al., 2018) and the mixed-catchment Palmones River Estuary, Spain (Rubio et al., 2003). Hydrodynamic energy over the intertidal zones of the central estuary is too low to create the shear required for the erosion of cohesive fine silts (Eyre, 2009). Accretion rates may be both high and non-linear in this zone as the water column is effectively squeezed and tidal flushing becomes less efficient.

7.2.3 Summary

Four of the six cores from Ahuriri Estuary exhibit sharp grain size changes between silts and sands indicative of a sudden change in the depositional environment. Using a combination of these visual cues, peaks in the Br/Inc marine organic matter ratio and peaks in the K/Inc terrigenous input ratio, these grain size changes have been attributed to the uplift caused by the 1931 Napier earthquake. In the silt-dominant upper estuarine cores, the K/Inc ratio and the Br/Inc ratio have been relied upon to indicate the 1931 uplift in the absence of sharp grain size changes. As a result, the 1931 Napier earthquake can be traced across the six cores from Ahuriri Estuary (Figure 7.2). This adds boundary depths for the exploration of the effect of Napier City's industrial development on the sediment chemistry of Ahuriri Estuary and allows the linkage of peaks in heavy metal concentrations to depositional timeframes using updated SAR from Table 7.1.

Figure 7.2: Compiled stratigraphic logs, graphed from west (left) to east (right): UAE, TAI, PUR, OTRB, SCAE, TT. Purple fill indicates deposition post-1931 earthquake.

7.4 Sub-catchment industrialisation and Ahuriri Estuary

7.4.1 Thames-Tyne discharge zone and Southern Central Ahuriri Estuary

The Pandora Industrial zone is dominated by 79% industrial land-use (Figure 5.7) and the TT core site is in the direct flow path of the Thames-Tyne waterway network which conveys storm and surface water from the industrial catchment. Relative to the other cores, the TT core shows a very high Pb and Zn count in the upper 18cm (Figure 6.3), with an extreme spike in Zn, Pb and Cu at 17.8cm depth. Using a combination of the averaged SAR between 1997 and 2021 in Table 7.1, and the estimations from Chagué-Goff et al. (2000), the date of the Cr peak at 14.0cm depth becomes 1985 and the 17.8cm peak in Zn, Cu and Pb becomes 1975 assuming SAR are relatively linear. Between 1969 and 1980, Pandora developed from 30.7% industrial land-use by area to 49.5% (Figure 7.3). During the estimated 1975 peak in Zn, Cu, and Pb, the fringing industrial zone was experiencing rapid development. This rapid reduction of surface water filtering grasslands and expansion of heavy impervious industrial surfacing was negatively affecting the sediment chemistry of the TT discharge zone. The sheer scale of the peak in Zn and Pb suggests a particularly problematic time in the development of the industrial estate, with high concentrations spanning 14.8mm vertical depth, or approximately 3.5 years between 1973 and 1976. The peak in Cu spans approximately 1.5 years.

The SCAE core is indirectly influenced by the Pandora Industrial zone on ebbing tides (Eyre, 2009). Zn trends about 6,000CPS in the upper 30cm of the SCAE core, leading into a peak occurring 32.8cm-34.7cm depth, namely 1977 and 1982 using estimated SAR. This coincides with the historic estuarine discharge of the Thames Waterway through the SCAE core zone prior to its confluence with the Tyne occurring after 1980 (Figure 5.5 and Figure 5.6). In the tidally influenced Thames-Tyne waterway network, this peak, alongside the peak in Cr at 36.1cm depth, further confirms that the 1980's was a time of high metal mobility from industrial development on the southern margin of Pandora's Thames Waterway.

The up-core increase in heavy metal counts for the TT and the SCAE cores culminates in an approximate zone of peak concentration at 17-35cm depth. Heavy metal levels then reduce toward the core surface. As an industrial zone housing metal processing plants, metal product manufacture is a very likely source of Zn, Cr, Cu, and Pb contamination. High heavy metal concentrations in both cores can be attributed to a lack of historic prioritisation around stormwater and surface water cleanliness resulting in contaminated water runoff and particulate-bound metal deposition to estuarine sediment (Jartun et al., 2008; Kennedy & Sutherland, 2008). Alongside a number of contaminated sites in the Pandora Industrial zone (Hawke's Bay Regional Council, 2009b), an historic unlined landfill also fringes Ahuriri Estuary (Hawke's Bay Regional Council, 1996) permitting free interaction with tidal shallow groundwater from the estuary itself. The slow capillary movement of the brackish groundwater would ensure its abrasiveness against buried historic waste and the subsequent potential for dissolved metal transportation, which may be impacting the sediment quality in the vicinity of both the TT and SCAE depositional sites.

7.4.2 Purimu and Old Tutaekuri Riverbed discharge zones

In the PUR core, none of the peaks in the counts of Zn, Cr, and Cu coincide though each heavy metal typically increases in concentration with decreasing depth (Figure 6.9). Zn counts trend about 6,000CPS within the uppermost 20cm, before peaking over 19.2cm-30.3cm, equating to approximately 1954-1975. Cr experiences a peak to 5,937CPS at 35.7cm depth from a trend of approximately 2,000CPS or a time of 1942 using averaged SAR. Conversely, Cu experiences an increasing trend with increasing depth to a peak of 1,966CPS at 48.4cm. Based on calculated SAR, this would have been deposited prior to the 1931 Napier Earthquake implying the Tutaekuri River's historic conveyance of excess copper from cropping application in the wider catchment (Gaw et al., n.d.).

Indicative depositional ages for the peak concentrations in the PUR core are ambiguous. This is due to the higher energy hydrodynamic environment of the discharge zone of the Purimu Waterway which is reflected in the stratigraphy of the PUR core. Contrasting with the other five cores, the upper 21.5cm of PUR is comprised of medium grained sand, despite residing in the discharge zone of the Purimu Waterway, which experiences excessive fine suspended sediment loading (Figure 3.32). The subtidal nature of the core site, combined with its location within the Ahuriri Estuary main channel, likely experiences too high flow velocities and bed shear to allow long-term settling of finer sediment grains. Heavy metal pollutants are typically associated with fine-grained sediments due to their negative charge and propensity for adhesion. This means this upper sand unit may not reflect the true degree of catchment-origin heavy metal pollutants and may show as comparatively lower in metal concentrations than the other six sediment cores.

In the OTRB core, Pb concentrations in the upper 33.2cm of the core are approximately 1,000CPS though a peak in Pb of 4,165CPS occurs at 26.6cm. Applying the SAR of 5.9mm yr^{-1} would place this peak in Pb concentrations at approximately 1976. Cr has three peaks at 33.7cm, 38.5cm and 50.2cm depth, representing approximate depositional timeframes of 1964, 1956, and 1936. Zn experiences a decreasing concentration with increasing depth, with a zone of maximum concentration at 12.4cm-17.2cm, equating to 1992-2000. This is prior to the construction of SH2 Bridge in the early 2000's when much of the surface water from Onekawa Industrial zone (and much of residential Napier) was discharging in the vicinity of the OTRB core. During this time, Onekawa industrial zone was comprised of approximately 70% highly productive, impervious surfacing (Figure 7.3 and Figure 5.10) which houses metal processing plants similar to the Pandora Industrial zone.

A peak in Cu of 1,934CPS at 14.7cm depth additionally reflects the location of the OTRB sediment core being within the primary impact zone for Onekawa's surface water discharge. Additional contaminated sites (Hawke's Bay Regional Council, 2009b) as well as another historic unlined landfill resides close to Onekawa (Hawke's Bay Regional Council, 1996) which may have contributed to poor waterway quality through shallow groundwater flow.

A lack of gravels is a distinguishing feature of the OTRB core. However, fluvial power may not have been enough to convey gravels to the core sites pre-1931 location in the central Ahuriri Lagoon (Figure 7.1) due to the topographically flat nature of Napier City. In addition, the control gate between the waterway and the estuary, which has been in place since at least 1936 (Napier City Council, n.d.-b) has potentially

impeded gravel exchange from the OTRB to the Ahuriri Estuary and vice versa – an additional effect of the built environment on Ahuriri Estuary's geomorphology.

7.4.3 Taipo discharge zone and Upper Ahuriri Estuary

The two cores from the upper estuary, TAI and UAE, are the least influenced by tidal flow (Eyre, 2009). The TAI core fringes the immediate discharge of the Taipo Waterway, which services a large residential catchment, and flows into Ahuriri Estuary untreated like the other Napier urban waterways. The TAI core is predominantly clayey silt, reflecting the low-velocity Taipo discharge zone, and presents good material for adhesion of heavy metals. Pb levels throughout the TAI core fluctuate at levels similar to the OTRB core which receives surface water from the Onekawa Industrial zone. Cu conversely declines in concentration with decreasing depth, with 3,279CPS at 82.3cm depth, to approximately 1,000CPS at the surface of the core. Zn is the only heavy metal to reflect the trend of increasing concentration with decreasing depth, peaking at 8,569CPS between 7.3 and 18.2cm. Using SAR, this reflects an approximate time of 1964-1994. This Zn increase in the TAI core can be explained by its vicinity to the slow-flowing, untreated Taipo Waterway, which receives surface water from the Taradale and Greenmeadows residential suburbs and the interconnecting road network. The Taipo catchment was historically dominated by undeveloped grassland (Figure 5.15). This gradual reduction in cropping land in the catchment for housing development may also contribute to the observed decrease in Cu concentrations through the decrease in copper-based pesticide application (Gaw et al., n.d.).

The propensity for heavy metal adhesion and settling is high in the UAE core due to its silt dominance (Jartun et al., 2008) and its residence in near-stagnant waters. Cu peaks near the surface of the core, reflective of its continued use in a wide range of urban and rural settings (Hwang et al., 2016; Salomons & Förstner, 1984), prior to declining and fluctuating about 0CPS from 22cm depth. Considering the estimated 1931 earthquake depth in the UAE core of 21.5cm, the accumulating Cu concentrations upcore is suggestive of increasing Cu mobilisation from the Poraiti hills from about the time of the earthquake. Cr and Zn are similar with trends declining to 26.1cm depth. Zn peaks at 6,199CPS at the surface of the core with a zone of high concentration between 0-5.2cm. Cr peaks at 4,156CPS at the same 5.2cm depth, or 1999 by estimate. While distant from the discharge zones of urban tributaries, the UAE core reflects the same increasing heavy metal trends observed across the other Ahuriri sediment cores, suggesting that much of Ahuriri is affected by land system change.

7.4.4 Caveats to interpretation of Itrax™ heavy metal data

A variety of factors such as sediment heterogeneity, grain size, exposure times, scan resolution and water content can affect the peak area data in Itrax™ sediment core scanning (MacLachlan et al., 2015). MacLachlan et al. (2015) suggest that above a 25% grain size by weight of sand and larger grains can affect peak areas of lighter elements such as silicon and calcium. Grain size and heterogeneity affecting scan resolution may be a direct result of the decreased surface area these larger sediments have for metal adhesion compared to fine silts and clays. In addition, sediment heterogeneity is affected by burrowing species which decrease the cohesiveness of fine sediment beds by permeation and subsequently changing the interstitial fluid content (Botto & Iribarne, 2000). Physical weathering and physicochemical diagenesis can also lead to reworking and disturbance of the sediment chronology

(Buggy & Tobin, 2008; Cundy et al., 2003): processes which make for a dynamic environment and can affect efforts of reconstructing estuarine quality history through sedimentary archives.

7.4.5 Summary

Linking peak heavy metal concentrations to approximate depositional timeframes using SAR calculated in Table 7.1, the early 1970s is a timeframe in common across five of the six Ahuriri Estuary cores and the five cores which are, or have been directly influenced by, urban tributary discharges (Table 7.2). This was a time where industrial coverage in the Onekawa and Pandora Industrial zones – which influences four of these cores – was approximately 50% of the total 293.5 focus area, or 59% of the total industrial coverage of 2018 (Figure 7.3). A pollution event captured in the TT core shows extremely high concentrations of Pb, Zn and Cu, each with the peak at the same 17.8cm depth or at 1975 using SAR calculated in Table 7.1.

Table 7.2: Depths of peak zones and subsequent depositional timeframes of heavy metal concentrations in each core.

Core	Urban tributary influence	Depth of peak heavy metal counts	Depositional timeframe
TT	Thames-Tyne	17.0cm – 18.5cm	1973 – 1976
SCAE	Thames (until after 1980)	14.6cm – 34.7cm	1977 – 2001
OTRB	Old Tutaekuri Riverbed	12.4cm – 26.6cm	1976 – 2000
PUR	Purimu	19.2cm – 30.3cm	1954 – 1975
TAI	Taipo	7.3cm – 18.2cm	1964 – 1994
UAE	-	0 – 5.2cm	1999 - 2021

The UAE site reflects the impact of modern urban land use in Zn and Cu concentrations in the upper 5.2cm. By contrast, heavy metal concentrations in the five urban tributary influenced samples reduces towards the surface of the cores above the depths of peak counts identified in Table 7.2.

Figure 7.3: Time series of industrial sub-catchment development; Onekawa Industrial and Pandora Industrial areas.

7.5 The current health of Ahuriri Estuary

7.5.1 Comparison of Ahuriri Estuary to other estuarine Itrax™ results

Being able to place the sediment quality of Ahuriri Estuary amongst studies which also employed Itrax™ XRF scanning techniques can assist in understanding the current health of the estuary in the context of this study. In addition to the Ahuriri Estuary XRF sediment core data deciphered by Chagué-Goff et al. (2000), studies by Gadd et al. (2015) and Rodríguez-Germade et al. (2015) undertook XRF scanning of estuarine-origin sediment in populated catchments. These studies discovered similar trends to the six Ahuriri Estuary sediment cores in that the concentrations of heavy metals Zn, Cu, Cr and Pb typically increase with decreasing depth, often with a zone of peak concentration around 5-25cm depth, depending on catchment use, localised SAR and sediment grain sizes (Chagué-Goff et al., 2000; Gadd et al., 2015; Rodríguez-Germade et al., 2015).

In the Spanish Ria de Huelva Estuary, the highest peak area Pb concentrations were approximately 10,000, Zn were approximately 13,000 and Cu trended between 20,000-30,000 (Rodríguez-Germade et al., 2015). Comparing Ahuriri Estuary to the Ria du Huelva Estuary which has a highly acidic fluvial tributary averaging pH <3 from a catchment supporting industrial metal mining, Zn levels from peak contamination zones identified in Table 7.2 are largely comparable across the board, while Pb levels and Cu levels are generally lower. The exceptions are the levels of Zn and Pb identified in the TT spike at 17.8cm depth which are 53 and 57 times the highest readings obtained in the Ria du Huelva respectively. However, direct comparison of peak intensities between studies is difficult, as it often does not allow consideration of the effect of individual sediment core composition.

The urbanised Australian Mill Creek catchment supports quarries, a landfill and a legacy nuclear waste site (Gadd et al., 2015). Cu and Pb counts from the six Ahuriri Estuary cores are akin to Mill Creek, both analytes residing around 500CPS throughout each of the cores. In Mill Creek, Ria du Huelva and Ahuriri Estuary, most cores exhibit a reduction in heavy metal concentrations towards the surface after a peak zone. This echoes the notion that modern prioritisation of waterway quality and subsequent improvements in land management can slow declining estuarine health.

7.5.2 Industrial coverage and heavy metals in Ahuriri Estuary sediment

Given mobilisation from stormwater, industrial activities are commonly identified as significant contributors of dissolved and particulate-bound heavy metals (Buggy & Tobin, 2008; Makepeace et al., 1995), nutrients (Mallin et al., 2009), hydrocarbons (Crane, 2019), compounds (Rossi et al., 2004), bacteria (Geldreich et al., 1968) and emerging contaminants (Pitt et al., 1995). Adsorption of such heavy metals and compounds to particulate sediment (Chester & Jickells, 2012; Jartun et al., 2008) and fine-grained sediment in particular (Chagué-Goff et al., 2000) is one of two primary hydrocycle contaminant transport methods (Buggy & Tobin, 2008).

Once contaminated sediment is in suspension in water, deposition becomes a result of a balance of grain size, flow velocity (Eyre, 2009) and flow type being laminar or turbulent (Chester & Jickells, 2012). Urban stormwater networks are typically designed to encourage higher velocities and laminar flow to keep sediment and debris in suspension and reduce maintenance costs of dredging channels and cleaning sediment from pipes (Rinas et al., 2019). Urban waterway tributaries in Napier City are

similarly designed to prioritise high flow drainage, evident in their channelised linearity (Figure 7.3). As a result, Napier City's urban waterway conveyance system is encouraging sediment deposition at the discharge environment.

After conveyance from the catchment to the Ahuriri Estuary depositional zone via freshwater tributaries, direct outfalls and catchment runoff, particulate-bound heavy metals and terrigenous sediment flocculate in the presence of converging saline and fresh water (Chester & Jickells, 2012; Dyer, 1988; Eyre, 2009). With contaminated particulates from Napier's urban tributaries requiring low velocities for deposition and with secretion of mucus from benthic organisms increasing shear stress for resuspension (Lelieveld et al., 2003), land-derived heavy metals can easily accrete in the fine-grained intertidal zones of Ahuriri Estuary (Eyre, 2009; Plater & Kirby, 2011) archiving historic water quality trends (Chester & Jickells, 2012; Cundy et al., 2003; Swales et al., 2002).

The Onekawa and Pandora Industrial areas have a modern influence over three of the six cores being TT, OTRB and PUR, and an historic influence over the SCAE core. While Cr and Cu levels are relatively similar across all cores, Zn and Pb levels indicate that more heavy metals have been mobilised from the Onekawa Industrial zone than the residential TAI sub-catchment and that the depositional zones of all sub-catchments are more enriched in heavy metals than the UAE zone. The two cores influenced by Pandora show levels of Pb and Zn far higher than the remaining four cores, identifying that the Pandora Industrial zone has contributed higher volumes of heavy metals to Ahuriri Estuary than the Onekawa Industrial zone and the residential Taipo catchment.

The highest industrial coverage across the Onekawa and Pandora focus area is exhibited in 2018 at 76.1% (Figure 7.3) though the zones of peak heavy metal concentration in sediment are largely representative of the 1970s (Table 7.1). During the 1970s, industrial coverage within the Onekawa and Pandora Industrial zones was 60.1% of the total land coverage. These peak heavy metal contamination zones including the extremities observed in the TT core show that a time beginning about the 1970s was a time of frequent pollution events, limited prioritisation around stormwater cleanliness and a lack of prioritisation of surface water quality in Napier City. Resultantly, contaminated water runoff and particulate-bound metal deposition to the sediment Ahuriri Estuary was chronic.

From the modern water quality readings from Napier City Council (2021b), both dissolved and particulate-bound Zn remains a widespread issue in the tributary waterways which partially explains high levels in the upper cores. Total and dissolved Pb do not show as an issue within the major urban tributary network from recent testing (Napier City Council, 2021b). This is indicative of a reduction in Pb usage in a wide range of industrial manufacturing processes, likely due to awareness of the extreme toxicity of Pb (Flora et al., 2012). Particulate-bound and dissolved Cu exceedances within Onekawa Industrial zone, as well as in the Purimu Waterway tributary Saltwater Creek, indicate that Cu remains prevalent in surface water with concentrations in excess of species protection concentrations (Charry et al., 2018; Napier City Council, 2021b). The universality of Cu, Pb and Zn is common amongst literature on estuarine sediment quality, as the three pollutants are and have been used in a wide range of processes and are considered environmentally persistent (Gadd et al., 2020; Hwang et al., 2016; Jartun et al., 2008; Kennedy & Sutherland, 2008; McKenzie et al., 2009; Pitt et al., 1995).

Prioritisation of surface water and waterbody protection is a modern effort (National Institute of Water and Atmospheric Research, n.d.-c) and this is evident through the gradual surficial reduction in heavy metal concentrations in the studies of Chagué-Goff et al. (2000), Gadd et al. (2015) and Rodríguez-Germade et al. (2015). This has also been observed in this study through the gradual decline in heavy metal counts in the very upper portion of the TT, SCAE, OTRB, PUR and TAI cores despite industrial intensification being at its highest in 2018. Prevention of land-based metal mobilisation is increasingly becoming a priority within Napier City, and subsequent management changes promoting catchment connectivity are proving effective, evident by this reduction in heavy metal counts in the urban tributary discharge zone sediments.

7.5.3 Effect of heavy metals in sediment on ecology

The zone of peak concentration across the six sediment cores may now be at a depth below primary biological activity. However, from studies undertaken in the previous decade such as the likes of Ludlow (2020) and Smith (2014), benthic biological health within the surficial sediment of the Ahuriri Estuary has been found to be generally poor with endemic species showing low individual counts within the TT and OTRB intertidal zones. Previous Ahuriri Estuary sediment samples by Ataria et al. (2007), Chagué-Goff et al. (2000), Kelly (2018), Smith (2014) and Strong (2005) still show the excessive amount of Zn, Cu and Pb in the surficial sediments of Ahuriri Estuary. Each of these studies identifies the Thames-Tyne discharge zone as a key area of concern as the depositional vicinity for surface water from the Pandora Industrial catchment. Charry et al. (2018) and Heinrich et al. (2016) collected sediment samples from Ahuriri Estuary to undertake toxicity testing, and both studies summarised that surface sediments in Ahuriri have high toxicity and toxic potential and are disruptive to basic benthic and biological functions. Charry et al. (2018) additionally compared Ahuriri Estuary sediment to the Waitangi Estuary 10km to the south, identifying Ahuriri Estuary's comparatively high toxicity. Despite heavy metal counts declining towards the surfaces of the six cores, these recent studies indicate that concentrations in the surficial sediments are bioavailable, biologically disruptive and are being metabolized. With benthic health a good indicator of the overall functionality of an estuarine system due to its low temporal variability, this provides evidence to the suggestion that Ahuriri Estuary is presently in a poor state of ecological health.

7.5.4 Summary

This section has shown that raw Itrax™ peak data and heavy metal trends in polluted estuarine sediment can be approximated to depositional timeframes using SAR. The 1970s has been identified as a common timeframe for peak heavy metal concentrations in sediment traceable across the five cores directly influenced by urban tributaries. A spike in Zn, Cu, and Pb observable in the TT core has been estimated to a depositional timeframe of 1975 using SAR from Table 7.1 – a time where the Pandora Industrial zone comprised approximately 40% industrial land use. The spike in Zn and the spike in Pb are at concentrations 53 and 57 times that of a contaminated, industrialised estuary, implying the sheer excessiveness of these two contaminants at this depth.

Heavy metal counts show reducing trends from the identified zones of peak concentrations towards the estuarine sediment surface. However, recent literature suggests that surficial heavy metal concentrations in depositional zones of urban tributaries remain at levels high enough to contribute

to a toxic sedimentary environment, disruptive of basic benthic functionality. This indicates that Ahuriri Estuary is in a poor ecological state, undermining the estuary's ability to support declining native aquatic species.

7.6 Additional contributing factors to the current health of Ahuriri Estuary

Several additional factors have influenced the current health of Ahuriri Estuary alongside sub-catchment industrialisation. These include vegetation clearance for urban development, the engineered diversion of the Tutaekuri River, channelisation of urban waterways and a non-cohesive governance framework.

7.6.1 Vegetation clearance for urban-industrial development

Vegetation clearance to accommodate productive urban-industrial land has increased contaminant mobilization and conveyance to coastal zones (Swales et al., 2005). Vegetation clearance for urban intensification affecting waterbodies is a common theme in that reduction of subsurface soakage, amplification of run-off by impervious surfaces and subsequent mobilization of exposed contaminants (Crane, 2019; Hwang et al., 2016; Jartun et al., 2008; Pitt et al., 1995), piped-network conveyance, waterway channelisation and stream width restrictions are key effects of urbanization on the hydrological cycle. Napier City is no exception, with 223ha of impervious surfacing for industrial activity across Onekawa and Pandora Industrial zones in 2018. The quality of the waterways in Napier City which service urban-industrial developments is similar to those across New Zealand which have been found in excess of guideline values for dissolved copper and dissolved zinc concentrations, with dissolved zinc directly related to impervious urban surface area (Gadd et al., 2020).

7.6.2 Diversion of the Tutaekuri River

The engineered diversion of the Tutaekuri River in 1936 would have significantly altered the ratio of freshwater to saline water in Ahuriri Estuary. Changes to ecological functions such as distribution, movement, growth and reproduction can be disrupted as a result of increased salinity and an increase in the reach of the tidal prism (Gillanders & Kingsford, 2002). Ahuriri Estuary's remaining freshwater sources are largely from the replacement of the Tutaekuri River with lower-volume urban drainage channels implying a lesser hydrodynamic flushing ability. These freshwater channels carry excessive volumes of sediment as well as high levels of nutrients, bacteria and heavy metals (Napier City Council, 2021b).

7.6.3 Waterway channelisation

Many of Napier's urban waterways have been channelized and straightened to ensure surface water is removed from urban areas in an efficient manner, decreasing the risk of household flooding. This drainage has typically been prioritized over waterway quality in Napier City, evident also by the lack of riparian margins which increase roughness and decrease flow during flood events (Alaoui et al., 2011). As a direct result of the particularly high dissolved phosphorus and total nitrogen available in

the waterway monitoring sites across Napier City, low shading over channelised waterways, combined with low flows encouraged by low gradients and drought conditions (Burke, 2020) create opportunity for cyanobacterial blooms. These blooms negatively affect water quality discharging to Ahuriri Estuary by reducing water clarity for aquatic macrophytes (Paerl & Otten, 2013).

7.6.4 Non-cohesive freshwater governance

The New Zealand governance structure has played a significant role in the development of surface water quality management tools, protection and awareness. The RMA is the directing legislation which rules that no person shall discharge contaminants where they may enter water (Parliamentary Counsel Office, 1991). With relevance to geographical water bodies, the RMA is largely administered by regional councils and unitary councils. The Local Government Act 2002 [LGA] directs territorial authorities (TAs) to develop bylaws specific to the territory (Parliamentary Counsel Office, 2002). Under the RMA, a person or entity can be fined up to $600,000 for discharge of contaminants into surface water (Parliamentary Counsel Office, 1991). A discrepancy between the RMA and the LGA is the LGA's maximum successful prosecution figure of $20,000 where a breach of a stormwater bylaw has occurred, such as a purposeful discharge of contaminants into a waterbody (Parliamentary Counsel Office, 2002). Where a regional council administers resource consents under the RMA to a TA for discharge of surface and stormwater from the city into a 'natural' water body, the territorial authority then largely holds the responsibility of its citizens and industry and may only recover up to the $20,000 of a potential $600,000 infringement. The discrepancy between these figures has likely discouraged action from TAs across New Zealand.

In the Ahuriri Estuary catchment, there are multiple key land management stakeholders including mana whenua, the Department of Conservation, NCC, HBRC, HDC, Pāmu Farm, the Hawke's Bay Airport, and residents and industry within the catchment. To add complexity to the management of the estuary, four of the seven major waterways which discharge via the southern margin have shared ownership and management by HBRC and NCC under a combined stormwater discharge consent (Hawke's Bay Regional Council, 2011). This multi-stakeholder system is highly complex which has likely challenged efforts to ensure local land-use development and land management rules align to reduce degradation of Ahuriri Estuary.

7.7 Recommendations for future management

To prevent further degradation of the Ahuriri Estuary, two key aspects of environmental management can be distinguished. The first is the prioritisation of preventing contaminant mobilisation from the built environment. The secondary aspect is the rehabilitation of captured historic contamination within the estuary itself.

This section aligns with Objective Four, being:

Prepare recommendations on the future management of Ahuriri Estuary to reduce known actions which catalyse contaminant accumulation and prevent further degradation of the estuary.

7.7.1 Land system & surface water management

Managing fine-grained estuarine sedimentation is a necessity for maintaining the integrity of benthic communities that provide foundational support for the aquatic food web (Kritzer et al., 2016; Magni, 2003) as well as protecting coastal settlements which face increasing sea level change and inundation pressures (Chester & Jickells, 2012; Dyer, 1988; McAnally & Metha, 2002; Thrush et al., 2004). As such, techniques for management of sediment runoff from hill country erosion, urban developments and developed industrial zones are becoming increasingly necessary to avoid benthic smother and estuarine infilling.

In urban zones, implementation of appropriate erosion and sediment control practices during large scale developments ensures that the risk of erosion of sediment from open grounds during windy or wet conditions is minimised (Jartun et al., 2008; Leersnyder et al., 2016). For sites in development as well as established sites in operation, vehicle movements can erode exposed sediment and transport it onto roads where it can be mobilised by stormwater and conveyed into the Napier urban waterway network, contributing to already excessive suspended sediment concentrations (Napier City Council, 2021b). Bunding the perimeter of sites containing exposed sediment and directing stormwater to sediment settling ponds while sites are in development will disrupt the urban sediment transport cycle. For sites already developed, local landowners, the regional authority and territorial authorities should ensure measures are in place to reduce sediment drag from heavy machinery, such as developing dedicated wheel wash pits at site exits (Leersnyder et al., 2016). Managing sediment mobilisation will reduce metal sorption and transport through the hydrocycle (Chester & Jickells, 2012), positively contributing to the observed gradual reduction in Zn, Pb, Cu and Cr concentrations in Ahuriri Estuary's surficial sediments, and subsequently ensuring the toxicity of these sediments is reduced in order to encourage a healthier estuarine ecosystem.

Much of the urban waterway network in Napier City lacks riparian margins, particularly where waterways travel through the Onekawa and Pandora Industrial zones (Napier City Council, n.d.-d). Depending on the spatiotemporal intensity of individual rainfall events (Alaoui et al., 2011), development of riparian margins will encourage water soakage to ground, encouraged by the flat topography of Napier City, and accordingly reduce runoff volumes. This would reduce urban-source bacteria and particulate-bound heavy contaminants in runoff discharging into waterways (Geldreich et al., 1968; Pitt et al., 1995; Rossi et al., 2004), as the roughness of riparian margins causes turbulent flow/eddying and encourages particulate settling (Alaoui et al., 2011; Gadd et al., 2020). Vegetated waterway margins additionally provide shelter and shade for freshwater species and benefit the shallow groundwater network through increasing soakage, reducing the risk of low flows and stagnation in urban waterways during summer months (Waddington et al., 1993; Westbrook et al., 2005).

7.7.2 Managing metal inputs

Two common modern phenomena affecting metal loading of surface water are galvanised building materials and vehicle movements which can result in Zn, Pb and Cu residues on roads (Kennedy & Sutherland, 2008; McKenzie et al., 2009; Pitt et al., 1995; Salomons & Förstner, 1984). As a universal

solvent, rainwater mobilises road residue and catalyses degradation of zinc-plated building materials (Jartun et al., 2008; McKenzie et al., 2009). Road systems should follow water sensitive urban design principles to reduce sediment and metal run off (Wong, 2006). Reducing zinc mobilisation from galvanised building materials requires a national approach.

Particularly in Napier City's industrial zones, ensuring sites are clean prior to rainfall and preventing spill events are imperative to improving urban waterway quality and the Ahuriri Estuary receiving environment. Social awareness through educational campaigns such as NCC's 'Stream to Coast' (Napier City Council, 2019) is an important contributor to freshwater protection (Sarkar et al., 2007). Where both point source and diffuse pollution occurs, enforcement tools such as the 2020 Napier City Stormwater Bylaw and the RMA should be enacted when appropriate to recover costs of associated clean-up and deter future events (Parliamentary Counsel Office, 1991, 2002).

Public infrastructure should be designed with natural disaster resilience, audited to reduce cross connections, and managed to avoid overflows. Potable water in Napier City contains chlorine, and public wastewater can contain a suite of contaminants, including chromium, detergents, microplastics, bacteria and industrial trade waste (Makepeace et al., 1995); all of which may negatively affect the ecological health of Ahuriri Estuary if managed improperly.

7.7.3 Freshwater and estuarine system governance

Focusing on the New Zealand national approach to surface water management, the discrepancy between the RMA and the LGA must be addressed in order to eliminate the inequity between successful prosecution fines. In theory, an environmentally catastrophic discharge into a waterway by a private entity could theoretically cause NCC to breach their resource consent, meaning that HBRC would be rightfully able to prosecute NCC for the maximum penalty under the RMA of $600,000, while NCC may only 'pass on' this prosecution of the private entity to a maximum penalty under the LGA of $20,000. This means that ratepayers are unfairly penalised for the actions of the private entity – an imbalance which requires a national approach to mitigate with priority.

With regard to local stakeholders for the health of Napier's urban tributaries and the Ahuriri Estuary, responsibilities and jurisdictions should be clarified and agreed in order to begin assessing rehabilitation approaches as a unified multi-stakeholder party. Such an essential process requires parity and transparency.

7.7.4 Estuarine rehabilitation

A study by Lange et al. (2020) recognizes that unless contaminated freshwater is chemically dosed, there is typically an adverse effect on the water quality of the discharge environment. In the major tributaries within the Ahuriri Estuary catchment, freshwater dosing has not been implemented, nor have ecological treatment options such as wetland zones been developed. Promoting the urban waterways throughout Napier City as important individual ecosystems as opposed to drainage channels will naturally improve the freshwater quality and the social connection to those waterways. In some particularly slow-flowing waterways, dosing and/or physical aeration of water may reduce algal bloom instances and improve the quality enough for habitation by indigenous aquatic species.

Focusing on the future of the Ahuriri Estuary catchment, establishment of high-risk land-uses such as heavy industry should be prevented in the fringing Pāmu and Lagoon Farms, as spill events in these areas would have a very limited response time for prevention of a discharge to Ahuriri Estuary.

For targeting historic contamination levels within Ahuriri Estuary's sediment, such as the 17.8cm zone of high Pb, Zn and Cu in the TT core, a thorough investigation on the current risk of metabolisation by benthic communities should be undertaken. If contamination is at a depth where this risk is minimal, maintaining the integrity of the overlying sediment cap may be preferred, as dredging can increase turbidity, reduce light and oxygen, and release previously captured contaminants (Thrush & Dayton, 2002).

7.8 Summary

Using a combination of grain size change cues and indications from peaks in the Br/Inc marine organic matter ratio, and the K/Inc terrigenous sediment ratio, the 1931 Napier earthquake has been identified across each of the six cores taken in Ahuriri Estuary (Figure 7.2). From the identification of these earthquake depths, average SAR have been identified for four of the six cores and updated SAR since the 1997 assessment by Chagué-Goff et al. (2000) have been calculated for the remaining TT and TAI cores. Using these SAR, peaks in heavy metal concentrations identified in Chapter 6 have been approximated to depositional timeframes.

The early 1970s is a timeframe in common across five of the Ahuriri Estuary cores which are, or have been directly influenced by urban tributary discharges (Table 7.2). During this time, Onekawa and Pandora were comprised of approximately 50% industrial land use. These industrial zones are high risk land uses for the mobilisation of heavy metals, high volumes of stormwater run-off and sediment transport. With multiple channelised urban tributaries flowing through the Onekawa Industrial zone and two tidally influenced waterways flowing through the Pandora Industrial zone, transportation of land-origin particulate-bound heavy metals to Ahuriri Estuary is straightforward.

Across all but the UAE core, heavy metal levels reduce toward the surface after identified individual peak contamination zones. This shows that urban-industrial land management practices are gradually improving and that surface water quality protection is becoming increasingly prioritised. However, urban tributary water testing shows excessive loadings of suspended sediment, excessive total zinc and zones of excessive total copper concentrations (Napier City Council, 2021b). In addition, recent testing of surface sediments from Ahuriri Estuary has shown toxicity levels enough to disrupt basic benthic and pelagic biological functions (Charry et al., 2018; Heinrich et al., 2016). This suggests that, while reduction in contamination is visible in the chemistry of the sediment cores, Ahuriri Estuary is still in a state of poor ecological health, unable to efficiently support declining native aquatic species who utilise the estuary as a spawning ground and nursery (Hawke's Bay Regional Council, 2004).

This thesis has identified and addressed a gap in the current state of knowledge in the health of Ahuriri Estuary through the connection of sub-catchment industrialisation and historic estuarine sediment heavy metal pollution trends. With internationally limited use investigating estuarine pollution, this

thesis has shown that, given SAR, Itrax™ raw data can be effective in identifying pollution trends and events. The results of this thesis can prompt quantitative environmental planning for the prevention of further degradation of the nationally significant Ahuriri Estuary.

7.8.1 Limitations of the thesis

There are several limitations to this thesis. Time constraints, as this is a 90 credit thesis conducted over 6 months, meant that the multi-temporal assessment of land development was focused on only the Onekawa and Pandora sub-catchments within the wider Ahuriri Estuary catchment. These two sub-catchments were focused on as they are the zones of primary industrial activity within the wider Ahuriri Estuary catchment, and the surface water from both sub-catchments is conveyed directly to the estuary via urban tributaries. The focus on these sub-catchments guided the thesis into emphasising the linkage between industrial land use and estuarine sediment quality. Given greater time and resources, a whole-of-catchment investigation would have elicited more thorough comparison of rurally-influenced, residentially-influenced, and industrially-influenced estuarine sediment. This would strengthen the conclusion of this thesis that industrial sub-catchments have conveyed high rates of heavy metal pollutants to Ahuriri Estuary, and prompt additional investigation into the effects of residential and rural sub-catchments on estuarine sediment quality.

Itrax™ XRF corescanning data is provided in the quantitative unit of counts per second, meaning that comparison to known qualitative guideline values such as the commonly used ANZECC 2000 sediment quality guidelines for the protection of aquatic species was not viable. Studies have shown that it is possible to calibrate Itrax™ data from CPS to concentrations, but without this calibration, only inferences of the true toxicity of the heavy metal levels on benthic species functionality can be made. In addition, there is limited number of studies which have utilised Itrax™ to investigate estuarine pollution. The low availability of studies with similar methodologies constrains the comparison of heavy metal trends and zones of peak concentration in the six Ahuriri Estuary cores to other estuaries.

Without undertaking radioisotope analyses on the six cores, the estimations of SAR have been limited by available sediment physicochemistry, which meant that SAR were averaged and assumed linear. With greater funding to undertake radioisotope analyses, dating pollution peaks would have been undertaken with greater accuracy. In addition, only four heavy metals were focused on to indicate historic sediment quality trends. Investigation of additional pollutants indicative of industrial influence such as hydrocarbons, pesticides, persistent organic pollutants, plasticisers, and flame retardants would have confirmed the degree of sediment degradation as a direct result of catchment activities.

These limitations provide the foundation of suggestions for future research discussed in Section 8.1.

8 CONCLUSION

This research has built on existing knowledge relating to the health of Ahuriri Estuary by undertaking a multi-temporal land-use change assessment and investigating linkages between industrial development and estuarine sediment chemistry. Methods for doing so were developed around the investigations of Al-Naswari et al. (2018), Arunyawat and Shrestha (2016), Birch et al. (2016), Chagué-Goff et al. (2000) and Swales et al. (2005). An investigation into previous Ahuriri Estuary research identified a gap in knowledge being a lack of information regarding heavy metal trends within the direct discharge zones of urban tributaries since 1931. This thesis aimed to extend knowledge of the effects of fringing industrial development on the health of Ahuriri Estuary.

Each of the four objectives of this thesis were met successfully and addressed individually in separate chapters. The objectives were:

1. *Review recent environment quality research undertaken in the Ahuriri Estuary, including geomorphology, hydrodynamics, sedimentary history, sediment quality, water quality, and ecology.*
2. *Undertake land system change analysis using aerial imagery to investigate gradual effects of industrial development on Ahuriri Estuary.*
3. *Utilise previous hydrodynamic modelling of the central estuary to guide sampling locations for extraction of sediment cores representing discharge depositional zones of different tributaries. Undertake physicochemical analysis on retrieved sediment core samples to investigate connections between industrial development and temporal sediment quality.*
4. *Prepare recommendations on the future management of Ahuriri Estuary to reduce known actions which catalyse contaminant accumulation and prevent further degradation of the estuary.*

The primary conclusion is that excessive heavy metal contamination has been delivered to Ahuriri Estuary via the urban tributaries with a peak contamination period beginning in the early 1970s. During this time, industrial land use within the 293.5ha focus area was 44.7%. Heavy metal contamination is prevalent in the cores adjacent the Pandora Industrial zone, highlighting the historic time of limited prioritisation of surface water cleanliness. In the TT core, extreme pollution levels from the Pandora Industrial zone lasting several years between 1973-1976 far exceeded Zn and Pb levels found in the limited literature of Itrax™ XRF-scanned estuarine core samples from similarly contaminated estuaries. Zn levels are relatively high across all core samples compared to the available literature with Pb levels also of concern. Cr showed occasional peaks though trends were limited. Cu trends largely reflect gradual catchment development though levels are comparatively of lesser concern than Zn. After this identified time of high heavy metal delivery to Ahuriri Estuary, trends across five of the six sediment cores reduce toward the surface. Although surface water management had been largely unconsidered in the 1970s, and governance around its integrity has been non-cohesive, efforts to improve awareness and discourage active contamination are recognisable in the sediment chemistry.

These results are consistent with previous research projects within Ahuriri Estuary, many of which conclude that the Thames-Tyne waterways which service the Pandora Industrial area have contributed to excessive Zn, Pb and Cu in the direct estuarine discharge zone. Previous research into benthic ecology within the Old Tutaekuri Riverbed discharge zone has also reflected similar conclusions in that

heavy metal levels are excessive which has led to toxicity issues in estuarine benthic communities. Previous research also compares Ahuriri Estuary to other mixed-catchment estuaries identifying that the estuary is in a comparatively poor state of health.

A combination of planting riparian margins along urban tributaries, managing urban sediment, challenging national and local surface water governance and reducing metal mobilisation will reduce contaminant transportation from the built environment to Ahuriri Estuary via the hydrocycle. With land-based contaminant mobilisation being minimised, rehabilitation options for contaminated sediment within Ahuriri Estuary can be investigated for feasibility.

The results show that sediment core scanning of estuarine sediment can be undertaken and analysed successfully. This is the first investigation to use raw data from Itrax™ XRF corescanning methodologies in Ahuriri Estuary within each of the urban tributary discharge zones. This shows that raw data can provide a great starting point for identifying key peaks and periods of contamination from industrialisation, to subsequently seed remediation efforts, as well as provide a solid foundation for building on in future studies.

Limitations of this thesis are in its narrow focus on the multi-temporal development of Napier City's two industrial zones as opposed to a thorough whole-of-catchment investigation. Itrax™ data were semi-quantitative, meaning direct comparisons to accepted species protection guidelines could not be made. In addition, the thesis focused solely on four heavy metals and the estimations of SAR are limited by the lack of updated radioisotope analyses, though constraints on resources are noted.

8.1 Recommendations for future research

Without restraint on resource or budget, additional sediment chemistry testing could be undertaken to further determine the effect of land use change on Ahuriri Estuary, including assessments of compound contaminants such as surfactants, polychlorinated biphenyls (PCB's), pharmaceuticals, polyfluoroalkyl substances (PFAS), organochlorine pesticides (OCP's), insecticides and PAH's. Each of these are environmentally persistent, anthropogenically-derived pollutants that can accumulate in estuarine systems and disrupt basic aquatic biological functions (Chagué-Goff et al., 2000; Feng et al., 1998; Gadd, 2020; Geldreich et al., 1968; Makepeace et al., 1995; Mallin et al., 2009; Pitt et al., 1995; Rossi et al., 2004). Such analysis would prompt an investigation into the bioavailability of such compounds for Ahuriri Estuary's benthic communities (Du Laing et al., 2008).

Additional research opportunities include whole-of-catchment multi-temporal georeferencing for a land system change assessment that examines more than just the Onekawa and Pandora Industrial zones. An expansion to more land-use categories such as roads, riparian margins, zinc roofs, native vegetation, exotic grasslands, horticultural and more, would allow estimation of urban run-off and subsequent waterway flow rates in rainfall events of varying intensities using known coefficients (Lang et al., 2013). This would allow assessment of heavy metal mobilisation from impervious surfaces, prompting quantitative goal setting for the reduction of land-origin pollutants being deposited to Ahuriri Estuary.

Cross-comparison and regression analyses of Itrax™ XRF data against analysis such as obtained by ICP-OES or ICP-MS methodologies would provide confidence in comparisons of peak contamination levels against accepted guideline values for each individual sediment core sample, such as per Gadd et al. (2015), Rodríguez-Germade et al. (2014) and Rodríguez-Germade et al. (2015). Future studies would be wise to undertake additional radioisotope analysis of each sample core to understand the differences in depositional behaviours within distinctive zones of the estuary such as per Chagué-Goff et al. (2000). Such analyses will allow a more holistic awareness of historic and current sediment physicochemistry to correctly manage SAR and particulate-bound contaminant accumulation encouraging land and surface water management planning for the prevention of estuarine smother.

8.2 Final summary

The six estuarine sediment cores reflect a period of high deposition of land-origin Cu, Pb and Zn, equating approximately to the 1970s with particularly high heavy metal mobilisation from the Pandora Industrial zone. Heavy metal levels appear to be reducing in the cores within the direct depositional zones of the urban tributaries indicating that the messaging and rules around the protection of surface water in Napier City are becoming more effective. Despite these recognisable reductions, recent sediment assessments highlight that Ahuriri Estuary's surficial sediment remains toxic enough to disrupt basic biological functionality, meaning continued contaminant mobilisation from the land is undermining the estuary's ability to behave as a nursery for spawning and juvenile native species. The findings of this study confirm that Ahuriri Estuary is in a poor state of ecological health and more needs to be done from an environmental management perspective to improve its condition.

This research has identified a gap in the current state of knowledge and addressed this gap successfully, connecting sub-catchment industrialisation of the land to the health of Ahuriri Estuary. This research has contributed important sediment quality information which can prompt quantitative environmental planning and management actions for the prevention of further degradation of a nationally significant wildlife reserve.

9 BIBLIOGRAPHY

Al-Naswari, A. K. M., Hamylton, S. M., & Jones, B. G. (2018). An assessment of anthropogenic and climatic stressors on estuaries using a spatio-temporal GIS-modelling approach for sustainability: Towamba estuary, southeastern Australia. *Environmental Monitoring and Assessment, 190*(375), 26. https://doi.org/10.1007/s10661-018-6720-5

Alaoui, A., Caduff, U., Gerke, H., & Weingartner, R. (2011). A preferential flow effects on infiltration and runoff in grassland and forest soils. *Vadose Zone Journal, 10*, 367-377. https://doi.org/10.2136/vzj2010.0076

Arunyawat, S., & Shrestha, R. (2016). Assessing land use change and its impact on ecosystem services in northern Thailand. *Sustainability, 8*, 768. https://doi.org/10.3390/su8080768

Ataria, J., Tremblay, C., Tremblay, L., Black, M., Kaukua, M., Kemp, R., & Mauger, J. (2007). *He Moemoea mō Te Whanganui-a-Orotū: A vision plan and health assessment for the Napier Estuary*. http://www.maramatanga.co.nz/

Birch, G. F., Gunns, T. J., Chapman, D., & Harrison, D. (2016). Development of an estuarine assessment scheme for the management of a highly urbanised catchment/estuary system, Sydney estuary, Australia. *Environmental Monitoring and Assessment, 188*(5), 1-14. https://doi.org/10.1007/s10661-016-5272-9

Birch, G. F., Robertson, E., Taylor, S. E., & McConchie, D. M. (2000). The use of sediments to detect human impact on the fluvial system [Article]. *Environmental Geology, 39*(9), 1015-1028. https://doi.org/10.1007/s002549900075

Borja, A., Basset, A., Bricker, S., Dauvin, J.-C., & Elliot, M. (2011). Classifying ecological quality and integrity of estuaries. *Treatise on Estuarine and Coastal Science, 1*, 125-162. https://doi.org/10.1016/B978-0-12-374711-2.00109-1

Botto, F., & Iribarne, O. (2000). Contrasting effects of two burrowing crabs (Chasmagnathus granulata and Uca uruguayensis) on sediment composition and transport in estuarine environments. *Estuarine, Coastal and Shelf Science, 51*(2), 141-151. https://doi.org/10.1006/ecss.2000.0642

Brooker's Ltd. (1995). *Te Whanganui-a-Orotu: A report to the Waitangi Tribunal*. Wai 55.

Buggy, C. J., & Tobin, J. M. (2008). Seasonal and spatial distribution of metals in surface sediment of an urban estuary. *Environmental Pollution, 155*, 308-319. https://doi.org/10.1016/j.envpol.2007.11.032

Burke, P. (2020). *Hawke's Bay's 'worst ever' drought?* www.ruralnewsgroup.co.nz

Burton, C. (2018). *The mixed governance of Te Whanganui-a-Orotū* [Unpublished map of wider Ahuriri Estuary catchments]. Napier City Council.

Cashman, S. C., & Kelsey, H. M. (1990). Forearc uplift and extension, southern Hawke's Bay, New Zealand: Mid-Pleistocene to present. *Tectonics, 9*(1). https://doi.org/10.1029/TC009i001p00023

Chagué-Goff, C., Nichol, S. L., Jenkinson, A. V., & Heijnis, H. (2000). Signatures of natural catastrophic events and anthropogenic impact in an estuarine environment, New Zealand. *Marine Geology, 167*. https://doi.org/10.1016/S0025-3227(00)00035-9

Chappel, P. R. (2013). The climate and weather of Hawke's Bay. (NIWA Science and Technology Series 58), 44. https://niwa.co.nz/

Charry, M. P., Keesing, V., Costello, M., & Tremblay, L. A. (2018). Assessment of the ecotoxicity of urban estuarine sediment using benthic and pelagic copepod bioassays. *Biodiversity and Conservation*, 1-19. https://doi.org/10.7717/peerj.4936

Chen, L., Dai, Y., Zhi, X., Xie, H., & Shen, Z. (2018). Quantifying nonpoint source emissions and their water quality responses in a complex catchment: A case study of a typical urban-rural mixed catchment. *Journal of Hydrology, 559*, 110-121. https://doi.org/10.1016/j.jhydrol.2018.02.034

Chester, R., & Jickells, T. (2012). *Marine geochemistry* (3rd ed.). Wiley-Blackwell.

Chmura, G. L., Anisfeld, S. C., Cahoon, D. R., & Lynch, J. C. (2003). Global carbon sequestration in tidal, saline wetland soils. *Global Biogeochemical Cycles, 17*(4), 22-21. https://doi.org/10.1029/2002GB001917

Clark, D. E., Pilditch, C. A., Pearman, J. K., Ellis, J. I., & Zaiko, A. (2020). Environmental DNA metabarcoding reveals estuarine benthic community response to nutrient enrichment – Evidence from an in-situ experiment. *Environmental Pollution, 267*, 115472. https://doi.org/10.1016/j.envpol.2020.115472

Crane, J. L. (2019). Distribution, toxic potential, and influence of land use on conventional and emerging contaminants in urban stormwater pond sediments. *Archives of Environmental Contamination and Toxicology, 76*(2), 265-294. https://doi.org/10.1007/s00244-019-00598-w

Cundy, A. B., Croudace, I. W., Cearreta, A., & Irabien, M. J. (2003). Reconstructing historical trends in metal input in heavily-disturbed, contaminated estuaries: studies from Bilbao, Southampton Water and Sicily. *Applied Geochemistry, 18*(2), 311-325. https://doi.org/10.1016/S0883-2927(02)00127-0

Davies, S. J., Lamb, H. F., & Roberts, S. J. (2015). Micro-XRF core scanning in palaeolimnology: Recent developments. In *Micro-XRF studies of sediment cores: Applications of a non-destructive tool for the environmental sciences* (Vol. 17). Springer.

Department of Conservation. (n.d.). *Ahuriri Estuary bird guide*. www.doc.govt.nz

Du Laing, G., Vos, R., Vandecasteele, B., Lesage, E., Tack, F., & Verloo, M. (2008). Effect of salinity on heavy metal mobility and availability in intertidal sediments of the Scheldt Estuary. *Estuarine, Coastal and Shelf Science, 77*, 589-602. https://doi.org/10.1016/j.ecss.2007.10.017

Dyer, K. R. (1988). Fine sediment particle transport in estuaries. In J. Dronkers & W. Leussen (Eds.), *Physical Processes in Estuaries* (pp. 295-310). Springer-Verlag.

ESRI Inc. (2019). *ArcGIS Pro.* In (Version 2.4.2) NZ Imagery basemap. www.esri.com

Eyre, T. M. (2009). *The sediment dynamics of Ahuriri Estuary, Napier, New Zealand* University of Waikato and Universität Bremen]. https://hdl.handle.net/10289/4290

Feng, H., Cochran, J. K., Lwiza, H., Brownawell, B. J., & Hirschberg, D. J. (1998). Distribution of heavy metal and PCB contaminants in the sediments of an urban estuary: The Hudson River. *Marine Environmental Research, 45*(1), 69-88. https://doi.org/10.1016/S0141-1136(97)00025-1

Finkl, C. W., & Khalil, S. M. (2005). Vibracore. In M. L. Schwartz (Ed.), *Encyclopedia of Coastal Science* (pp. 1026-1036). Springer Netherlands. https://doi.org/10.1007/1-4020-3880-1_335

Flora, G., Gupta, D., & Tiwari, A. (2012). Toxicity of lead: A review with recent updates. *Interdisciplinary toxicology, 5*(2), 47-58. https://doi.org/10.2478/v10102-012-0009-2

Gadd, J. (2020). *Sediment sampling in the Thames-Tyne waterways* [Unpublished report for Napier City Council]. National Institute of Water and Atmospheric Research.

Gadd, J., Snelder, T., Fraser, C., & Whitehead, A. (2020). Current state of water quality indicators in urban streams in New Zealand. *New Zealand Journal of Marine and Freshwater Research, 54*(3), 354-371. https://doi.org/10.1080/00288330.2020.1753787

Gadd, P., Heijnis, H., Chagué, C., Zawadzki, A., Fierro, D., Atahan, P., Croudace, I., & Goralewski, J. (2015). iTrax core scanner capabilities combined with other geochemical and radiochemical techniques to evaluate environmental changes in a local catchment, South Sydney, NSW, Australia. In *Micro-XRF studies of sediment cores: Applications of a non-destructive tool for the environmental sciences* (pp. 13). Springer. https://doi.org/10.1007/978-94-017-9849-5_17

Gaw, S. K., Kim, N. D., Wilkins, A. L., & Palmer, G. T. (n.d.). *Contaminated horticultural land, a developing issue for New Zealand*. www.wasteminz.org.nz

Geldreich, E. E., Best, L. C., Kenner, B. A., & Van Donsel, D. J. (1968). The bacteriological aspects of stormwater pollution. *Journal (Water Pollution Control Federation), 40*(11), 1861-1872. http://www.jstor.org/

Gillanders, B., & Kingsford, M. (2002). Impact of changes in flow of freshwater on estuarine and open coastal habitats and the associated organisms. *Oceanography and Marine Biology: An Annual Review, 40*, 233-309. https://doi.org/10.1201/9780203180594.ch5

Google. (n.d.-a). *Google Earth aerial imagery of Ahuriri Estuary, Napier, New Zealand [Aerial imagery], taken from 8512m elevation.* In (Version 9.120.0.2) Google Earth. https://earth.google.com/

Google. (n.d.-b). *Google Earth aerial imagery of Napier, New Zealand [Aerial imagery], taken from 24000m elevation.* In (Version 9.120.0.2) Google Earth. https://earth.google.com/

Hawke's Bay Regional Council. (2004). *Ahuriri Estuary: Environmental evaluation*. www.hbrc.govt.nz

Hawke's Bay Regional Council. (2009a). *Industrial stormwater design* (HBRC Plan number 4107). (Hawke's Bay waterway guidelines, Issue 1). www.hbrc.govt.nz

Hawke's Bay Regional Council. (2009b). *List of HOTSPOT sites*. http://static.stuff.co.nz/

Hawke's Bay Regional Council. (1996). *Resource consent: Permits for Napier City Council to discharge into or onto land: DP950085L, DP950086L, DP950087L, DP950511L, DP950088L, DP950089L, DP950090L.* Hawke's Bay Regional Council. consents.hbrc.govt.nz

Hawke's Bay Regional Council. (2007). *Resource consent: Coastal permit to discharge stormwater collected from the Burns Road catchment area to the Bridge Street end of the Iron Pot: CD070023W*. Hawke's Bay Regional Council. consents.hbrc.govt.nz

Hawke's Bay Regional Council. (2011). *Resource consent: Coastal permit to discharge stormwater from part of Napier City urban area and surrounding rural land into the Ahuriri Estuary via the Westshore Tidal Gates: CD990516Wa*. Hawke's Bay Regional Council. consents.hbrc.govt.nz

Hayward, B. W., Grenfell, H. R., Sabaa, A. T., Carter, R., Cochran, U., Lipps, J. H., Shane, P. R., & Morley, M. S. (2006). Micropaleontological evidence of large earthquakes in the past 7200 years in southern Hawke's Bay, New Zealand. *Quaternary Science Reviews, 25*(11-12), 1186-1207. https://doi.org/10.1016/j.quascirev.2005.10.013

Hayward, B. W., Grenfell, H. R., Sabaa, A. T., Clark, K. J., Cochran, U. A., & Palmer, A. S. (2015). Subsidence-driven environmental change in three Holocene embayments of Ahuriri Inlet, Hikurangi Subduction Margin, New Zealand. *New Zealand Journal of Geology and Geophysics, 58*(4), 344-363. https://doi.org/10.1080/00288306.2015.1077872

Heinrich, P., Petschick, L. L., Northcott, G. L., Tremblay, L. A., Ataria, J., & Braunbeck, T. (2016). Assessment of cytotoxicity, genotoxicity and 7-ethoxyresorufin-Odeethylase (EROD) induction in sediment extracts from New Zealand urban estuaries. *Ecotoxicology, 26*(2). https://doi.org/10.1007/s10646-016-1756-1

Hull, A. G. (1986). Pre-a.d. 1931 tectonic subsidence of Ahuriri Lagoon, Napier, Hawke's Bay, New Zealand [Article]. *New Zealand Journal of Geology and Geophysics, 29*(1), 75-82. https://doi.org/10.1080/00288306.1986.10427524

Hull, A. G. (1990). Tectonics of the 1931 Hawke's Bay earthquake. *New Zealand Journal of Geology and Geophysics, 33*(2), 309-320. https://doi.org/10.1080/00288306.1990.10425689

Hume, T., Gerbeaux, P., Hart, D., Kettles, H., & Neale, D. (2016). *A classification of New Zealand's coastal hydrosystems*. National Institute of Water and Atmospheric Research (NIWA).

Hwang, H.-M., Fiala, M. J., Park, D., & Wade, T. L. (2016). Review of pollutants in urban road dust and stormwater runoff: part 1. Heavy metals released from vehicles. *International Journal of Urban Sciences, 20*(3), 334-360. https://doi.org/10.1080/12265934.2016.1193041

Jartun, M., Ottesen, R. T., Steinnes, E., & Volden, T. (2008). Runoff of particle bound pollutants from urban impervious surfaces studied by analysis of sediments from stormwater traps. *Science of The Total Environment, 396*(2), 147-163. https://doi.org/10.1016/j.scitotenv.2008.02.002

Jarvis, S., Croudace, I. W., & Guy Rothwell, R. (2015). Parameter optimisation for the Itrax core scanner. In *Micro-XRF studies of sediment cores: Applications of a non-destructive tool for the environmental sciences* (Vol. 17). Springer.

Johnson, L. E., Bishop, T. F. A., & Birch, G. F. (2017). Modelling drivers and distribution of lead and zinc concentrations in soils of an urban catchment (Sydney estuary, Australia). *Science of The Total Environment, 598*, 168-178. https://doi.org/10.1016/j.scitotenv.2017.04.033

Jones, R. (2002). Algorithms for using a DEM for mapping catchment areas of stream sediment samples. *Computers & Geosciences, 28*(9), 1051-1060. https://doi.org/10.1016/S0098-3004(02)00022-5

Kelly, S. (2018). *Ahuriri Estuary: Effects of stormwater contaminants on benthic ecology*. Coast & Catchment Ltd.

Kennedy, P., & Sutherland, S. (2008). *Urban sources of copper, lead and zinc.* Technical report 2008/023). Auckland Regional Council.

Komar, P. D. (2007). *Summary report: The coast of Hawke's Bay: Processes & erosion problems.* (AM 07/02).

Kritzer, J. P., DeLucia, M.-B., Greene, E., Shumway, C., Topolski, M. F., Thomas-Blate, J., Chiarella, L. A., Davy, K. B., & Smith, K. (2016). The Importance of benthic habitats for coastal fisheries. *BioScience, 66*(4), 274-284. https://doi.org/10.1093/biosci/biw014

Laing, D. (2021). *Napier's Red Sea probably harmless algae bloom* www.nzherald.co.nz

Lang, M., Li, P., & Yan, X. (2013, Aug 1). Runoff concentration and load of nitrogen and phosphorus from a residential area in an intensive agricultural watershed. *Sci Total Environ, 458-460*, 238-245. https://doi.org/10.1016/j.scitotenv.2013.04.044

Lange, K., Österlund, H., Viklander, M., & Blecken, G.-T. (2020). Metal speciation in stormwater bioretention: Removal of particulate, colloidal and truly dissolved metals. *Science of The Total Environment, 724*, 138121. https://doi.org/10.1016/j.scitotenv.2020.138121

Leersnyder, H., Bunting, K., Parsonson, M., & Stewart, C. (2016). *Erosion and sediment control guide for land disturbing activities in the Auckland region* (Auckland Council Guideline Document, Issue GD2016/005).

Lelieveld, S. D., Pilditch, C. A., & Green, M. O. (2003). Variation in sediment stability and relation to indicators of microbial abundance in the Okura Estuary, New Zealand. *Estuarine, Coastal and Shelf Science, 57*, 123-136. https://doi.org/10.1016/S0272-7714(02)00336-0

Ludlow, H. M. (2020). *Annual environmental report: Resource consent DP110266W* (2019/20). Napier City Council.

MacLachlan, S. E., Hunt, J. E., & Croudace, I. W. (2015). An empirical assessment of variable water content and grain-size on X-Ray fluorescence core-scanning measurements of deep sea sediments. In *Micro-XRF studies of sediment cores: Applications of a non-destructive tool for the environmental sciences* (Vol. 17). Springer.

Magni, P. (2003). Biological benthic tools as indicators of coastal marine ecosystems health. *Chemistry & Ecology, 19*(5), 363-372. https://doi.org/10.1080/0275754031000160371 8

Makepeace, D. K., Smith, D. W., & Stanley, S. J. (1995). Urban stormwater quality: Summary of contaminant data. *Critical Reviews in Environmental Science and Technology, 25*(2), 93-139. https://doi.org/10.1080/10643389509388476

Mallin, M. A., Johnson, V. L., & Ensign, S. H. (2009). Comparative impacts of stormwater runoff on water quality of an urban, a suburban, and a rural stream. *Environmental Monitoring and Assessment, 159*(1-4), 475-491. https://doi.org/10.1007/s10661-008-0644-4

McAnally, W. H., & Metha, A. J. (2002). Significance of aggregation of fine sediment particles in their deposition. *Estuarine, Coastal and Shelf Science, 54*, 643-653. https://doi.org/10.1006/ecss.2001.0847

McDowall, R. M. (1976). The role of estuaries in the life cycle of fishes in New Zealand. *New Zealand Ecological Society, 23*, 27-32. www.newzealandecology.org

McKenzie, E. R., Money, J. E., Green, P. G., & Young, T. M. (2009). Metals associated with stormwater-relevant brake and tire samples. *The Science of the total environment, 407*(22), 5855-5860. https://doi.org/10.1016/j.scitotenv.2009.07.018

McLintock. (1966). *Hawke's Bay land district*. Te Ara - the Encyclopedia of New Zealand. http://www.teara.govt.nz/

Ministry for the Environment. (2020). *New Zealand's environmental reporting series: Our freshwater 2020*. http://www.mfe.govt.nz/

Ministry for the Environment, & Ministry of Health. (2003). *Microbiological water quality guidelines for marine and freshwater recreational areas*. Ministry for the Environment & Ministry of Health.

Museum Theatre Gallery Hawke's Bay. (n.d.). *Napier - 100 years of progress map*. mtghawkesbay.wordpress.com

Napier City Council. (2011). *Napier operative district plan*. Napier City Council. www.napier.govt.nz

Napier City Council. (2019). *Stream to coast - Napier's stormwater education campaign*. www.youtube.com

Napier City Council. (2021a). *Ahuriri Masterplan: city-wide waterway monitoring project 2019 - 2022* [Mapped, unpublished database].

Napier City Council. (2021b). *Bubble plot maps of city-wide urban surface water study 2019-2022* [Unpublished data].

Napier City Council. (n.d.-a). *Napier City Council IntraMaps*. www.gis.napier.govt.nz/

Napier City Council. (n.d.-b). *Napier City Council IntraMaps: Aerial photos 1936*. Retrieved February 2, 2021 from www.gis.napier.govt.nz/

Napier City Council. (n.d.-c). *Napier City Council IntraMaps: Aerial photos 2004*. Retrieved February 2, 2021 from www.gis.napier.govt.nz/

Napier City Council. (n.d.-d). *Napier City Council IntraMaps: Aerial photos 2018*. Retrieved February 2, 2021 from www.gis.napier.govt.nz/

Napier City Council. (n.d.-e). *Napier City Council IntraMaps: Countours*. Retrieved March 17, 2021, from www.gis.napier.govt.nz/

Napier City Council. (n.d.-f). *Napier City Council IntraMaps: Stormwater mains*. Retrieved March 17, 2021 from www.gis.napier.govt.nz/

National Institute of Water and Atmospheric Research. (n.d.-a). *CLUES – Catchment Land Use for Environmental Sustainability model*. https://niwa.co.nz/

National Institute of Water and Atmospheric Research. (n.d.-b). *Neon Network: Napier Nelson Park external weather station*. https://neon.niwa.co.nz/

National Institute of Water and Atmospheric Research. (n.d.-c). *Stormwater - an introduction*. https://niwa.co.nz

O'Brien, A., Townsend, K., Hale, R., Sharley, D., & Pettigrove, V. (2016). How is ecosystem health defined and measured? A critical review of freshwater and estuarine studies. *Ecological Indicators, 69*, 722-729. https://doi.org/10.1016/j.ecolind.2016.05.004

Ogden, J., Deng, Y., Horrocks, M., Nichol, S., & Anderson, S. (2006). Sequential impacts of Polynesian and European settlement on vegetation and environmental processes recorded in sediments at Whangapoua Estuary, Great Barrier Island, New Zealand. *Regional Environmental Change, 6*, 25-40. https://doi.org/10.1007/s10113-005-0006-5

Paerl, H. W., & Otten, T. G. (2013). Harmful cyanobacterial blooms: Causes, consequences, and controls. *Microbial Ecology, 65*(4), 995-1010. https://doi.org/10.1007/s00248-012-0159-y

Parliamentary Counsel Office. (1991). *New Zealand Resource Management Act*. Retrieved October 9, 2020 from http://www.legislation.govt.nz/

Parliamentary Counsel Office. (2002). *New Zealand Local Government Act*. Retrieved October 9, 2020 from http://www.legislation.govt.nz/

Parsons, P. (1992). *Te Whanganui-a-Orotu (The Napier Inner Harbour): Traditional use and environmental change* (A Report to the Waitangi Tribunal, Issue WAI 55).

Pethick, J. (2001). Coastal management and sea-level rise. *Catena, 42*, 307-322. https://doi.org/10.1016/S0341-8162(00)00143-0

Pitt, R., Field, R., Lalor, M., & Brown, M. (1995). Urban stormwater toxic pollutants: assessment, sources, and treatability. *Water Environment Research, 67*(3), 260-275. https://www.jstor.org/stable/25044552

Plater, A., & Kirby, J. (2011). Sea-level change and coastal geomorphic response. *Treatise on Estuarine and Coastal Science, 3*, 39-72. https://doi.org/10.1016/B978-0-12-374711-2.00304-1

RetroLens. (2016). *Napier City 1980: Crown_5752_I_18* [Aerial imagery]. https://retrolens.co.nz/

RetroLens. (2019a). *Napier City 1964: Crown_1654_3845_38* [Aerial imagery]. https://retrolens.co.nz/

RetroLens. (2019b). *Napier City 1964: Crown_1654_3846_38* [Aerial imagery]. https://retrolens.co.nz/

RetroLens. (2020). *Napier City 1969: Crown_3183_4199_25* [Aerial imagery]. https://retrolens.co.nz/

RetroLens. (n.d.). *RetroLens: Historical image resource*. https://retrolens.co.nz/

Rinas, M., Tränckner, J., & Koegst, T. (2019). Sediment transport in sewage pressure pipes, part I: Continuous determination of settling and erosion characteristics by in-situ TSS monitoring inside a pressure pipe in northern Germany. *Water, 11*(10), 1-16. https://doi.org/10.3390/w11102125

Rodríguez-Germade, I., Rubio, B., & Rey, D. (2014). XRF scanners as a quick screening tool for detecting toxic pollutant elements in sediments from Marín harbour in the Ría de Pontevedra (NW Spain). *Marine Pollution Bulletin, 86*(1), 458-467. https://doi.org/10.1016/j.marpolbul.2014.06.029

Rodríguez-Germade, I., Rubio, B., Rey, D., & Borrego, J. (2015). Detection and monitoring of REEs and related trace elements with an iTrax™ Core Scanner in the Ría de Huelva (SW Spain). *Water, Air, & Soil Pollution, 226*(5), 137. https://doi.org/10.1007/s11270-015-2389-3

Rossi, L., Alencastro, L., Kupper, T., & Tarradellas, J. (2004). Urban stormwater contamination by polychlorinated biphenyls (PCBs) and its importance for urban water systems in Switzerland. *Science of The Total Environment, 322*, 179-189. https://doi.org/10.1016/S0048-9697(03)00361-9

Rothwell, R. G., & Croudace, I. W. (2015). Twenty years of XRF core scanning marine sediments: What do geochemical proxies tell us? In *Micro-XRF studies of sediment cores: Applications of a non-destructive tool for the environmental sciences* (Vol. 17). Springer.

Rubio, L., Linares-Rueda, A., Dueñas, C., Fernández, M. C., Clavero, V., Niell, F. X., & Fernández, J. A. (2003). Sediment accumulation rate and radiological characterisation of the sediment of Palmones River estuary (southern of Spain). *Journal of Environmental Radioactivity, 65*(3), 267-280. https://doi.org/10.1016/s0265-931x(02)00102-9

Salomons, W., & Förstner, U. (1984). Metals in the hydrocycle. 63-98. https://doi.org/10.1007/978-3-642-69325-0_3

Sarkar, S., Saha, M., Takada, H., Bhattacharya, A., Mishra, P., & Bhattacharya, B. (2007). Water quality management in the lower stretch of the River Ganges, East Coast of India: An approach through environmental education. *Journal of Cleaner Production, 15*, 1559-1567. https://doi.org/10.1016/j.jclepro.2006.07.030

Shi, P., Yuan, Y., Zheng, J., Wang, J., Ge, Y., & Qiu, G. (2007). The effect of land use/cover change on surface runoff in Shenzhen region, China. *Catena, 69*, 31-35. https://doi.org/10.1016/j.catena.2006.04.015

Smith, J., Barber, J., Ellmers, J., Fake, D., Haidekker, S., Harper, S., Hicks, A., Kozyniak, K., Lyncy, B., Madarasz-Smith, A., Norris, T., Rushworth, G., Sessions, L., Shanahan, B., Waldron, R., &

Wilding, T. (2018). *Our Hawke's Bay Environment*. Hawke's Bay Regional Council. https://www.hbrc.govt.nz/

Smith, S. (2014). *Monitoring of benthic effects of stormwater discharges at sites in the Ahuriri Estuary, Napier* (HBRC Publication No. 4896 Report No. RM16-78,). TripleFin Consulting Ltd.

Strong, J. (2005). *Background sediment trace metal concentrations of major estuarine, riverine, and lagoon systems in the Hawke's Bay region, New Zealand: A tool for the management of these resources* University of Auckland].

Swales, A., Ovenden, R., Budd, R., & Hawkes, J. (2005). *Whaingaroa (Raglan) Harbour: Sedimentation and the effects of historical catchment landcover changes* (2005/36). Environment Waikato. https://www.waikatoregion.govt.nz/

Swales, A., Williamson, R. B., Van Dam, L. F., Stroud, M. J., & McGlone, M. S. (2002). Reconstruction of urban stormwater contamination of an estuary using catchment history and sediment profile dating. *Estuaries, 25*(1), 43-56. https://doi.org/10.1007/BF02696048

Thrush, S., Hewitt, J., Cummings, V., Ellis, J., Hatton, C., Lohrer, A., & Norkko, A. (2004). Muddy waters: elevating sediment input to coastal and estuarine habitats. *Frontiers in Ecology and the Environment, 2*(6), 299-306. https://doi.org/10.1890/1540-9295(2004)002[0299:Mwesit]2.0.Co;2

Thrush, S. F., & Dayton, P. K. (2002). Disturbance to marine benthic habitats by trawling and dredging: implications for marine biodiversity. *Annual Review of Ecology and Systematics, 33*, 449-473. http://www.jstor.org/stable/3069270

Tjallingii, R., Röhl, U., Kölling, M., & Bickert, T. (2007). Influence of the water content on X-ray fluorescence core-scanning measurements in soft marine sediments. *Geochemistry, Geophysics, Geosystems, 8*(2). https://doi.org/10.1029/2006GC001393

University of Otago. (n.d.). *Itrax™ XRF Corescanner*. https://www.otago.ac.nz/

Vasconcelos, R. P., Reis-Santos, P., Costa, M. J., & Cabral, H. N. (2011). Connectivity between estuaries and marine environment: Integrating metrics to assess estuarine nursery function. *Ecological Indicators, 11*(5), 1123-1133. https://doi.org/10.1016/j.ecolind.2010.12.012

Waddington, J. M., Roulet, N. T., & Hill, A. R. (1993). Runoff mechanisms in a forested groundwater discharge wetland. *Journal of Hydrology, 147*(1), 37-60. https://doi.org/10.1016/0022-1694(93)90074-J

Westbrook, S. J., Rayner, J. L., Davis, G. B., Clement, T. P., Bjerg, P. L., & Fisher, S. J. (2005). Interaction between shallow groundwater, saline surface water and contaminant discharge at a seasonally and tidally forced estuarine boundary. *Journal of Hydrology, 302*(1), 255-269. https://doi.org/10.1016/j.jhydrol.2004.07.007

Wong, T. H. F. (2006). Water sensitive urban design - the journey thus far. *Australasian Journal of Water Resources, 10*(3), 213-222. https://doi.org/10.1080/13241583.2006.11465296

Wu, J., & Sun, Z. (2016). Evaluation of shallow groundwater contamination and associated human health risk in an alluvial plain impacted by agricultural and industrial activities, mid-west China. *Exposure and Health, 8*, 311-329. https://doi.org/10.1007/s12403-015-0170-x

Yeager, K. M., Schwehr, K. A., Schindler, K. J., & Santschi, P. H. (2018). Sediment accumulation and mixing in the Penobscot River and estuary, Maine. *Science of The Total Environment, 635*, 228-239. https://doi.org/10.1016/j.scitotenv.2018.04.026

Zeldis, J., Skilton, J., South, P., & Schiel, D. (2011). *Effects of the Canterbury earthquakes on Avon-Heathcote Estuary / Ihutai ecology* (U11/14).

Zingaro, M., Refice, A., Giachetta, E., D'Addabbo, A., Lovergine, F., De Pasquale, V., Pepe, G., Brandolini, P., Cevasco, A., & Capolongo, D. (2019). Sediment mobility and connectivity in a catchment: A new mapping approach. *Science of The Total Environment, 672*, 763-775. https://doi.org/10.1016/j.scitotenv.2019.03.461

Appendix A: Supplementary data file – Itrax raw scan data

Description:

The accompanying .zip file contains six csv spreadsheets of the raw Itrax™ XRF Corescanner data from the University of Otago for each of the six sediment cores.

Included files:

Itrax raw scan data - OTRB sediment core.csv
Itrax raw scan data - PUR sediment core.csv
Itrax raw scan data - SCAE sediment core.csv
Itrax raw scan data - TAI sediment core.csv
Itrax raw scan data - TT sediment core.csv
Itrax raw scan data - UAE sediment core.csv